Unit of Physiology and Program in Neuroscience
Department of Medicine
University of Fribourg
(Switzerland)

Anti-Nogo-A antibody treatment enhances functional recovery and sprouting of the corticospinal tract after spinal cord injury in adult primates

INAUGURAL-DISSERTATION
to attain the degree of
Doctor rerum naturalium
of the Faculty of Science of the University of Fribourg in Switzerland

Presented by

Patrick Freund
from
Germany

Thesis n° 1592
Uni Print Fribourg
2008

Accepted by the Faculty of Science of the University of Fribourg in Switzerland at the request of Prof. Volker Dietz, Prof. Marco Celio, Prof. Eric Rouiller and Dr. Thierry Wannier.

Fribourg, 28.01.2008

Ph.D. supervisor: **Dean:**

…….. …….

Chapter 1: Introduction

Chapter 2: Anti-Nogo-A specific antibody treatment enhances sprouting and functional recovery after cervical lesion in adult primates

Chapter 3: Anti-Nogo-A antibody treatment promotes recovery of manual dexterity after unilateral cervical lesion in adult primates: further behavioral data

Chapter 4: Anti-Nogo-A antibody treatment enhances sprouting of CS axons rostral to a unilateral cervical spinal cord lesion in adult macaque monkey

Acknowledgements

The present work was conducted between March 2005 and December 2007 in the Department of Medicine of the Faculty of the University of Fribourg.

I would like to express my gratitude to Eric Rouiller and Thierry Wannier who both guided and supported me throughout my thesis in very different important ways.

From Thierry Wannier, in particularly I learned in an unmistakable way that to defend ones own hypothesis knowledge about the field of interest is one of the tools a scientist has to acquire. Moreover, criticism is an attitude pushing things backward, but at the same time forward. It just has to be considered as objective. Thank you for your continuous support.

Eric Rouiller supported me in a very special way. I remember especially one moment. In front of the microscope I realized regenerated axons had innervated the territory below the lesion. In my excitement I jumped up and run into Eric's office and spread the news. Instantly he convinced himself and realized: "The brain is like a gold mine, it just has to be exploited". Thank you for your enthusiasm, your broad insight into neuroscience, your great ability to fill a blank sheath of paper and your continuous support.

I am very grateful to all the people working in the laboratory for their help and friendship all along the three years. I especially enjoyed the interesting conservation during the coffee breaks and of course during the EMG experiments with Abderraouf Belhaj. Special thanks go out to my wonderful Assistant Georgette Fischer who always amused me with her cheerful singing during her work with the monkeys.

I thank Professor Marco Celio at the University of Fribourg and Professor Volker Dietz at the Balgrist University Hospital for critically reviewing the present thesis as co-examiners.

I would like to especially thank my parents, sister and brothers for their never ending support. Always being interested in what I was doing they listened for

hours and hours to my thoughts, concerns and ideas. Without their support I would not have achieved. Thank you all.

Last but not least, I thank Theo Freund who hold so tight to his life during the decades being bound to the wheelchair. Through him I realized as a very little boy how important nerves are and how devastating it is not to feel a body part seemingly so intact.

Table of Abbreviations

BDA	Biotine dextran amine
C7	Spinal segment at cervical level 7
C8	Spinal segment at cervical level 8
CNS	Central nervous system
CS	Corticospinal
CST	Corticospinal tract
ER	Endoplasmatic Reticulum
fMRI	Functional magnetic resonance imiging
ICMS	Intracortical microstimulation
IN-1 mAb	Monoclonal antibody against Nogo-A
M1	Primary motor cortex
MAG	Myelin-associated glycoprotein
NgR	Nogo-Receptor
OMgP	Oligodendrocytes-myelin glycoprtein
PM	Premotor cortex
RN	Red nucleus
RNm	magnocellular part of RN
RNp	parvocellular part of RN
ROCK	Rho Kinase
RSNs	Rubrospinal neurons
RST	Rubrospinal tract
SCI	Spinal cord injury
Th2	Spinal segment at thoracic level 2

Zusammenfassung

Eine vollständige Rückenmarksdurchtrennung führt zu einem totalen funktionellen Verlust jeglicher willentlicher Kontrolle unterhalb der Läsion. Die Ursache für diesen Verlust ist der limitierten Zellernneuerung und der ausbleibenen axonalen Regeneration zu zuschreiben. Erste Hinweise deuten daraufhin, dass die Präsenz von Myelin-assozierten inhibitorischen Wachstumsfaktoren, wie zum Beispiel Nogo-A, dafür verantworlich sind. Eine therapeutische Massnahme um diesen inhibitorischen Effekt entgegen zu wirken, ist die Applikation von Antikörpern welche diese Stoffe neutralisieren. Am Rattenmodel wurde erfolgreich gezeigt das nach einer Rückenmarksverletzung und einer zweiwöchigen Applikation eines neutralisierendes Antikörpers gegen das Protein Nogo-A, Nervenzellen dazu stimulierten wieder auszuwachsen und funktionelle Verknüpfungen herzustellen. Diese neuen Verbindungen ermöglichten den anti-Nogo-A behandelten Tieren im Vergleich zu Unbehandelten zu einer verbesserte Motorik.

Das Ziel dieser These war es zu prüfen, ob die Translation dieser therapeutischen Anwendung am Primaten bevor es zur ersten klinischen Anwendung an querschnittsgelähmten Patienten gelangt. Der Translationschritt ist in sofern unumgänglich, da er zum einen erlaubt zu prüfen, ob die Neutralsierung und die folgliche Stimulierung von Nervenwachstum nicht irrtürmlicher Weise zu falschen Verbindungen führen könnte mit heftigen Nebenwirkung als Folge und zum anderen ob die Applizierung des Antikörpers am Primaten zu wessen Gruppe der Mensch zählt, funktioniert.

Insgesamt wurden 13 adulten Makaken einer unilateralen zervikalen Läsion ausgesetzt. Sieben Tiere erhielten den neutralieserendem Antikörper gegen Nogo-A während vier Wochen und die Anderen sechs Tiere erhielten eine Kontrollantikörper Behandelung. Kontrollantikörper behandelte Tiere wiesen eine läsionsgrössen-abhängige motorische Genesung für einen

Dexteritätstest auf mit sehr limitertem axonalen Wachstum des Kortikospinalen Tractes kaudal der Läsion. Im scharfen Gegensatz wiesen behandelte Tiere vermehrtes axonales Wachstum und eine vollständige funktionelle Erholung für diesen spezifischen Dexteritätstest auf (**Kapitel 1, 2 und 3**). Desweiteren führte die Neutrilaztion von Nogo-A zu einer verstärkten Reorganization des Kortikospinalen Trakt rostral der Läsion (**Kapitel 4**).

Auf dem Nivieau des Kortex und des Pons wurden retrograde degenerative Veränderungen gemessen anhand der Zellgrösee und Anzal von Neuronen im motrischen Kortex und im Rotem Nucleus. In beiden untersuchten Arealen kam es zu eienr deutlichen vermindureung der Zellsomagrösse auf der lädierten Seite. Im Gegensatzt zum motorischen Kortex wo kein signifikanter Unterschied von Zell Anzahl gefunden wurde gab es zudem im Roten Nucleus eine deutlich Reduzierung der Anzahl von Neuronen auf der lädierten Seite. Diese degenerativen Vorgängen wurden nicht durch die anti-Nogo-A Behandlung vermindert (**Kapitel 5 und 6**).

Zusammengefasst zeigen die Resultate dieser These dass eine Neutralization von einem Myelin-assoziertem Protein Nogo-A nach einer Rückenmarksverletzung zu einer verbesserten Motorik und vermehrtem axonalen Wachstum auf der Höhe der Läsion im adulten Primaten fürht, in Abwesenheit von Nebenwirkungen.

1 Summary

After injury to the adult central nervous system (CNS), permanent deficits remain to a large part due to limited cell renewal, axonal regeneration and re-establishment of functional connectivity. Evidence indicate that the lack of axonal regeneration is partly due to the myelin-associated inhibitory factor Nogo-A. A therapeutical strategy to overcome this inhibition is to prevent the neurite outgrowth inhibitor Nogo-A from interacting with its neural receptors by using antibodies specifically binding to Nogo-A, thereby neutralizing its action. Experiences in the rodent model subjected to spinal cord injury have shown that neutralizing Nogo-A, by using specific antibodies not only promotes axonal regeneration but also leads to significant functional recovery.

The aim of this thesis was to investigate whether this treatment strategy also leads to axonal regeneration and functional recovery in non-human adult primates subjected to a partial section of the spinal cord. This assessment is a crucial step towards a safe clinical application. Thirteen macaque monkeys were subjected to a unilateral cervical lesion at the border between the C7 and C8 segments. A group received intrathecal injections of a control antibody whereas the other animals received a monoclonal antibody recognizing Nogo-A. Functional recovery was tested using several motor tasks mainly focusing on manual dexterity. Control antibody treated monkeys showed a recovery that depends on lesion size. In contrast, anti-Nogo-A antibody treated monkeys recovered better and even returned to pre-lesion score levels in a manual dexterity task (**Chapters 2 and 3**).

We further investigated, using light-microscopy, if the process of functional recovery is paralleled by an anatomical reorganization of the injured corticospinal tract (CST). At the spinal level, the area rostral and caudal to injury was analyzed for axonal regeneration. Compared to control antibody treated monkeys, an enhanced number of fibers presumably due to regenerative sprouting was observed rostral to the lesion in anti-Nogo-A antibody treated monkeys. Caudal to injury, a higher cumulated axonal arbor

length and a higher number of axonal swellings were observed in anti-Nogo-A treated animals (**Chapters 2 and 4**).

We also investigated the consequences of the lesion on corticospinal (CS) and rubrospinal (RS) neurons and whether the anti-Nogo-A antibody treatment had an influence on these effects. For this purpose the number and size of CS and RS neurons were measured in both sides of the brain using light-microscopy in intact, in control antibody as well as in anti-Nogo-A antibody treated monkeys.

At the level of the motor cortex the number of pyramidal neurons remains similar on both hemispheres, but their somata shrunk on the side opposite to the lesion. In this case, the neutralization of Nogo-A did not protect the cells from shrinkage.

In the red nucleus, the lesion also induced shrinkage of the soma of the neurons detected in the contralesional magnocellular part of the red nucleus (RNm). In contrast to cortical level, here, the number of cells detected in the contralesional RNm was consistently lower to that in the ipsilesional RNm, suggesting either cell loss or shrinkage beyond detection. Thus, the neutralization of Nogo-A by antibody infusion at the lesion side did not prevent the phenomena of cell somata shrinkage nor cell disappearance (**Chapters 5 and 6**).

In summary the results reported in this thesis demonstrate that the neutralization of the neurite outgrowth inhibitor Nogo-A promotes axonal regeneration on the level of the spinal cord in adult monkeys subjected to a unilateral spinal cord lesion. This effect is paralleled by significant functional recovery. However, histological changes in the red nucleus and motor cortex were not prevented or attenuated by the anti-Nogo-A antibody treatment.

2 Introduction

In patients suffering from spinal cord injury the connections linking the brain to the centres controlling limb movements are often interrupted. Currently no treatments to re-establish these lost connections are available. Patients with high cervical lesions present tetraplegia, a paralysis of all four limbs, whereas patients with thoracic and/or lower lesions present paraplegia, paralysis of the lower part of the body. Depending on the lesion extent and level, injuries are classified according to the American Spinal Injury Association (ASIA) as complete (ASIA A) or incomplete (ASIA B-D). Both types of injury represent different challenges to basic as well as clinical research. In case of complete lesion questions have to be addressed whether it is possible to enable injured axons to cross the lesion scar in order to reconnect the two stumps. As in the present case of incomplete injuries, injured axons may not need to regenerate through the lesion site, but sprout around the lesion using spared tissue as a bridge or onto spared pathways not affected by the lesion.

At present, focus on treating spinal cord injured (SCI) patients remains limited to management of bladder dysfunction, spasticity and neuropathic pain. However, tetra- as well as paraplegic patients experience limited functional recovery that can be promoted by rehabilitative means (Dietz, 1997). For example it was shown that regular locomotor training, by walking on a treadmill under weight support conditions, can aid some incomplete patients to regain their capability of weight bearing and walking (Dietz, 1995; Dietz et al., 1998). Nevertheless, in all cases, SCI patients have to learn to make compensatory use of spared motor functions.

Repair of large lesions to the spinal cord requires lesioned axons to regenerate across the lesion scar and/or compensatory sprouting of spared fibers. After a lesion, both types of neurite growth are abundant in the newborn CNS but not in the mature CNS. The time point at which this capacity to nerve regeneration ceases depends on the species. In rodents (Kalil and Reh, 1982) and in humans (Chen et al., 2002) this occurs within a few weeks postnatally. Simultaneously, the cellular composition of the maturing CNS changes by the differentiation of oligodendrocytes and the myelination of axons (Kapfhammer and Schwab, 1994). However, adult CNS

neurons have not lost the intrinsic capacity to regenerate (Fig. 1), because, when provided with a permissive environment such as a portion of a peripheral nerve, they will extend long processes into the graft that somewhat penetrate CNS tissue (David and Aguayo, 1981).

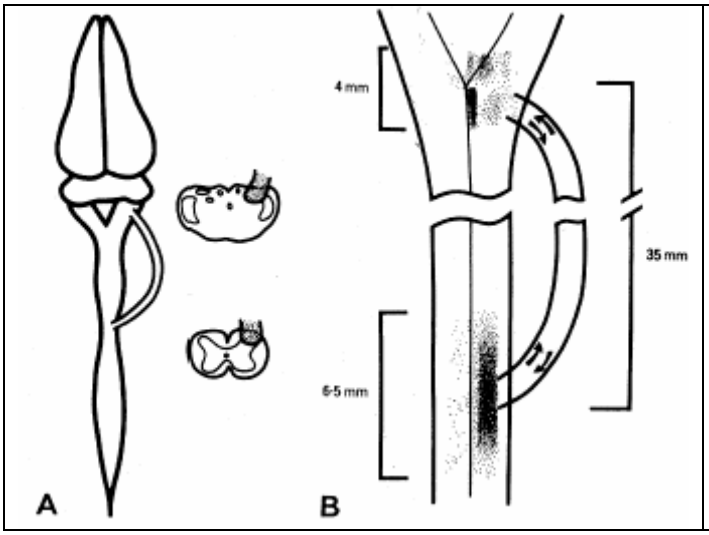

Figure 1 A: Axons of the adult CNS use a tissue bridge to regenerate over long distance in a PNS environment
Panel B: Anterograde and retrograde labeled CNS neurons after grafting (David and Aguayo, 1981)

To restore function following SCI, molecular therapeutic interventions shall promote neuron survival, axonal growth and enhance conductivity. In recent times, several pharmacological approaches have led to long distance regeneration of injured axons and compensatory sprouting being paralleled by enhanced functional recovery in the rodent model of SCI.

For example, it has been shown that *neurotrophic* factors applied after injury promote the survival and maintenance of a variety of injured neurons in the mammalian adult CNS (Giehl and Tetzlaff, 1996; Schnell et al., 1994; Tobias et al., 2003; Weidner et al., 1999) and survival, sprouting and outgrowth of injured fibres within the grey matter, but never within the white matter (Grill et al., 1997; Ramer et al., 2000).

Also the delivery of intracellular cyclic AMP (cAMP) induces axonal sprouting of injured sensory neurons in vivo (Lu et al., 2004). Another approach, the *inactivation of Rho k inase (RO CK),* a protein family of GTPases, promoted functional recovery and had a neuroprotective effect *(Dergha m et al., 2002; Fournier et al., 2003).* One of the most recently evolved strategies to allow successful reconnection of neurons to deprived targets is the neutralization of the inhibitory effects imposed by the glia scar, by enzymatically degrading the axon-inhibitory chondrotin sulphate proteoglycans (David and Lacroix, 2003).

The failure of axonal regeneration is largely attributable to growth inhibitors expressed in myelin by oligodendrocytes (Fig. 2), a cell type only found in the white matter (Caroni et al., 1988). Numerous myelin associated proteins have been found that exert inhibitory properties on neurite outgrowth (Fig. 3). These proteins include Nogo-A (Chen et al., 2000; Schwab and Bartholdi, 1996), MAG and OMgp (Filbin, 2003).

Nogo-A was found to be the most expressed inhibitory protein and represent an important factor in the restriction of neurite growth after injury. The application of the monoclonal antibody IN-1 (mAb IN-1), which was raised against a protein later identified as Nogo-A, allowed long distance growth of axons and compensatory fiber growth in vitro and in vivo (Caroni and others, 1988; Schnell and Schwab, 1990). Interestingly, these new grown fibers seem to establish functionally meaningful connections with adequate targets. Thereafter, several studies have shown that this morphological reorganization after SCI is paralleled by motor recovery of skilled forelimb movements and locomotion in rats and mice in absence of malfunction, such as neuropathic pain (Bradbury et al., 2002; Bregman et al., 1995; Li and Strittmatter, 2003). Therefore, the neutralization of endogenous nerve growth inhibitors represents a promising approach for therapeutic application to repair the CNS in humans. In order to translate these advances the use of the non-human primate model is essential (Courtine et al., 2007). In accordance with this idea, the aims of this study were to investigate the anatomical fibre plasticity and functional recovery in control and in anti-Nogo-A antibody treated macaques subjected to a partial cervical spinal cord lesion.

In the following sections of this chapter the main characteristics of Nogo-A and its implication in the repair of spinal cord lesion and functional recovery will be outlined. Special attention will be paid to the implication of the corticospinal tract in and its contribution to functional recovery.

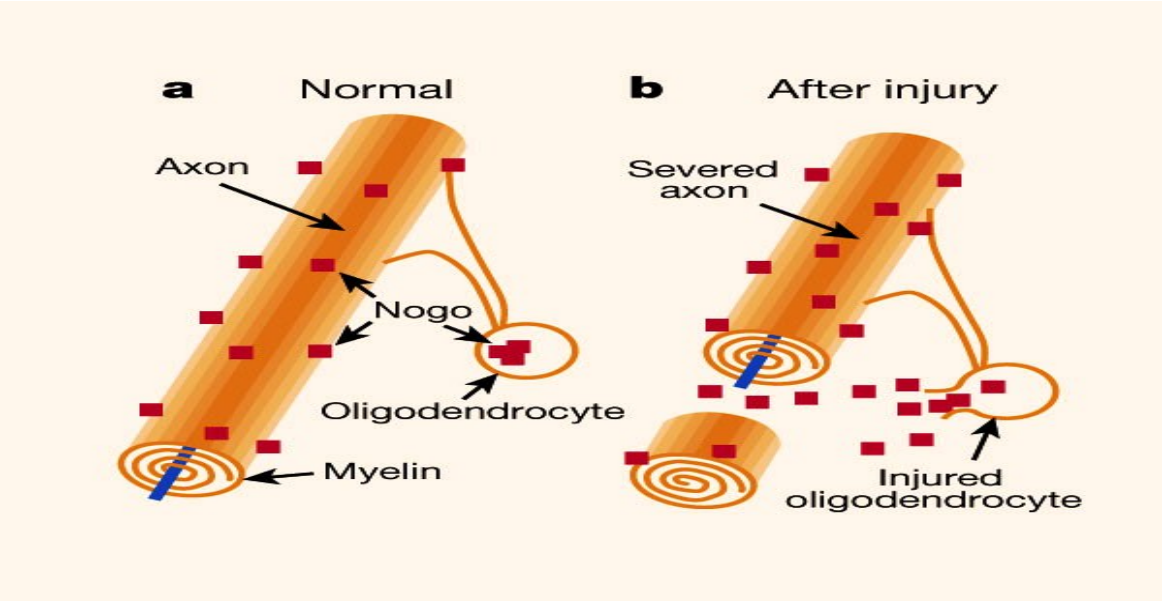

Figure 2 Inhibition of axon regeneration. A) Myelin-associated inhibitors, such as Nogo, are found on the inner and outer myelin leaflets and may normally prevent axonal sprouting in the uninjured CNS. B) After injury, damaged myelin and oligodendrocytes contribute to the prevention of regeneration (Goldberg and Barres, 2000).

2.1 Axonal growth inhibition and its implication in spinal cord repair

2.1.1 Modulation of interactions with the myelin inhibitor Nogo-A

The N*ogo* protein is a member of the Reticulon family which comprises proteins that are usually associated with the endoplasmatic reticulum (ER). The Nogo gene is differentially spliced to generate three isoforms each having different N-termini which result into: Nogo-A, Nogo -B and Nogo-C (Chen et al., 2000) (Fig. 3). Nogo-A, the largest form, is predominantly expressed in the CNS; Nogo-B is a minor isoform and concentrated in the ER of endothelial cells; Nogo-C is enriched in the periphery, especially in skeletal muscle (Huber et al., 2002). The biological function of Nogo B and C are currently unknown. Nogo-A though, has been identified as a protein which exerts a strong inhibitory action on neurite outgrowth. It is localized on the surface of oligodendrocytes (Chen and others, 2000) and into the inner and outer loops

of myelin (Huber et al., 2002). Its topology, predicted from amino acid composition and immunohistochemistry, showed that all the three main products of the gene encoding Nogo have 188 amino acids at their carboxy terminus in common. It is this specific amino acid chain which is in common with the Reticulon protein family (Chen and others, 2000; Fournier et al., 2001; GrandPré et al., 2000; Oertle et al., 2003).

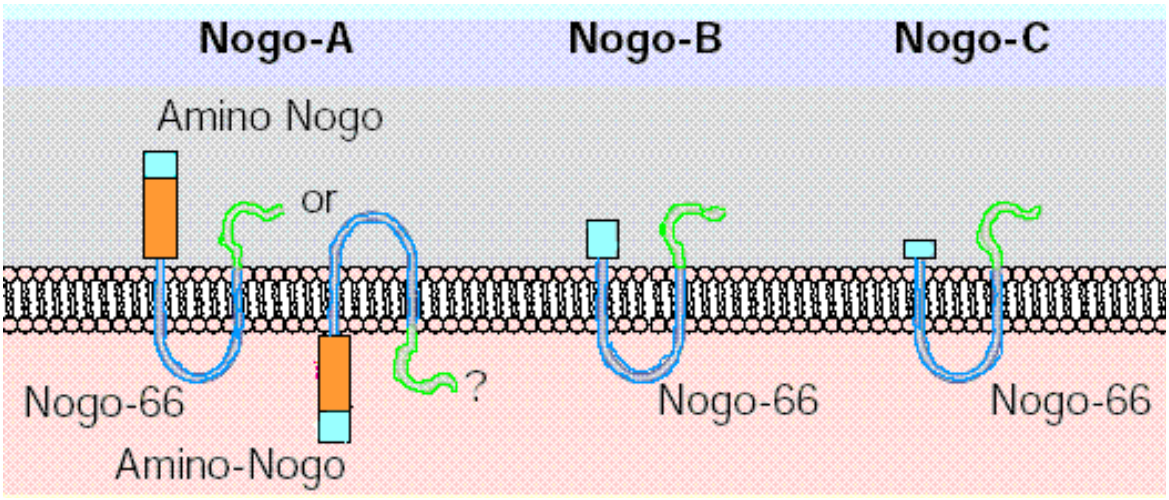

Figure 3 Structures of three inhibitors of axonal regeneration identified in myelin; Nogo exists in three isoforms A, B and C. Their hypothesized topologies are shown here. Sequences that are common to all three isoforms are shown in blue and green (Filbin, 2003).

Three different extracellular exposed peptide chains are involved in the process of inhibition. In particular, the N-terminal region of Nogo-A inhibits strongly the neurite outgrowth whereas the C-terminal region (Nogo 66) and a stretch encoded by the Nogo-A-specific exon leads to growth cone collapse. In addition the latter is capable of restricting neurite outgrowth and cell spreading. Besides, the N-terminal and C-terminal domains are likely to be located on the cytoplasmic side (Oertle and others, 2003). These different inhibitory action sites might satisfy the need of a developing neuron to get to its correct place (i.e. Nogo-66) and/or restrict its plasticity and regeneration (i.e. Nogo-A) by using its different binding sites to the receptors.

In what ways Nogo acts on the neuron is not yet fully understood, though some functionality has been discovered. A protein which binds to the extracellular domain of the Nogo protein (Nogo-66) (Fig. 4) was identified (GrandPré and others, 2000). Nogo-66 is common to Nogo-A, -B, -C and leads to growth cone collapse when a connection between the two molecules is established, hence proving that the protein recognizes a Nogo-66 receptor (NgR) (Fournier and others, 2001).

The Nogo receptor is predominantly expressed in the CNS in neurons and their axons (Josephson et al., 2001; Wang et al., 2002) and is attached to the outer leaflet of the plasma membrane by a glycosylphosphatidylinositol moiety, implying a need for further subunits to efficiently transfer the information to the intercellular space (Fig. 3) (McGee and Strittmatter, 2003). The Nogo-NgR complex needs to associate with the neutrophin coreceptors p75 (Wang et al. 2002) and Lingo-1, a nervous-system specific Nogo receptor interacting protein (Mi et al., 2004), to transduce the signal across the plasma membrane. This then triggers the activation of RHoA GTPase downstream of NgR and thus controls axon growth and extension during development and after injury (Niederöst et al., 2002).

However, that NgR is not the only crucial receptor which is active during the signaling process received potential evidence through the findings that cross talk between pathways involved in neurotrophin signalling and signalling by axon growth inhibitors does exist. The N-terminal region of Nogo-A (amino-Nogo), for example, can inhibit neurite outgrowth independent of NgR via an unknown receptor (He et al. 2004). Furthermore, at least two other inhibitory components of myelin, though with a less inhibitory activity, have been found binding to the same NgR as Nogo-66, i.e. the myelin-associated glycoprotein (MAG) and the oligodendrocyte-myelin glycoprotein (OMgp) (Filbin, 2003).

MAG is found in both the CNS and the PNS, where it is located in the periaxonal membrane, and is therefore ideally placed to interact with an axonal receptor (i.e. NgR) (Filbin, 2003). OMgp is a relatively minor component of myelin, and it is believed to be localized largely in the paranodal loops, next to the node of Ranvier (Wang et al 2002). Like MAG and Nogo, OMgp induces growth cone collapse and inhibits neurite outgrowth when it binds to NgR (Niederöst and others, 2002).

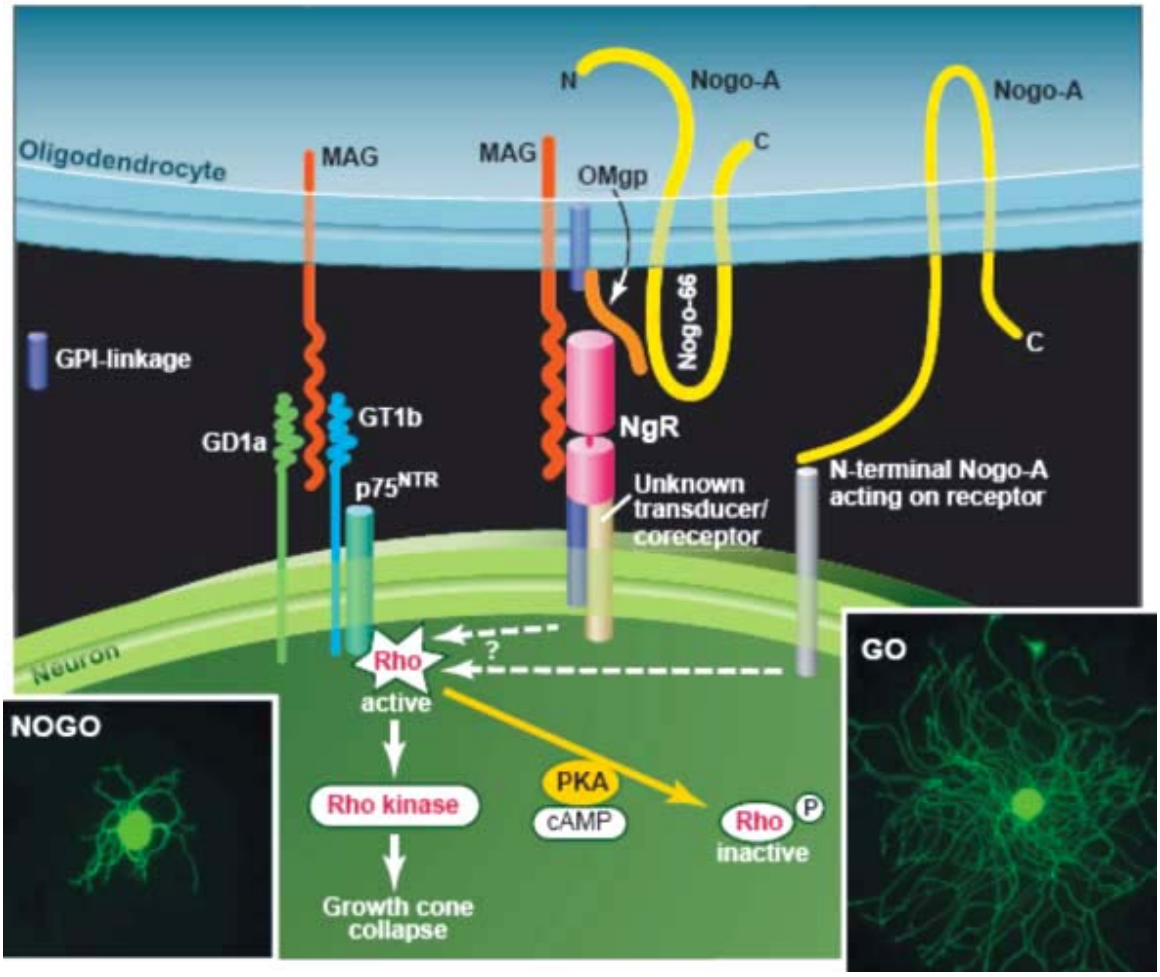

Figure 4: A schematic representation of known myelin-associated inhibitors and their receptor complexes. Three major myelin inhibitors, including the extracellular domain of Nogo-A (Nogo-66), MAG, and OMgp, all bind to NgR with high affinity. This complex in turn associates with coreceptors as p75 to transduce the signal across the plasma membrane. In addition, the N-terminal region of Nogo-A (amino-Nogo) can inhibit neurite outgrowth independently of NgR. It seems that the different activation pathways all converge onto the ROCK cascade inside the neuron, leading to an inhibition of neurite growth (Woolf and Bloechlinger, 2002).

2.1.2 Neutralizing Nogo-A enhances axonal sprouting and functional recovery in rodents

The IN-1 monoclonal antibody (mAb IN-1)(Caroni and others, 1988) which is an IgM that recognizes the region specific to Nogo A (Brösamle et al., 2000; Brösamle et al., 2000; Brösamle et al., 2000) neutralizes the action of Nogo-A in vivo.

To investigate plasticity and compensatory fiber growth after SCI, the corticospinal tract (CST) was sectioned unilaterally at the level of the pyramids in adult rats. Control or anti-Nogo-A producing hybridoma cells were implanted in the hippocampus. In control treated animals sprouting was minimal within the spinal cord, the red nucleus and pontine nuclei. In contrast, in anti-Nogo-A treated rats sprouting of cortico-bulbar fibers and establishment of cortico-rubral and cortico-pontine connections occurred. In addition, the uninjured CST sprouted across the midline and branched into the denervated dorsal and ventral part of the spinal cord along the entire spinal cord (Thallmair et al., 1998). Anti-Nogo-A treated rats showed almost full recovery for sensory and a motor task demanding skilled forelimb reaching (Z'Graggen et al., 1998).

The bilateral interruption of the CS connections at the level of the pyramids can be compensated by corticorubral and rubrospinal sprouts of these pathways. It was observed that following lesion, sprouts grew into the ventral grey matter of the cervical cord where they made close apposition to motoneurons of forelimb muscles (Raineteau et al., 2002) (Fig. 5). Interestingly, in intact animals the rubrospinal tract does not project directly to this region (Raineteau et al., 2001). In the anti-Nogo-A treated rats, fast muscle EMG responses were evoked following cortical microstimulation. However, these responses were abolished after injection of mucimol, a GABA antagonist, into the red nucleus, showing the presence of new cortico-rubro-spinal pathways in anti-Nogo-A antibody treated rats (Raineteau et al., 2002).

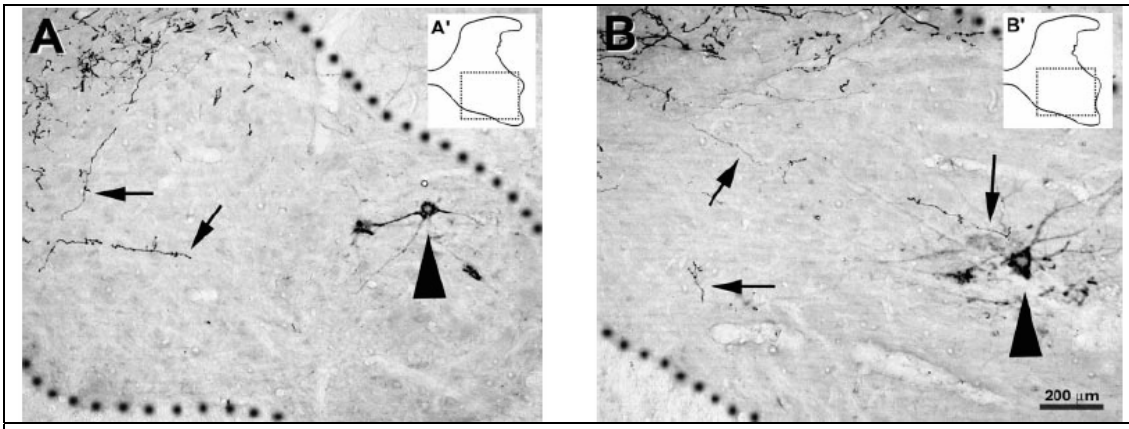

Figure 4: Photomicrographs depicting the penetration of BDA-labeled rubrospinal tract sprouts in the ventral horn of the spinal cord in rats treated with the IN-1 antibody. Panel A shows axon sprouts at C6 level and in panel B at C7 level (Raineteau et al., 2002).

It has been reported that, in adult rats, subjected to lesion of the dorsal column of the spinal cord, improved functional recovery occurred in anti-Nogo-A treated animals (Bregman and others, 1995). In this lesion paradigm, control or anti-Nogo-A producing hybridoma cells were implanted in the proximity of the ventricular system allowing the antibodies to penetrate along the entire CNS. Sprouting and regeneration of CST axons paralleled functional recovery. The behavioral findings were confirmed by electromyographic examinations (Raineteau et al., 2002). Muscle EMG activity was measured in control and anti-Nogo-A treated animals during treadmill walking of flexor and extensor muscles. In contrast to control animals, in anti-Nogo-A treated animals these EMG recordings confirmed the improved step-cycle duration, rhythmicity, and coupling of the hindlimbs (Fig. 6).

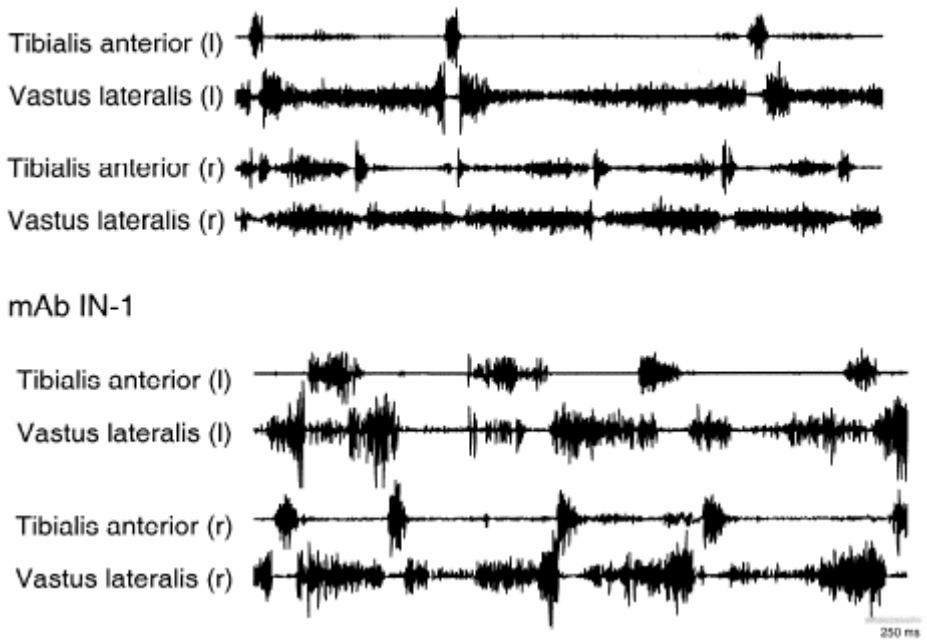

Figure 6: Muscle EMG activity recorded in SCI rats during treadmill walking. In the top panel a control animal clearly shows an abnormal stepping pattern, whereas the pattern of an anti-Nogo-A treated animal is close to normal (Fouad et al., 2001).

The above outlined results indicate a clearly improved functional recovery suggesting that the increased plastic and regenerative capabilities of the CNS after Nogo-A neutralization result in a functionally meaningful rewiring of the motor systems.

In a further step towards the clinic the mAb IN-1 was partially humanized by replacing the murine constant domains with human domains, in order to make it more accessible to the human immune system (Brösamle et al., 2000). Indeed, this recombinant Fab fragment (rIN-Fab) itself was again able to stimulate injured adult rat axons to regenerate over long distance in the spinal cord as represented schematically in Fig. 7

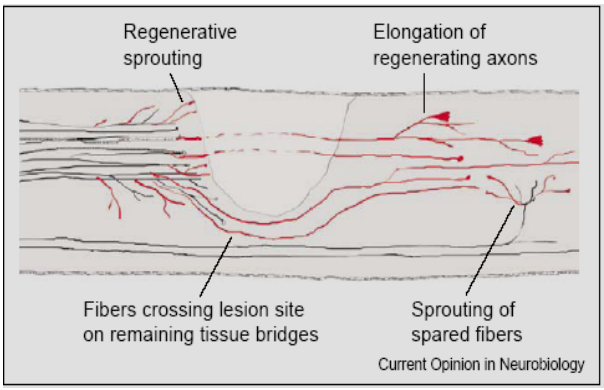

Figure 7: Longitudinal sagittal view of a rat or mouse dorsal spinal cord lesion, transecting the main corticospinal tract which shows minor spontaneous sprouting (black). Nogo-A neutralizing antibodies can lead to enhanced sprouting of fibers rostral to the lesion and to fibres crossing the lesion on remaining tissue bridges into the caudal spinal cord and growing down the spinal cord over long distances (drawn in red). Spared fibres also show enhanced sprouting in the caudal spinal cord (Schwab, 2004).

2.1.3 Proof of principle-way to the clinic

Nogo-A is present in humans (Prinjha et al., 2000; Spillmann et al., 1997), making its inactivation a possible treatment for SCI patients. Before the translation of this technique to humans, an important step is to establish how the antibody should be delivered and to show its efficacy in primates. In humans to allow a controlled application over weeks, the antibody will be applied using implanted pumps. Infusion of antibodies via osmotic minipumps proved to be an efficient way to apply antibodies to the CNS of both rat and monkeys. Indeed it was shown that in these species the antibody reached its antigen via diffusion in the CSF or inside the CNS tissue and was able to downregulate Nogo-A expression (Weinmann et al., 2006). Whether the application of the anti-Nogo-A antibody onto humans increases plasticity and regenerative growth remains unknown. However, application of Nogo-A antibodies in the marmoset subjected to spinal injury confirmed that sprouting occurred into, through and around the lesion in a primate (Fouad et al., 2004). However, the latter study did not address the questions of functional recovery and negative side effects, such as allodynia, through aberrant sprouting. We investigated these questions in the macaque monkey subjected to unilateral

cervical lesion by evaluating their hand and leg function and their recovery when Nogo-A is neutralized.

Why use the non-human primate model? In a recent discussion examining whether the non-human primates can expedite the translation of treatments for spinal cord injury in humans it was concluded that this animal model can probe the effect of therapy-induced neural plasticity on various aspects of functional recovery with a precision which cannot be achieved in rodents (Courtine et al., 2007). Three major points justify this conclusion:

First, the general organisation of the CS system in monkeys is very much like that in human subjects, in contrast to the rat. Whereas the CST tract in rats run in the dorsal columns without making direct corticomotoneural connection, in the primate as in humans, the main crossed part of the CST tract runs in the dorsolateral funiculus and the uncrossed part run either in the dorsolateral or anterior ventral funiculus on the contralateral side.

Second, the CS projection system is involved, as far as the forelimb is concerned, in sophisticated dexterous movements typical of primates (Lawrence and Hopkins, 1976; Lemon, 1993; Porter et al., 1985; Porter, 1987). Along this line, behavioural assessment of manual dexterity is more pertinent in monkeys than in rodents, the formers being capable of fractionated dexterous movements of the fingers as human subjects. Third, neutralization of Nogo-A may not only favour regeneration or sprouting of lesioned axons, but may also induce an unspecific growth of axons which may cause undesired pathologies, such as allodynia.

2.2 Investigating regeneration and functional recovery in non-human primate

Proving the efficacy and safety of a treatment in the non-human primate provides strong support for the translation of this treatment to the clinics (Courtine et al., 2007). Investigations have already been conducted to establish whether an anti-Nogo-A antibody treatment induces regeneration. To study the action of a regenerative treatment on the level of functional

recovery in the non-human primate, we have chosen to perform a unilateral partial section of the spinal cord at the border between the C7 and C8 spinal segments. The reasons accounting for this choice and some of the consequences expected from this lesion with their characteristics are presented below.

2.2.1 : Lesion level

The distribution of spinal motoneurons is topographically organized. At a segmental level, the motoneurons innervating the axial muscles lie most medially in the grey matter of the spinal cord, whereas those innervating the most distal muscles in the limbs are found most laterally in the ventral horn. From an anatomical point of view these latter motoneurons are located most closely to the lateral corticospinal tract and receive the highest density of CS projections (Holstege, 1991; Ralston and Ralston, 1985).

Along the neuroaxis, motoneurons innervating a specific muscle are grouped in close proximity to each others. Jenny and Inukai (1983) determined the topographic organization of these motoneurons pools for the segments involved in controlling arm, wrist, and hand (finger) movement (Jenny and Inukai, 1983). As illustrated in Fig. 7, each single motoneurons pool spreads over two or more segments. The motoneurons projecting to hand muscles are located in the spinal segments C8 to Th 2, whereas the cervical segments C5 and C7 contain motoneurons controlling forearm muscles as well as biceps and triceps.

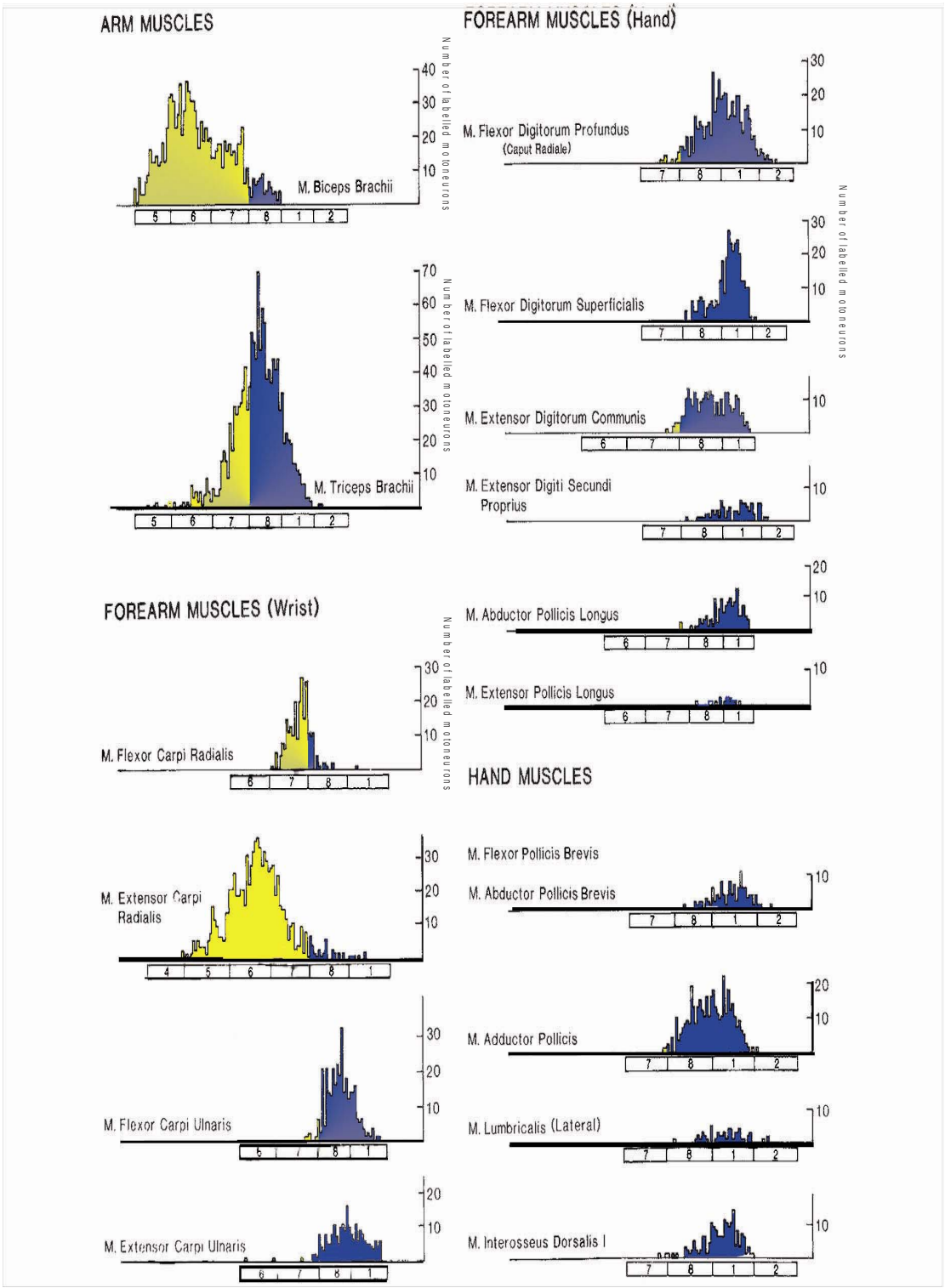

Figure 7: Segmental distribution of motoneurons innervating selected muscles of the macaque monkey forelimb expressed as the number of retrogradly labeled motoneurons after HRP injections in the forelimb muscles. In addition the regions affected following a hemi-section lesion between the spinal cord segments C7/C8 as done in the present thesis work, are marked blue; the motoneurons not affected are shown in yellow (Jenny and Inukai, 1983)

2.3 *Functional consequences of a spinal cord injury in primates*

2.3.1 Anatomy of the corticospinal tract and its contribution to voluntary movement

The capacity to perform a precise opposition of the thumb and the forefingers and independent movements of the fingers depends on the CS system integrity, especially on the direct monosynaptic input from primary motor cortical areas to motoneurons in the cervical spinal cord, the so called corticomotorneural (CM) system (Kuypers, 1981; Lemon, 1993; Phillips, 1971). CS projections arise from spatially discrete and somatopically organized cortical regions (Fig 8). For example, the macaque monkey possesses at least six CS neural subpopulations located within the frontal, cingulate, parietal and insular cortices (Galea and Darian-Smith, 1994; Galea and Darian-Smith, 1995; Kuypers, 1981).

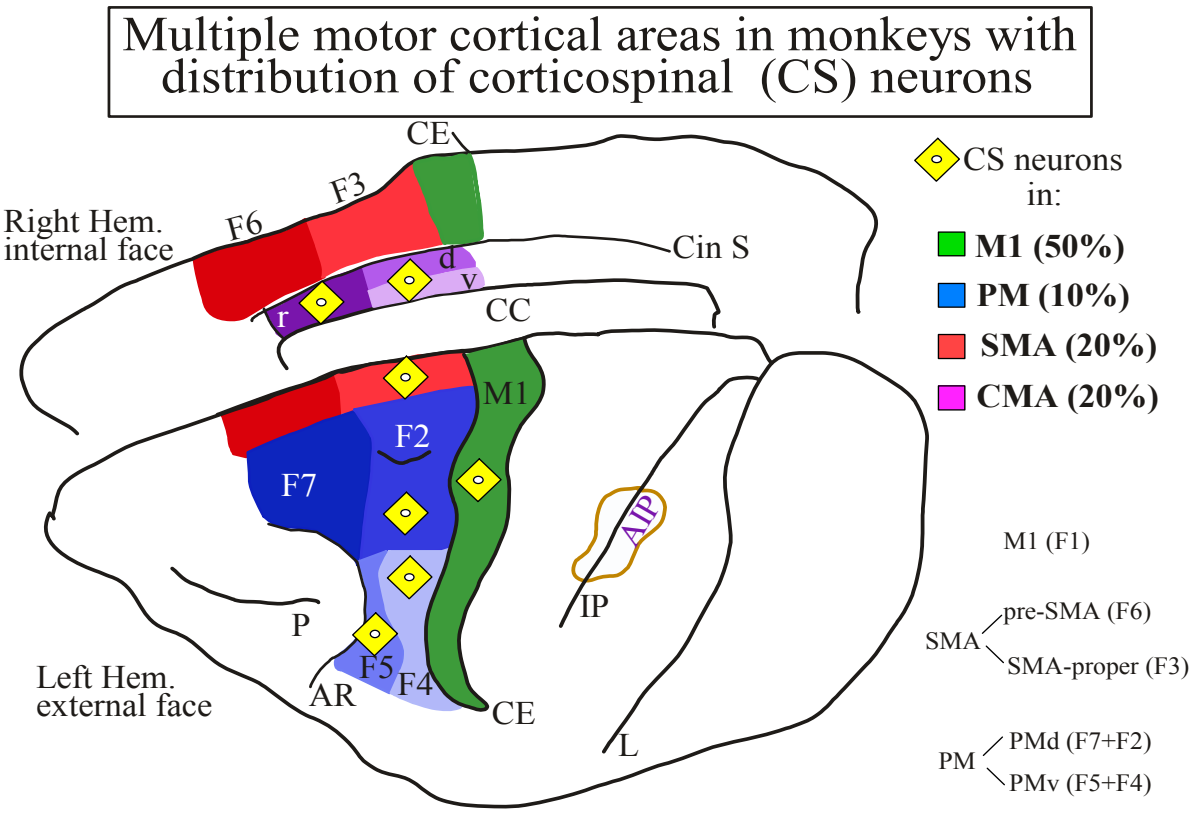

Figure 8: The organization of the motor cortical areas in the macaque monkey and the qualitative distribution of corticospinal (CS) neurons. Fifty percent of the CS neurons of the

frontal lobe are in M1, whereas the other 50% are distributed in the other three motor regions (Premotor Area (PM), Supplementary Motor Area (SMA), Cingulate Motor Area (CMA)).

Inside these cortical motor areas CS neurons are situated in the deepest part of lamina V (Asanuma, 1981; Humphrey and Corrie, 1978; Porter, 1981). The majority (about 90%) of the CS fibres decussate and project contralaterally (Kuypers, 1981; (Holstege, 1991). Together with other corticofugal fibres they project via the internal capsule into the ipsilateral cerebral peduncle. From there the largest part of the fibres emerges from the cerebral peduncle and continues caudally along the ventral surface of the medulla oblongata towards the pyramidal decussation point at the caudal end of the brainstem. After decussating they continue on the contralateral side of the spinal white matter as the '*lateral corticospinal tract*' representing 90-95 percent of all descending fibers (Lacroix et al., 2004; Rouiller et al., 1996)(Fig. 9, 10). The other 10 percent emerge in the same manner, but either enter the '*medial (anterior) corticospinal tract*' by descending ipsilateral, hence not crossing the sides at the level of the medulla oblongata, or by descending first and then crossing the dorsolateral funiculus at lower spinal segments (Galea and Darian-Smith, 1997; Kuypers, 1981; Phillips, 1979).

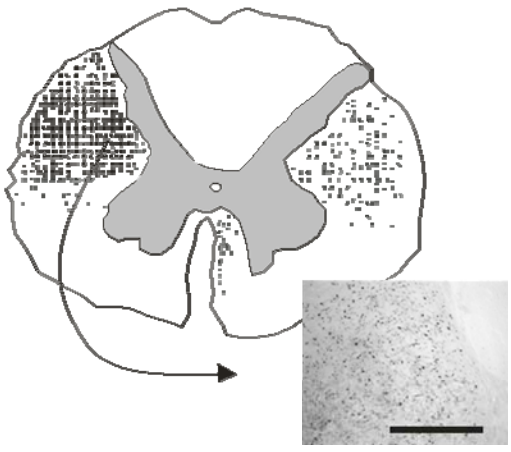

Figure 9 : After unilateral injection of the anterograde tracer BDA into the hand representing area of M1 the CST is labeled within the spinal cord. Here at C5 level, on a frontal section of the cervical cord, black dots indicate the location and distribution of the CS axons, forming the dorsolateral funiculus (dlf) contralateral to the injection site (left half of the cord) and the uncrossed CS axons, present in the dorsolateral and ventral funiculi ipsilateral to the injection site (right side of the cord).

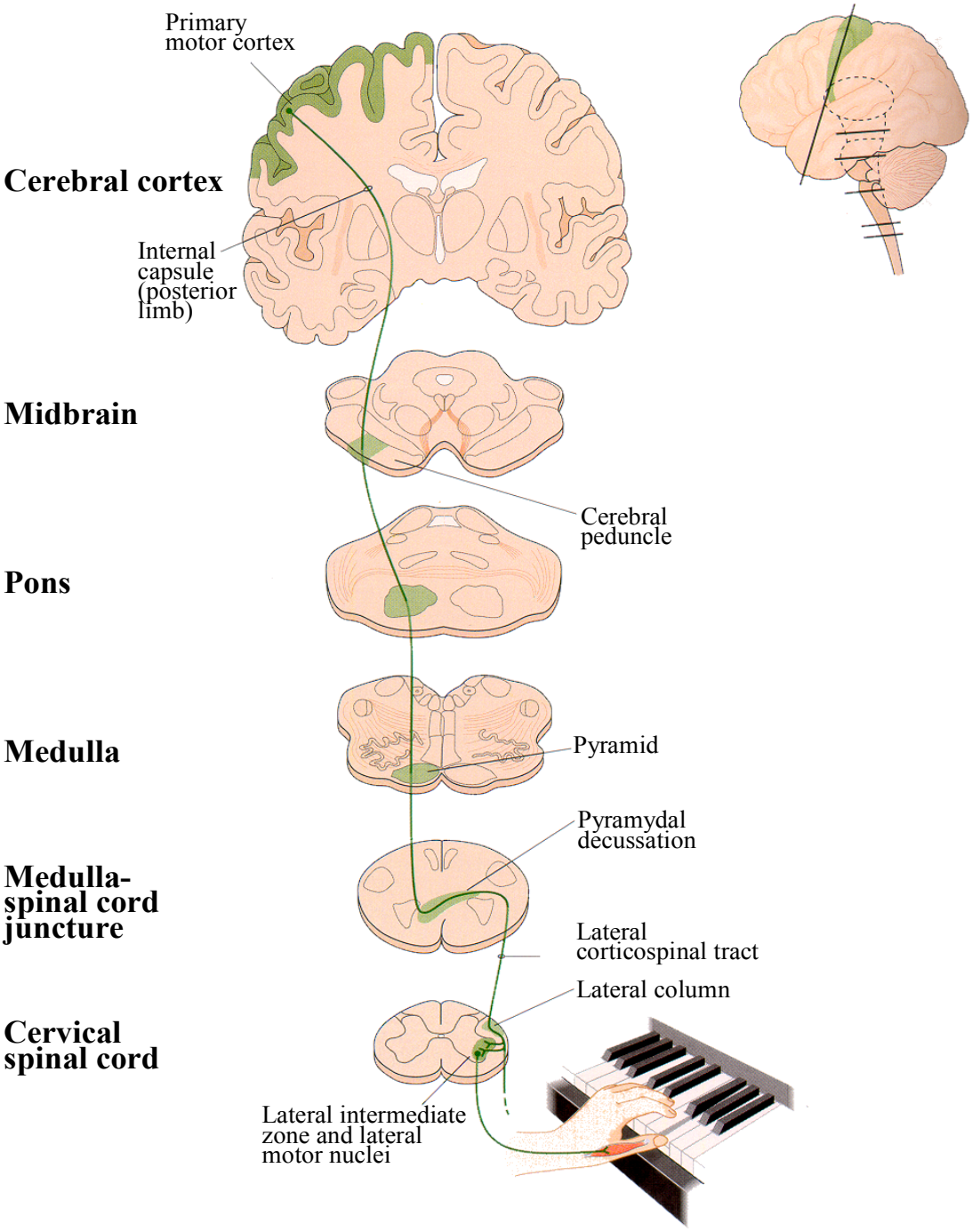

Figure 10: Schematic illustration of the main component of the CST. The origin of the control of voluntary movements mainly mediated by direct CM connections. The green line represents the crossed corticospinal pathway throughout its course from its cortical origin till the lateral intermediate zone and lateral motor nuclei.

At their level of termination, axons of the CST leave the dorsolateral funiculus and establish connections with spinal motoneurons. In primates, a portion of these fibers make direct contact with motoneurons. Other fibers leave the CS tract as early as in the pyramids or even rostral to it to innervate the cranial nerve motor nuclei or other brain stem nuclei. These fibers are known as the *corticobulbar tract* (Holstege, 1991; Kuypers, 1981).

Most CS fibres are myelinated (Ralston and Ralston, 1985). In total the CST tract consists of approximately one million nerve fibres in humans and of about four-hundred thousand in the macaque monkey.

CS fibers project to all of the spinal segments and some have a distinct termination pattern onto motoneurons. In macaque monkeys, the CST terminates most heavily in the medial part of Rexed lamina VI of the spinal grey matter where interneurons of various types are located (Fig.11) (Armand et al., 1997; Kuypers, 1981; Peschanski and Ralston, 1985).

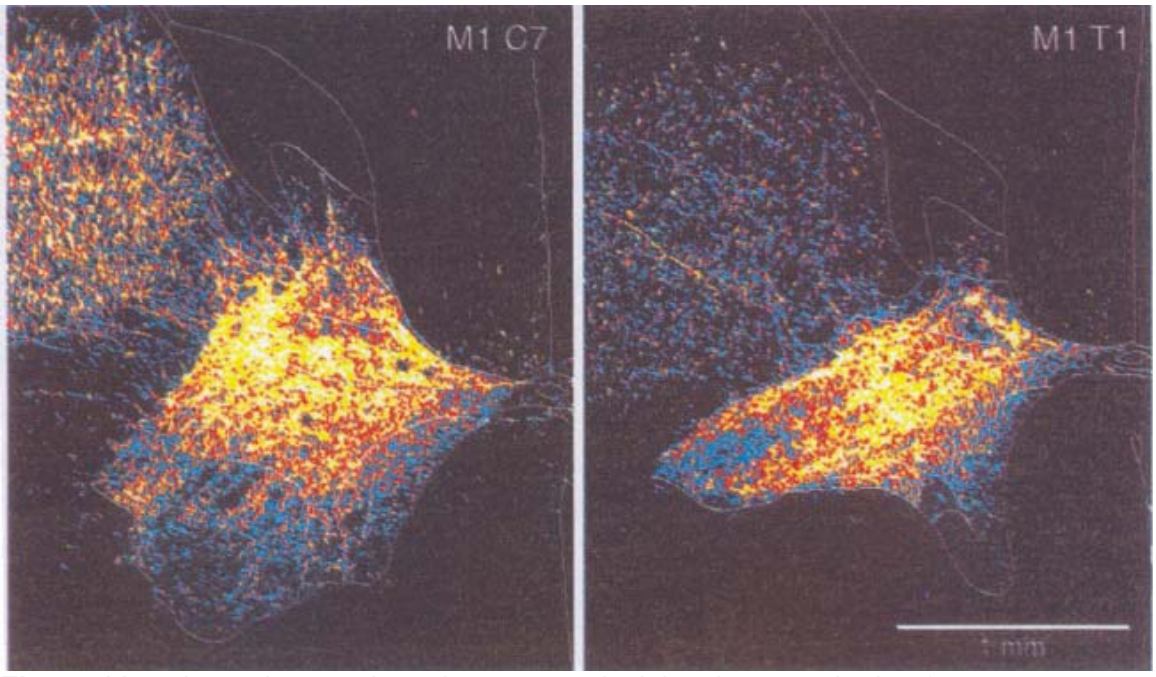

Figure 11 : Photomicrographs taken at cervical level C7 and Th1 from a macaque monkey illustrating the projections patterns of the CST from M1 WGA-HRP injections. At both levels the CST terminates mainly within the intermediate layer of the spinal gray. However within the hand motor nuclei the density of labeled fibers arising from SMA was much lower than the density of labeled fibers arising from M1 (Dum and Strick, 1996).

As a result of selectively sectioning the CST at the level of the pyramids in the nonhuman primate is the permanent deterioration in the ability to make fine finger, independent movement of the digits (Tower, 1940); the loss of contractual hand orientation (Denny-Brown, 1966) and the degree of recovery depending on several factors such as lesion size and age of the animal (Hepp-Reymond, 1988). These severe disturbances in monkeys following pyramidotomy probably reflect the increased importance of the direct cortico-motoneural connections for individual digit control. The observation that digital control is impaired also in the animals such as the cat, rat and hamster in which CM connections are few or absent, allows to suggest that the effects seen in the primate do not involve the CM projections alone.

The medial termination pattern onto interneurons as seen in Fig 11 emphasizes the importance of indirect control which parallels the direct CM connections. The importance of indirect motor control can be illustrated in the cat having no direct CM projections. In this species a system has been described of short propriospinal neurons located in the cervical spinal cord. These interneurons project monosynsaptically to the motoneurons in the forelimb segments and receive convergent inputs from the cortico-, rubro-, reticulo- and tectospinal descending pathways, as well as afferent input from forelimb nerves. At least in the cat, this propriospinal systems stands as an integrator between cortex and the motoneurons for cortical motor command (Alstermark and Ohlson, 2000; Illert et al., 1977). Similar experiments carried out from two different groups in macaque monkeys showed that if propriospinal neurons similar to those in the cat are present in the macaque monkey, the contribution of this system to the normal control of the forelimb is questionable (Lemon et al., 2004; Maier et al., 1998; Maier et al., 2002). In a recent review it has been pointed out that these pathways could gain importance as soon as other systems fail to transfer the cortical information such following an incomplete SCI (Jankowska and Edgley, 2006).

2.3.2 The rubrospinal tract

The mammalian red nucleus (RN) processes sensorimotor information from the frontoparietal cortex and the cerebellar cortex. It transmits the transformed signals back to the cerebellum through the rubroolivary projection and to the spinal cord through the rubrospinal (RS) neurons. In the macaque these two efferent pathways originate from cytoarchitecturally distinct areas, a parvocellular part (RNp) located in the rostral part of the nucleus and a magnocellular part (RNm) located caudally.

The RS pathway is a crossed pathway and sends direct fibres, mainly within the dorsolateral funiculus towards motoneuron cell groups in the ventral horn of the cervical enlargement of the spinal cord (Fig. 12). The RS fibers are about a 100 x less numerous than the corticospinal fibres in nonhuman primates (Holstege et al., 1988; Ralston et al., 1988). Functionally, the RS tract is implicated in control of hand movements in parallel to the CS tract, in particular during coordinated, whole limb movements.

The lower number of RS fibers compared to CS fibers (100 x less) may be the main reason why the rubrospinal system in monkeys cannot completely compensate for the loss of direct cortical control on the distal musculature. Indeed, in macaque monkeys subjected to pyramidotomy, a specific lesion of the CS system which spares the rubrospinal pathway a drastic loss of dexterity on the side of the lesion is the consequence. The major difference compared with a hemisection, which destroys the corticospinal and rubrospinal pathways, is the fact that a more rapid recovery of hand function follows.

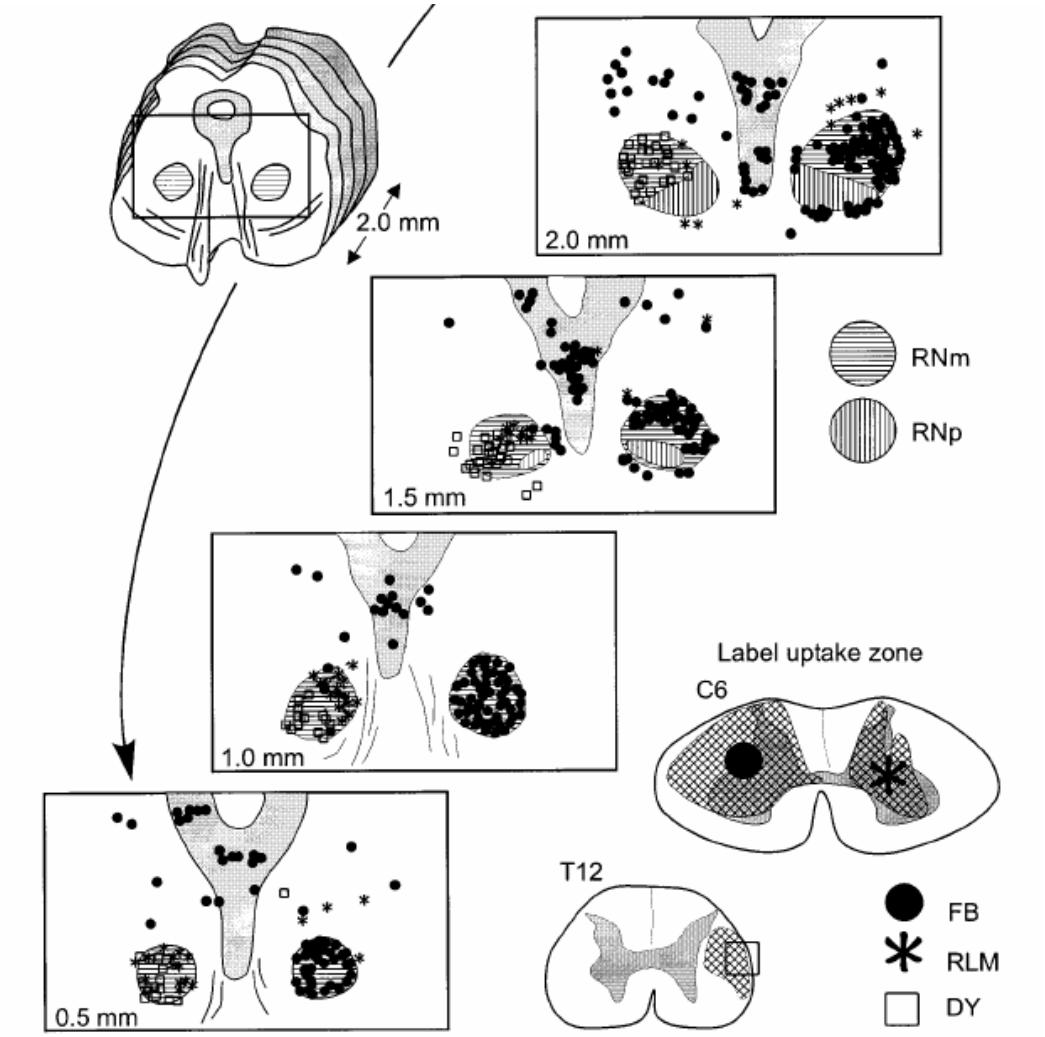

Figure 12: The injection of three different retrograde tracers within the spinal cord of macaque monkeys revealed the distribution of neurons retrograde stained in the RN. The amount of labeled neurons differed within the main two part of the RN: The pars magnocellularis RNm received most whereas very few in the pars parvocellularis RNp (Burman et al., 2000; Burman et al., 2000).

2.3.3 Effects of lesions to the corticospinal system

Following spinal cord injury, transected axons of the adult mammalian central nervous system (CNS) fail to re-grow. Immediately after onset of injury, a series of structural changes proximal and distal to the point of transection occurs. Whereas the distal stump of the axon degenerates, corresponding to the so-called Wallerian degeneration, the proximal stump of the axon dies back (i.e. retracts) on a distance of several hundreds microns, as observed for instance in the corticospinal tract of mice (Kerschensteiner et al., 2005). A typical feature of the transected axonal stumps proximal to lesion is the formation of a terminal retraction bulb (Kao et al., 1977). Two opposing forces, acting simultaneously, may account for the formation of retraction terminal bulbs: 1) the pressure of the axoplasmic flow towards the cut ends of the transected axons and 2) interferences of structural changes within the axon and myelin sheaths (Kao et al., 1977). Once a terminal retraction bulb is formed, the axon becomes stabilized and ceases to retract but fails to re-grow (Kalil and Schneider, 1975).

Up to present the question whether axotomized neurons die is a matter of debate. Some studies targeting the corticospinal (CS) tract following pyramidotomy or spinal cord lesion, revealed a significant loss of corticospinal neurons (Holmes and May, 1909; Levin and Bradford, 1938; Pernet and Hepp-Reymond, 1975), whereas other studies concluded that most CS neurons survived (Tower 1940). In a recent study in monkeys based on a specific marker of pyramidal neurons (SMI-32, including the CS neurons), after hemi-section of the cervical cord, there was evidence for a survival of the axotomized CS neurons, but their soma shrank as compared to the population of intact CS neurons in the opposite hemisphere (Wannier et al., 2005).

Lesions to the CST either at the pyramids or at cervical level lead to behavioral deficits in the non-human primate. However, a major difference between these two approaches to lesion the CST tract has to be kept in mind: a pyramidotomy interrupts selectively the CST whereas a cervical lesion represents a more complex injury situation. A cervical section impacts on both descending and ascending projections, such as it affects the crossed CS

projections from the opposite motor cortex and the uncrossed CS projections from the ipsilateral motor cortex, as well as other descending tracts like the rubrospinal and the reticulospinal tracts. All ascending sensory information and the propriospinal system are affected as well, though not the uncrossed CS axons coming from the contralesional motor cortex.

The behavioral consequences following bilateral pyramidotomy are a loss of posture and limb movements which after 6-8 months post injury return to normal. However, control over independent finger movements is only little recovered (Fig. 11) (Hepp-Reymond and Wiesendanger 72). Animals with unilateral pyramidal lesions show no impairment of the hand contralateral to the lesion, while the ipsilateral hand exhibited an improved recovery than monkeys subjected to bilateral pyramidal lesions (Lawrence and Kuypers, 1968). These results led to the conclusion that CM connections to the cervical cord are responsible for the control of voluntary movements.

Following a unilateral lesion of the midcervical cord interrupting the dorsolateral funiculus, lateral and ventral columns, macaque monkeys recover rapidly their ability to use their hand successfully during a prehension task demanding a precision grip. The degree of recovery of manual dexterity depends on lesion level and lesion size (Freund et al., 2006; Galea and Darian-Smith, 1994; Galea and Darian-Smith, 1995). In contrast to the bilateral pyramidotomy a hemisection spares the undecussated descending CST fibers which constitute up to 10% of the total amount of CS axons (Rouiller et al., 1996). Recently it has been proposed that these spared fibers may be responsible for the marked recovery of manual dexterity (Jankowska and Edgley, 2006).

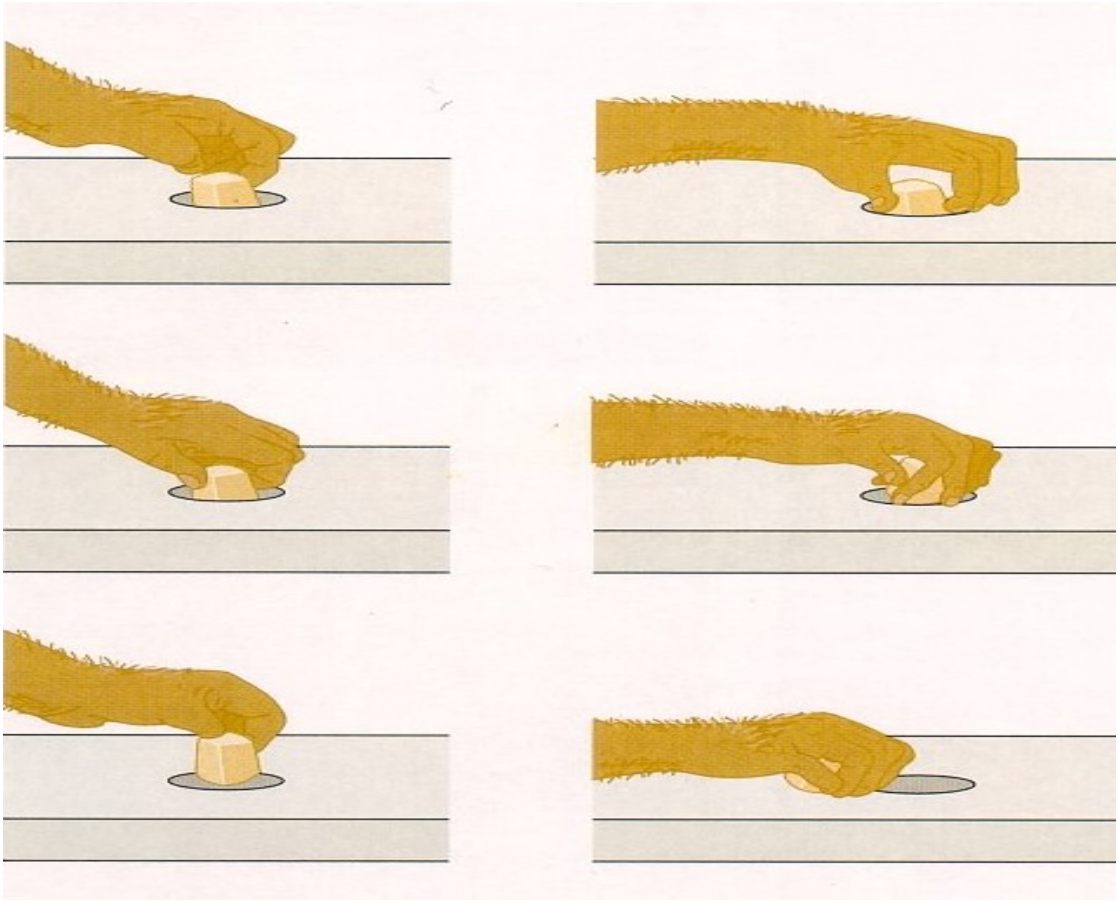

Figure 13: On the left: Macaque monkey applying the precision grip, the opposition between the tip of the index finger and the tip of the thumb. This has been an object for investigating the independent control of finger movement and the ones of the upper limbs. On the right: Immediately following a section of the corticospinal tract the monkey has lost its capacity of independent finger movement and the skill of exerting the precision grip. Instead it can only remove food from the slot by grabbing with the whole hand (power grip).

2.4 Aims of the present thesis

The aim of this thesis was to prove the principle whether the anti-Nogo-A antibody treatment strategy leads to axonal regeneration and functional recovery in non-human adult primates subjected to a partial section of the spinal cord.
In particular, to asses the behavioral evolution of the anti-Nogo-A antibody treatment the following questions were addressed:

1) Does the anti-Nogo-A antibody treatment lead to enhanced recovery of manual dexterity as assessed by using a battery of tasks demanding the execution of the precision grip and other movements such as a ballistic arm movement and hindlimb grasping?

2) Does the infusion of the antibody over a period of four weeks trigger inflammatory responses?

3) Does the anti-Nogo-A antibody treatment induce chaotic sprouting leading to negative side effects, such as allodynia?

The anterograde labeling of CS axons originating from the contralesional hemisphere, allowed us to address the following issues:

4) Does the proximal part of the axotomized CS axons retract from the lesion? If yes, in what proportion of CS axotomized axons does such a retraction occur and what is the distance of retraction?

5) Does anti-Nogo-A antibody treatment prevent such retraction of CS axons?

6) Do some axotomized CS axons attempt to re-approach and eventually enter the lesion? If yes, does the anti-Nogo-A antibody treatment make such attempts more successful?

7) Above the cervical lesion, do the axotomized CS axons sprout, giving rise to collaterals medially into the grey matter?

8) Do axotomized CS axons grow around the injury on spared tissue bridges to re-innervate the denervated zone caudal to the lesion?

9) Do axotomized CS and RS neurons die or atrophy? If so, can this be prevented when Nogo-A is neutralized?

3 Material and Methods

Overview of the experimental protocol

The experimental events from the point of time when the monkey was habituated to enter the primate chair/cage to the time of sacrifice, ranged between eight up to twenty months. Detailed information concerning the individual steps is provided in the Material and Method section of the chapters 2, 3, 4, 5 and 6.

In short 16 young adult macaque monkeys (Macaca mulatta and fascicularis; 3.5 to 6.9 years at sacrifice), of either sex were used for these experiments. Retention and experimental protocol were in accordance with the Swiss federal rules for animal protection and controlled by the local veterinary authorities. During the first couple of weeks the monkeys were habituated to the animal housekeeping environment and to their room-mates. Usually four monkeys of one sex were housed in a detention room of 13 m^3 (245cm x 220cm x 240cm) in size. The retention room contained two smaller cages into which the monkeys were transferred by the animal room keepers at 7 am during weekdays. Once habituated to their new environment, the monkeys were trained for a subsequent transfer into a primate chair or cage. This usually took two to four weeks. In the further course, the monkeys were then brought into the laboratories in which they were presented with a set of behavioural tasks. At the beginning all monkeys were habituated to perform a unimanual dexterity task the so-called “modified Brinkman board test”, with each of the two hands. Monkeys were trained on a five day per week basis during 14-60 days. Then other tests assessing additional aspects of the manual dexterity (e.g. a test where the position of the hand during the prehension task had to be dynamically controlled, the capacity to perform rapid catching movements or the ability to grasp using the hindlimbs) were introduced selectively to several monkeys (see **Chapters 2 and 4**). Scoring started after the monkeys were habituated to all tests. At least 20-40 sessions were taken to establish the level of the pre-lesion baseline.

Then, a unilateral cervical spinal cord section was introduced under aseptic conditions in the fully anesthetized animal between the 7th and 8th cervical spinal cord segments. Immediately following the transsection, an osmotic pump containing either a control antibody or an anti-Nogo-A antibody was placed under the skin and delivered, via a catheter ending intrathecally a few millimeters above the lesion, the antibody during a period of four weeks. Following surgery the monkeys were placed separately in a cage to allow better conditions for recovery than in the usual group housing with other monkeys. After 30 to 60 minutes the monkeys woke up and were rapidly able to sit upright in the cage despite their paresis on the ipsilesional side. During the next 2-5 days the monkeys regained their mobility to such extent that they were again placed together with the other monkeys. Post-lesion data acquisition started at the same time and depending on the lesion size the monkeys started to recover their manual dexterity within the first four weeks. Generally the time course of recovery for the individual monkeys overlapped, reaching stable level of performance at 60 to 80 days. When the acquisition of behavioral data was finished, biotinylated dextran amine (BDA), an anterograde tracer, was injected in the contralesional motor cortex under aseptic conditions in the fully anesthetized animal. Another tracer (Dextran Fluresocein) was injected into the ipsilesional motor cortex. A survival period of approximately 60-80 days was used to allow optimal labeling of the descending corticospinal tract within the spinal cord.

At the end of the survival period, the animals were sacrificed by a lethal injection of pentobarbital and perfused transcardiacally. The perfusion was continued with 4% paraformaldehyde solution in phosphate buffer and then with solutions of the same fixative containing increasing concentrations of sucrose. The brain and spinal cord were dissected and placed in a 30% solution of sucrose for cryoprotection for a few days. Frozen sections (50 µm thick) of the brain were cut in the frontal plane whereas frozen sections (50 µm thick) of the cervical cord (approximately the segments C6-Th2) were cut in the parasagittal longitudinal plane and collected in three series for later histological processing. Additional material originating from segments placed just rostral and caudal to this tissue were cut in the frontal plane at 50 µm thick and collected in three series. BDA and Dextran-Fluorescein staining was

revealed in two series of spinal cord sections. The third series of spinal cord sections were immunohistochemically processed using the marker SMI-32, an antibody recognizing a non-phosphorylated form of neurofilaments.

The lesion site was reconstructed from camera lucida drawings of individual consecutive SMI-32 labeled or BDA stained sections of the cervical cord. An alignment of the drawings allowed reconstruction of the location and extent of the lesion on a frontal view of the cord.

Morphometrical analysis was conducted using Neurolucida® software. BDA labeled sections of the cervical cord were analyzed for regenerative sprouting and the neurons of the primary motor cortex (M1) and of the magnocellular part of the red nucleus were analyzed for soma surface area using the SMI-32 stained brain tissue.

References

Dietz V. 1997. Locomotor recovery after spinal cord injury. Trends Neurosci 20:346-347.

Dietz V, Wirz M, Colombo G, Curt A. 1998. Locomotor capacity and recovery of spinal cord function in paraplegic patients: a clinical and electrophysiological evaluation. Electroencephalogr Clin Neurophysiol Electromyogr Motor Control 109:140-153.

Dietz V. 1995. Locomotor training in paraplegic patients. Ann Neurol 38:965.

Kalil K, Reh T. 1982. A light and electron microscopic study of regrowing pyramidal tract fibers. J Comp Neurol 211:265-275.

Chen R, Cohen LG, Hallett M. 2002. Nervous system reorganization following injury. Neuroscience 111:761-773.

Kapfhammer JP, Schwab ME. 1994. Inverse patterns of myelination and GAP-43 expression in the adult CNS: Neurite growth inhibitors as regulators of neuronal plasticity? J Comp Neurol 340:194-206.

David S, Aguayo AJ. 1981. Axonal elongation into peripheral nervous system "bridges" after central nervous system injury in adult rats. Science 214:931-933.

David S, Aguayo AJ. 1981. Axonal elongation into peripheral nervous system "bridges" after central nervous system injury in adult rats. Science 214:931-933.

Schnell L, Schneider R, Kolbeck R, Barde Y-A, Schwab ME. 1994. Neurotrophin-3 enhances sprouting of corticospinal tract during development and after adult spinal cord lesion. Nature 367:170-173.

Tobias CA, Shumsky JS, Shibata M, Tuszynski MH, Fischer I, Tessler A, Murray M. 2003. Delayed grafting of BDNF and NT-3 producing fibroblasts into the injured spinal cord stimulates sprouting, partially rescues axotornized red nucleus neurons from loss and atrophy, and provides limited regeneration. Experimental Neurology 184:97-113.

Weidner N, Blesch A, Grill RJ, Tuszynski MH. 1999. Nerve growth factor-hypersecreting Schwann cell grafts augment and guide spinal cord axonal growth and remyelinate central nervous system axons in a phenotypically appropriate manner that correlates with expression of L1. J Comp Neurol 413:495-506.

Giehl KM, Tetzlaff W. 1996. BDNF and NT-3, but not NGF, prevent axotomy-induced death of rat corticospinal neurons *in vivo*. Eur J Neurosci 8:1167-1175.

Grill R, Murai K, Blesch A, Gage FH, Tuszynski MH. 1997. Cellular delivery of neurotrophin-3 promotes corticospinal axonal growth and partial functional recovery after spinal cord injury. J Neurosci 17:5560-5572.

Ramer MS, Priestley JV, McMahon SB. 2000. Functional regeneration of sensory axone into the adult spinal cord. Nature 403:312-316.

Lu P, Yang H, Jones LL, Filbin MT, Tuszynski MH. 2004. Combinatorial therapy with neurotrophins and cAMP promotes axonal regeneration beyond sites of spinal cord injury. J Neurosci 24:6402-6409.

Dergham P, Ellezam B, Essagian C, Avedissian H, Lubell WD, McKerracher L. 2002. Rho signaling pathway targeted to promote spinal cord repair. J Neurosci 22:6570-6577.

Fournier AE, Takizawa BT, Strittmatter SM. 2003. Rho kinase inhibition enhances axonal regeneration in the injured CNS. J Neurosci 23:1416-1423.

David S, Lacroix S. 2003. Molecular approaches to spinal cord repair. Annu Rev Neurosci 26:411-440.

Caroni P, Savio T, Schwab ME. 1988. Central nervous system regeneration: oligodendrocytes and myelin as non-permissive substrates for neurite growth. Prog Brain Res 78:363-370.

Schwab ME, Bartholdi D. 1996. Degeneration and regeneration of axons in the lesioned spinal cord. Physiol Rev 76:319-370.

Chen MS, Huber AB, Van der Haar ME, Franck M, Schnell L, Spillmann AA, Christ F, Schwab ME. 2000. Nogo-A is a myelin-associated neurite outgrowth inhibitor and an antigen for monoclonal antibody IN-1. Nature 403:434-438.

Filbin MT. 2003. Myelin-associated inhibitors of axonal regeneration in the mammalian CNS. Nat Rev Neurosci 4:703-713.

Schnell L, Schwab ME. 1990. Axonal regeneration in the rat spinal cord produced by an antibody against myelin-associated neurite growth inhibitors. Nature 343 no 6255:269-272.

Li S, Strittmatter SM. 2003. Delayed systemic Nogo-66 receptor antagonist promotes recovery from spinal cord injury. J Neurosci 23:4219-4227.

Bradbury EJ, Moon LDF, Popat RJ, King VR, Bennett GS, Patel PN, Fawcett JW, McMahon SB. 2002. Chondroitinase ABC promotes functional recovery after spinal cord injury. Nature 416:636-640.

Bregman BS, Kunkel-Bagden E, Schnell L, Dai HN, Gao D, Schwab ME. 1995. Recovery from spinal cord injury mediated by antibodies to neurite growth inhibitors. Nature 378:498-501.

Courtine G, Bunge MB, Fawcett JW, Grossman RG, Kaas JH, Lemon R, Maier I, Martin J, Nudo RJ, Ramon-Cueto A, Rouiller EM, Schnell L, Wannier T, Schwab ME, Edgerton VR. 2007. Can experiments in nonhuman primates expedite the translation of treatments for spinal cord injury in humans? Nat Med 13:561-566.

Goldberg JL, Barres BA. 2000. Nogo in nerve regeneration. Nature 403:369-370.

Huber AB, Weinmann O, Brösamle C, Oertle T, Schwab ME. 2002. Patterns of Nogo mRNA and protein expression in the developing and adult rat and after CNS lesions. J Neurosci 22:3553-3567.

Huber AB, Weinmann O, Brösamle C, Oertle T, Schwab ME. 2002. Patterns of Nogo mRNA and protein expression in the developing and adult rat and after CNS lesions. J Neurosci 22:3553-3567.

Fournier AE, GrandPré T, Strittmatter SM. 2001. Identification of a receptor mediating Nogo-66 inhibition of axonal regeneration. Nature 409:341-346.

Oertle T, Van der Haar ME, Bandtlow CE, Robeva A, Burfeind P, Buss A, Huber AB, Simonen M, Schnell L, Brösamle C, Kaupmann K, Vallon R, Schwab ME. 2003. Nogo-A inhibits neurite outgrowth and cell spreading with three discrete regions. J Neurosci 23:5393-5406.

GrandPré T, Nakamura F, Vartanian T, Strittmatter SM. 2000. Identification of the NOGO inhibitor of axon regeneration as a reticulon protein. Nature 403:439-444.

Josephson A, Widenfalk J, Widmer HW, Olson L, Spenger C. 2001. NOGO mRNA expression in adult and fetal human and rat nervous tissue and in weight drop injury. Exp Neurol 169:319-328.

Wang KC, Koprivica V, Kim JA, Sivasankaran R, Guo Y, Neve RL, He Z. 2002. Oligodendrocyte-myelin glycoprotein is a Nogo receptor ligand that inhibits neurite outgrowth. Nature 417:941-944.

McGee AW, Strittmatter SM. 2003. The Nogo-66 receptor: focusing myelin inhibition of axon regeneration. Trends in Neurosciences 26:193-198.

Mi S, Lee X, Shao Z, Thill G, Ji B, Relton J, Levesque M, Allaire N, Perrin S, Sands B, Crowell T, Cate RL, McCoy JM, Pepinsky RB. 2004. LINGO-1 is a component of the Nogo-66 receptor/p75 signaling complex. Nat Neurosci 7:221-228.

Niederöst B, Oertle T, Fritsche J, McKinney RA, Bandtlow CE. 2002. Nogo-A myelin-associated glycoprotein mediate neurite growth inhibition by antagonistic regulation of RhoA and Rac1. J Neurosci 22:10368-10376.

Woolf CJ, Bloechlinger S. 2002. It takes more than two to NOGO. Science 297:1132-1134.

Brösamle C, Huber AB, Fiedler M, Skerra A, Schwab ME. 2000. Regeneration of lesioned corticospinal tract fibers in the adult rat induced by a recombinant, humanized IN-1 antibody fragment. J Neurosci 20:8061-8068.

Brösamle C, Huber AB, Fiedler M, Skerra A, Schwab ME. 2000. Regeneration of lesioned corticospinal tract fibers in the adult rat induced by a recombinant, humanized IN-1 antibody fragment. J Neurosci 20:8061-8068.

Brösamle C, Huber AB, Fiedler M, Skerra A, Schwab ME. 2000. Regeneration of lesioned corticospinal tract fibers in the adult rat induced by a recombinant, humanized IN-1 antibody fragment. J Neurosci 20:8061-8068.

Thallmair M, Metz GAS, Z'Graggen WJ, Raineteau O, Kartje GL, Schwab ME. 1998. Neurite growth inhibitors restrict plasticity and functional recovery following corticospinal tract lesions. Nature Neurosci 1:124-131.

Z'Graggen WJ, Metz GAS, Kartje GL, Thallmair M, Schwab ME. 1998. Functional recovery and enhanced corticofugal plasticity after unilateral pyramidal tract lesion and blockade of myelin-associated neurite growth inhibitors in adult rats. J Neurosci 18:4744-4757.

Raineteau O, Fouad K, Bareyre FM, Schwab ME. 2002. Reorganization of descending motor tracts in the rat spinal cord. Eur J Neurosci 16:1761-1771.

Raineteau O, Fouad K, Noth P, Thallmair M, Schwab ME. 2001. Functional switch between motor tracts in the presence of the mAb IN-1 in the adult rat. Proceedings of the National Academy of Sciences of the United States of America 98:6929-6934.

Raineteau O, Fouad K, Bareyre FM, Schwab ME. 2002. Reorganization of descending motor tracts in the rat spinal cord. Eur J Neurosci 16:1761-1771.

Raineteau O, Fouad K, Bareyre FM, Schwab ME. 2002. Reorganization of descending motor tracts in the rat spinal cord. Eur J Neurosci 16:1761-1771.

Raineteau O, Fouad K, Bareyre FM, Schwab ME. 2002. Reorganization of descending motor tracts in the rat spinal cord. Eur J Neurosci 16:1761-1771.

Fouad K, Volker D, Schwab ME. 2001. Improving axonal growth and functional recovery after experimental spinal cord injury by neutralizing myelin associated inhibitors. Brain Res Rev 36:204-212.

Brösamle C, Huber AB, Fiedler M, Skerra A, Schwab ME. 2000. Regeneration of lesioned corticospinal tract fibers in the adult rat induced by a recombinant, humanized IN-1 antibody fragment. J Neurosci 20:8061-8068.

Schwab ME. 2004. Nogo and axon regeneration. Curr Opin Neurobiol 14:118-124.

Prinjha R, Moore SE, Vinson M, Blake S, Morrow R, Christie G, Michalovich D, Simmons DL, Walsh FS. 2000. Inhibitor of neurite outgrowth in humans. Nature 403:383-384.

Spillmann AA, Amberger VR, Schwab ME. 1997. High molecular weight protein of human central nervous system myelin inhibits neurite outgrowth: an effect which can be neutralized by the monoclonal antibody IN-1. Eur J Neurosci 9:549-555.

Weinmann O, Schnell L, Ghosh A, Montani L, Wiessner C, Mir A, Schwab ME. 2006. Intrathecally infused antibodies against Nogo-A penetrate the rat CNS and downregulate the endogenous Neurite growth inhibitor Nogo-A. In.

Fouad K, Klusman I, Schwab ME. 2004. Regenerating corticospinal fibers in the Marmoset (*Callitrix jacchus*) after spinal cord lesion and treatment with the anti-Nogo-A antibody IN-1. Eur J Neurosci 20:2479-2482.

Lawrence DG, Hopkins DA. 1976. The development of motor control in the Rhesus monkey: evidence concerning the role of corticomotoneuronal connections. Brain 99:235-254.

Porter JD, Guthrie BL, Sparks DL. 1985. Selective retrograde transneuronal transport of wheat germ agglutinin-conjugated horseradish peroxidase in the oculomotor system. Exp Brain Res 57:411-416.

Porter R. 1987. Functional studies of motor cortex. In: Bock G, editor. Motor ares of the cerebral cortex. Chichester: CIBA Foundation, J. Wiley and Sons. p 83-97.

Lemon RN. 1993. Cortical control of the primate hand. Exp Physiol 78:263-301.

Holstege G. 1991. Descending motor pathways and the spinal motor system: limbic and non-limbic components. Prog Brain Res 87:307-403.

Ralston DD, Ralston HJI. 1985. The terminations of corticospinal tract axons in the macaque monkey. J Comp Neurol 242:325-337.

Jenny AB, Inukai J. 1983. Principles of motor organization of the monkey cervical spinal cord. J Neurosci 3:567-575.

Phillips CG. 1971. Evolution of the corticospinal tract in primates with special reference to the hand. In: Proceedings of the Third International Congress of Primatology, Vol 2. Basel: Karger. p 2-23.

Kuypers HGJM. 1981. Anatomy of descending pathways. In: Brooks VB, editor. Handbook of Physiology (The Nervous System), vol. II, part 1. Bethesda, MD: Am. Physiol. Soc. p 597-666.

Galea MP, Darian-Smith I. 1994. Multiple corticospinal neuron populations in the macaque monkey are specified by their unique cortical origins, spinal terminations, and connections. Cereb Cortex 4:166-194.

Galea MP, Darian-Smith I. 1995. Postnatal maturation of the direct corticospinal projections in the macaque monkey. Cereb Cortex 5:518-540.

Kuypers HGJM. 1981. Pyramidal Tract. In: Handbook APS. p 1018-1020.

Humphrey DR, Corrie WS. 1978. Properties of pyramidal tract neuron system within a functionally. J Neurophysiol 41:216-243.

Porter R. 1981. Internal organization of the motor cortex for input-output arrangements. Handbook Physiol (Section 1) 2 (II):1063-1081.

Asanuma H. 1981. The pyramidal tract. In: Brooks VB, editor. Handbook of Physiology (The Nervous System), vol. II. Bethesda, MD: Am. Physiol. Soc. p 703-733.

Rouiller EM, Moret V, Tanné J, Boussaoud D. 1996. Evidence for direct connections between the hand region of the supplementary motor area and cervical motoneurons in the macaque monkey. Eur J Neurosci 8:1055-1059.

Lacroix S, Havton LA, McKay H, Yang H, Brant A, Roberts J, Tuszynski MH. 2004. Bilateral corticospinal projections arise from each motor cortex in the macaque monkey: A quantitative study. J Comp Neurol 473:147-161.

Phillips CG. 1979. The cortical.Spinal pathway of primates. In: Asanuma H, Wilson VJ, editors. Integration in the nervous system. Tokyo: p 263-278.

Galea MP, Darian-Smith I. 1997. Corticospinal projection patterns following unilateral section of the cervical spinal cord in the newborn and juvenile macaque monkey. J Comp Neurol 381:282-306.

Armand J, Olivier E, Edgley SA, Lemon RN. 1997. Postnatal development of corticospinal projections from motor cortex to the cervical enlargement in the macaque monkey. J Neurosci 17:251-266.

Peschanski M, Ralston HJI. 1985. Light and electron microscopic evidence of transneuronal labeling with WGA-HRP to trace somatosensory pathways to the thalamus. J Comp Neurol 236:29-41.

Dum RP, Strick PL. 1996. Spinal cord terminations of the medial wall motor areas in macaque monkeys. J Neurosci 16:6513-6525.

Tower SS. 1940. Pyramidal lesion in the monkey. Brain 63:36-90.

Denny-Brown D. 1966. The Cerebral Control of Movements. Liverpool: Liverpool University Press.

Hepp-Reymond M-C. 1988. Functional organization of motor cortex and its participation in voluntary movements. In: Seklis HD, Erwin J, editors. Comparative Primate Biology, Vol 4: Neurosciences. New York: Alan R. Liss. p 501-624.

Illert M, Lundberg A, Tanaka R. 1977. Integration in descending motor pathways controlling the forelimb in the cat. 3. Convergence on propriospinal neurones transmitting disynaptic excitation from the corticospinal tract and other descending tracts. Exp Brain Res 29:323-346.

Alstermark B, Ohlson S. 2000. Origin of corticospinal neurones evoking disynaptic excitation in forelimb motoneurones mediated via C3-C4 propriospinal neurones in the cat. Neuroscience Research 37:91-100.

Maier MA, Illert M, Kirkwood PA, Nielsen J, Lemon RN. 1998. Does a C3-C4 propriospinal system transmit corticospinal excitation in the primate? An investigation in the macaque monkey. J Physiol (Lond) 511:191-212.

Maier MA, Armand J, Kirkwood PA, Yang HW, Davis JN, Lemon RN. 2002. Differences in the corticospinal projection from primary motor cortex and supplementary motor area to macaque upper limb motoneurons: An anatomical and electrophysiological study. Cereb Cort 12:281-296.

Lemon RN, Kirkwood PA, Maier MA, Nakajima K, Nathan P. 2004. Direct and indirect pathways for corticospinal control of upper limb motoneurons in the primate. Prog Brain Res 143:263-279.

Jankowska E, Edgley SA. 2006. How can corticospinal tract neurons contribute to ipsilateral movements? A question with implications for recovery of motor functions. Neuroscientist 12:67-79.

Holstege G, Blok BF, Ralston DD. 1988. Anatomical evidence for red nucleus projections to motoneuronal cell groups in the spinal cord of the monkey. Neurosci Lett 95:97-101.

Ralston DD, Milroy AM, Holstege G. 1988. Ultrastructural evidence for direct monosynaptic rubrospinal connections to motoneurons in macaca mulatta. Neurosci Lett 95:102-106.

Burman K, Darian-Smith C, Darian-Smith I. 2000. Macaque red nucleus: Origins of spinal and olivary projections and terminations of cortical inputs. J Comp Neurol 423:179-196.

Burman K, Darian-Smith C, Darian-Smith I. 2000. Geometry of rubrospinal, rubroolivary, and local circuit neurons in the macaque red nucleus. J Comp Neurol 423:197-219.

Kerschensteiner M, Schwab ME, Lichtman JW, Misgeld T. 2005. *In vivo* imaging of axonal degeneration and regeneration in the injured spinal cord. Nature Med 11:572-577.

Kao CC, Chang LW, Bloodworth JMBJr. 1977. Electron microscopic observations of the mechanisms of terminal club formation in transected spinal axons. J Neuropathol Exp Neurol 36:140-156.

Kalil K, Schneider GE. 1975. Motor performance following unilateral pyramidal tract lesions in the hamster. Brain Res 100:170-174.

Pernet U, Hepp-Reymond M-C. 1975. Retrograde Degeneration der Pyramidenbahnzellen im motorischen Kortex beim Affen (Macaca fascicularis). Acta Anat (Basel)552-561.

Holmes GL, May WP. 1909. On the exact origin of the pyramidal tracts in man and other mammals. Brain 32:1-42.

Levin PM, Bradford FK. 1938. The exact origin of the cortico-spinal tract in the monkey. J Comp Neurol 68:411-422.

Wannier T, Schmidlin E, Bloch J, Rouiller EM. 2005. A unilateral section of the corticospinal tract at cervical level in primates does not lead to measurable cell loss in motor cortex. In.

Lawrence DG, Kuypers HGJM. 1968. The functional organization of the motor system. I. The effects of bilateral pyramidal lesions. Brain 91:1-14.

Freund P, Schmidlin E, Wannier T, Bloch J, Mir A, Schwab ME, Rouiller EM. 2006. Nogo-A-specific antibody treatment enhances sprouting and functional recovery after cervical lesion in adult primates. Nature Med 12:790-792.

Chapter 2

Nogo-A-specific antibody treatment enhances sprouting and functional recovery after cervical lesion in adult primates

This chapter has been adapted from an article originally published in Nature Medicine (Patrick Freund [1], Eric Sch midlin[1], Thierry Wannier [1], Jocelyne Bloch, Anis Mir, Martin E. Schwab an d Eric M. Rouiller; Nat Med 12:790-792, 2006)

(1) These authors contributed equally to the study.

1.1 Abstract

In rodents, after spinal lesion, neutralizing the neurite growth inhibitor Nogo-A promotes axonal sprouting and functional recovery. To evaluate this treatment in primates, twelve monkeys were subjected to cervical lesion. Manual dexterity recovery and corticospinal axonal sprouting were enhanced in anti-Nogo-A antibody treated monkeys as compared to control-antibody treated monkeys.

1.2 Introduct ion

Following injury, the adult mammalian central nervous system has limited capacity to repair. Transected nerve fibers do not spontaneously re-grow, due in part to myelin-associated neurite growth inhibitors such as Nogo-A(Oertle et al., 2003; Liebscher et al., 2005). After section of the corticospinal (CS) tract in adult rats, neutralizing Nogo-A with monoclonal antibodies leads to enhancement of axonal re-growth and compensatory sprouting, accompanied by increased motor recovery (Oertle and others, 2003; Schmidlin et al., 2004; Weinmann et al., 2006). The neutralization of Nogo-A represents a promising approach for therapy after lesion if its enhancement of functional recovery can be transposed to primates. First, the general organization of the CS system is similar in monkeys and humans, in contrast to the rat (Liu and Rouiller, 1999). Second, the CS system is involved, as far as the hands are concerned, in dexterous movements typical of primates (Kazennikov et al., 1994; Rouiller et al., 1996; Kazennikov et al., 1998). Behavioral assessment of manual dexterity is more pertinent in monkeys than rodents, the former being capable of fractionated dexterous movements of the fingers as humans. Third, neutralization of Nogo-A may not only favor sprouting of lesioned axons, but may induce unspecific growth of axons, causing undesired pathologies. The monkey model offers more possibilities than rodents to detect such changes of behavior.

Neutralization of Nogo-A was found to promote CS axonal sprouting in marmosets (Kermadi et al., 2000).

The aim of our study was to extend these anatomical data to macaque monkeys and assess whether neutralization of Nogo-A enhances motor recovery from spinal lesion in primates.

1.3 M aterial and Methods

Anti-Nogo-A antibodies

Two monoclonal antibodies (mAbs) against different sites of Nogo-A were used: the mouse **mAb 11C7** (Liebscher,T. *et al.*, 2005) was raised against a 18 amino acid peptide of rat Nogo-A (aa623 – 640), close to the most inhibitory region of the Nogo-A protein (Oertle,T. *et al.*, 2003), which cross-reacts with mouse and monkey Nogo-A. The second antibody used, **mAb hNogo-A** is directed against the Nogo-A specific region of the human Nogo-A sequence. Both antibodies recognize primate Nogo-A monospecifically on Western blots (Oertle,T. *et al.*, 2003). Both antibodies increase neurite outgrowth in vitro and penetrate deeply the CNS in vivo in monkeys (Weinmann,O. *et al.*, 2006). The antibodies were purified as IgGs and concentrated to 3.7-10 mg/ml in phosphate buffered saline (PBS).

Control antibodies

Purified IgG of a mouse mAb directed against wheat auxin (AMS Biotechnology, Oxon/UK) was used as control antibody.

Behavioral testing

The experiments were carried out on twelve (3-4 years old) rhesus (*Macaca mulatta*) or cynomolgus (*Macaca fascicularis*) monkeys of either sex (Table 1), ranging from 2.5 to 5.5 kg, in accordance to the Guide for the Care and Use of Laboratory Animals (ISBN 0-309-05377-3; 1996) and approved by local (Swiss) veterinary authorities. Monkeys were housed in our animal facilities in rooms of

12 m^3, each containing usually 4 monkeys free to move in the room and to interact among each others. In the morning (7 am), before behavioral testing, the animal keeper placed the monkeys in temporary cages for subsequent transfer to the primate chair by the experimenter. The monkeys had free access to water and were not food deprived. The rewards obtained during the behavioral tests represented the first daily access to food. After the tests, the monkeys received additional food (fruits, cereals). To reduce inter-animal variability, "pairs" of two monkeys were formed, placed under the responsibility of the same experimenter, and were subjected simultaneously to the same experimental protocol. Within each "pair" of monkey, one animal was treated with the anti-Nogo-A antibody while the other was treated with the control antibody. However, in most cases, this information was not available to the experimenter (“double-blind" procedure; see Table 1). The ID codes refer to individual monkeys, as indicated in Table 1, and comprise for sake of clarity in the text a “C” or a “A” at the fourth digit position, indicating whether the monkey was control-antibody treated or anti-Nogo-A treated, respectively. However, in the course of the experiments, the animals had different names from which the experimenter could not know which antibody was infused, at least for the “pairs” of monkeys in which the double blind procedure was applied (see Table 1). With the goal to reduce variability, part of the data are presented by comparing monkeys within a “pair” (see Fig. 1a, b, c; Fig. 2c, d; Fig. 4a2; Fig. 5a, b).

The manual dexterity of each hand was assessed in all lesioned monkeys with a finger prehension task (Fig. 1e), namely our so-called “modified Brinkman board” quantitative test, as described in detail earlier (Rouiller et al., 1998; Liu and Rouiller, 1999; Schmidlin et al., 2005). Briefly, tests were done using a Perspex board (10 cm x 20 cm) containing 50 randomly distributed wells, each filled with a food pellet at the beginning of the test. Twenty-five wells were oriented horizontally and twenty-five vertically. The dimension of the wells was 15 mm long, 8 mm wide and 6 mm deep. Retrieval of the food pellets required fractionated finger movements, consisting normally in a dexterous opposition of the index finger and the thumb, corresponding to the so-called "precision grip".

This manual prehension dexterity task was executed daily, alternatively with one or the other hand, 4 to 5 times per week for several months before and after the unilateral cervical cord lesion. A daily behavioral session typically lasted 60 minutes. The performance of each hand was videotaped. The behavioral scores were established by counting the number of wells from which the food pellets were successfully retrieved and brought to the mouth during 30 seconds (Fig. 1a-c). After the monkeys reached a stable level of performance (usually after 30-60 days), as indicated by a plateau of behavioral performance, 30-50 daily sessions were considered to establish a stable pre-lesion behavioral score. Functional recovery was expressed quantitatively as the ratio in percent of the plateau post-lesion score to the pre-lesion score.

Other behavioral tests were considered to assess further the motor capacity of the monkeys, such as the previously described natural "reach and grasp drawer" task (Kazennikov and others, 1994; Kermadi et al., 1997; Kazennikov and others, 1998; Kermadi et al., 1998; Wannier et al., 2002) (see also *www.unifr.ch/neuro/rouiller/motorcontcadre.htm*). Originally, this task was developed to study quantitatively bimanual coordination but, in the present case, it was executed only unimanually, testing one hand after the other. In addition to test grasping while the monkey retrieved the pellet from the drawer, the reach and grasp drawer task also allowed assessment of the precise timing for the reaching phase towards the drawer as well as the pulling phase during which the monkey has to produce enough force to open the drawer while holding firmly the drawer's knob. More specifically, in the present report, control-antibody treated- and anti-Nogo-A antibody treated-monkeys will be compared for the reaching and pulling components of the reach and grasp drawer task (Fig. 2a and Fig. 4a1,a2).

Motor capacity was tested further qualitatively using other tests performed on a weekly basis, at the end of a behavioral session. For instance, “Ballistic Arm Movements” (BAM test) were captured on video sequences while the monkey caught, using the two hands or sometimes one hand, pieces of food thrown by the experimenter from a distance of about 1 meter (see also

www.unifr.ch/neuro/rouiller/motorcontcadre.htm). In the BAM test, synchrony of the two hands was assessed as well as the pre-shaping ability to open the fingers before retrieving the approaching piece of food (Fig. 2b and Fig. 4b).

The capacity to grasp with the hindlimb was also tested qualitatively by presenting to the animal a large piece of food accessible only with one or the other foot, before transferring it from the hindlimb to the hand. This "hindlimb grasp" test thus allowed assessment of another motor function affected by the cervical lesion, but for which the corresponding motoneurons are located at a much greater distance from the lesion (lumbar cord) than motoneurons involved in manual capacity (Fig. 4c; see also *www.unifr.ch/neuro/rouiller/motorcontcadre.htm*).

Before each daily session, to follow the general health condition of the animal, the body weight was measured daily (except on week-end), in eight of the twelve monkeys involved in the present study (see Supplementary Figure 3f and Supplementary Note). The body weight analysis did not include the four initial monkeys Mk-AF, Mk-AS, Mk-CS and Mk-CC because their body weight was not systematically measured daily but only weekly.

Table 1: List of cervical cord lesioned monkeys included in the present study with identification code.

	Mk-CC	**Mk-CP**	**Mk-C G**	**Mk-CS**	**Mk-CB**	**Mk-CH**	**Mk- AS**	**Mk- AF**	**Mk- AP**	**Mk- AA**	**Mk- AM**	**Mk- AC**
species	mul.	fasc.	fasc.	mul.	fasc.	fasc.	mul.	mul.	fasc.	mul.	fasc.	fasc.
Antibody Treatment	**Control** antibody	**Control** antibody	**Control** antibody	**Control** antibody	**Control** antibody	**Control** antibody	**Anti-Nogo-A** (11C7)	**Anti-Nogo-A** (11C7)	**Anti-Nogo-A** (11C7)	**Anti-Nogo-A** (11C7)	**Anti-Nogo-A** (hNogo)	**Anti-Nogo-A** (hNogo)
"Double-blind" procedure	No	Yes	Yes	No	Yes	Yes	No	No	Yes	No	Yes	Yes
ICMS	Yes			Yes				Yes				
Hemi-section Extent (%)	**38**	**45 51 63 75**				**90 41 56 58 72 80**						**85**
Functional Recovery (%)	**83**	**83 90 22 78**				**53 100**		**57 99 88 96**				**100**
Completeness of dlf section	No	No (BDA)	**Yes*** (BDA)	**Yes**	**Yes** (BDA)	**Yes** (BDA)	No (BDA)	**Yes** (BDA)	**Yes** (BDA)	No (BDA)	**Yes** (BDA)	**Yes** (BDA)

Extent of dorsal column lesion (%)	0	14	39	47	31	72	9	2	48	100	74	44
Extent of CS and RS territory lesion (%)	61	64	70	87	93	100	48	73	100	57	100	100
Extent of ventral lesion (%)	30	24	0	19	38	60	12	0	8	43	5	100
Rostro-Caudal extent oflesion (in m)	505	632	617	925	578	715	488	783	880	1189	1075	1367
Normalized axon ar bor length (˜ m)	-	**171.3**	**48.8**	**- 36.7**		**8**	**- - 59.3**			**- 46**		**79.9**
Normalized nb.of swellings	-	**0.57 0.1**		-	**0.05 0.01**		-	-	**0.4**	-	**0.26 0.44**	
Nb. of BDA-labeled CS axons at C5	-	927	1005	-	1186	780	-	-	1250	-	1148	270
% of uncrossed CS axons at C5	-	10	4.5	-	9	3	-	-	5	-	5	7.0
Volume of BDA injected (in l)	24	24	24	13	20	20	22	25.5	24	40	19	20
Nb. of BDA injection sites	12	12	12	6	10	10	11	17	12	20	10	10
Survival time (in days)	21	78	70	35	78	62	72	71	81	74	69	64

At the time of the experiment, the monkeys had different names, not indicating whether the animal was infused with the control or the anti-Nogo-A antibody. New names were assigned to the monkeys during the writing of the manuscript to improve its readability.

Under species, "mul." is for macaca mulatta while "fasc." is for macaca fascicularis.

The six control antibody treated monkeys are in the six leftmost columns, whereas the six anti-Nogo-A treated monkeys are in the six rightmost columns ("Anti-Nogo-A") with indication of which of the two antibodies was used (mAB11C7 or mAB hNogoA).

Under "double-blind procedure", "Yes" refers to monkeys for which the collaborators delivering the antibodies (control or anti-Nogo-A) did not know to which monkey they were aimed for. On their side, the experimenters taking care of the monkeys did not know which antibody has been administered to the corresponding animal.

Under ICMS (intracortical microstimulation), "Yes" refers to the three monkeys subjected to extensive ICMS sessions in the primary motor cortex (M1), whose data have been reported previously (Schmidlin and others, 2004; Schmidlin and others, 2005).

Functional recovery was assessed here based on the "modified Brinkman board" task, by giving in percent the ratio of the post-lesion score to the pre-lesion score.

In the row “completeness of CS (dlf) section”, “Yes” and “No” indicates whether the dorsolateral funiculus (dlf) was or was not completely transected unilaterally, respectively. When “BDA” is indicated between parentheses, it means that completeness of the section of the dorsolateral funiculus unilaterally was assessed based on the BDA-labeling of the CS tract immediately above the lesion, in addition to the location and extent of the lesion itself.

* In the monkey Mk-CG, a very small contingent of CS axons, labeled with BDA, escaped from the lesion ventrally. However, these few axons then ran ventrally in the white matter, without giving rise to collaterals into the area immediately caudal to the lesion, and continued their trajectory further below to low thoracic segments. As a consequence, these few preserved CS axons did not participate to the reconstruction of the CS tract in the segments immediately caudal to the lesion and therefore the lesion of the dorsolateral funiculus was considered as complete in this animal too.

For the sake of completeness of information, the extent of the lesion in percent was given separately for three sub-territories of white matter in the lesioned hemi-cord. The three territories are: the dorsal column (from midline dorsally up to the dorsal rootlet entrance); the ventral column (from midline ventral to the ventral rootlet exit) and, laterally, the territory between the dorsal and ventral rootlets corresponding mainly to the territories occupied by the CS and rubrospinal (RS) tracts. A value of 100%, for instance in the dorsal column, means that 100 % of the dorsal column sub-territory was lesioned in the corresponding monkey.

Survival time: number of days separating the injection of BDA in the contralesional M1 and the day of sacrifice of the animal.

Surgical procedures: partial cervical cord section

Pre-anaesthesia was induced by intramuscular injection of ketamine (Ketalar®; Parke-Davis, 5 mg/kg, i.m.). Atropine was injected i.m. (0.05 mg/kg) to reduce bronchial secretions. Before surgery, the animal was treated with the analgesic Carprofen (Rymadil®, 4 mg/kg, s.c.). An intravenous catheter was placed in the femoral vein for continuous perfusion (0.1 ml/min/kg) with a mixture of 1% propofol (Fresenius®) and a 4% glucose solution (1 volume of Propofol and 2 volumes of glucose solution), inducing a deeper and stable anaesthesia. Methylprednisolone (Solu-Medrol®, Pfizer) was added to the perfusion solution (1 mg/ml). The animal was then placed in a stereotaxic framework, with local anaesthetic put on the ear bars in order to reduce pain possibly originating from the ear canals. During the surgery under aseptic conditions, the following parameters were monitored: heart rate, respiration rate, expired CO_2, arterial O_2 saturation and body temperature. In the initial experiments, an extra intravenous bolus of 0.5 mg of ketamine diluted in saline (0.9%) was added i.v. at potentially more painful steps of the surgical procedure, such as laminectomy. In the other and more recent experiments, ketamine was added to the perfusion solution (65 mg/100 ml) thus administered i.v. continuously throughout the whole surgery. Placed in a ventral decubitus position, the spinal processes from C2 to Th1 were exposed. The paravertebral muscles were retracted and the laminae of the segments C6, C7 and Th1 were dissected. A complete C6 laminectomy and an upper C7 hemi-laminectomy were then performed. The ligamentum flavum was removed. The dura mater was exposed and incised longitudinally. Under the microscope, the dorsal root entry zones were easily identified. A unilateral incomplete section of the cervical cord at the C7/C8 border was performed using the dorsal root entry zone as the most medial landmark. From this target, a surgical blade (no 11, Paragon®) was inserted 4 mm in depth perpendicularly to the spinal cord, and the section was prolonged laterally to completely cut the dorsolateral funiculus. From previously available anatomical material, the rostro-caudal level where the dorsal rootlets entering respectively the 7^{th} and the 8^{th} cervical spinal segments meet was determined, corresponding to the rostral zone

of the spinal portion covered by the 6th cervical lamina. The aimed lesion was located caudal with respect to the pool of biceps motoneurons but rostral to the pool of triceps, forearm and hand muscle motoneurons[13] (see also Fig. 3a). The muscles and the skin were sutured. The animal usually recovered from anesthesia 15-30 minutes after interruption of the perfusion with propofol and was treated post-operatively with an antibiotic (Ampiciline 10%, 30 mg/kg, s.c.). Additional doses of Carprofen were given daily during one week (pills of Rymadil mixed with food). After the spinal lesion, the animal was kept alone in a separate cage for a couple of days, to allow better conditions for recovery than the usual group housing with other monkeys.

Antibody treatments

The treatment with control (six monkeys) or anti-Nogo-A (six monkeys) antibodies lasted during 4 weeks post-lesion delivered from an osmotic pump (Alzet ®, 2ML2), placed in the back of the animal, using a small silastic tube positioned intrathecally 3-5 mm above the cervical lesion. The pump was implanted within a few minutes after the lesion of the cervical cord. The pump had a volume of 2 ml, allowing treatment during 2 weeks, after which it was replaced under anaesthesia by a second pump for another 2 weeks treatment. In five monkeys (pilot animals), the experimenters knew which one of the two antibodies was contained in the pumps (Table 1). For the seven other monkeys, the antibody contained in the pump was blind for the experimenters (Table 1) until the end of the experiments (sacrifice of the animal and reconstruction of the cervical lesion). After four weeks of treatment, the pump and the silastic tube were removed. When removed, each pump was checked for the volume left in order to ensure that the antibody was indeed delivered.

Post-lesion behavioral, electrophysiological and pharmacological investigations

The manual dexterity assessment using the "modified Brinkman board" task was pursued along a period of two to three months post-lesion, in order to reach a plateau (Fig. 1a-c). Then an amount of 30-50 daily sessions were considered to

establish the “post-lesion” behavioral score, corresponding to the so-called “functional recovery” expressed in percent of the pre-lesion behavioral score. In three monkeys (“Mk-CC”, “Mk-CS” and “Mk-AF”), extensive intracortical microstimulation (ICMS) sessions were conducted in the motor cortex bilaterally in order to study the post-lesional plasticity of the motor map both in the contralesional (Schmidlin,E. et al., 2004) and ipsilesional (Schmidlin,E. et al., 2005) hemispheres. In the same three monkeys, the post-lesional ICMS sessions were followed by reversible inactivation sessions by infusing the GABA agonist muscimol in the contralesional or ipsilesional hand representation area in M1 (Schmidlin,E. et al., 2004, 2005).

Tracing experiments and histological assessment of the lesion

After completion of the post-lesion behavioral and electrophysiological (ICMS) sessions, the anterograde tracer “Biotinylated Dextran Amine” (BDA, Molecular Probe®) was injected in the contralesional hemisphere. In the three monkeys subjected to electrophysiological mapping, the chronic chamber allowed positioning of Hamilton syringes containing BDA at sites in the M1 hand area identified based on the pre- and post-lesion ICMS data. In order to obtain an uptake of BDA also from more proximal CS neurons, BDA was also injected at ICMS sites corresponding to forearm territories (wrist, elbow, shoulder) as well as more medially in M1 leg territories. In the other monkeys, using stereotaxic landmarks, a craniotomy was performed under propofol anesthesia to expose the central and arcuate sulci contralesionally. Injections of BDA were performed in M1, i.e. in the rostral bank of the central sulcus, following the central sulcus going from lateral (hand representation) to medial (leg representation). A second series of BDA injections were performed more rostrally with respect to the central sulcus, also going from lateral to medial, but at a depth aiming for the part of M1 located on the surface of the cerebral cortex. The parameters of BDA injections are given for each monkey in Table 1. In the first two monkeys (Mk-CC, Mk-CS), the survival time after BDA injection was set to three weeks, as used before in

intact monkeys[15]. However, the cervical lesion substantially slowed down the anterograde axonal transport of BDA and therefore the tracer did not reach the cervical segments. These animals were not considered further for the anatomical analysis (Table 1). In contrast, a much longer survival time (60 days) allowed transport of BDA up to thoracic level in the other ten monkeys (Table 1). The animals were finally sacrificed under deep, lethal anaesthesia (90 mg of sodium pentobarbital/kg body weight) by transcardiac perfusion with 0.9% saline (400 ml) and continued with fixative (3 liter of 4% phosphate buffered paraformaldehyde in 0.1 M phosphate buffer, pH=7.6). Perfusion was continued with solutions (2 liters each) of the same fixative containing increasing concentrations of sucrose (10, 20 and and 30%). The brain and spinal cord were dissected and placed in a 30% solution of sucrose (in phosphate buffer) for cryoprotection during seven days. Frozen sections (50 µm thick) of the brain were cut in the frontal plane and collected in eight series, whereas frozen sections (50 µm thick) of the cervical cord (approximately segments C6-T3) were cut in the paralongitudinal plane and collected in 3 series for later histological processing. Upper cervical segments and lower thoracic spinal segments were cut in the frontal plane at 50 µm thick and sections were also collected in three series. One series of spinal sections were revealed for BDA staining, as described in detail in previous reports[15,16]. The second series of spinal cord sections were immunohistochemically processed to visualize the corticospinal axons using the marker SMI-32, as recently reported, a series of sections also used to reconstruct the location and extent of the cervical lesion, as described in detail earlier (Schmidlin,E. et al., 2004, Wannier,T. et al. 2005).

As other descending motor tracts (e.g. rubrospinal, reticulospinal) may also contribute to recovery, the overall extent of the lesion was quantitatively assessed by the percentage of hemi-cord lesioned. In other words, the extent of the cervical lesion was expressed quantitatively in percent, given by the ratio of the reconstructed lesion area (as shown by the red or blue area in Fig. 3b online) to the total area of the corresponding hemi-cervical cord. The extent of the cervical lesion ranged across monkeys from 38% to 90% of the spinal hemi-cord

(Table 1). The rostrocaudal extent of the cervical lesion ranged from 488 to 1367 m (see also Table 1). The third series of sections were processed to visualize another anterograde tracer (Dextran-Fluorescein) injected in the ipsilesional hemisphere, but these data will not be presented here.

Measurement of CS axonal arborization

On every paralongitudinal section processed for BDA (150 µm interval), the presence of BDA labelled CS axonal arbors was investigated caudal to the lesion at 200x magnification on a light microscope (Olympus®). Using neurolucida® software, each BDA-labelled axonal segment was traced and the location of boutons *terminaux* and *en passant* were registered. The same software allowed counts of axonal swellings and the cumulated length of axonal arbors labeled with BDA caudal to the lesion. Boutons *en-passant* were defined as a swelling with a diameter twice the diameter of the axonal branch before and after the swelling itself. For each monkey, the contour of the lesion (vertical arrow in Fig. 4c-d and Fig. 5a-b) and the labeled CS axonal segments were plotted on a drawing of superimposed reconstructions of paralongitudinal sections of the cervical-thoracic cord (Fig. 4c-d and Fig. 1a-b). Rostral to the lesion, the densely packed line segments represent the BDA-labeled CS tract above the lesion and interrupted by the transection of the dorsolateral funiculus (Fig. 4c-d and Fig. 5a-b). Some of the transected CS axons exhibited a retraction from the rostral limit of the lesion (data not presented here).

Out of the ten monkeys injected with BDA and for which a survival time was long enough (Table 1), the seven monkeys conducted according to the “double-blind” procedure were selected for the quantitative analysis of BDA labeling caudal to the lesion. The expected number of CS axonal arbors and swellings labeled with BDA depends on the size of the BDA injection in M1, on the efficiency of tracer uptake and axonal transport. In order to normalize the data across monkeys, the number of BDA-labeled CS axons was counted rostral to the lesion, at C5 level on a frontal section. Then the cumulated length of CS axonal arbors caudal to the lesion was divided by the total number of labeled CS

axons at C5 level (Fig. 4e and g). A similar normalization was performed for the number of CS axonal swellings (Fig. 4f-g).

The statistical comparisons between the two groups of monkeys (anti-Nogo-A treated versus control-antibody treated) regarding functional recovery and CS axonal sprouting were conducted using the non parametric Mann and Whitney test.

1.4 Results

The motoneurons controlling hand muscles in macaque monkeys are located at cervical and thoracic levels (Jenny and Inukai, 1983) (Fig.1a). Deficits of manual dexterity were produced in twelve monkeys by unilateral cervical cord lesion at C7-C8 border, rostral to the hand motoneurons (Fig.1a,b; Methods and Materals; Table1), aimed unilaterally at the dorsolateral funiculus, which was completely interrupted in eight monkeys. In four monkeys, the lesion was incomplete with a few CS axons preserved in the dorsolateral funiculus. The monkeys exhibited dramatic post-lesion loss of manual dexterity ipsilesionally, accompanied by hindlimb dysfunction.

The deficit of manual dexterity was followed by a progressive recovery. However, in a first "pair" of monkeys (Fig.2a) subjected to a large lesion, recovery was fast and complete in the anti-Nogo-A treated animal (Mk-AM), in contrast to the control-antibody treated monkey (Mk-CH). In a second "pair" of monkeys (Fig.2b), the anti-Nogo-A treated monkey (Mk-AC) had a larger lesion but exhibited faster recovery than the control-antibody treated monkey (Mk-CG). Similarly, in a third "pair" of monkeys (Fig.2c), the anti-Nogo-A treated monkey (Mk-AF) recovered better than the control-antibody treated one (Mk-CS). The functional recovery, plotted as a function of lesion extent (Fig.2d), was significantly higher

Based on a “reach and grasp drawer” test (Fig.3a1, a2), assessing ability to generate force with the fingers, the anti-Nogo-A treated monkeys tended to

recover faster the capacity to pull the drawer post-lesion than the control-antibody treated monkeys (*P*=0.27), especially in case of large lesions (Fig.4a). The difference was statistically significant when excluding the monkey MK-CP with incomplete lesion of the dorsolateral funiculus (*P*=0.05). Catching an object thrown to the monkey ("ballistic arm movements" test; Fig.3b) also revealed faster recovery of the capacity to pre-shape the hand (extension of fingers) in the anti-Nogo-A treated monkeys (Fig.4b), a trend however not statistically significant (*P*=0.12 without monkey Mk-CP). No difference between the two groups of monkeys regarding capacity of prehension with the hindlimb was observed (Fig.3c).

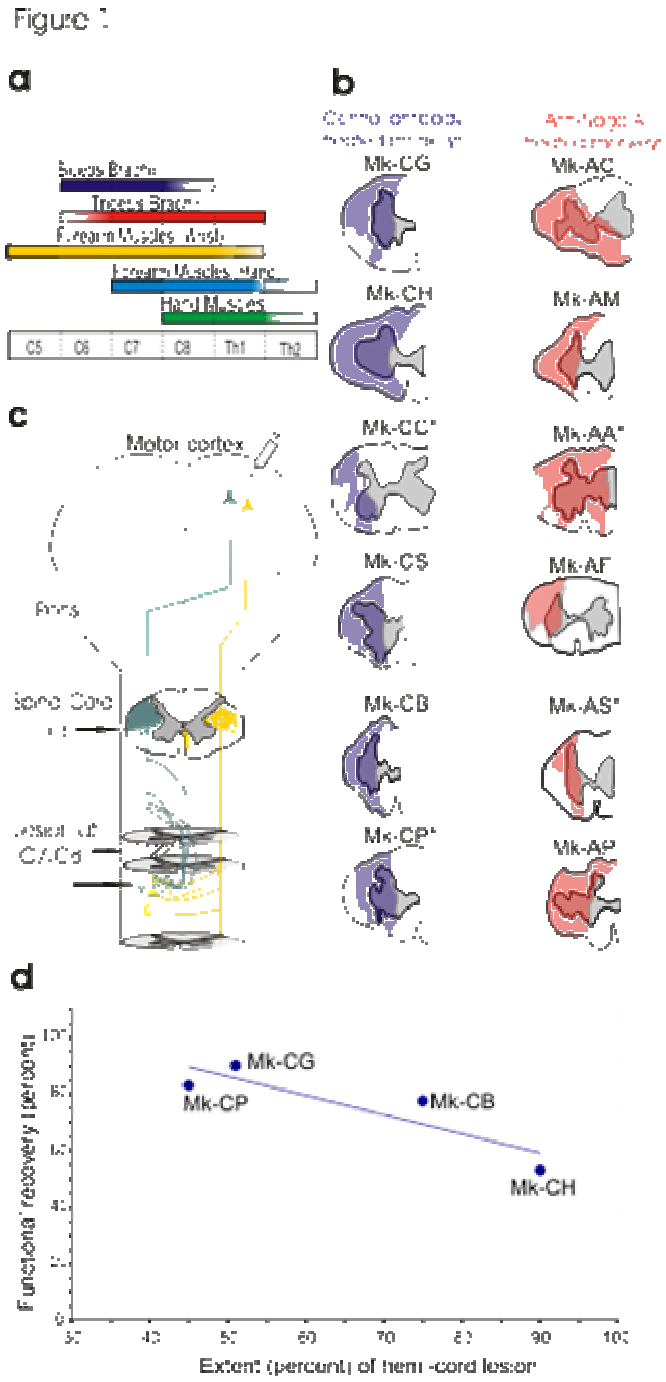

Legend to Figure 1

Organization of the CS projection in the macaque monkey and reconstructions of the cervical lesions performed in the 12 monkeys.

(**a**) Location of motoneurons in cervical and thoracic cord segments controlling forelimb muscles in the macaque monkey (Re-drawn from Jenny and Inukai[10]).

(**b**) Reconstruction in the frontal plane, from paralongitudinal sections, of the lesion extent at cervical level C7/C8 (see **Table1**). The gray area represents the spinal gray matter. Note some distortion of the hemi-cord on the lesional side. The dorsolateral funiculus was completely interrupted in eight monkeys, whereas in four monkeys (asterisks) it was incompletely transected.

(**c**) Schematic representation of the macaque monkey corticospinal (CS) projection from the right motor cortex. The cervical lesion (gray bent line segments) did not interrupt the uncrossed CS axons originating from the contralesional hemisphere, except in Mk-AC. The arrow below the lesion points to the spinal cord region in which the presence for BDA axonal arbors was quantitatively assessed in the present study.

(**d**) The behavioral data derived from the assessment of manual dexterity based on the "**modified B rinkman b oard**" test are shown here exclusively for the group of control-antibody treated monkeys excluding the two animals subjected to intracortical microstimulation (thus corresponding to the blue symbols of **Fig. 1 d**). As indicated by the regression line for these 4 control-antibody treated monkeys (coefficient of correlation of R=-0.879), the data indicate that, in control-antibody treated monkeys, functional recovery of manual dexterity is inversely correlated to the extent of the hemi-cord lesion.

Figure 2

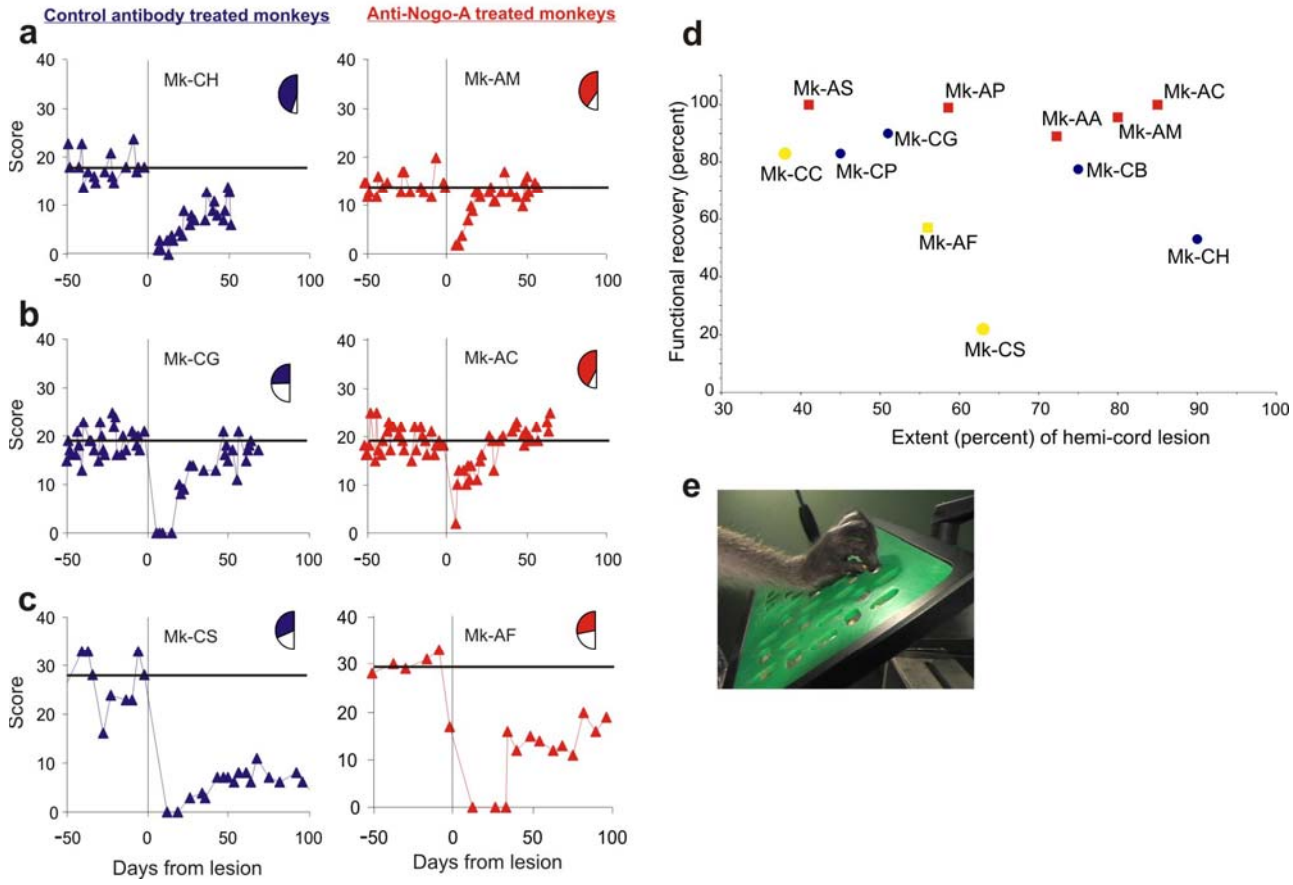

Figure 2
Quantitative assessment of manual dexterity pre- and post-lesion.
To reduce inter-individual variability, direct comparisons were performed first between two monkeys forming a so-called "pair" (**Methods**).
(**a-c**) For three "pairs" of monkeys, comparison of behavioral scores assessing manual dexterity, before and after the lesion (day 0), derived from the "**modified Brinkman b oard**" task (number of pellets retrieved within 30 seconds) for the hand affected by the cervical lesion. The extent of the blue/red zones in the "semicircular figurines" represents the extent of the hemi-cord lesion for each monkey (but does not indicate the location of the lesion). The two monkeys displayed in **c** were subjected to intracortical stimulation (ICMS), possibly explaining the less prominent recovery than in the other monkeys.
(**d**) Relationship between the extent of the hemi-cord lesion and the degree of functional recovery for the "**modified Brinkman board**" test. The blue circles are for control-antibody treated monkeys, whereas the anti-Nogo-A treated monkeys are represented by red squares. Three monkeys were plotted separately (yellow symbols) because being subjected to extensive ICMS (Schmidlin,E. *et al.* 2005; Rouiller,E.M. et al.1996), a procedure that may have reduced their manual capacity. The recovery of manual dexterity was significantly higher (Mann-Whitney test, P=0.028) in the five anti-Nogo-A treated monkeys (red squares) than in the four control-antibody treated monkeys (blue circles). A statistically significant difference was also found if all twelve monkeys are included (Mann-Whitney test, P=0.037). (**e**) Left hand of a monkey performing the "**modified Brinkman board**" task, using the precision grip (opposition of thumb and index finger).

Figure 3

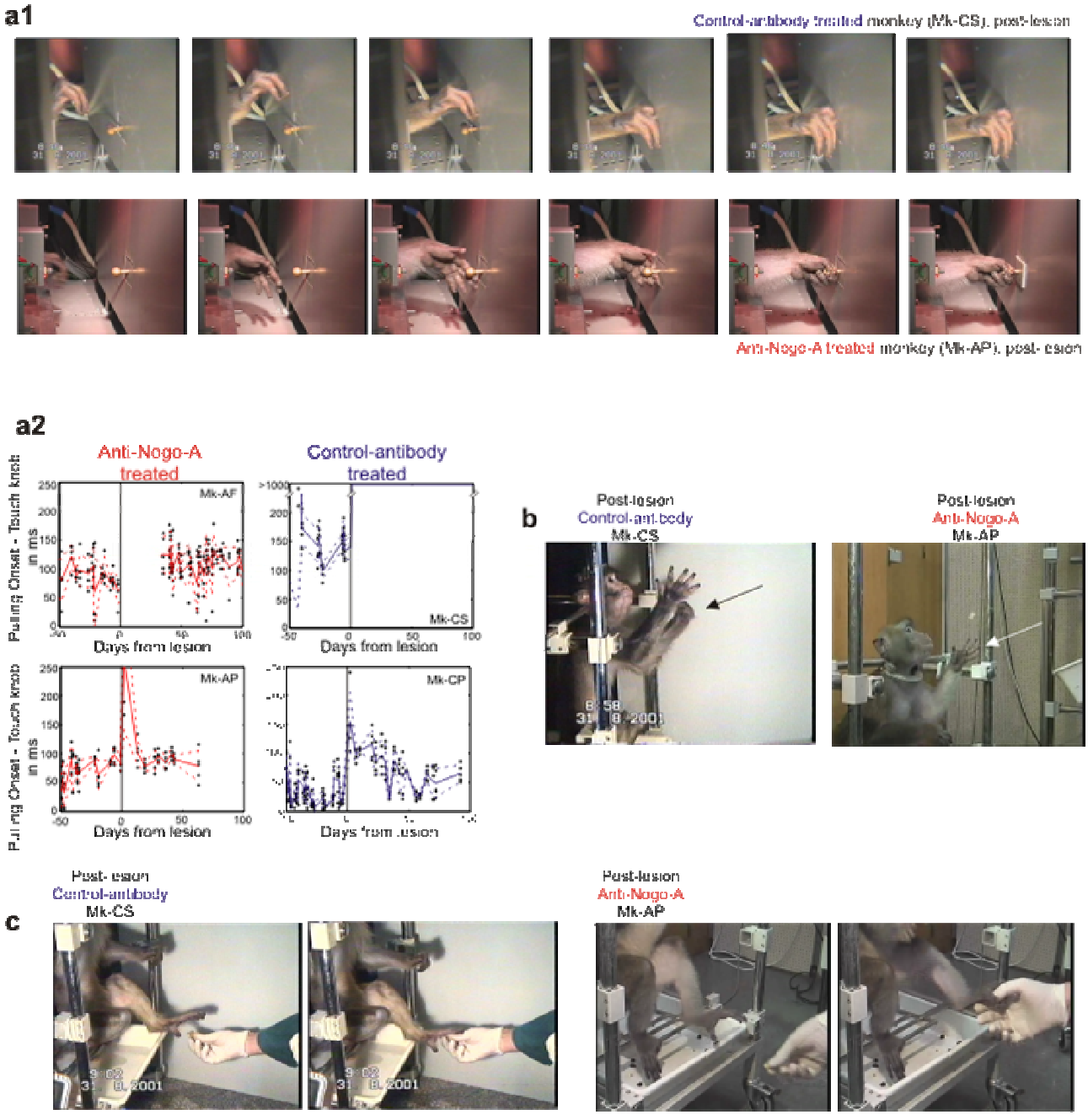

Figure 3
Assessment of motor capacity of fore- and hind-limbs.

(**a1, b, c**) Views extracted from video sequences of one representative trial performed post-lesion by a control-antibody treated monkey (Mk-CS) and an anti-Nogo-A treated monkey (Mk-AP) in the "**reach and grasp drawer**", "**ballistic arm movements**" and "**hindlimb grasp**" tests, respectively. The control-antibody treated monkey did not grasp properly the drawer knob and did not develop enough force to pull the drawer as the knob slipped in between the fingers. The control-antibody treated monkey did not pre-shape the

ipsilesional hand (absence of fingers extension: see arrow) in the ballistic task and did not recover foot grasping. The anti-Nogo-A treated monkey successfully opened the drawer and pre-shaped the hand (fingers extension) in the ballistic task but foot grasping was not recovered.

(**a2**) Quantitative assessment of the "**reach and gra sp drawer**" task in two anti-Nogo-A treated monkeys (Mk-AF; Mk-AP) and two control-antibody treated monkeys (Mk-CS; Mk-CP). The time interval (in ms) between contact with the knob and pulling onset was plotted as a function of the corresponding daily session, before (days -50 to 0) and after (days 0 to 100) the lesion. The thick red/blue line represents the average time interval derived from five trials (with SD given by the red/blue dots), whereas all observations are represented by a "+" sign. The anti-Nogo-A treated monkeys recovered a time interval comparable to pre-lesion, whereas the control-antibody treated monkeys did not (Mk-CS did not recover at all the drawer task).

CS axons were labeled by injecting the anterograde tracer BDA in the contralesional motor cortex (Fig.1c). In the "pair" of monkeys Mk-CH and Mk-AM, CS axonal arbors were more numerous caudal to the lesion in the anti-Nogo-A treated than in the control-antibody treated monkey (Fig.4c-d). After normalization (Table 1; Fig.5a-b), in six monkeys with complete CS transection in which BDA-labeling data could be quantified caudal to the lesion, the normalized cumulated axonal arbor length was larger in the anti-Nogo-A treated than in the control-antibody treated monkeys (Fig.4e), a trend however not statistically significant (P=0.12). The normalized number of CS axonal swellings caudal to the lesion was significantly larger (Fig.4f) in the anti-Nogo-A treated than in the control-antibody treated monkeys with complete lesion (P<0.05; if monkey Mk-CP is included, the difference is not statistically significant: P=0.29). Accordingly, the normalized number of axonal swellings plotted as a function of normalized axonal arbor length was higher in the anti-Nogo-A treated monkeys (Fig.4g). Sprouting was observed on a total distance of about 10-12 mm and occurred from axotomized CS axons (Fig.4c) but sprouting from intact CS axons from both hemispheres may also have occurred.

The monkeys treated with anti-Nogo-A antibodies did not lose weight (Fig.5f) and remained cooperative with the experimenter. Furthermore, the monkeys did not exhibit signs of discomfort or pain when the experimenter touched their body or

manipulated their limbs. These observations suggest that the rewiring induced by the anti-Nogo-A treatment did not generate chronic pain (see Discussion).

Figure 4

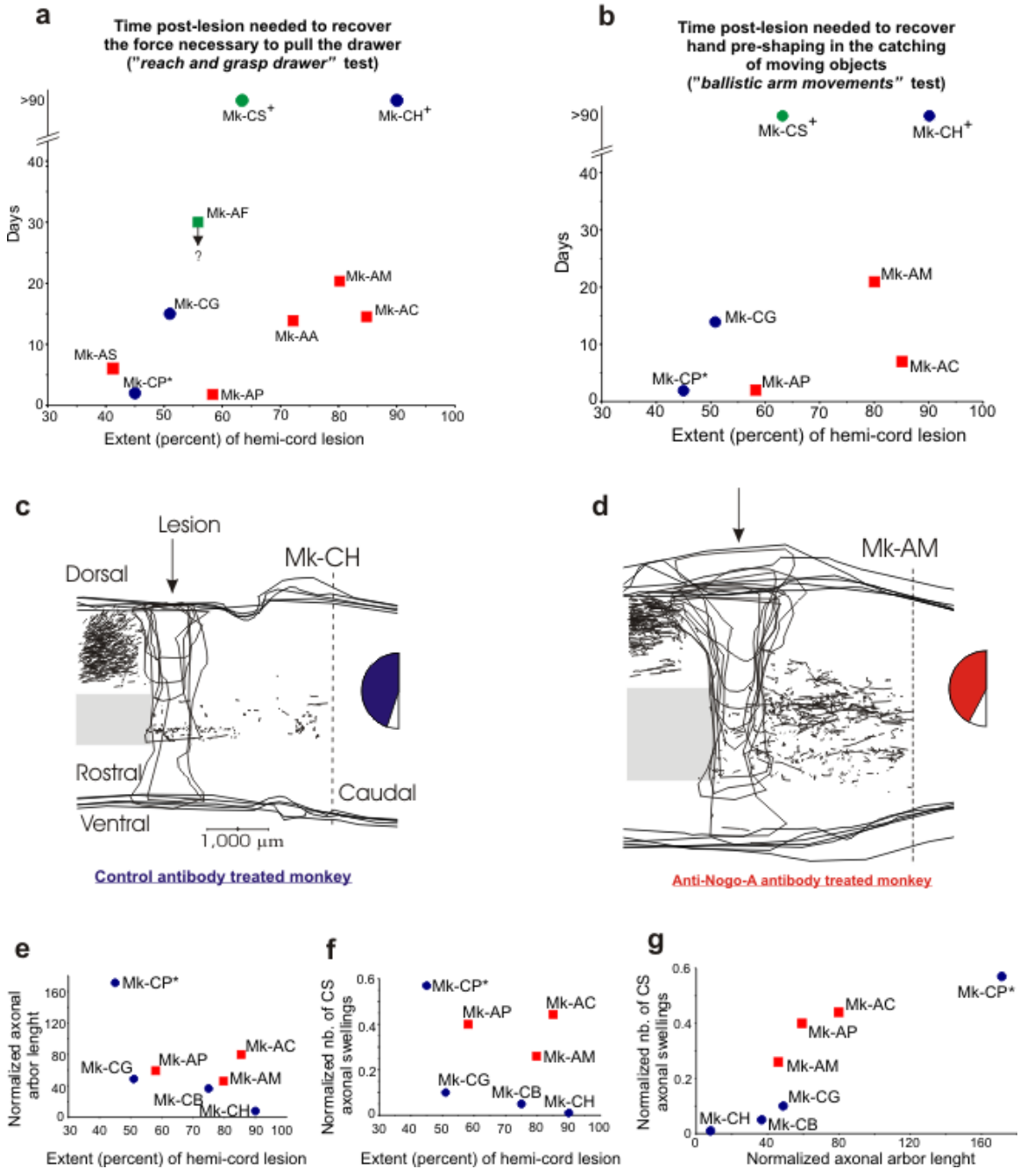

Legend to Figure 4

Anti-Nogo-A enhanced motor recovery and CS axonal sprouting.

Days required post-lesion to recover the ability to perform the **reach and grasp drawer** (**a**) and **ballistic arm movement** (**b**) tasks plotted as a function of lesion extent. Monkey Mk-AF was not tested before 30 days for technical reasons. In monkey Mk-CP (asterisk), the dorsolateral funiculus was not completely interrupted, possibly explaining the rapid recovery. Two monkeys did not recover during the three months of observation (+signs).

(**c-d**): CS axons were labeled by multiple, widespread BDA injections in the contralesional motor cortex. In two monkeys, in which all labeled CS axons were interrupted, BDA-labeled axonal arbors caudal to the lesion were more numerous in the anti-Nogo-A treated (Mk-AM) than in the control-antibody treated monkey (Mk-CH). The gray area rostral to the lesion delineates the gray matter.

In the seven monkeys in which BDA-labeling was quantitatively analyzed caudal to the lesion, the normalized cumulated CS axonal arbor length (mm) and the normalized number of axonal swellings emitted by CS axons (representing putative re-established contacts with interneurons or motoneurons deprived of inputs as a result of the lesion) were plotted as a function of lesion extent (**e-f**). Monkey Mk-CP, with incomplete section of the dorsolateral funiculus (asterisk), exhibited profuse sprouting from spared CS axons. The number of CS axonal swellings was plotted as a function of the cumulated CS axonal arbor length (in mm) for the seven monkeys (**g**).

(See legend of **Fig.2** for symbol and semicircular figurine conventions)

1.5 Discussion

Neutralization of Nogo-A promotes re-growth of CS (and possibly other) axons around the lesion and into the denervated spinal cord in macaque monkeys, in line with previous observation in marmoset (Fouad et al., 2004). For the first time in primates, anti-Nogo-A antibody treatment also led to considerable functional recovery. The time course and limitation of spontaneous manual dexterity recovery in the control-antibody treated monkeys are consistent with earlier reports for monkeys subjected to lesion at C3-C5 level (Galea and Darian-Smith, 1997; Sasaki et al., 2004). This time course was shortened and the recovery of skilled hand function was nearly complete when neutralizing Nogo-A (Figs.2-4). Neutralization of Nogo-A by specific antibodies infused intrathecally leads to impressive functional recovery and enhanced regenerative axonal sprouting and elongation not only in spinal cord lesioned adult rats but also in adult primates, in absence of detectable malfunctions. These observations represent an important proof of principle on the way to a novel therapy of spinal cord and brain lesions in humans.

The position and size of the cervical sections were inevitably variable across the monkeys (Fig. 1b). However, it turned out that the most crucial requirement for the validity of the present model was to completely transect the dorsolateral funiculus unilaterally, a condition achieved in eight out of the twelve monkeys, leading to substantial manual deficit of the ipsilesional hand. Complete CS tract lesions were even more necessary for the interpretation of the anatomical data caudal to the lesion.

Figure 5

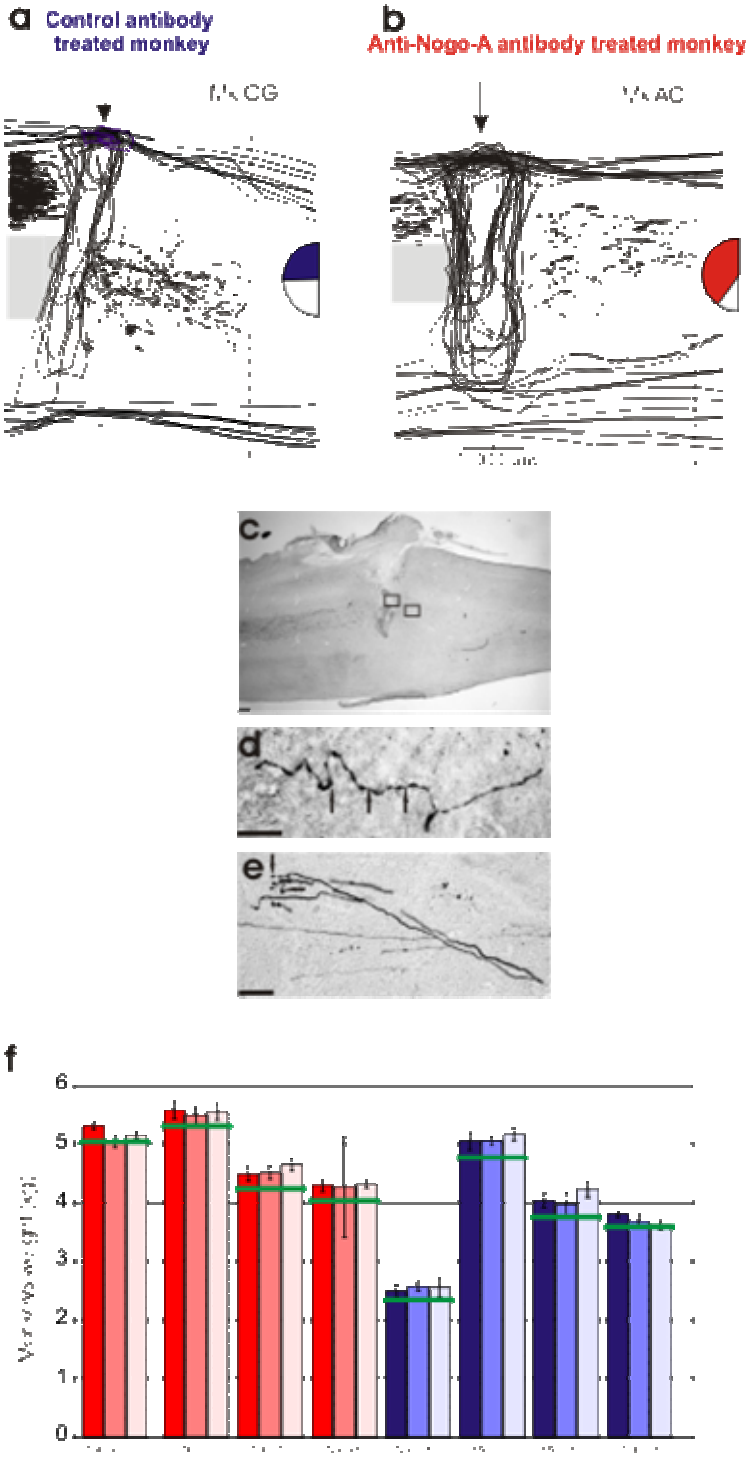

Legend to Figure 5

Morphological analysis of labeled CS axons; health condition of monkeys.

(**a**, **b**) Same data (BDA-labeled CS axons) as in **Fig.2c-d**, but for two other monkeys. Paradoxically, more BDA-labeled CS axonal arbors caudal to the lesion were found in the control-antibody treated (Mk-CG) than in the anti-Nogo-A treated (Mk-AC) monkey. However, the cortical BDA injections labeled quite different amounts of CS axons, namely 1,005 in Mk-CG and 270 in Mk-AC, respectively. After normalization with respect to the total number of CS axons labeled, the cumulated axonal arbors length and the number of axonal swellings were actually larger in the anti-Nogo-A treated monkey (Mk-AC) than in the control-antibody treated monkey (Mk-CG; see **Table 1**).

The two photomicrographs **d** and **e** illustrate the appearance of BDA-labeled CS axonal arbors at locations caudal to the lesion, as indicated in **c**, on a paralongitudinal section of the cervical-thoracic cord. Arrows point to axonal swellings (boutons *terminaux* and *en passant*). Scale bars: 1 mm in **c**, 100 m in **d** and 200 m in **e**.

(**f**) Average body weight (with SDs), pre-lesion (30 days; leftmost bar), post-lesion during infusion of the antibodies (30 days; middle bar) and after offset of antibody administration (30 days; rightmost bar), as an indicator of health condition (see **Discussion**), in four anti-Nogo-A treated monkeys (red) and four control-antibody treated monkeys (blue). The green horizontal lines represent, for each monkey, a level corresponding to a loss of 5% from the average body weight pre-lesion.

The size of the cervical lesion remains a crucial concern. For ethical reasons, nearly complete spinal lesions were discarded, in particular to keep the animals in decent post-lesion health condition. The extent of the lesion was aimed at generating a significant deficit of manual dexterity, exhibiting however a clear enhancement by the anti-Nogo-A. Moreover, further extension of the lesion more ventrally in the white matter or medially in the gray matter may also affect the degree of recovery, involving other descending tracts such as the rubrospinal, reticulospinal, tectospinal and vestibulospinal tracts (Hashimoto and Fukuda, 1991; Feraboli-Lohnherr et al., 1997; Raineteau et al., 2001; Schucht et al., 2002; Raineteau et al., 2002; Ruitenberg et al., 2003; Fouad et al., 2005)}, as well as a more indirect contribution via propriospinal projections, as shown in rats (Bareyre et al., 2004). However, the possible role played by the propriospinal projection in monkeys for manual dexterity remains controversial (Sasaki and others, 2004; Lemon, 2004).

Descending tracts other than the CS projection were not labeled in the present investigation and therefore how much they were affected by the lesion remains uncertain, as well as to what extent the anti-Nogo-A treatment enhanced sprouting of the rubrospinal, reticulospinal, tectospinal and vestibulospinal tracts for instance. In addition, the spread of the lesion into the dorsal and ventral columns may also affect the behavioral data. Table 1 indicates for each monkey the extent of the lesion (given in percent) affecting three sub-territories of the white matter, namely the dorsal column, the ventral column and the lateral zone of the white matter (in between the dorsal and ventral rootlets), corresponding to the location of the partly overlapping corticospinal and rubrospinal (RS) tracts. From these data, due to the limited number of monkeys, it was not possible to extract a systematic relationship between the functional recovery and the extent of the lesion within one or the other of these three sub-territories of the white matter. Indeed, the functional roles of these different sub-territories are not independent and, to address the impact of lesioning one of them, would require the comparison of several monkeys with the same lesion of the RS and CS tracts and assess the effects of lesions of graded extent aimed at the ventral column for

instance. Due to restrictions in the use of non-human primates, the contribution to manual deficits of damage to separate territories of the cervical cord could not be addressed in the present study.

Recovery of manual dexterity following cervical cord lesion paralleled the density of CS axonal arbors, which have re-innervated the territory immediately caudal to the lesion, containing the motoneurons controlling hand muscles. Such partial reconstruction of the lesioned CS tract was clearly enhanced by anti-Nogo-A treatment, thus possibly promoting better and faster recovery as compared to control-antibody treated monkeys. Among the possible mechanisms leading to the partial reconstruction of the CS tract caudal to the lesion, sprouting from the CS tract originating from the ipsilesional hemisphere was ruled out in control-antibody treated monkeys because reversible inactivation of the ipsilesional motor cortex did not affect the recovered manual dexterity score (Schmidlin,E. et al., 2004, 2005). On the other hand, reversible inactivation of the contralesional motor cortex completely suppressed the recovered manual dexterity score (Schmidlin et al., 2005), indicating that the limited, spontaneous reconstruction of the CS tract caudal to the lesion occurs from axons originating from the contralesional hemisphere in the form of sprouting of the transected CS axons (green solid lines in Fig. 1c) and/or sprouting of the undecussated CS projection not affected by the lesion, crossing the midline below the lesion (yellow solid lines in Fig. 1c; see also in the rat Weidner,N., et al. 2001). A significant role played in the recovery by the axotomized CS axons in the form of sprouting (green lines in Fig. 1c) is compatible with previous observations that most axotomized CS neurons in the contralesional hemisphere do not die(Davison, 1937; Tower, 1940; Lassek, 1942; Wannier et al., 2005). As far as the anti-Nogo-A treated monkeys are concerned, reversible inactivation experiment conducted in one monkey indicates that the enhanced reconstruction of the CS tract caudal to the lesion also derives from sprouting of the CS tracts originating from the contralesional hemisphere (green and yellow lines in Fig. 1c). However, in the anti-Nogo-A treated monkeys, one cannot rule out at that step a possible

contribution of sprouting of the CS tract originating from the ipsilesional hemisphere.

As observed previously in rodents {Bregman, 1995 9875 /id;Schwab, 2004 22523 /id;Liebscher, 2005 24410 /id, anti-Nogo-A enhanced sprouting of the CS tract was limited to 10-12 mm caudal to the lesion (Fig. 4c-d; Fig. 5a-b), sufficient however to re-address the hand motoneurons denervated after the lesion, thus possibly promoting recovery of manual dexterity. The extent of sprouting was not sufficient to reach the lumbar segment, thus explaining the absence of functional recovery of grasping with the hindlimb in anti-Nogo-A treated monkeys (Fig. 3c).

As a result of multiple, widespread BDA injection in the right motor cortex, the following distribution of CS axons was observed in the cervical cord (Fig. 1c). The main (crossed) CS tract (90-95% of axons) runs in the cervical cord in the opposite dorsolateral funiculus (green dots at C5 level), whereas the uncrossed CS projection (5-10% of CS axons) runs in the homolateral dorsolateral and ventral funiculi (yellow dots at C5 level), in line with previous reports (Rouiller,E.M. et al., 1996; Wannier,T et al. 2005). Such distribution of CS components is also consistent with a recent report at the level of the lumbar cord ({Lacroix, 2004 22711 /id}.

.

The general health condition of the monkeys was assessed quantitatively by their body weight measured regularly, in general before each daily behavioral session. The body weight data are presented for eight monkeys (Fig. 5f). Note that none of the monkeys exhibited a loss of weight post-lesion (during the 30 days of antibody infusion) larger than 5%. According to the guidelines established by the local veterinary authorities, a loss of body weight of 10% or greater is considered as an indicator of pain or discomfort, prompting the exclusion of the animal from the daily protocol (e.g. ICMS, behavioral test, etc). In parallel to a generally stable body weight, the monkeys did not exhibit any reduction of co-operatively and motivation to perform the behavioral tests. No signs of epilepsy, aggression or excessive fear with respect to the experimenter

and animal keeper were observed. Acceptance of passive manipulation of the limbs by the experimenter was unaffected by the treatment. The general social behavior of the anti-Nogo-A antibody treated monkeys with respect to the other monkeys sharing the same detention room was not modified, in particular the grooming behavior. Furthermore, when moving freely in the detention room, the anti-Nogo-A treated monkeys did not take action to avoid contacts of the affected body side with the floor, the walls or other objects.

1.6 References

Bareyre FM, Kerschensteiner M, Raineteau O, Mettenleiter TC, Weinmann O, Schwab ME. 2004. The injured spinal cord spontaneously forms a new intraspinal circuit in adult rats. Nat Neurosci 7:269-277.

Davison C. 1937. Syndrome of the anterior spinal artery of the medulla. Arch Neurol 37:91-107.

Feraboli-Lohnherr D, Orsal D, Yakovleff A, Ribotta MGY, Privat A. 1997. Recovery of locomotor activity in the adult chronic spinal rat after sublesional transplantation of embryonic nervous cells: Specific role of serotonergic neurons. Exp Brain Res 113:443-454.

Fouad K, Klusman I, Schwab ME. 2004. Regenerating corticospinal fibers in the Marmoset (Callitrix jacchus) after spinal cord lesion and treatment with the anti-Nogo-A antibody IN-1. Eur J Neurosci 20:2479-2482.

Fouad K, Schnell L, Bunge MB, Schwab ME, Liebscher T, Pearse DD. 2005. Combining Schwann cell bridges and olfactory-ensheathing glia grafts with chondroitinase promotes locomotor recovery after complete transection of the spinal cord. J Neurosci 25:1169-1178.

Galea MP, Darian-Smith I. 1997. Manual dexterity and corticospinal connectivity following unilateral section of the cervical spinal cord in the macaque monkey. J Comp Neurol 381:307-319.

Hashimoto T, Fukuda N. 1991. Contribution of serotonin neurons to the functional recovery after spinal cord injury in rats. Brain Res 539:263-270.
Jenny AB, Inukai J. 1983. Principles of motor organization of the monkey cervical spinal cord. J Neurosci 3:567-575.

Kazennikov O, Hyland B, Wicki U, Perrig S, Rouiller EM, Wiesendanger M. 1998. Effects of lesions in the mesial frontal cortex on bimanual co-ordination in monkeys. Neuroscience 85:703-716.

Kazennikov O, Wicki U, Corboz M, Hyland B, Palmeri A, Rouiller EM, Wiesendanger M. 1994. Temporal structure of a bimanual goal-directed movement sequence in monkeys. Eur J Neurosci 6:203-210.

Kermadi I, Liu Y, Rouiller EM. 2000. Do bimanual motor actions involve the dorsal premotor (PMd), cingulate (CMA) and posterior parietal (PPC) cortices? Comparison with primary and supplementary motor cortical areas. Somatosensory and Motor Research 17:255-271.

Kermadi I, Liu Y, Te mpini A, Calciati E, Rouiller EM. 1998. Neur onal activity in the primate supple mentary m otor ar ea and the prim ary m otor cort ex in r elation to s patio-temporal bimanual coordination. Somatosens Mot Res 15:287-308.

Kermadi I, Liu Y, Tempini A, Rouiller EM. 1997. Effects of reversible inactivation of the supplementary m otor ar ea (SMA) on uni manual gr asp and bi manual pull and grasp performance in monkeys. Somatosens Mot Res 14:268-280.

Lassek AM . 1942. The pyra midal tract. A st udy of retrograde de generation in the monkey. Arch Neurol 48:561-567.

Lemon RN. 2004. Cortico- motoneuronal sy stem and dexterous finger movements. J Neurophysiol 92:3601.

Liebscher T, S chnell L, S chnell D , S choll J, Schneider R, G ullo M, Fouad K, Mir A, Rausch M, Kindler D, Ha mers FPT, Schwab ME. 2005. Nogo- A antibody im proves regeneration and locomotion of spinal cord-injured rats. Ann Neurol 58:706-719.

Liu Y, Rouiller EM. 1999. Mechanis ms of r ecovery of dexterity following unilater al lesion of the sensorimotor cortex in adult monkeys. Exp Brain Res 128:149-159.

Oertle T, Van der Haar ME, Bandtlow CE, Robeva A, Bu rfeind P, Buss A, Huber AB, Simonen M, Schnell L, Brösamle C, Kaupmann K, Vallon R, Schwab ME. 2003. Nogo-A inhibits neu rite ou tgrowth a nd cell spread ing w ith three discrete regions. J Neurosci 23:5393-5406.

Raineteau O, Fouad K, Bar eyre FM, Schwab M E. 2002. Reorganization of des cending motor tracts in the rat spinal cord. Eur J Neurosci 16:1761-1771.

Raineteau O, Fouad K, Noth P, Thall mair M, Schwab ME. 2001. Functional switch between motor tracts in the pres ence of the mAb IN-1 in the adult rat. Proceedings of the National Academy of Sciences of the United States of America 98:6929-6934.

Rouiller EM, Moret V, Tanné J, Boussaoud D. 1996. Evidence for direct connections between the hand region of the sup plementary mo tor area and cervic al m otoneurons in the macaque monkey. Eur J Neurosci 8:1055-1059.

Rouiller EM, Tanné J , More t V, Ker madi I , Boussaoud D, Welker E. 1998. Dual morphology and topography of the corticothala mic ter minals originating from the primary, supplementary motor, and dorsal premotor cortical areas in macaque monkeys. J Comp Neurol 396:169-185.

Ruitenberg MJ, Plant GW, Ha mers FPT, Wort el J, Blits B, Dij khuizen PA, Gispen WH, Boer GJ, Verhaagen J. 2003. Ex vivo adenoviral vector- mediated neurotrophin gen e transfer to olfactory ensheathing glia: Effects on rubros pinal tract rege neration, lesion

size, and functional recovery after implantation in the injured rat spinal cord. J Neurosci 23:7045-7058.

Sasaki S, Isa T, Pettersson LG, Alstermark B, Naito K, Yoshimura K, Seki K, Ohki Y. 2004. Dexterous finger movements in primate without monosynaptic corticomotoneuronal excitation. J Neurophysiol 92:3142-3147.

Schmidlin E, Wannier T, Bloch J, Belhaj-Saïf A, Wyss A, Rouiller EM. 2005. Reduction of the hand representation in the ipsilateral primary motor cortex following unilateral section of the corticospinal tract at cervical level in monkeys. BMC Neuroscience 6:56.

Schmidlin E, Wannier T, Bloch J, Rouiller EM. 2004. Progressive plastic changes in the hand representation of the primary motor cortex parallel incomplete recovery from a unilateral section of the corticospinal tract at cervical level in monkeys. Brain Research 1017:172-183.

Schucht P, Raineteau O, Schwab ME, Fouad K. 2002. Anatomical correlates of locomotor recovery following dorsal and ventral lesions of the rat spinal cord. Experimental Neurology 176:143-153.

Tower SS. 1940. Pyramidal lesion in the monkey. Brain 63:36-90.
Wannier T, Liu J, Morel A, Jouffrais C, Rouiller EM. 2002. Neuronal activity in primate striatum and pallidum related to bimanual motor actions. NeuroReport 13:143-147.

Wannier T, Schmidlin E, Bloch J, Rouiller EM. 2005. A unilateral section of the corticospinal tract at cervical level in primate does not lead to measurable cell loss in motor cortex. Journal of Neurotrauma 22:703-717.

Weinmann O, Schnell L, Ghosh A, Montani L, Wiessner C, Wannier T, Rouiller E, Mir A, Schwab ME. 2006. Intrathecally infused antibodies against Nogo-A penetrate the CNS and downregulate the endogenous neurite growth inhibitor Nogo-A. Mol Cell Neurosci 32:161-173.

Chapter 3

Anti-Nogo-A antibody treatment promotes recovery of manual dexterity after unilateral cervical lesion in adult primates: further behavioural data

This chapter has been adapted from an article originally submitted to Journal of Neuroscience: (Patrick Freund*, Eric Schmidlin*, Thierry Wannier*, Jocelyne Bloch, Anis Mir, Martin E. Schwab and Eric M. Rouiller, 2007)

- The three first authors contributed equally to the study.

1.1 Abs tract

In rodents and primates subjected to spinal cord lesion, neutralizing the neurite growth inhibitor Nogo-A promoted regenerative axonal sprouting and functional recovery (Liebscher et al., 2005; Freund et al., 2006). In the latter report, the recovery of manual dexterity was based on a single quantitative behavioural readout. The goal of the present report was to extend these data using refined behavioural analyses and statistical assessments. The recovery of manual dexterity following unilateral cervical lesion was investigated in thirteen adult monkeys, seven receiving an anti-Nogo-A antibody, whereas a control antibody was infused in six monkeys.

Monkeys were trained to perform the “modified Brinkman board” task requiring opposition of the index finger and thumb to grasp food pellets, placed in vertical and horizontal oriented slots. Two parameters were quantified before and following spinal cord injury: 1) the “score” as defined by the number of pellets retrieved within 30 seconds; 2) the “contact time” as defined by the duration of digit contact with the food pellet before successful retrieval. During a few postoperative weeks, the hand was severely impaired in all monkeys, followed by progressive functional recovery. In control monkeys, the recovery of manual dexterity was inversely correlated to lesion extent, with residual impairment for both parameters, whereas anti-Nogo-A antibody treated monkeys recovered better and completely (or nearly so), irrespective of lesion size. The difference of functional recovery between the two groups of monkeys was statistically significant (Mann and Whitney tests, $p<=0.05$) for both parameters and for both vertical and horizontal slot orientations.

1.2 Introduction

In the adult mammalian central nervous system (CNS), lesions lead to persistent motor and sensory deficits, to an extent depending on the location and size of injury. Transected nerve fibres do not spontaneously re-grow in the CNS of adult mammals, due in part to the presence of myelin-associated neurite growth inhibitors such as Nogo-A (Yiu and He, 2006; Schwab, 2004). After section of the corticospinal (CS) tract in adult rat, neutralizing Nogo-A with monoclonal antibodies led to enhancement of axonal re-growth and compensatory sprouting, in parallel to increased functional recovery (Schnell and Schwab, 1990; Bregman et al., 1995; Thallmair et al., 1998; Brösamle et al., 2000; Schwab, 2004; Liebscher et al., 2005).

Following incomplete spinal cord injury, non-human primates show spontaneous, but incomplete functional recovery with persisting post-lesion deficits (Galea and Darian-Smith, 1997a,b; Sasaki et al., 2004; Schmidlin et al., 2004). Recently, extending the above data in rat, adult non-human primates were subjected to spinal cord injury and treated with the neutralizing antibody against the neurite outgrowth inhibitor Nogo-A. They showed an enhancement of functional recovery, in parallel to an increased sprouting of the CS tract, both caudal and rostral to the lesion site (Freund et al., 2006, 2007). These studies emphasized the importance of using adult non-human primate models of spinal cord injury for a proof of principles before going into clinical trials (Courtine et al., 2007; Lemon and Griffiths, 2005). In particular, the advantages to use non-human primate in this matter is for instance the fact that the general organisation of the CS system is very alike to that of human subjects, in contrast to the rat (Nudo and Frost, 2006).

The present report provides a new and more detailed behavioural and statistical analysis than the recent report by Freund et al. (2006). These new results demonstrate that anti-Nogo-A antibody treatment significantly enhanced the recovery of manual dexterity after cervical cord lesion, as compared to control antibody treated adult monkeys. More specifically, the present study aimed first at refining previously shown statistical analysis of the behavioural scores derived from the standard behavioural assessment of manual dexterity (the so-called “modified Brinkman board” task). Second, more importantly, a new parameter is introduced here for the same task, namely the “contact time”, defined as the time required grasping the first food pellet aimed by the monkey. This new parameter demonstrates more accurately the manual dexterity as it reflects the precision grip between thumb and index finger, a prerogative of primates including humans (see Lemon and Griffiths, 2005 for review).

1.3 Materials and Methods

The experiments were carried out on thirteen (3.5-6.9 years old) rhesus (Macaca mulata) or cynomolgus (Macaca fascicularis) monkeys of either sex, ranging from 3.0 to 5 Kg, in accordance to the Guide for the Care and Use of Laboratory Animals (ISBN 0-309-05377-3; 1996) and approved by local (Swiss) veterinary authorities. Three recent reports (Freund et al., 2006,2007; Wannier et al., 2005) described in detail the behavioural task considered in the present report ("modified Brinkman board" task; see Fig. 1E and also *www.unifr.ch/neuro/rouiller/motorcontcadre.htm)*, the surgical procedures (including transaction of the CS tract in the cervical cord at C7/C8 level), the treatment with the anti-Nogo-A (n=7) or the control (n=6) antibodies and the neuroanatomical investigations (including the assessment of spinal lesion location and extent). The antibodies' characteristics and the issue of antibody penetration in the CNS were reported elsewhere (Weinmann et al., 2006; Freund et al., 2007).

The present study includes the same twelve recently reported monkeys (Freund et al., 2006) and a thirteenth monkey (Mk-AK), on which the experiment was completed later, belonging also to the group of anti-Nogo-A antibody treated monkeys (Fig. 1B), but in Mk-AK antibody infusion was initiated seven days post-lesion (Fig. 1A), in contrast to immediate infusion on the day of the lesion in the other six anti-Nogo-A antibody treated monkeys. In all anti-Nogo-A antibody treated monkeys, the antibody was delivered during four weeks.

The monkeys ID codes to refer to individual monkeys (Table 1 in Freund et al., 2006) comprise for sake of clarity in the text a "C" or an "A" at the fourth digit position, indicating whether the monkey was **c**ontrol antibody treated or **a**nti-Nogo-A antibody treated, respectively. However, in the course of the experiments, the animals had different names from which the experimenter could not deduce which antibody was infused, at least for the "pairs" of monkeys in which the "double blind" procedure was applied (Table 1 in Freund et al., 2006).

A new statistical test was introduced to assess the overlap/segregation between two groups of data (Figures 2E,F; 4C,D), taking into account two parameters, namely the extent of the lesion and the percent of functional recovery. We use Fisher's linear discriminant function providing maximal separation between the two groups (see e.g. Everitt B. (2005), An R and S-plus Companion to Multivariate Analysis, Springer). The idea is to find a linear function of the observed variables such that the ratio of the between-group variance to its within-group variance is maximized. We used the R package to get the two axes of each Figures 2E,F and 4C,D. Axis 1 (dashed line) yields maximal separation, and the projected sample is provided on the orthogonal axis 2 (solid line).

Then, the axis 2 was proportionally enlarged and positioned vertically (green arrows). As regards of statistics, the sample size does not permit to rely on normality assumptions, and we considered the statistical problem of separation of the projected samples using the non-parametric Mann and Whitney U test.

1.4 Resul ts

The general schedule of the experiment is represented in Figure 1A. In three of the thirteen monkeys (Mk-CS, Mk-CC and Mk-AF) a comprehensive intracortical microstimulation (ICMS) mapping of M1 hand area was conducted on both hemispheres (Schmidlin et al., 2004, 2005), a procedure which may have in part reduced their manual dexterity recovery. The location and extent of the cervical cord lesion is represented for the thirteen monkeys in Figure 1, including four animals in which the CS tract was not completely transected (asterisks). A typical lesion is shown in Figure 1D for monkey Mk-AK, at a sagittal plane where it covers the entire dorso-ventral extent of the cervical cord.

Fig. 1

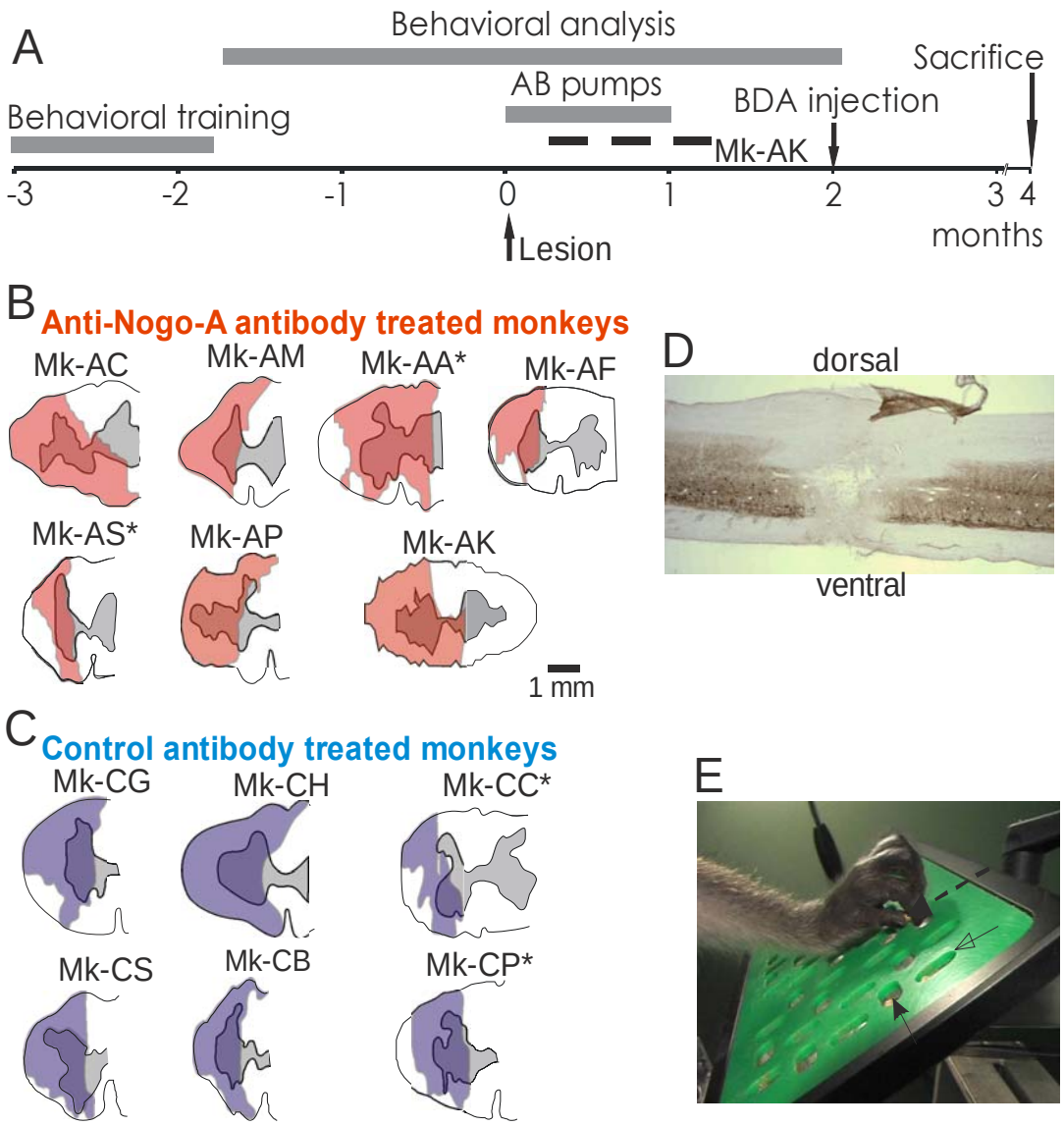

Figure 1

Experimental time course, lesion histology and manual dexterity tests

Panel A: Time course of the experiment. AB=osmotic pump implanted to deliver the antibody (control or anti-Nogo-A) at the time of the lesion in 12 monkeys. The antibody infusion was delayed by one week in monkey Mk-AK (dashed line). The neuroanatomical tracer BDA was injected in the contralesional motor cortex (Freund et al., 2006, 2007).

Panels B and C: Reconstruction in the frontal plane, from paralongitudinal sections, of the lesion extent at cervical level C7/C8 in all monkeys. The grey area represents the grey matter of the cervical cord. Note that, due to the lesion, the hemi-cord on the side of the lesion has been distorted to some extent. In four monkeys (asterisk), the dorsolateral funiculus was not completely transected (see Table 1 in Freund et al., 2006). The lesion for twelve monkeys (all except Mk-AK) has been illustrated in previous reports (Freund et al., 2006, 2007).

Panel D: Photomicrograph of a sagittal section of the cervical cord taken from monkey Mk-AK, illustrating the lesion site. Scale bar= 1mm.

Panel E: Photograph illustrating the "Modified Brinkman Board" task used to assess manual dexterity pre- and post-lesion (modified from Freund et al., 2006). The board comprises 50 slots containing a food pellet (dashed arrows), 25 oriented vertically (open arrow) and 25 horizontally (filled arrow). The monkey grasps the pellet by performing the precision grip (opposition of index finger and thumb).

1. Behavioural assessment of post-lesion recovery of manual dexterity using scores

Following unilateral cervical injury, the manual dexterity of the ipsilesional hand was severely impaired, as assessed by the "**modified Brinkman board**" test. In our previous report (Freund et al., 2006), only the total score was presented whereas, here, scores for the vertical and horizontal slots (number of pellets retrieved in 30 sec) are presented separately (Fig. 2). Retrieval from the horizontal slots is expected to more difficult as it requires a rotation of the hand in addition to the precision grip. For two monkeys conducted in parallel by the same experimenter and having a comparable lesion (Fig. 2A), the anti-Nogo-A antibody treated monkey (Mk-AM) exhibited a faster and better recovery (100% and 75% of the pre-lesion scores for the vertical and horizontal slots) than the control antibody treated monkey (Mk-CH: 60% and 40%, respectively). Along the same line (Fig. 2B), in two other monkeys conducted in parallel, the anti-Nogo-A antibody treated monkey (Mk-AC) with a clearly larger lesion recovered faster and slightly better (100% for both orientations) than the control antibody treated monkey (Mk-CG: 95% and 85% for the vertical and horizontal slots, respectively).

The relationship between lesion extent and recovery of manual dexterity in all monkeys, for vertically and horizontally oriented slots (Fig. 2C, D), shows that the control antibody treated monkeys (blue circles) are characterized by an inverse significant

correlation between lesion extent and the percent of recovery (r=-0.942 for vertical and r=-0.841 for horizontal slots). In contrast, in the anti-Nogo-A antibody treated monkeys (red squares), the recovery was substantially enhanced and, most importantly, reached 90-100% irrespective of the lesion extent.

Fig. 2

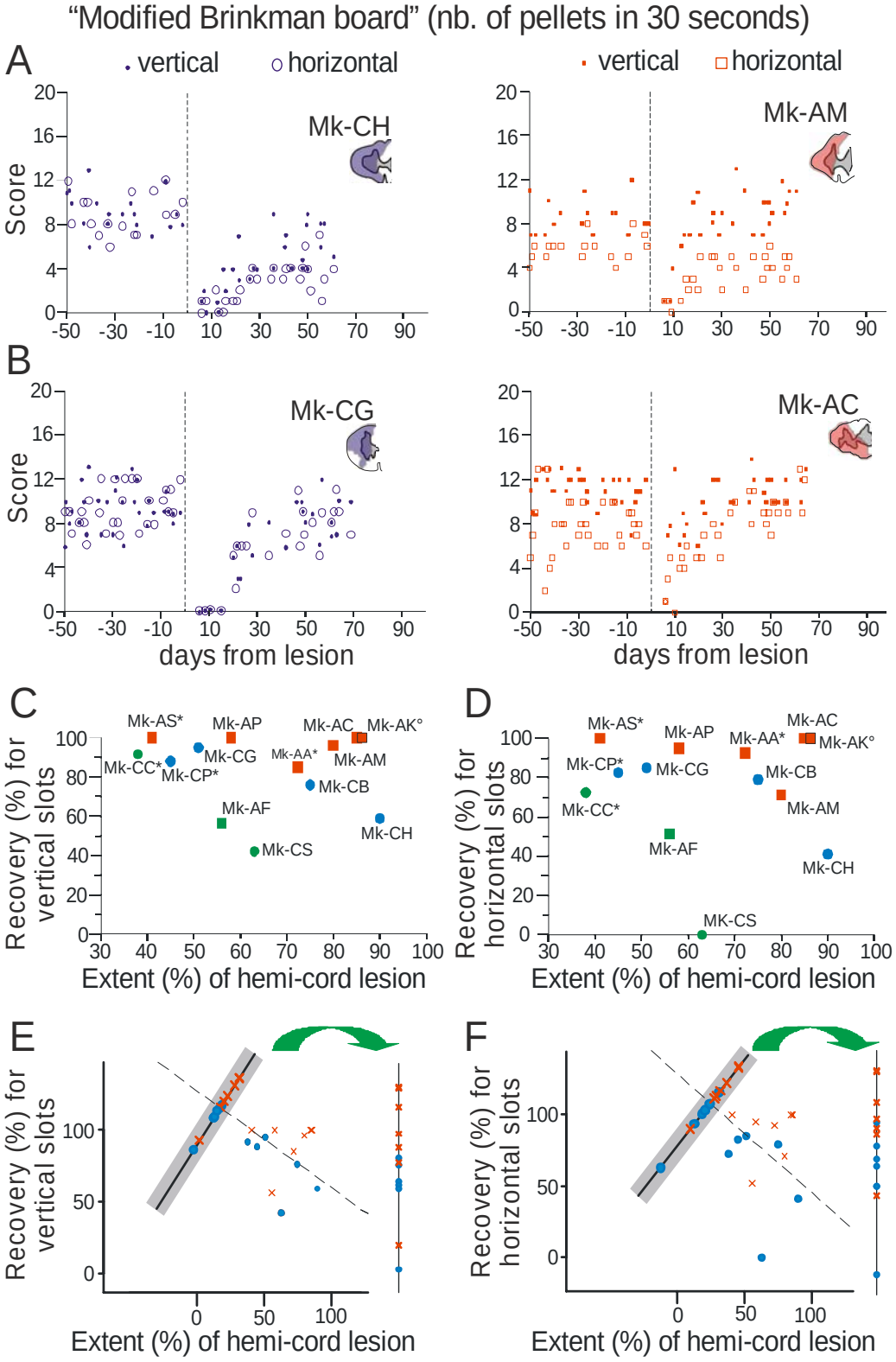

Figure 2

Quantitative assessment of manual dexterity based on "scores"

Panels A-B: For two "pairs" of monkeys, comparison of the behavioural scores obtained before and after the lesion (day 0, represented by the vertical dashed line) derived from the "Modified Brinkman board" task (number of pellets retrieved in 30 seconds), for the hand affected by the cervical lesion. The control antibody treated monkeys are in the left column (blue symbols) and the anti-Nogo-A antibody treated monkeys in the right column (red symbols). The scores were plotted separately for the vertical (dots) and horizontal (open symbols) slots. Monkeys in the same "pair" were assessed in parallel under the same behavioural protocol and by the same experimenter. For each plot, the inset on the upper right is a reminder of the lesion location and extent.

Panels C, D: Relationship between the extent of the hemi-cord lesion in % and the degree of functional recovery in % for the "Modified Brinkman board" test for vertically (C) and horizontally (D) oriented slots (blue circles for control antibody treated monkeys and red squares for anti-Nogo-A antibody treated monkeys). Three monkeys were plotted separately (green symbols) because the experimental protocol was different (they were subjected to extensive intracortical microstimulation).

Panels E, F: Illustration of the statistical analysis conducted on the data presented in panels C and D, respectively (for better visualization, circles are for control antibody treated monkeys whereas crosses are for anti-Nogo-A antibody treated monkeys). A line was searched for which the sum of distances between each data point and its projection onto the line was minimal (dashed lines in Figs. 2E,F). Then, the data points were projected in the direction given by this line onto an orthogonal line segment (full line inside the grey box; note that the values on that segment are independent of the y axis of the initial plot). The green arrow points to an enlargement of the solid line onto which the data points were projected (n=6 for the control antibody treated monkeys and n=7 for the anti-Nogo-A antibody treated monkeys). The rank of the values on the projected segment was statistically analysed using the Mann-Whitney U test.

In our previous report (Freund et al., 2006), the statistical analysis between the two groups of monkeys (anti-Nogo-A and control antibody treated monkeys) was based on a Mann and Whitney test taking into consideration only the manual dexterity score, but not the lesion extent, a crucial parameter in the present matter, especially for the control antibody treated monkeys (Fig. 2C, D). A new statistical procedure was introduced to consider both the behavioural score and the lesion extent by plotting the data as in Figures 2C and D but computing a line defined by minimizing the sum of distances between each data point and its projection onto the line (dashed lines in Figs. 2E,F). Then, data points were projected in the direction given by this line onto an orthogonal line segment (the values on that segment are independent of the y axis of the initial plot). Finally, the overlap between the two treatment groups of monkeys (blue circles for control antibody treated

monkeys and red crosses for anti-Nogo-A antibody treated monkeys) was assessed using the Mann and Whitney test. The two groups of monkeys are significantly different for the vertical slots (p=0.03) and horizontal slots (p=0.05).

2. Behavioural assessment of post-lesion recovery of manual dexterity using contact time

The data presented above, based on the standard analysis of the "modified Brinkman board" task (score given by the total number of pellets retrieved in 30 seconds), reflect not only the grasping ability but also other components of the movements such as the reaching phase, thus introducing more variability. Another source of variability may be the level of motivation and attention of the animal, changing from one day to another as well as along a daily session, thus affecting the data when considering a sustained performance lasting as much as 30 seconds. In order to investigate solely the capacity of fine finger movement (i.e. the precision grip between index finger and thumb), the grasping phase was analysed by measuring the so-called "contact time". It is defined as the time interval separating the first "contact" of the index finger with the food pellet and the final successful grasping using pad to pad opposition of the index finger and thumb (when the pellet left the slot), respectively for the first vertical and the first horizontal slots visited by the monkey's hand.

For the same two pairs of monkeys as in Figure 2, the "contact time" was plotted as a function of time pre- and post-lesion (Figs. 3A, B). Before lesion, all monkeys exhibited a short and fairly stable "contact time", which increased substantially immediately after the lesion, becoming more variable from one daily session to the next. However, the anti-Nogo-A antibody treated monkeys (red symbols in Figs. 3A, B) recovered faster and better than the control antibody treated monkeys (blue symbols in Figs. 3A,B).

The "contact time" in the vertical and horizontal slots has been plotted for all thirteen monkeys (box and whisker plots in Figs. 3C, D), showing the pre-lesion values compared with the post-lesion values at plateau, after recovery. For the vertical and the horizontal slots, the "contact time" values were significantly longer post-lesion than pre-lesion in four of the six control antibody treated monkeys (Mann and Whitney: $p<0.05$; Fig. 3C), corresponding to an incomplete recovery. In sharp contrast, the post-lesion "contact time" values in six of the seven anti-Nogo-A treated monkeys were not statistically different (Mann and Whitney: $p>0.05$) from the pre-lesion values (Fig. 3D), thus reflecting substantial functional recovery. Furthermore, the post-lesion "contact time" values are less variable in the anti-Nogo-A antibody treated than in the control antibody treated monkeys.

The "contact time" values were plotted in percent of recovery for the vertical and horizontal slots, respectively (Figs. 4A, B). The data were processed statistically as

described above (Figs. 2E, F). The anti-Nogo-A antibody treated monkeys were statistically different from the control antibody treated monkeys with respect to recovery of “contact time” for both the vertical slots (Mann and Whitney: $p<0.01$; Fig. 4C) and the horizontal slots ($p<0.01$; Fig. 4D).

Fig. 3

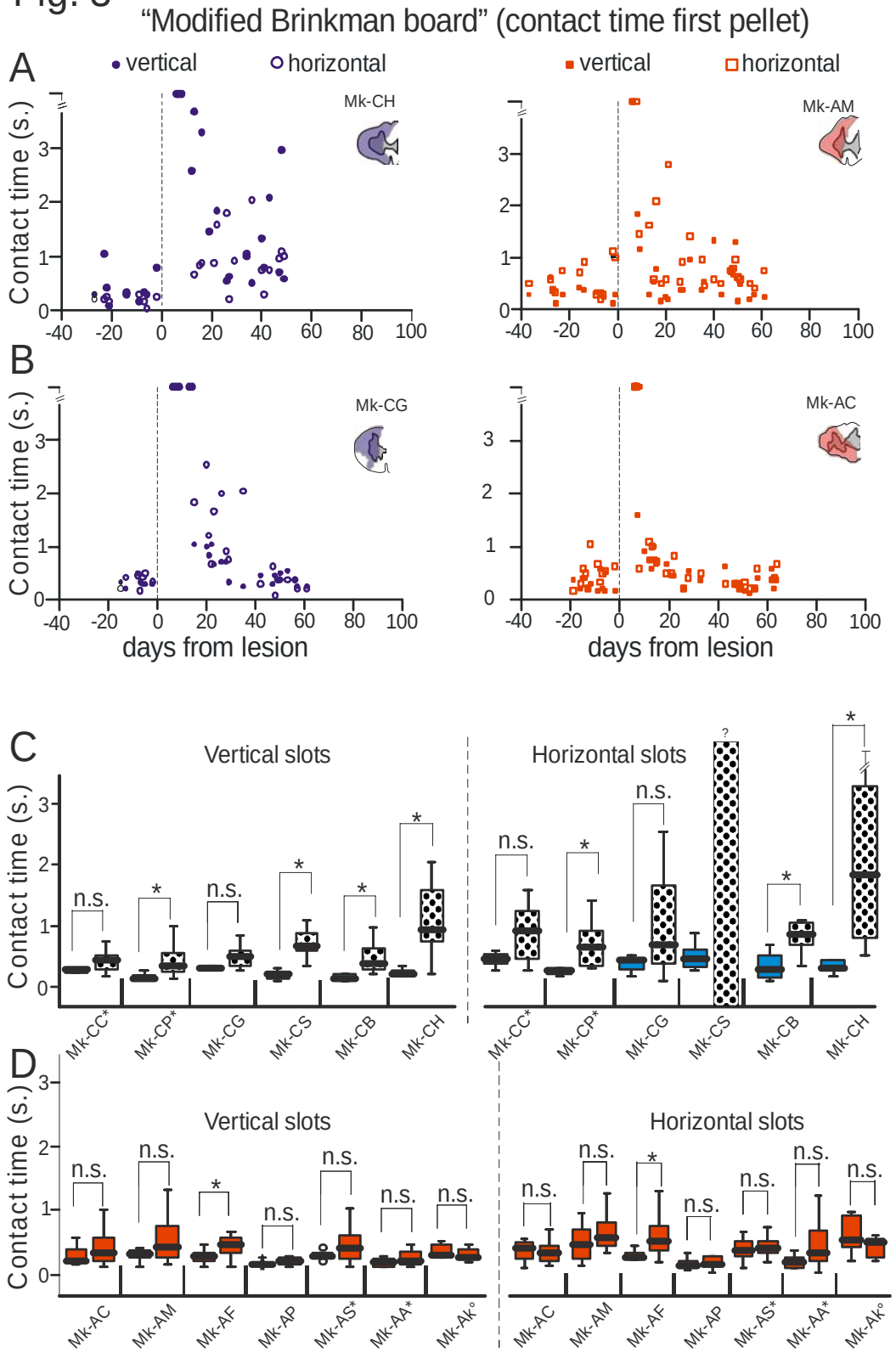

Figure 3

Quantitative assessment of manual dexterity based on "contact time"

Panels A, B: The contact time (in seconds), i.e. the time needed for a successful picking using the opposition of index finger and thumb in a pad to pad fashion, was plotted for two pairs of monkeys as a function of time (days) with respect to the lesion. The control antibody treated monkeys are in the left column (blue) and the anti-Nogo-A antibody treated monkeys in the right column (red). Data are shown before the lesion and over the post-lesion weeks for the vertically (filled symbols) and horizontally (open symbols) oriented slots. On the abscissa, day zero (vertical dashed line) is for the time point of the cervical lesion. For each plot, the inset on the upper right is a reminder of the lesion location and extent.

Panels C, D: The contact times measured before lesion and within the last ten post-lesion sessions in the plateau reflecting the recovery are distributed in the form of box and whisker plots. For each monkey, the left bar is for pre-lesion data whereas the right bar is for post-lesion data. In the box and whisker plots, the thick horizontal line in the box corresponds to the median value, whereas the top and bottom of the box are for the 75 and 25 percentile values respectively. The top and bottom extremities of the vertical lines on each side of the box are for the 90 and 10 percentile values, respectively. The asterisks indicate a statistically significant difference between pre- and post-lesion contact time values (Mann and Whitney test, $p<=0.05$) whereas "n.s." is for a non-significant difference ($p>0.05$).

As compared to our recent report (Freund et al., 2006), an additional monkey was introduced here (Mk-AK), in which the anti-Nogo-A antibody was infused after a delay of one week post-lesion. The recovery of manual dexterity was complete in this delayed treatment monkey (Mk-AK), both for the score (Fig. 2C,D) and the contact time (Fig. 4A,B) parameters, as it was observed in most anti-Nogo-A antibody treated monkeys subjected to immediate post-lesion treatment.

Fig. 4

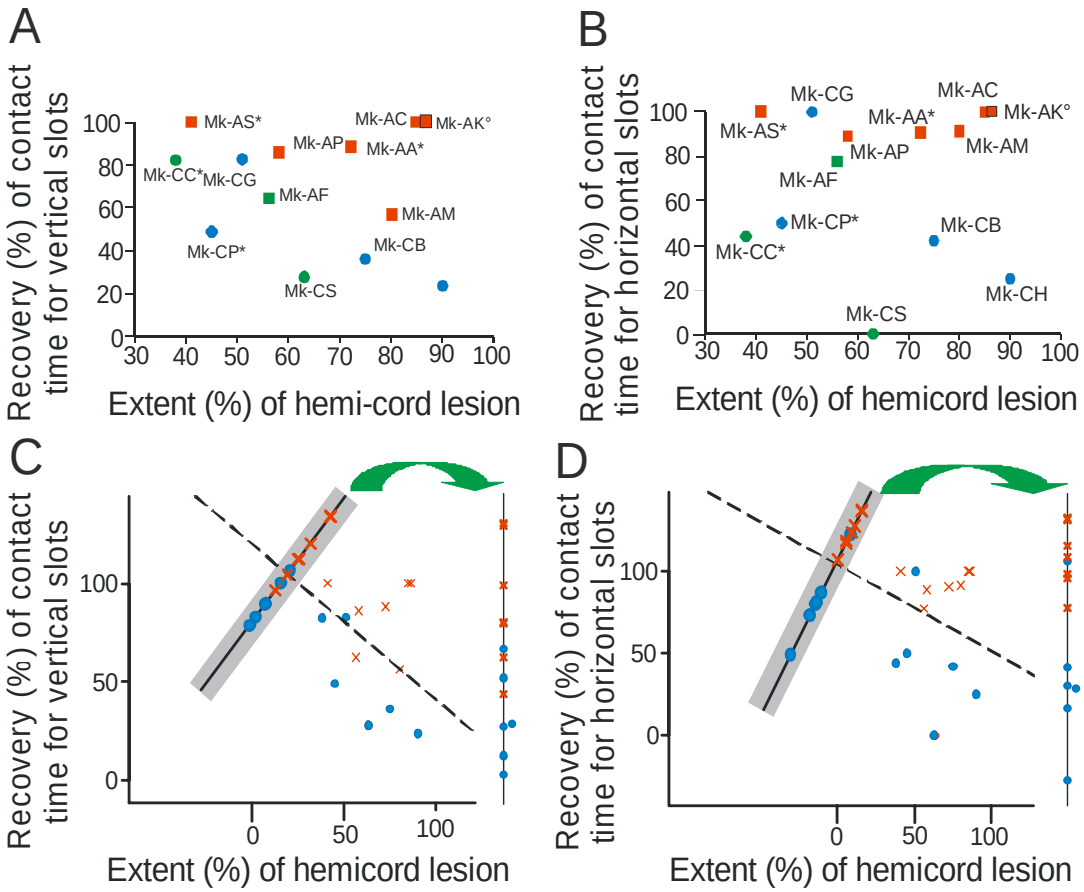

Figure 4

Relationship between contact time and hemi-cord lesion extent

Panel A, B: Relationship between the extent of the hemi-cord lesion and the functional recovery for the contact time needed for the first successful picking. Same conventions as in Figure 2C,D.

Panel C, D: Graphic illustration of the statistical analysis conducted on the contact times for the vertical (C) and horizontal (D) slots. Same conventions as in Figure 2E,F.

1.5 Dis cussion

Using a more detailed behavioural analysis with a new parameter (“contact time”), specifically reflecting finger dexterity, and introducing a new statistical test, the present report extends our initial observations (Freund et al., 2006) and demonstrates quantitatively that anti-Nogo-A antibody treatment in adult Macaque monkeys promotes functional recovery from cervical hemi-section. The anti-Nogo-A antibody enhanced recovery is paralleled by an increase of corticospinal axonal sprouting both caudal and rostral to the lesion (Freund et al., 2006, 2007).

An intrinsic difficulty of such lesion study is the considerable variability between individuals; the impact being even more substantial on an animal model (monkeys) for which ethical considerations drastically limits the number of animals. In rodents, the inter-individual variability is dealt with in part by increasing the number of animals included in the treated and control groups. In the present study, the inter-individual variability is due to inevitable variations in the location and extent of the lesion, as well as parameters related to motivational and attentional states of the monkeys. The variability related to the lesion extent was taken into account here statistically, in contrast to our previous report (Freund et al., 2006), by introducing a non-parametric statistical test comparing the anti-Nogo-A antibody treated (n=7) and control antibody treated monkeys (n=6) with assessment of both the percent of recovery and lesion extent. The statistical comparisons shown in Figures 2E and F (scores) and 4C and D (“contact time”) include all monkeys, irrespective of differences related to the lesion (Fig. 1B) or to the experimental protocol, such as the inclusion of three monkeys subjected to extensive ICMS sessions (green symbols in Figs. 2C,D and 4A,B). The new statistical test demonstrates that the anti-Nogo-A antibody treated monkeys (n=7) recovered their manual dexterity significantly better than the control antibody treated monkeys (n=6), as assessed either with the score (number of pellets retrieved for both vertical and horizontal slots) or with the contact time to retrieve the first pellet from the vertical or horizontal slots. Note however that, on contrary to what was expected, the recovery was comparable for the vertical and horizontal slots.

Whereas twelve monkeys were the same as those described in Freund et al. (2006), a thirteenth monkey was included here, belonging to the group of anti-Nogo-A antibody treated monkeys (Mk-AK). This animal differed from the other six monkeys of the same group by a delayed onset of anti-Nogo-A antibody infusion by one week. The goal here was to tentatively test the impact of such delay, which may be required in spinal cord injured patients to allow their stabilization before any intervention. These very preliminary data in a single monkey suggest that a delay of one week does not impact on the anti-Nogo-A antibody enhanced recovery. However, a larger number of animals with delayed

infusion are needed to confirm this observation and to determine the length of delay from which a decrease of efficacy occurs.

The originality of the present report is the newly introduced readout of manual dexterity (the “contact time” in the “modified Brinkman board” task) coupled to a new statistical analysis, forming together a pertinent, sensitive and robust assessment of functional recovery after cervical lesion in a non-human primate model, in spite of an inevitable inter-individual variability related to lesion characteristics. The new readout (contact time with the first pellet) reduces the impact of motivational variability and focuses on the finger dexterity, characteristic of primates (see Lemon and Griffiths, 2005 for review), by assessing the retrieval time itself without taking into account the less controlled inter-pellet time interval. The inter-individual variability mainly due to lesion properties is in line with the strong variability also encountered in spinal cord injured patients, thus making the present behavioural model in monkey clinically relevant. In spite of this inter-individual variability, the original behavioural readout (contact time) and bi-variate statistical assessment clearly demonstrate that anti-Nogo-A antibody treatment indeed promotes functional recovery from spinal cord lesion in primates. The Nogo-A antibody treatment thus represents a promising approach for improved clinical intervention in spinal cord injured patients, most likely in combination with complementary strategies.

Acknowledgements

The authors wish to thank the technical assistance of Georgette Fischer, Véronique Moret, Christine Roulin and Françoise Tinguely (histology and behavioural evaluations), Josef Corpataux, Bernard Bapst and Bernard Morandi (animal house keeping), André Gaillard (mechanics), Bernard Aebischer (electronics), Laurent Monney (informatics). Special thanks are due to Prof. J.P. Gabriel, Prof. Ch. Mazza and Mr. Th. Fournier (Department of Mathematics, University of Fribourg) for their contribution to the newly introduced statistical analysis.

Grant Sponsors: Swiss National Science Foundation, grants No 31-61857.00 (EMR) and No 31-63633.00 (MES), and 4038043918/2 (PNR-38); Novartis Foundation; The National Centre of Competence in Research (NCCR) on "Neural plasticity and repair", and the Christopher Reeves Foundation (Springfield, NJ). The antibodies were provided by Novartis Pharma.

Address for correspondence: Prof. Eric M. Rouiller, Unit of Physiology, University of Fribourg, Chemin du Musée 5, CH-1700 Fribourg, Switzerland. Phone: 0041 26 300 86 09. Fax: 0041 26 300 96 75. E-mail: Eric.Rouiller@unifr.ch

1.6 References

Bregman BS, Kunkel-Bagden E, Schnell L, Dai HN, Gao D, Schwab ME (1995) Recovery from spinal cord injury mediated by antibodies to neurite growth inhibitors. Nature 378:498-501.

Brösamle C, Huber AB, Fiedler M, Skerra A, Schwab ME (2000) Regeneration of lesioned corticospinal tract fibers in the adult rat induced by a recombinant, humanized IN-1 antibody fragment. J Neurosci 20:8061-8068.

Courtine G, Bunge M, Fawcett JW, Grossman RG, Kaas JH, Lemon R, Maier I, Martin J, Nudo RJ, Ramon-Cueto A, Rouiller EM, Schnell L, Wannier T, Schwab ME, Edgerton R (2007) Can experiments in nonhuman primates expedite the translation of treatments for spinal cord injury in humans? Nat. Med. 13:561-566.

Filbin MT (2003) Myelin-associated inhibitors of axonal regeneration in the mammalian CNS. Nat Rev Neurosci 4:703-713.

Freund P, Schmidlin E, Wannier T, Bloch J, Mir A, Schwab ME, Rouiller EM (2006) Nogo-A-specific antibody treatment enhances sprouting and functional recovery after cervical lesion in adult primates. Nature Med 12:790-792.

Freund P, Wannier T, Schmidlin E, Bloch J, Mir A, Schwab ME, Rouiller EM (2007) Anti-Nogo-A antibody treatment enhances sprouting of corticospinal axons rostral to a unilateral cervical spinal cord lesion in adult macaque monkey. J Comp Neurol 502:644-659.

Galea MP, Darian-Smith I (1997a) Corticospinal projection patterns following unilateral section of the cervical spinal cord in the newborn and juvenile macaque monkey. J Comp Neurol 381:282-306.

Galea MP, Darian-Smith I (1997b) Manual dexterity and corticospinal connectivity following unilateral section of the cervical spinal cord in the macaque monkey. J Comp Neurol 381:307-319.

Lemon RN, Griffiths J (2005) Comparing the function of the corticospinal system in different species: organizational differences for motor specialization? Muscle and Nerve 32: 261-279.

Liebscher T, Schnell L, Schnell D, Scholl J, Schneider R, Gullo M, Fouad K, Mir A, Rausch M, Kindler D, Hamers F PT, Schwab ME (2005) Nogo-A antibody improves regeneration and locomotion of spinal cord-injured rats. Ann Neurol 58:706-719.

Nudo RJ, Frost SB (2006) The evolution of motor cortex and motor systems. In: Krubitzer L, Kaas J, editors. Evolution of nervous systems, vol. 4.

Sasaki S, Isa T, Pettersson LG, Alstermark B, Naito K, Yoshimura K, Seki K, Ohki Y (2004) Dexterous finger movements in primate without monosynaptic corticomotoneuronal excitation. J Neurophysiol 92:3142-3147.

Schmidlin E, Wannier T, Bloch J, Rouiller EM (2004) Progressive plastic changes in the hand representation of the primary motor cortex parallel incomplete recovery from a unilateral section of the corticospinal tract at cervical level in monkeys. Brain Research 1017:172-183.

Schmidlin E, Wannier T, Bloch J, Belhaj-Saïf A, Wyss A, Rouiller EM (2005) Reduction of the hand representation in the ipsilateral primary motor cortex following unilateral section of the corticospinal tract at cervical level in monkeys. BMC Neuroscience 6:56.

Schnell L, Schwab ME (1990) Axonal regeneration in the rat spinal cord produced by an antibody against myelin-associated neurite growth inhibitors. Nature 343:269-272.

Schwab ME (2004) Nogo and axon regeneration. Curr Opin Neurobiol 14:118-124.

Thallmair M, Metz GAS, Z'Graggen WJ, Raineteau O, Kartje GL, Schwab ME (1998) Neurite growth inhibitors restrict plasticity and functional recovery following corticospinal tract lesions. Nature Neurosci 1:124-131.

Wannier T, Schmidlin E, Bloch J, Rouiller EM (2005) A unilateral section of the corticospinal tract at cervical level in primate does not lead to measurable cell loss in motor cortex. J Neurotrauma 22:703-717.

Weinmann O, Schnell L, Ghosh A, Montani L, Wiessner C, Wannier T, Rouiller E, Mir A, Schwab ME (2006) Intrathecally infused antibodies against Nogo-A penetrate the CNS and downregulate the endogenous neurite growth inhibitor Nogo-A. Molec Cell Neurosci 32:161-173.

Yiu G, He ZG (2006) Glial inhibition of CNS axon regeneration. Nat Rev Neurosci 7: 617-627.

Chapter 4

Anti-Nogo-A antibody treatment enhances sprouting of corticospinal axons rostral to a unilateral cervical spinal cord lesion in adult macaque monkey

This chapter has been adapted from an article originally published in Journal of Com parative Neurology (Patrick Freund [*], Thierry Wannier [*], Eri c Schmidlin[*], Jocelyne Bloch, Anis Mir, Ma rtin E. Schwab and Eric M. Rouiller; 502:644-659, 2007)

- These authors contributed equally to the study.

1.1 Abstract

After injury, re-growth of axons in mammalian adult central nervous system is highly limited. However, in monkeys subjected to unilateral cervical lesion (C7-C8 level), neutralization of an important neurite outgrowth inhibitor, Nogo-A, stimulated axonal sprouting caudal to the lesion, accompanied by enhanced functional recovery of manual dexterity, as compared to lesioned monkeys treated with a control antibody (Freund et al., 2006). The present study aimed at comparing the same two groups of monkeys for axonal sprouting rostral to the cervical lesion. The corticospinal tract was labeled by injecting the anterograde tracer BDA in the contralesional motor cortex. The corticospinal axons were interrupted at the level of the lesion, accompanied by retrograde axonal degeneration (axon dieback), reflected by the presence of terminal retraction bulbs. The number of terminal retraction bulbs was lower in anti-Nogo-A antibody treated monkeys and, when present, they were found closer to the lesion than in control antibody treated monkeys. As compared to control antibody treated monkeys, the anti-Nogo-A antibody treated monkeys exhibited an increased cumulated axon arbor length and a higher number of axon arbors going in the medial direction from the white to the grey matter. Higher in the cervical cord (at C5 level), the anti-Nogo-A treatment enhanced the number of corticospinal fibers crossing the midline, suggesting axonal sprouting. Thus, the anti-Nogo-A antibody treatment enhanced axonal sprouting rostral to the cervical lesion; some of these fibers grew around the lesion and into the caudal spinal segments. These processes paralleled the observed improved functional recovery.

1.2 Introduction

Following spinal cord injury, the re-growth of injured axons in the adult mammalian central nervous system (CNS) is extremely limited. Immediately after onset of injury, a series of structural changes occur that are proximal and distal to the point of transection. Whereas the distal stump of the axon degenerates, corresponding to the so-called Wallerian degeneration, the proximal stump of the axon dies back (i.e. retracts) by several hundreds microns, as observed for example in the corticospinal (CS) tract of mice (Kerschensteiner et al., 2005). A typical feature of the transected axonal stumps proximal to the lesion is the formation of a terminal retraction bulb (Kao et al. 1977a,b; Kalil and Schneider, 1975; Houle and Jin, 2001).

The fate of axotomized CS neurons in the monkey is controversial, with claims of significant loss (e.g. Pernet and Hepp-Reymond, 1975; Wolfarth, 1932; Holmes and May, 1909; Levin and Bradford, 1938), contrasting with evidence for survival of most CS neurons (Lassek, 1948; Tower 1940). In a recent study, we confirmed that most CS neurons survived the axotomy, but their soma shrink (Wannier et al., 2005). In spite of the survival of their cell body, only a very limited re-growth of injured nerve fibers may take place in the adult mammalian CNS due to the presence of neurite outgrowth inhibitors, such as Nogo-A (e.g. Caroni et al., 1988; Schwab 2004) within the CNS myelin. In fact, a therapeutic approach based on the application of antibodies neutralizing Nogo-A resulted in enhanced re-growth or regenerative sprouting of CS axons following spinal cord lesion in rats (e.g. Schnell and Schwab, 1990; Bregman et al., 1995; Thallmair et al., 1998; Brösamle et al., 2000; Liebscher et al., 2005; see Schwab 2004 for review), in marmosets (Fouad et al., 2004) and in macaque monkeys (Freund et al., 2006). Compared with animals also subjected to a spinal cord lesion and treated with a control antibody, the anti-Nogo-A antibody treatment promoted sprouting of CS axons caudal to the lesion, in the area of denervated motoneuron pools. In rats (Bregman et al., 1995; Thallmair et al, 1998; Schwab, 2004; Liebscher et al., 2005) and macaque monkeys (Freund et al., 2006), the sprouting of CS axons caudal to the lesion, promoted by anti-Nogo-A antibody

treatment, was paralleled by an enhancement of functional motor recovery for various specific behavioral tasks, even leading to a complete recovery of performance on some of them.

Knowing that the re-growth of CS fibers caudal to a cervical spinal lesion occurred in parallel with better functional recovery of the hand in monkeys (Freund et al., 2006), the aim of the present study was to investigate, anatomically, how a cervical cord hemi-section affects the CS axons rostral to the lesion in terms of die-back and formation of terminal retraction bulbs (see Fig. 1A). A specific goal was to assess whether the anti-Nogo-A antibody treatment may reduce or prevent axonal retraction effects proximal to the lesion and, in addition, favor local axonal sprouting. Thirteen macaque monkeys were therefore subjected to a cervical cord lesion unilaterally interrupting the dorsolateral funiculus; seven monkeys were treated with an anti-Nogo-A antibody whereas the other six received a control antibody. The anterograde labeling of CS axons originating from the contralesional hemisphere, allowed us to address the following issues:

- Does the proximal part of the axotomized CS axons retract from the lesion? If yes, in what proportion of CS axotomized axons does such a retraction occur and what is the distance of retraction? Does anti-Nogo-A antibody treatment prevent such retraction of CS axons?

- Do some axotomized CS axons attempt to re-approach and eventually enter the lesion? If yes, does the anti-Nogo-A antibody treatment make such attempts more successful?

- Above the cervical lesion, do the axotomized CS axons sprout, giving rise to collaterals medially into the grey matter and/or growing around the lesion thus possibly contributing to the enhanced presence of CS axons observed caudal to the lesion in anti-Nogo-A antibody treated monkeys (Freund et al., 2006)

1.3 M aterials and Methods

Animals

The experiments were conducted on sixteen adult macaque monkeys (Macaca mulatta and fascicularis, Tables 1 and 2; see also Supplementary Table 1 in Freund et al., 2006) of either sex. Surgical procedures and animal care were conducted in accordance with the Guide for the Care and Use of Laboratory Animals (ISBN 0-309-05377-3; 1996) and approved by local (Swiss) veterinary authorities. Conditions of housing of the animals as well as the behavioral procedures aimed at assessing the manual dexterity of monkeys before and after the lesion were described in detail earlier (Schmidlin et al., 2004; 2005; Freund et al., 2006). Only the methods specifically relevant for the present study will be described below in detail. Out of the sixteen monkeys, thirteen were subjected to a unilateral cervical cord lesion (see below). The lesioned monkeys were 3.5 to 6.9 years old at time of sacrifice, thus corresponding to young adult monkeys, and their weight ranged from 3.0 to 5.0 kg. The other three monkeys (see Table 2 for age and weight) were intact and were considered here for comparison of some tracing data (Fig. 5E and F) with the lesioned monkeys. One of the three intact monkeys was used in a previous tracing study describing the CS projection originating from the primary motor cortex (Rouiller et al., 1996).

Surgical procedures: unilateral lesion of the dorsolateral funiculus

In thirteen monkeys a unilateral cervical cord lesion was performed as follows. Intramuscular injection of ketamine (Ketalar®; Parke-Davis, 5 mg/kg, i.m.) was performed to induce anesthesia and atropine was injected i.m. (0.05 mg/kg) to reduce bronchial secretions. Before surgery, the animal was treated with the analgesic Carprofen (Rymadil®, 4 mg/kg, s.c.). Then, a continuous perfusion (0.1 ml/min/kg) through an intravenous catheter placed in the femoral vein with a mixture of 1% propofol (Fresenius ®) and a 4% glucose solution (1 volume of propofol and 2 volumes of glucose solution) induced a deep and stable anaesthesia. The animal was then placed in a stereotaxic headholder, using ear bars covered at their tip with local anesthetic. Surgery was carried out

under aseptic conditions. The following parameters were monitored: heart rate, respiration rate, expired CO_2, arterial O_2 saturation and body temperature. In early experiments, an extra intravenous bolus of 0.5 mg of ketamine diluted in saline (0.9%) was added at potentially more painful steps of the surgical procedure, such as laminectomy. In later experiments, ketamine was added to the perfusion solution and delivered throughout surgery (0.0625 mg/min/kg). Placed in a ventral decubitus position, the spinal processes from C2 to Th1 were exposed. The paravertebral muscles were retracted and the laminae of the segments C6, C7 and Th1 were dissected. A complete C6 laminectomy and an upper C7 hemi-laminectomy were then performed. The ligamentum flavum was removed in order to expose the dura mater, which was incised longitudinally. From previously available anatomical material, the rostro-caudal level at which the dorsal rootlets entered respectively the 7^{th} and the 8^{th} cervical spinal segments corresponded to the rostral zone of the spinal cord covered by the 6^{th} cervical lamina. The dorsal root entry zone at the C7/C8 border was then identified, providing a medial landmark for placing a surgical blade (no 11, Paragon®), which was used to perform an incomplete section of the cervical cord at this level. The surgical blade was inserted 4 mm in depth perpendicular to the spinal cord, and the section was prolonged laterally to completely cut the dorsolateral funiculus. In most cases, such a section completely interrupted the CS tract unilaterally. As illustrated in detail in a recent report (Freund et al., 2006), the lesion was aimed at a site caudal to the biceps motor nucleus but rostral to the nuclei of triceps, forearm and intrinsic hand muscles (Jenny and Inukai, 1983). The muscles and the skin were sutured. The animal usually recovered from anesthesia 15-30 minutes after interruption of the perfusion with propofol and was treated post-operatively with an antibiotic (Ampiciline 10%, 30 mg/kg, s.c.). During the week following the surgery, additional doses of Carprofen were given daily (pills of Rymadil mixed with food). After the spinal lesion, the animal was kept alone in a separate cage for a couple of days in order to perform a careful watch of its condition.

In addition, the transient separation in a cage allowed better conditions for recovery than the usual group housing with other monkeys, in which the animal was usually replaced two to five days after surgery. Some of the behavioral deficits due to the lesion were described previously (Freund et al., 2006), as well as the time course of recovery observed with various motor tasks.

Anti-Nogo-A antibody treatment

The treatment lasted 4 weeks, using either the anti-Nogo-A antibody or control antibody (14.8 mg in 4 weeks) delivered from an osmotic pump, placed in the back of the animal a few minutes after the lesion of the cervical cord. A small silastic tube, attached at one of its extremity to the pump, was positioned intrathecally 3-5 mm rostral to the cervical lesion. The pump had a volume of 2 ml but one or the other of two types of pumps were used, allowing treatment during 4 or 2 weeks. In the latter case, after 2 weeks of treatment, the first pump was replaced under anesthesia by a second pump for another 2 weeks treatment. Seven monkeys received either one of two monoclonal antibodies (mAbs) against different sites of Nogo-A (Table 1): the mouse mAB **11C7** (Liebscher et al., 2005) was raised against a 18 amino acid peptide of rat Nogo-A (aa623 – 640), close to the most inhibitory region of the Nogo-A protein (Oertle et al., 2003), which cross-reacts with mouse and monkey Nogo-A. The second antibody used, **mAb hNogo-A** was raised by immunization with the whole Nogo-A specific region of the human Nogo-A sequence. The characterization of the two anti-Nogo-A antibodies was performed as follows. Cynomologus monkey brain tissue (cerebral cortex) was homogenized in T-PER lysis buffer (Pierce) using a rotor stator. For Western Blots, aliquots corresponding to 10 µg total protein were separated on a 4-12% NuPAGE gel (Invitrogen). The protein bands were transferred to a nitrocellulose membrane. The membrane was blocked for 1 hour at room temperature in blocking buffer (2% blocking reagent (Amersham) in TBS-T), then incubated with either 0.1 nM hNogoA mAB or 1nM 11C7 antibody in blocking buffer for 2 hours, followed by 1 hour incubation with either anti-human or anti-mouse peroxidase coupled secondary antibodies (1:500 000

dilution in blocking buffer). Signals were detected using ECL-Advance Western Blot detection reagents (Amersham) and exposure to film for 1 minute. Both antibodies recognize primate Nogo-A monospecifically on Western blots (Figure 1B; see also Oertle et al., 2003). The antibodies were purified as IgGs and concentrated to 3-10 mg/ml in phosphate buffered saline (PBS). In the other six monkeys, a control antibody was infused, corresponding to a purified IgG of a mouse mAb directed against wheat auxin (AMS Biotechnology, Oxon/UK).

In safety studies conducted in the monkey, remaining antibodies were retrieved form the pump at the end of the treatment (after 4 weeks), when the osmotic pumps were removed. The antibody hNogoA mAB was found to be completely stable. Both anti-Nogo-A antibodies used were shown to be distributed with the flow of CSF over most of the spinal cord and brain within 7 days of infusion and to penetrate deeply into the parenchyma (Weinmann et al, 2006). They are internalized together with endogenous Nogo-A protein into endosomal and lysosomal structures, leading to a down regulation of Nogo-A (Weinmann et al, 2006). The concentrations chosen for the anti-Nogo-A antibody treatment (3-10 mg/ml) are high in relations to the high sub-nanomolar affinities of the antibody for Nogo-A. Therefore, differences in efficacy are not expected at these concentrations. Due to the limited number of monkeys treated either with one (11C7) or the other (hNogoA) of the two anti-Nogo-A antibodies, the issue of whether there was a difference in efficacy between the two could not be addressed.

In the first six lesioned monkeys included in the study (pilot animals), the identity of the antibody contained in the pump was known to the experimenters (Supplementary Table 1 in Freund et al., 2006). For the seven other lesioned monkeys, the experimenters were blind as to the antibody contained in the pump (Supplementary Table 1 in Freund et al., 2006) until the end of the experiment (sacrifice of the animal and reconstruction of the lesion). The pump and the silastic tube were removed after four weeks of treatment. Each pump was then checked for the volume left in order to ensure that the antibody has been properly delivered.

Tracing experiments and histological assessment of the lesion

The anterograde tracer Biotinylated Dextran Amine (BDA, Molecular Probe®) was injected in the contralesional hemisphere (motor cortex) of the thirteen lesioned monkeys to label the CS tract, using Hamilton syringes. Similarly, for comparison, BDA was injected unilaterally in the motor cortex of three additional intact monkeys (Table 2). Under propofol anesthesia (see above), a craniotomy was performed to expose the central and arcuate sulci. Injections of BDA were performed in the primary motor cortex (M1), i.e. in the rostral bank of the central sulcus, in a territory corresponding mainly to the hand representation. Based on previously available monkeys in which the hand representation was determined by intracortical microstimulation (Rouiller et al., 1996, 1998; Schmidlin et al., 2004, 2005), the hand territory was estimated to be located immediately rostral to the central sulcus, extending medio-laterally between 10 to 15 mm from midline, with its most lateral extent roughly corresponding to the genu of the arcuate sulcus. In this territory of about 5-6 mm along the medio-lateral axis, three to four syringe penetrations were aimed perpendicularly to the cortical surface, at 1.5 to 2 mm distance from each other. To cover most of the rostral bank of the central sulcus, BDA was typically deposited along each syringe penetration at two (rarely three) depths, usually at sites located 3 and 7 mm below the pial surface. Usually one to three additional syringe penetrations were performed more medially, still along the central sulcus, to cover the representation of more proximal territories (wrist, elbow, shoulder, trunk). The detailed parameters of BDA injections are given for each monkey in Table 1. Based on our previous experience with tracing the CS tract with BDA in monkeys (Rouiller et al., 1996), the survival time after BDA injection was set to three weeks for the first two lesioned animals. However, it turned out that the cervical lesion substantially slowed down the anterograde axonal transport of BDA and therefore the tracer did not reach the cervical segments of interest. For this reason, a much longer survival time (around 60-80 days) was applied to the other eleven lesioned monkeys, allowing transport of BDA up to

thoracic level. Furthermore, it appeared that in two lesioned monkeys, the BDA staining was not dense enough in the cervical cord for a full anatomical analysis. Consequently these four animals (too short survival time or insufficient staining) were not considered further in the present study. The list of the nine lesioned monkeys considered in the present study for the analysis of CS axons rostral to the cervical lesion is given in Table 1.

At the end of the survival period, the animals were sacrificed under deep (lethal) anaesthesia (90 mg of sodium pentobarbital/Kg body weight) by transcardiac perfusion with 0.9% saline (400 ml). The perfusion was continued with fixative (3 liters of 4% phosphate buffered paraformaldehyde in 0.1 M phosphate buffer, pH=7.6) and solutions (2 liters each) of the same fixative containing increasing concentrations of sucrose (10, 20 and 30%). The brain and spinal cord were dissected and placed in a 30% solution of sucrose (in phosphate buffer) for cryoprotection for seven days. Frozen sections (50 µm thick) of the brain were cut in the frontal plane whereas frozen sections (50 µm thick) of the cervical cord (approximately the segments C6-T3) were cut in the parasagittal longitudinal plane and collected in three series for later histological processing. Upper cervical segments and lower thoracic spinal segments were cut in the frontal plane at 50 µm thick and sections were also collected in three series. BDA staining was revealed in one series of spinal cord sections, as described in detail in previous reports (Rouiller et al., 1996, 1998). The second series of spinal cord sections were immunohistochemically processed to visualize corticospinal axons using the marker SMI-32, as recently reported (Wannier et al., 2005), a series of sections also used to reconstruct the location and extent of the cervical lesion (Fig. 1C), as described in detail earlier (Schmidlin et al., 2004; Wannier et al., 2005). The third series of sections was processed to visualise another anterograde tracer (Dextran-Fluorescein) injected in the ipsilesional hemisphere, but these data will not be presented here. A light microscope (Olympus) and Neurolucida® software were used for analyses of CS axon numbers, retraction, arbor length, sprouting and trajectories.

Normalization of BDA labeled CS axons

Due to variations in the uptake of the tracer BDA (Table 1; see also Supplementary Table 1 in Freund et al., 2006), the number of BDA labeled CS axons varied from one animal to the next. In order to normalize the BDA data across monkeys, the total number of BDA-labeled CS axons was counted at C5 level on a frontal section in the white matter, in the two dorsolateral funiculi and in the ventral funiculus ipsilateral to the BDA injection in the cerebral cortex (Table 1).

Measurement of retraction of lesioned CS axons and number of CS axons with terminal retraction bulbs

On the photomicrographs of the parasagittal cervical cord sections processed for BDA visualization, a first line was drawn along the rostral border of the lesion using CorelDraw® software. A second line, parallel to the first one, was drawn 600 µm more rostrally, following the orientation of the axons. The first line offered a fixed point of reference for measuring the distance of CS axonal retraction (Fig. 2A). The distance of the center of each terminal bulb (identified as being at least twice the axon caliber) to the lesion border was measured within this space. Only CS axons with terminal bulbs located in the white matter at a maximal distance of 600 µm from the edge of the lesion were used for this analysis (Fig. 2A). A more specific question was addressed to the terminal bulbs located in the first 100 µm from the rostral border of the lesion. CS axon arbors displaying no such terminal bulbs were not taken into consideration for measurement, because it could not be excluded that the cut end of the axons was leaving the plane of the section, thereby continuing on an adjacent section. The cumulated number of CS axon with terminal bulbs observed on the BDA sections analyzed was finally divided by the total number of BDA-labeled CS axons observed at C5, for normalization as explained above. The above assessments of the number of CS axons with terminal retraction bulbs (Figs. 2D and 2F) and the distance of retraction (Fig. 2E) are represented schematically by the numbers "1" and "2" in Figure 1A.

Measurement of CS axon arborization and CS sprouting

In the grey matter, the presence of BDA labeled CS axon arbors was investigated at the immediate border of the lesion and within an area extending up to 500 µm away from the rostral limit of the lesion at a total magnification of 200x. For this analysis (schematically represented by the number "3" in Figure 1A), all parasagittal spinal cord sections processed for BDA visualization (150 µm intervals) on the ipsilesional cervical side were chosen. Using neurolucida® software, each BDA-labeled axon segment in the grey matter was traced. Then the cumulated axon arbor length was computed and normalized with respect to the total number of CS axons labeled at C5 level, as described above.

Using the software neurolucida® as well, the BDA-labeled CS axon arbors which attempted to enter the lesion by crossing the rostral limit of the lesion were drawn. The cumulated number of CS axon arbors intercepting the rostal border of the lesion was determined in each monkey (analysis represented schematically by the number "4" in Fig. 1A).

To analyze further the sprouting of the CS axons in the region rostral to the lesion, BDA-labeled CS axon arbors entering into the grey matter were counted up to a distance of 3 mm away from the rostral border of the lesion on the parasagittal sections (number "5" in Fig. 1A). For this analysis, histological sections exhibiting BDA-stained CS axons in the white and grey matter were selected (ranging from 5 to 9 slides across animals). At their crossing with the white/grey matter border, these axon arbors were generally oriented along a perpendicular axis, although some of them showed an orientation that was slightly oblique from the axis perpendicular to the white/grey matter border.

Furthermore, at more rostral levels in the cervical cord, five frontal sections taken at C5 level were selected to count the number of CS fibers crossing the midline at C5 (analysis represented schematically by the number "6" in Fig. 1A). Using neurolucida® software, a vertical line was superimposed onto the midline of the frontal section of the cervical cord at C5 level and two additional vertical lines were drawn at a distance of 250 µm on each side away from the line on the

midline (Fig. 5C). CS axon arbors crossing these lines were counted (if the same axon arbor was long enough to intercept two or three lines, it was counted once) and the cumulated number for the five frontal sections were normalized by dividing by the total number of CS axons present at C5 level in the white matter, as described above.

Fig.1

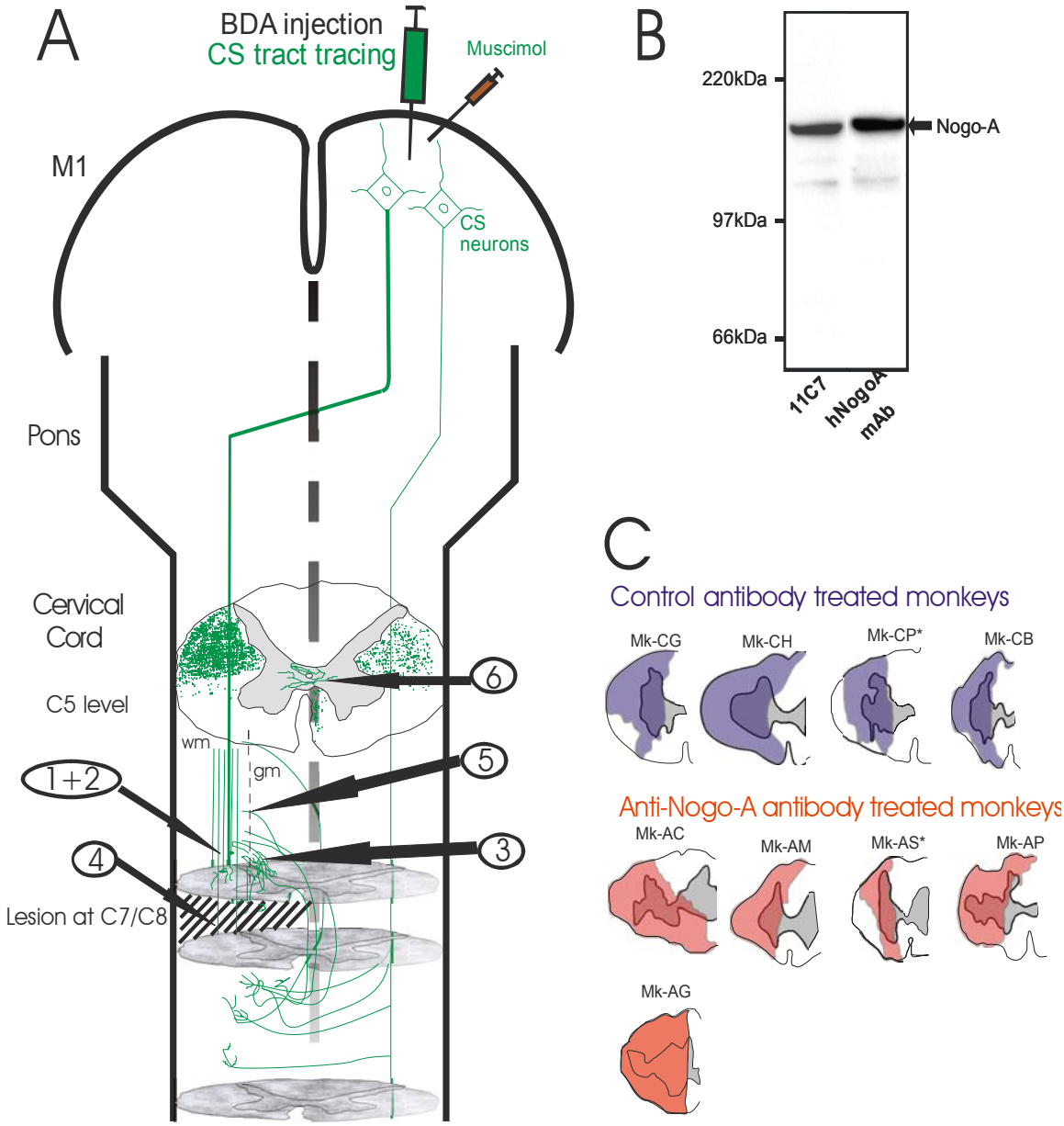

Figure 1

Panel A: Schematic representation of the macaque monkey corticospinal (CS) projection originating from the right primary motor cortex (M1) as seen at cervical cord level, as a result of BDA injection (green syringe) in the right motor cortex. At C5 level, on a frontal section of the cervical cord, green dots indicate the location and distribution of the CS axons, forming the dorsolateral funiculus (dlf) contralateral to the injection site and the uncrossed CS axons, present in the dorsolateral and ventral funiculi ipsilateral to the injection site. At C7/C8 level, the ensemble of black oblique lines represent the cervical lesion performed in the present study in

thirteen monkeys. Rostral to the lesion, parallel green thick lines represent CS axons in the dorsolateral funiculus, interrupted by the lesion. Axonal sprouting is represented by thinner lines arising from the thick green lines. The numbers "1" to "6" point to the six sites of the quantitative analyses performed in the present study as explained in the method section. The brown syringe is for pharmacological reversible inactivation experiments of the contralesional primary motor cortex (M1), as previously reported (Schmidlin et al., 2004) and mentioned in the discussion. The thick vertical dashed line represents midline, whereas the thin vertical dashed line represents the boundary between the white (wm) and the grey (gm) matter.

Panel B: Both monoclonal antibodies against Nogo-A, 11C7 and anti-hNogo-A, recognize a single band running at the expected molecular weight of Nogo-A in cortex homogenates of adult macaque monkeys separated by SDS polyacrylamide gel electrophoresis.

Panel C: Reconstruction from parasagittal sections in the frontal plane of the location and extent of the lesion at C7/C8 lesion performed in the nine monkeys included for the present analysis of the CS tract rostral to the lesion. Lesions in blue are for the control antibody treated monkeys (n=4) whereas red represents the lesion in the anti-Nogo-A antibody treated monkeys (n=5). The asterisks point to the two monkeys with incomplete lesion of the dorsolateral funiculus (see text).

1.4 Results

Morphology of the unilateral cervical cord lesion

Following unilateral injection of BDA in the contralesional primary motor cortex (M1) mainly in the hand representation, the main CS tract was found at cervical cord level (C5) in the left dorsolateral funiculus, representing 90-95% of the whole CS population (Fig. 1A). The uncrossed CS projection (representing 5-10% of CS axons) was found in the dorsolateral and ventral funiculi homolateral to the BDA injection (Fig 1A). These figures are consistent with a recent report on the distribution of CS axons at the level of the lumbar cord (Lacroix et al., 2004). The unilateral section of the cervical cord was aimed at transecting the crossed CS tract in the left dorsolateral funiculus (Fig. 1C). In seven out of nine lesioned monkeys included in the present anatomical analysis, the dorsolateral funiculus was indeed completely interrupted, as assessed on the basis of the location and extent of the lesion (Fig. 1C) in comparison to the location and extent of the dorsolateral funiculus in an intact monkey after BDA injection in M1. In addition, BDA labeling of CS axons in the white matter provided evidence that

all axons in the dorsolateral funiculus were indeed sectioned in these seven monkeys. On the other hand, in two monkeys (indicated by an asterisk in Fig. 1C), the lesion did not completely interrupt the dorsolateral funiculus in its most ventro-lateral extent and therefore some CS fibers were spared. The intact BDA-labeled CS fibers were easily detectable, because of their straight course in the white matter; they were excluded from the anatomical analysis.

The lesion territory was easily distinguishable from the intact spinal cord tissue. A scar consisting of non-homogenous tissue and of cysts of various diameters was observed, acting as a clear physical impediment for axonal re-growth in the rostro-caudal direction (Fig. 3A).

Effects of anti-Nogo-A antibody treatment on CS axons in the region rostral to the cervical cord lesion

In order to evaluate whether the anti-Nogo-A antibody treatment favored the maintenance, growth and/or sprouting from the CS axons in the area rostral to the cervical cord lesion, six quantitative morphological analyses were conducted at specific locations, represented schematically by the numbers "1 to 6" in Figure 1A, and presented below in the paragraphs numbered accordingly. The detailed results obtained for these six analyses are given for each individual lesioned monkey in Table 1.

Fig.2

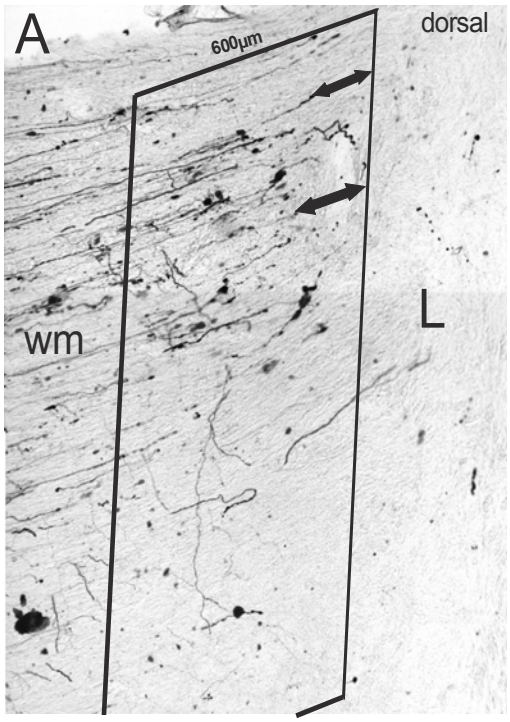
A
600μm
dorsal
wm
L

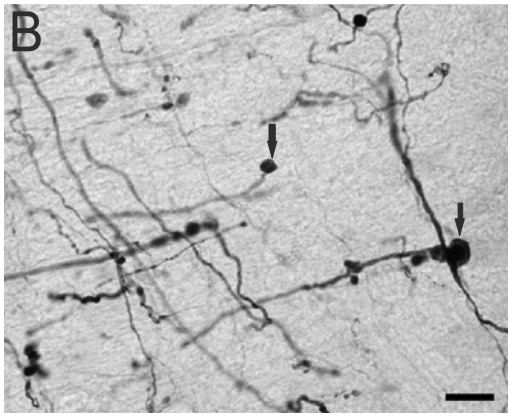
B

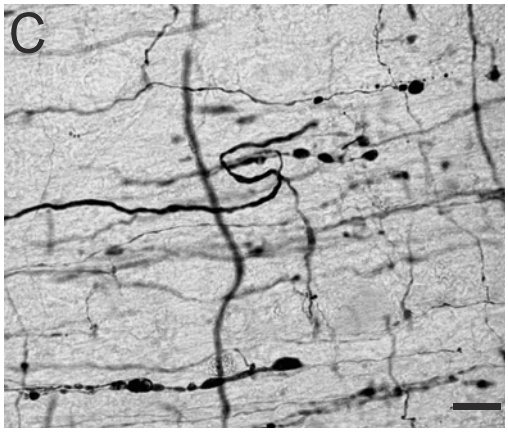
C

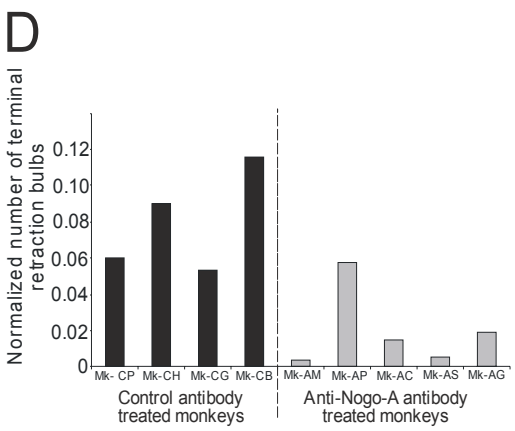
D
Normalized number of terminal retraction bulbs
0.12
0.10
0.08
0.06
0.04
0.02
0
Mk- CP
Mk-CH
Mk-CG
Mk-CB
Mk-AM
Mk-AP
Mk-AC
Mk-AS
Mk-AG
Control antibody treated monkeys
Anti-Nogo-A antibody treated monkeys

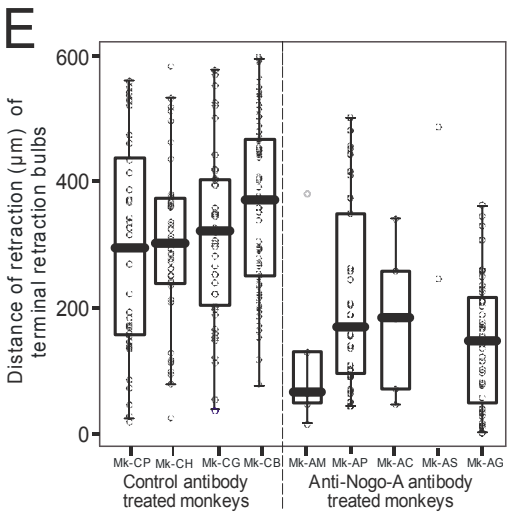
E
Distance of retraction (μm) of terminal retraction bulbs
600
400
200
0
Mk-CP
Mk-CH
Mk-CG
Mk-CB
Mk-AM
Mk-AP
Mk-AC
Mk-AS
Mk-AG
Control antibody treated monkeys
Anti-Nogo-A antibody treated monkeys

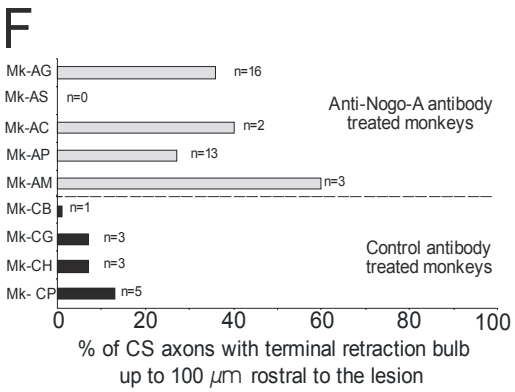
F
Mk-AG
n=16
Mk-AS
n=0
Mk-AC
n=2
Mk-AP
n=13
Mk-AM
n=3
Mk-CB
n=1
Mk-CG
n=3
Mk-CH
n=3
Mk- CP
n=5
Anti-Nogo-A antibody treated monkeys
Control antibody treated monkeys
0
20
40
60
80
100
% of CS axons with terminal retraction bulb up to 100 μm rostral to the lesion

Figure 2

Panels A-C: The panel A photomicrograph displays transected BDA-labeled CS fibers at the proximity of the rostral border of the lesion in the white matter. The lesion border appears as non-homogenous axon free tissue distinct from more rostral intact spinal cord tissue. The arrows with double heads illustrate how the distance was measured between a terminal retraction bulb and the rostal border of the lesion. L=Lesion; wm, white matter. The panels B and C photomicrographs illustrate at higher magnification BDA labeled CS axons close to the lesion forming retraction bulbs (arrows). Scale bars=50μm.

Panel D: Normalized number of terminal retraction bulbs observed within a territory extending 600 □m away from the lesion border in the rostral direction for the nine lesioned monkeys included in the present study, separately for the control antibody treated monkeys (n=4) and the anti-Nogo-A antibody treated monkeys (n=5). The site of this analysis is schematically represented by the number “1” in Figure 1A.

Panel E: For each monkey, the distance between each terminal retraction bulb observed and the rostal limit of the lesion was plotted. Superimposed on the individual measurements, the box and whisker plot depicts the median value (horizontal bar in the middle of the box) and the 25 and 75 percentiles (bottom and top extremities of the box, respectively). The site of this analysis is schematically represented by the number “2” in Figure 1A.

Panel F: Instead of considering a territory of 600 □m away from the lesion in the rostral direction (panels A, D and E), a more restricted area only 100 □m away from the lesion was considered. The horizontal bar represents the % of the total number of terminal retraction bulbs observed up to 600 □m away from the lesion which terminates not further than 100 □m from the rostral border of the lesion.

1) Appearance and number of terminal retraction bulbs on transected BDA labeled CS axons

In all monkeys subjected to cervical cord lesion, BDA-labeled CS axons displaying terminal retraction bulbs were found rostral to the lesion (Fig. 2A, B and C), corresponding to a common feature for transected axons that underwent retrograde degeneration (Kao et al., 1977a,b; Kalil and Schneider, 1975; Houle and Jin 2001). To investigate the influence of anti-Nogo-A antibody treatment upon the transected CS axons, the region rostral to the lesion was scanned at high magnification for CS axons exhibiting terminal retraction bulbs.

Terminal retraction bulbs in the area rostral to the lesion, in a territory of white matter extending 600 µm away from the lesion border, were counted in each monkey and cumulated for all parasagittal sections analyzed. For normalization, the cumulated numbers of terminal retraction bulbs in each monkey were divided by the total number of BDA-labeled CS fibers in the white matter at C5 level. Strikingly, in anti-Nogo-A antibody treated monkeys, the normalized cumulated numbers of CS axons exhibiting terminal retraction bulbs were significantly lower (approximately 4x on average) than in control antibody treated monkeys (Fig. 2D). This difference was statistically significant (Mann and Whitney test: $P<0.05$). Furthermore, from a qualitative point of view, anti-Nogo-A antibody treated monkeys, instead of exhibiting the standard terminal retraction bulbs, often showed outgrowing sprouts being tortuous in shape and decorated with varicosities, strongly resembling boutons *en passant* and *terminaux* that approached the lesion border (Fig. 3B and C).

Figure 3

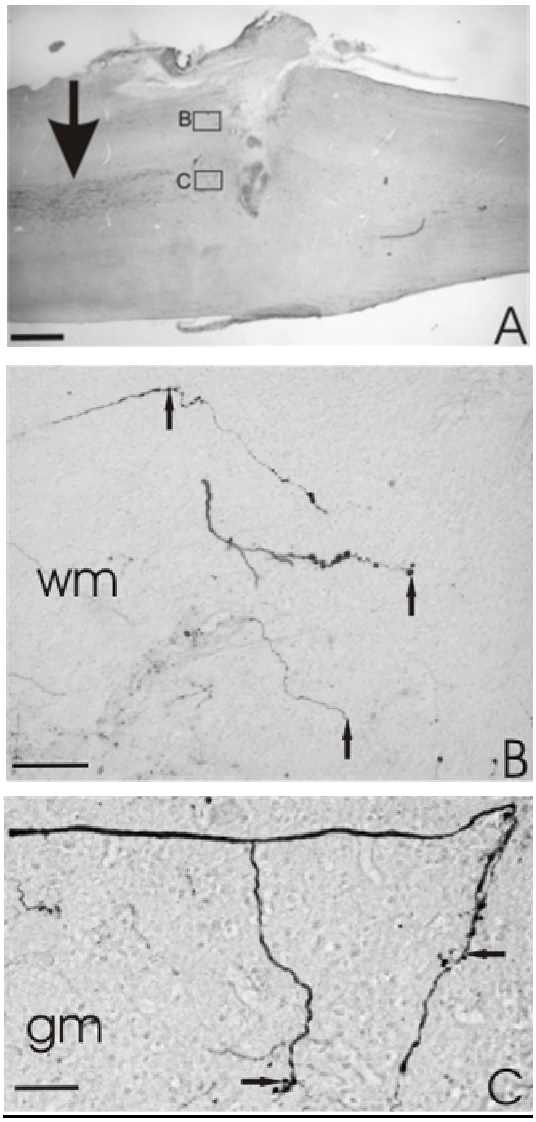

Figure 3

Panel A: Photomicrograph of a parasagittal spinal cervical-thoracic cord section illustrating the appearance of BDA-labeled CS fibers in the grey matter, rostral to the lesion (arrow). The section was taken from an anti-Nogo-A antibody treated monkey. The CS axons in the white matter and the CS axon arbors in the grey matter, shown at higher magnification below in panels B and C, are located in the cervical cord as indicated by the two rectangles.

Panels B and C: Typical examples of sprouting from transected CS axons in the white (B) and grey matter (C) giving rise to collaterals directed towards the lesion border. These axons were tortuous and irregular in growth with varying diameter and varicosities (arrows) along their course and at their termination. wm=white matter; gm=grey matter.

Scale Bar=1 mm in panel A, 100 □m in panel B and 50 □m in panel C.

2) CS axonal retraction (axonal dieback)

To address the issue of a response of the transected CS axons to anti-Nogo-A antibody treatment, the distance of retraction from the lesion for the CS axons exhibiting a terminal retraction bulb was measured. All terminal retraction bulbs within a distance of 600 μm from the rostral limit of the lesion were included.

The average retraction distance from the lesion border was markedly reduced in anti-Nogo-A antibody treated monkeys as compared to the control

antibody treated monkeys (Fig. 2E). This difference was not statistically significant (Mann and Whitney test, P>0.05). However, because of the large variability across monkeys and because of the much lower number of CS axons with terminal retraction bulbs in the anti-Nogo-A antibody treated monkeys with regard to that in the control antibody treated monkeys, the conditions were not favorable to detect a possible treatment-induced population difference (Fig. 2E).

A prominent difference appeared, however, when focusing on a more restricted area, within 100 µm of the rostral limit of the lesion (Fig. 2F). About 10% of transected CS axons displaying a terminal retraction bulb were found in the control antibody treated monkeys. In contrast, this proportion ranged between 27 and 60% in the anti-Nogo-A antibody treated monkeys (see also Table 1). As the total number of terminal retraction bulbs was much higher in the control antibody treated monkeys (Fig. 2D), the data of Figure 2F indicate that the transected CS axons in anti-Nogo-A antibody treated monkeys rarely formed terminal retraction bulbs, but when they did, they were located close to the lesion. In contrast, the numerous terminal retraction bulbs in the control antibody treated monkeys had generally retracted further from the lesion.

3) Density of CS axon arbors in the grey matter rostral to the lesion

To investigate whether anti-Nogo-A antibody treatment induced changes within the grey matter of the cervical cord above the lesion, the BDA-labeled CS axon arbors within the spinal cord 500 µm rostral to the lesion on parasagittal sections were traced bilaterally at a magnification of 200x. The sections were then superimposed (Fig. 4A-D), showing for each animal the density of axon arbors in the white matter rostral to the lesion (brown lines) as well as in the grey matter rostral to the lesion (black lines on the left side of the lesion in Fig. 4A-D). For completeness of the information, BDA-labeled CS axon arbors caudal to the lesion were also represented. However, these data were described in a recent report (Freund et al., 2006) and will therefore not be considered further. At first sight, numerous BDA-labeled CS axon arbors are present in the grey matter rostral to the lesion (Fig. 4A-D), without obvious difference between the two

groups of monkeys. To quantify the density of CS axon arbors in the grey matter rostral to the lesion, their cumulated length was measured (see methods). The cumulated axon arbor length was then normalized by dividing by the total number of BDA-labeled CS axons present at C5 level in the white matter, and plotted as a function of the extent (in % of the hemi-cord) of the lesion (Fig. 4E). If one excludes the animal Mk-CP (asterisk in Fig. 4E) which had an incomplete lesion of the CS tract, there is a clear trend showing that anti-Nogo-A antibody treated monkeys (red squares in Fig. 4E) displayed a higher cumulated axon arbor length than the control antibody treated monkeys (blue circles), thus indicating that the anti-Nogo-A antibody treatment enhanced axon sprouting in the grey matter rostral to the cervical lesion. However, this trend was not statistically significant (Mann and Whitney test, $P>0.05$).

More labeled CS axon arbors are visible rostral and caudal to the lesion in Mk-CG (control antibody treated) than in Mk-AC (anti-Nogo-A antibody treated): this apparent contradiction is due to the much higher (4 times) total number of CS axons labeled with BDA in Mk-CG than in Mk-AC (see Table 1). If normalized according to the total number of CS axons labeled with BDA, then Mk-AC exhibits a larger cumulated axon arbor length rostral to the lesion (Fig. 4E) and a higher number of axon swellings caudal to the lesion (Fig. 4F) than Mk-CG (see also Freund et al., 2006). Furthermore, the extent of the lesion was smaller in Mk-CG than in Mk-AC.

4) CS axon arbors entering the lesion

On the parasagittal reconstructed sections used for the CS axon arbor length measurements, special attention was paid to CS axon arbors entering the scar tissue of the lesion. Examples are shown in Figure 5A, where more CS axons entered the lesion in three anti-Nogo-A antibody treated monkeys (red) than in one control antibody treated monkey (blue). For quantification, BDA-labeled CS axon arbors that crossed the rostral border of the lesion were counted in each monkey, normalized (according to the total number of BDA-stained CS axons at C5) and compared between the two groups of monkeys

(Fig. 5D). All anti-Nogo-A antibody treated animals exhibited a higher number of CS axon arbors entering the scar tissue than the highest number of such axons found in the group of control monkeys (Fig. 5D, Table 1). This difference between the two groups of monkeys is statistically significant (Mann and Whitney test: $p<0.05$). Typically, the course of these fibers was highly irregular, showing that they were regenerating rather than surviving fibers. Nevertheless, even in anti-Nogo-A antibody treated monkeys, the number of CS axons entering the lesion remains very low (Fig. 5D). Furthermore, none of these CS fibers reached the caudal border of the lesion. These results indicate that the CS axon arbors observed caudal to the lesion (Freund et al., 2006) did not arise from transected CS axons which would have regenerated straight through the lesion but rather from regenerating axons having grown around the lesion on bridges of spared white and grey matter.

5) CS axon collaterals entering the grey matter rostral to the cervical lesion

To determine whether anti-Nogo–A antibody treatment possibly enhanced CS axon collateral sprouting, the number of axon arbors leaving the cervical white matter and entering the grey matter was counted in the two groups of monkeys. Axons were counted within a territory extending as far 3 mm rostral from the lesion (Figs. 1A and 5B). Only six monkeys (Mk-CB, Mk-CH, Mk-CP, Mk-AP, and Mk-AM, Mk-AG) fulfilled the criterion of sufficient quality of BDA staining to identify clearly such CS axon arbors leaving the white matter and entering the grey matter. The numbers of such CS axon arbors was normalized and plotted as a function of the extent of the hemi-cord lesion (Fig. 5E). The number of CS axon arbors passing from the white to the grey matter was lower in the three control antibody treated monkeys than in the three anti-Nogo-A antibody treated monkeys, without any obvious relationship to lesion size in either group of monkeys (Fig. 5E). For comparison, the same measurement was conducted in an intact monkey (Mk-I3; Table 2), exhibiting a normalized number of CS axon arbors entering the grey matter rostral to the lesion slightly lower than the three control antibody treated monkeys subjected to cervical cord lesion (Fig. 5E).

6) CS axons crossing the midline at C5

In the case of complete hemi-section of the spinal cord, CS axons growing around the lesion in an attempt to re-innervate the denervated spinal cord caudal to the lesion, would have to cross the spinal cord midline. For this reason, we examined the frontal sections taken at the level C5 to determine whether BDA-labeled CS axons crossed the midline in the grey matter and if such midline crossing was enhanced by the anti-Nogo-A antibody treatment (Fig. 5C; see also methods sections). The sum of CS axons crossing the midline at C5 in each monkey was normalized to the total number of labeled CS axons and plotted as a function of the lesion extent (Fig. 5F). The anti-Nogo-A antibody treated monkeys exhibited a higher number of midline crossing CS axons than the control antibody treated monkeys (Fig. 5F). There was no relationship to the lesion extent in either group of monkeys. For comparison, the same analysis was conducted in three intact monkeys (Table 2), exhibiting a normalized number of CS axons crossing the midline at C5 equal or lower than the four control antibody treated monkeys subjected to cervical cord lesion (Fig. 5F).

Fig.4

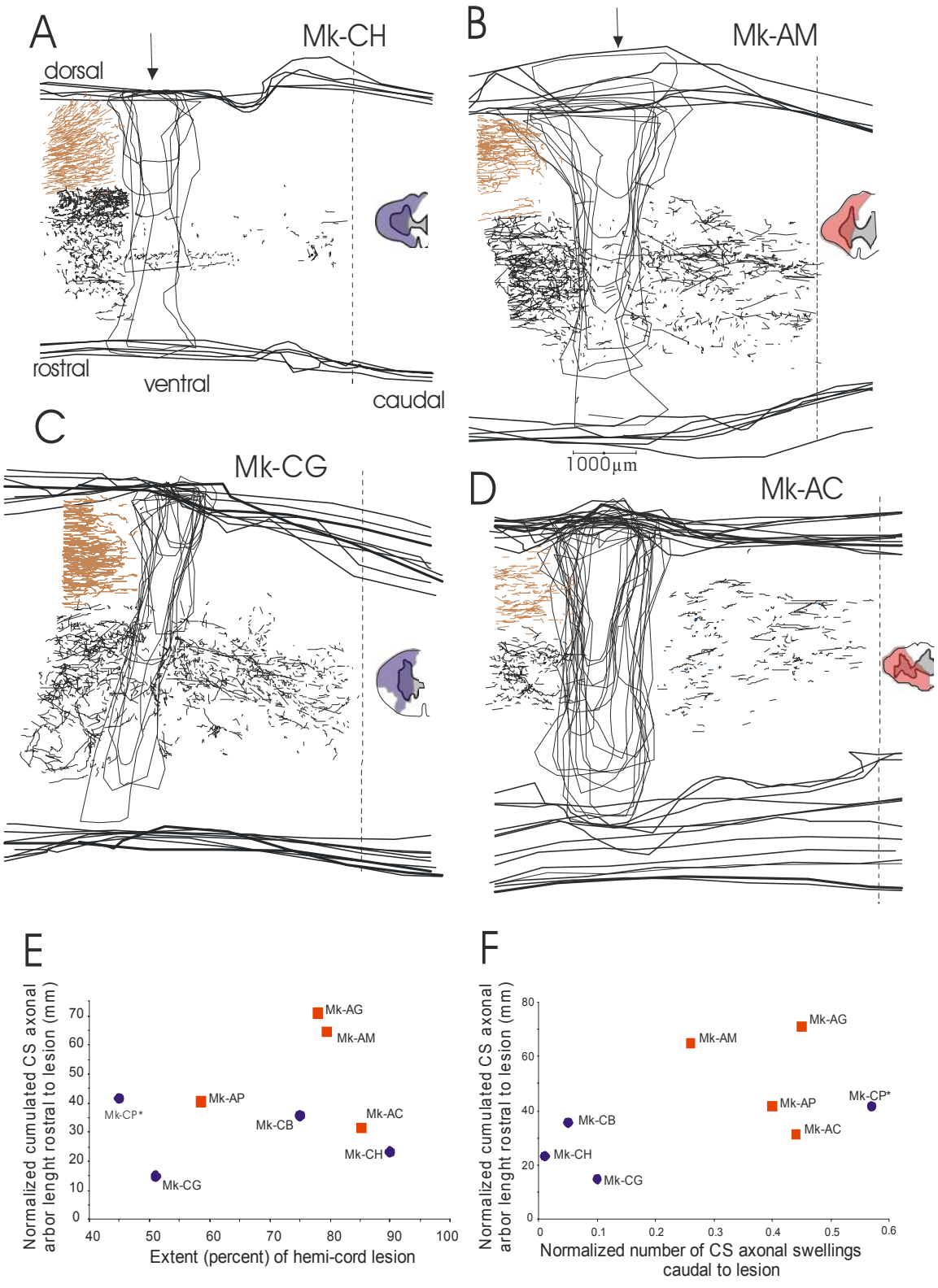

Figure 4

Panels A-D: Superimposed reconstructions of parasagittal sections of the cervical-thoracic cord showing the lesion (vertical arrow) as well as the density of BDA-labelled CS axon arbors present around the lesion, in four different monkeys (with a reminder of their lesion extent). Two monkeys received the control antibody (Mk-CH and Mk-CG in panels A and C) whereas in the other two monkeys the anti-Nogo-A antibody was delivered (Mk-AM and Mk-AC in panels B and D). Rostral to the lesion, the densely packed brown line segments represent the BDA-labelled CS axons in the white matter, interrupted by the transection of the dorsolateral funiculus. The position of the rostral stump of CS fibers in the white matter and of the axon arbors in the grey matter is schematic, as derived from a superimposition of sections, some of which were located more lateral than those for which their contour is represented here. The black line segments represent the CS axon arbors traced rostrally in the grey matter and caudally to lesion. In these four monkeys, the dorsolateral funiculus was completely transected. A less detailed version of these 4 reconstructions has been previously published in Freund et al. (2006), where the CS axon arbors rostral to the lesion were not represented.

Panel E: Relationship between the normalized cumulated axon arbor length in the grey matter rostral to the lesion as a function of the extent (in %) of the hemi-cord lesion. Cumulated axon arbor lengths were measured only rostral to the lesion. Blue circles are for control antibody treated monkeys whereas red squares are for the anti-Nogo-A antibody treated monkeys. The site of this analysis is schematically represented by the number “3” in Figure 1A.

Panel F: The present data about the axonal sprouting of the CS tract rostral to the lesion (reflected here by the normalized cumulated axon arbor length) was plotted as function of the normalized number of CS axonal swellings observed caudal to the lesion, as reported recently (Freund et al., 2006).

1.5 Discussion

The present study provides evidence that, after unilateral cervical lesion that sections the dorsolateral funiculus, anti-Nogo-A antibody treatment decreased the normally occurring retrograde degeneration of the CS axotomized axons: the number of terminal retraction bulbs formed by the axotomized CS axons was smaller in the group of anti-Nogo-A antibody treated monkeys than in the group of control antibody treated monkeys (Fig. 2D) and the terminal retraction bulbs were closer to the lesion (Fig. 2E and F). Thus, anti-Nogo-A antibody treatment prevented to some extent the phenomenon of axonal dieback. More CS axons grew into the lesion scar, but their regeneration through the scar tissue remained unsuccessful. In contrast, increased numbers of CS axon arbors were seen in the anti-Nogo-A antibody treated spinal cord rostral to the lesion. Some of these fibers arborized in the spinal cord caudal to the injury, as recently reported (Freund et al., 2006).

With respect to the question of direct regeneration of the cut stem axon or collateral axonal sprouting, there is evidence here that both were enhanced by anti-Nogo-A antibody treatment. Axotomized CS axons growing and penetrating into the lesion area were more numerous in the anti-Nogo-A antibody treated monkeys than in the control antibody ones. However, none of the CS axons penetrating the scar seemed to be able to reach its distal end. Scar associated growth inhibition factors probably account for this blockade of regeneration (Rhodes and Fawcett, 2004).

CS axons rostral to the injury gave rise to collaterals. The anti-Nogo-A antibody treatment enhanced the presence of CS axon arbors in the grey matter rostral to the lesion, the number of CS axon arbors (possibly corresponding to CS axon collaterals) passing from the white to the grey matter and, finally, the number of CS axon arbors crossing the segmental midline at C5 level. These measurements show that axonal sprouting took place rostral to the cervical lesion, and that some of these fibers were in position to grow around the lesion in order to re-innervate the spinal cord territory caudal to the lesion deprived of CS input. The anti-Nogo-A antibody treatment enhanced CS axonal sprouting

and re-growth, confirming previous observations in anti-Nogo-A antibody treated rats (Liebscher et al., 2005).

The larger number of CS axon arbors observed caudal to the lesion in the anti-Nogo-A antibody treated monkeys correlates with enhancement of functional recovery, especially of manual dexterity, i.e. functions known to depend on direct inputs from CS fibers (Freund et al., 2006). As further discussed hereunder, in our view the present data suggest a mechanism of functional recovery relying on collateral sprouting that arises from the axotomized CS axons rostral to the lesion, possibly contributing to the increased presence of CS axonal arbors in the grey matter of the spinal segments caudal to the lesion (green curved lines in Fig. 1A). Again, these data are consistent with previous data in rodents showing that "regenerative sprouting" enhanced in anti-Nogo-A antibody treated rats consisted of CS collaterals growing around the lesion on remaining tissue bridges (e.g. von Meyenburg et al., 1998; Brösamle et al., 2000; Schwab, 2004; Liebscher et al., 2005).

The present study did not address the possibility that some CS axon arbors observed caudal to the lesion (Freund et al., 2006) could result from sprouting arising from the undecussated CS axons not affected by the cervical lesion (Fig. 1A). In rats subjected to a spinal cord lesion interrupting the main CS tract, axon sprouting from the intact ventral CS tract was indeed found to play an important role in the spontaneous post-lesion recovery (Weidner et al., 2001). CS fibers from the intact side have been seen to cross the spinal cord midline in rats after unilateral pyramidotomy and anti-Nogo-A antibody application (Thallmair et al., 1998). In earlier studies in macaques, we found that reversible inactivation by intracortical muscimol infusion in the contralesional hemisphere several months post-lesion leads to a loss of recovered manual dexterity (Schmidlin et al., 2004; see brown syringe in Fig. 1A). In contrast, reversible inactivation of the ipsilesional hemisphere in control antibody treated monkeys did not affect the post-lesional functional recovery (Schmidlin et al., 2005), indicating that the decussated CS tract originating from the ipsilesional hemisphere does not play a major role in the recovery. Altogether, the present data as well as our recent

report (Freund et al., 2006) favor the notion that collateral sprouting and growth of the axotomized CS tract after cervical cord lesion may play a role in the post-lesion functional recovery.

It remains to be determined whether other descending tracts (rubrospinal, reticulospinal, long propriospinal projections) may also contribute, as shown in the rat (e.g. Hashimoto and Fukuda, 1991; Feraboli-Lohnherr et al., 1997; Raineteau et al., 2001; Schucht et al., 2002; Ruitenberg et al., 2003; Bareyre et al., 2004; Fouad et al., 2001). The possibility that the rubrospinal and reticulospinal tracts may play a role in the functional recovery is consistent with the observation reported in Freund et al. (2006) that the two control antibody treated monkeys with a lesion leaving intact a significant portion of these two tracts spontaneously recovered much better than the control antibody treated animal in which the lesion interrupted these two tracts completely.

The correlation between the anti-Nogo-A antibody enhancement of CS sprouting rostral to the cervical lesion (present study) and the density of CS tract axons caudal to the lesion (Freund et al., 2006) is shown in Figure 4F. The normalized cumulated axon arbors length as determined rostral to the lesion (present study) was plotted as a function of the normalized number of CS axonal swellings found caudal to the lesion, as reported recently (Freund et al., 2006). The control antibody treated monkeys subjected to complete transection of the dorsolateral funiculus exhibited no or only few CS axonal swellings caudal to the lesion; this was correlated with limited axonal sprouting rostral to the lesion in these animals (Fig. 4F: three blue circles on the left of the plot). In sharp contrast, the four anti-Nogo-A antibody treated monkeys, all subjected to complete transection of the dorsolateral funiculus, exhibited much higher numbers of CS axonal swellings caudal to the lesion. This again correlated with a significantly higher density of CS axon arbors arising from sprouts rostral to the lesion (red squares in Fig. 4F). The control antibody treated monkey Mk-CP (with an asterisk in Fig. 4F) needs to be considered separately because the lesion of the dorsolateral funiculus was incomplete (Fig. 1C), leaving a small bundle of CS axons intact. The intact CS axons reaching the region caudal to the lesion

sprouted profusely at that level, giving rise to numerous axon arbors and swellings. This animal showed a much better functional recovery than the other control antibody treated monkeys (Freund et al., 2006).

Comparison with previous studies

The present model of cervical cord lesion in the monkey can be compared, at least from a behavioral point of view, to previous studies in which macaque monkeys were subjected to a lesion of the cervical cord (Galea and Darian-Smith, 1997; Sasaki et al., 2004). Although the transection of the dorsolateral funiculus was aimed at lower cervical segments (C7/C8) than in these two studies (C3-C4), we observed an extent and a time course of functional recovery (Freund et al., 2006) largely comparable to that reported by Galea and Darian-Smith (1997). In contrast, Sasaki et al. (2004) reported an even faster, if not immediate, time course of recovery of precision grip and independent finger movements (1-28 days), although weakness in force and deficit in pre-shaping lasted longer. The two studies of lesion at C3-C4 level (Galea and Darian-Smith, 1997; Sasaki et al., 2004) did not analyze the plasticity of the CS tract in the vicinity of the cervical lesion, thus preventing a comparison with the present anatomical data.

A different neutralizing antibody against Nogo-A, mAbIN-1, was applied in marmosets with a thoracic lesion (Fouad et al., 2004). CS fibers growing around the lesion and into the caudal spinal cord were observed (Fouad et al., 2004), but the animals were not tested behaviorally preventing correlation with functional recovery.

A post-lesion sprouting of the CS tract was shown to be present in hamster only at perinatal ages (Kuang and Kalil, 1990). Adult hamsters subjected to pyramidotomy exhibited a retraction of the axons rostral to the lesion by a substantial distance, up to about 6-7 mm after several months. The present data, derived from macaque monkeys subjected to cervical lesion, are markedly different because the distance of retraction was much smaller. Indeed, after 4-6 months post-injury, most terminal retraction bulbs were located not more than 1

mm from the lesion. Furthermore, in the marmoset as well, the terminal retraction bulbs appeared to be located close to the lesion after two weeks post-injury (Fouad et al., 2004). These data are in line with earlier reports in monkey and man that retrograde degeneration of axotomized CS axons was limited to the region immediately above the lesion (Tower, 1940; Bronson et al., 1978). In rats, axonal dieback following spinal cord lesion was studied for the rubrospinal and reticulospinal tracts (Houle and Jin, 2001). The authors observed an average retraction of the axons over a mean distance of about 500 µm, which is in the same order as the retraction of the CS axons seen in monkeys (Fouad et al., 2004; present study). The limited axonal dieback is thus favorable for a regenerative sprouting from the axotomized axons, giving rise to collaterals which can grow in the caudal direction around the lesion in order to re-innervate the region caudal to the lesion.

In the present study, young adult monkeys (3.5 – 6.9 years old at time of sacrifice) were subjected to the spinal cord lesion (Table 1). It cannot be excluded that some of the axonal sprouting (although limited) observed in the control antibody treated monkeys occurred due to the relatively juvenile state of some of the animals and would not have taken place in older animals. Similarly, it is not established whether the enhancement of sprouting due to the anti-Nogo-A treatment would have reached the same extent in older animals. Nevertheless, most of our animals (except maybe Mk-AG) had an age at the time of the lesion (3.5 years or more) at which the myelination of the CS tract reached the adult stage, as full myelination was reported to last as long as 36 months (Olivier et al., 1997). As far as the CS tract is concerned, the animals included in the present study can thus be considered as adult monkeys.

As a result of BDA injection in M1, the number of CS labeled axons observed at C5 level on transverse sections (up to 2282; see Table 1) appears low considering that the total number of CS axons was estimated to be 400'000 and that the number of CS neurons retrogradely labeled after tracer injection in the upper spinal cord amounted up to 72'000 in the entire frontal lobe (Dum and Strick, 1991). A few explanations may account for this. First of all, only 50% of

the precentral CS axons originate from M1 (Dum and Strick, 1991; He et al., 1993, 1995). Second, the BDA injections formed patchy territories leaving in between zones where there was no or less uptake. Third, the BDA injections did not cover the entire M1; instead they were focused to the hand (forelimb) representation. Fourth, a contingent of CS axons terminates above C5. In addition, BDA infusion was limited to the rostral bank of the central sulcus and therefore the whole rostral part of M1 was not injected. Furthermore, as compared to other anterograde tracers such as WGA-HRP for instance, the uptake of BDA appears less prominent. However, to explain the surprisingly low number of CS axons labeled with BDA in the present study, one may consider the likely possibility that the very fine axons making the majority of the CS tract are not labeled or escaped detection at light microscopy level, as suggested by our observation that most BDA labeled CS axons visible in our material at C5 level are relatively large in diameter. In this context, for the same reason, one cannot exclude that some fine CS axons unlabeled with BDA or undetected at light microscopic level were spared by the lesion.

In conclusion, the present study demonstrates quantitatively that anti-Nogo-A antibody treatment attenuated the retraction of axotomized CS axons after cervical cord injury and enhanced axonal sprouting rostral to the lesion. Within the scar tissue, growth of these fibers is blocked by inhibitory factors other than Nogo-A. Some fibers, however, succeeded in bypassing the scar, presumably by remaining on grey matter bridges. These axons growing around the lesion probably make an important contribution to the incomplete but significantly enhanced reconstruction of the CS fiber plexus caudal to the lesion in the anti-Nogo-A antibody treated monkeys (Freund et al., 2006), more so than the fibers attempting to regenerate and to re-enter the lesion itself. The contingent of CS axons growing around the lesion in the grey matter is believed to be an anatomical correlate of the functional recovery observed in the anti-Nogo-A antibody treated animals.

	Mk-CP	Mk-CG	Mk-CB	Mk-CH	Mk-AP	Mk-AG	Mk-AM	Mk-AS	Mk-AC
Species	fasc.	fasc.	fasc.	fasc.	fasc.	fasc.	fasc.	mul	fasc.
Anti-Nogo-A treatment	**No No No**			**No Yes**	(11C7)	**Yes** (hNogoA)	**Yes** (hNogoA)	**Yes** (11C7)	**Yes** (hNogoA)
"Double-blind" procedure	Yes	Yes	Yes	Yes	Yes	No	Yes	No	Yes
Completeness of CS (dlf) section	**No** (BDA)	**Yes** (BDA)	**Yes** (BDA)	**Yes** (BDA)	**Yes** (BDA)	**Yes** (BDA)	**Yes** (BDA)	**No** (BDA)	**Yes** (BDA)
Extent of hemi-cord lesion (%)	45	51	75	90	58	78	80	41	85
Extent of grey matter cut (%)	77	73	81	74	85	81	71	86	100
Number of BDA-labeled CS axons at C5	927	1005	1186	780	1250	2282	1148	168	270
% of uncrossed CS axons at C5	10	5	9	3	5	9	5	11	7
Volume of BDA Injected (in □l)	24	24	20	20	24	28	19	22	20
Number of BDA Injection sites	12	12	10	10	12	15	10	11	10
Total nb. of injection tracks	6	6	5	5	6	7	6	4	6
Survival time post BDA injection (days)	78	70	78	62	81	70	69	72	64
Nb. of days between lesion and BDA injection	81	70	147	76	79	42	69	210	71
Age of the animal at sacrifice (years)	6.9	~4	5	~4	6.5	3.5	~4	6.25	~4
(1) Number of retraction bulbs / number of CS axons at C5	0.06	0.053	0.116	0.09	0.058	0.019	0.004	0.006	0.015

Number of CS axons with terminal bulbs	56	53	137	70	72	44	5	2	4
(2) Mean distance of axonal retraction in □m (std-dev)	291.5 (98.3)	326 (292.3)	407.5 (171.2)	310.7 (154.5)	240.8 (144.5)	145.9 (101.8)	116.5 (155.3)		179.4 (143.8)
% of terminal retraction bulbs 100□m rostral to the lesion	13%	7%	1%	7%	27%	36%	60%	0%	40%
(3) Normalized axon arbor length rostral to lesion	41.624	14.961	35.769	23.33	41.914	71.12	64.752		31.307
(4) Normalized number of CS axotomized axons entering lesion area	0.003	0.0039	0.0093	0.014	0.03	0.022	0.0366		0.0851
(5) Normalized number of CS axons going from white to grey matter	0.135		0.111	0.128	0.213	0.301	0.169		
(6) Normalized number of CS axons crossing midline at C5	0.045	0.028	0.025	0.041	0.06	0.06	0.05		

Table 1: List of the lesioned monkeys included in the present study with identification code

Detailed information on the nine monkeys included in the present anatomical study. Eight of the nine monkeys were part of the previous report, describing the behavioral recovery and the properties of the CS axon collaterals caudal to the lesion (Freund et al., 2006; see their Table 1). One additional animal (Mk-AG) was newly introduced in the present study.

At the time of the experiment, the monkeys had different names, not indicating whether the animal was infused with the control or the anti-Nogo-A antibody.

Under species, "mul." is for macaca mulata while "fasc." is for macaca fascicularis.

The four control antibody treated monkeys ("Anti-Nogo-A treatment: **No**") are in the four leftmost columns, whereas the five anti-Nogo-A antibody treated monkeys are in the five rightmost columns ("Anti-Nogo-A treatment: **Yes**") with indication of which of the two antibodies was used (mAB11C7 or mAB hNogoA).

Under "double-blind procedure", "Yes" refers to monkeys for which the collaborators delivering the antibodies (control or anti-Nogo-A) did not know to which monkey they were aimed for. On their side, the experimenters taking care of the monkeys did not know which antibody has been administered to the corresponding animal.

In the row “completeness of CS (dlf) section”, “yes” and “No” indicate whether the dorsolateral funiculus (dlf) was or was not completely transected unilaterally, respectively. “BDA”, indicated between parentheses, means that completeness of the section of the dorsolateral funiculus unilaterally was assessed based on the BDA-labeling of the CS tract immediately above the lesion. If "yes", this means that there was no BDA-labeled axon spared by the lesion in the aimed dorsolateral funiculus. If "no", this means that few BDA-labeled axons in the dorsolateral funiculus were spared by the lesion.

For four animals, their age was not precisely determined when they were received in our animal facility and was estimated to be around 3 years old at that time. Therefore, their age was estimated to be around 4 years old when sacrificed.

The grey cells in the table are for parameters that could not be determined in the corresponding monkeys.

	Mk-I1 Mk-I2	Mk-I3	
Species	fasc.	fasc.	fasc.
Age at sacrifice (year); weight (kg)	4; ~5	8.3; ~10	7.7; ~10
Volume of BDA injected (in □l)	10	22.5	25.5
Number of injection sites	7	15	17
Number of injection tracks	3	9	11
Survival time post-injection (days)	25	42	48
Normalized number of CS axons going from white to grey matter	+	++	**0.078**
Normalized number of CS axons crossing midline at C5	**0.02 0.021**		**0.025**
Number of CS axons in the white matter at C5 (for normalization)	1766	984	1922
Number of crossed CS axons at C5 (% of total)	1620 (91.7%)	859 (87.3%)	1735 (90.3%)
Number of uncrossed CS axons at C5 (% of total)	146 (8.3%)	125 (12.7%)	187 (9.7%)

Table 2: List of the three “intact” monkeys included in the present study with identification code

The data (in Bold) derived from these three intact (unlesioned, untreated) animals were used to establish a baseline for the analyses presented for the lesioned monkeys in Figures 5E and 5F.

In the two intact monkeys (Mk-I2 and Mk-I3), injection of tracer in the motor cortex was the unique intervention, following the protocol described in the method section. Mk-I1 was used in a previous tracing study (Rouiller et al., 1996), in which the primary motor cortex was mapped using intracortical microstimulation before BDA injection.

Under species, "fasc." is for macaca fascicularis.

+ In Mk-I1, the cervical segment C6-T3 was not cut in the sagittal plane (but in the frontal plane) and therefore the assessment of the number of axons entering the grey matter could not be made.

++ In Mk-I2, the quality of the BDA reaction at C6-T3 did not allow the assessment of the number of axons entering the grey matter. In contrast, the block including C5 (sectioned in the frontal plane) was processed separately and the BDA reaction allowed the determination of the number of CS axons crossing midline.

1.6 References

Bareyre FM, Kerschensteiner M, Raineteau O, Mettenleiter TC, Weinmann O, Schwab ME. 2004. The injured spinal cord spontaneously forms a new intraspinal circuit in adult rats. Nat Neurosci 7:269-277.

Bregman BS, Kunkel-Bagden E, Schnell L, Dai HN, Gao D, Schwab ME. 1995. Recovery from spinal cord injury mediated by antibodies to neurite growth inhibitors. Nature 378:498-501.

Bronson R, Gilles FH, Hall J, Hedley-Whyte ET. 1978. Long term post-traumatic retrograde corticospinal degeneration in man. Hum Pathol 9:602-607.

Brösamle C, Huber AB, Fiedler M, Skerra A, Schwab ME. 2000. Regeneration of lesioned corticospinal tract fibers in the adult rat induced by a recombinant, humanized IN-1 antibody fragment. J Neurosci 20:8061-8068.

Caroni P, Savio T, Schwab ME. 1988. Central nervous system regeneration: oligodendrocytes and myelin as non-permissive substrates for neurite growth. Prog Brain Res 78:363-370.

Dum RP and Strick PL. 1991. The origin of corticospinal projections from the premotor areas in the frontal lobe. J Neurosci 11:667-689.

Feraboli-Lohnherr D, Orsal D, Yakovleff A, Ribotta MGY, Privat A. 1997. Recovery of locomotor activity in the adult chronic spinal rat after transplantation of embryonic nervous cells: Specific role of serotonergic neurons. Exp Brain Res 113:443-454.

Fouad K, Volker D, Schwab ME. 2001. Improving axonal growth and functional recovery after experimental spinal cord injury by neutralizing myelin associated inhibitors. Brain Res Rev 36:204-212.

Fouad K, Klusman I, Schwab ME. 2004. Regenerating corticospinal fibers in the Marmoset (Callitrix jacchus) after spinal cord lesion and treatment with the anti-Nogo-A antibody IN-1. Eur J Neurosci 20:2479-2482.

Freund P, Schmidlin E, Wannier T, Bloch J, Mir A, Schwab ME, Rouiller EM. 2006. Nogo-A-specific antibody treatment enhances sprouting and functional recovery after cervical lesion in adult primates. Nature Med 12:790-792.

Galea MP, Darian-Smith I. 1997. Manual dexterity and corticospinal connectivity following unilateral section of the cervical spinal cord in the macaque monkey. J Comp Neurol 381:307-319.

Hashimoto T, Fukuda N. 1991. Contribution of serotonin neurons to the functional recovery after spinal cord injury in rats. Brain Res 539:263-270.

He SQ, Dum RP, Strick PL. 1993. Topographic organization of corticospinal projections from the frontal lobe: Motor areas on the lateral surface of the hemisphere. J. Neurosci 13: 952-980.

He SQ, Dum RP, Strick PL. 1995. Topographic organization of corticospinal projections from the frontal lobe: Motor areas on the medial surface of the hemisphere. J Neurosci 15: 3284-3306.

Holmes GL, May WP. 1909. On the exact origin of the pyramidal tracts in man and other mammals. Brain 32:1-42.

Houle JD, Jin Y. 2001. Chronically injured supraspinal neurons exhibit only modest axonal dieback in response to a cervical hemisection lesion. Exp Neurol 169:208-217.

Jenny AB, Inukai J. 1983. Principles of motor organization of the monkey cervical spinal cord. J Neurosci 3:567-575.

Kalil K, Schneider GE. 1975. Motor performance following unilateral pyramidal tract lesions in the hamster. Brain Res 100:170-174.

Kao CC, Chang LW, Bloodworth JMBJr. 1977a. Electron microscopic observations of the mechanisms of terminal club formation in transected spinal axons. J Neuropathol Exp Neurol 36:140-156.

Kao CC, Chang LW, Bloodworth JMBJr. 1977b. The mechanisms of spinal cord cavitation following spinal cord transection. J Neurosurg 46:745-756.

Kerschensteiner M, Schwab ME, Lichtman JW, Misgeld T. 2005. In vivo imaging of axonal degeneration and regeneration in the injured spinal cord. Nature Med 11:572-577.

Kuang RZ, Kalil K. 1990. Specificity of corticospinal axon arbors sprouting into denervated contralateral spinal cord. J Comp Neurol 302:461-472.

Lacroix S, Havton LA, McKay H, Yang H, Brant A, Roberts J, Tuszynski MH. 2004. Bilateral corticospinal projections arise from each motor cortex in the macaque monkey: A quantitative study. J Comp Neurol 473:147-161.

Lassek AM. 1942. The pyramidal tract. A study of retrograde degeneration in the monkey. Arch Neurol 48:561-567

Levin PM, Bradford FK. 1938. The exact origin of the cortico-spinal tract in the monkey. J Comp Neurol 68:411-422.

Liebscher T, Schnell L, Schnell D, Scholl J, Schneider R, Gullo M, Fouad K, Mir A, Rausch M, Kindler D, Hamers FPT, Schwab ME. 2005. Nogo-A antibody improves regeneration and locomotion of spinal cord-injured rats. Ann Neurol 58:706-719.

Oertle T, Van der Haar ME, Bandtlow CE, Robeva A, Burfeind P, Buss A, Huber AB, Simonen M, Schnell L, Brösamle C, Kaupmann K, Vallon R, Schwab ME. 2003. Nogo-A inhibits neurite outgrowth and cell spreading with three discrete regions. J Neurosci 23:5393-5406.

Olivier E, Edgley SA, Armand J, Lemon R. 1997. An electrophysiological study of the postnatal development of the corticospinal system in the macaque monkey. J Neurosci 17:267-276.

Pernet U, Hepp-Reymond M-C. 1975. Retrograde Degeneration der Pyramidenbahnzellen im motorischen Kortex beim Affen (Macaca fascicularis). Acta Anat (Basel)552-561.

Raineteau O, Fouad K, Noth P, Thallmair M, Schwab ME. 2001. Functional switch between motor tracts in the presence of the mAb IN-1 in the adult rat. Proceedings of the National Academy of Sciences of the United States of America 98:6929-6934.

Rhodes KE, Fawcett JW. 2004. Chondroitin sulphate proteoglycans:preventing plasticity or protecting the CNS? J Anat 204:33-48.

Rouiller EM, Moret V, Tanné J, Boussaoud D. 1996. Evidence for direct connections between the hand region of the supplementary motor area and cervical motoneurons in the macaque monkey. Eur J Neurosci 8:1055-1059.

Rouiller EM, Tanné J, Moret V, Kermadi I, Boussaoud D, Welker E. 1998. Dual morphology and topography of the corticothalamic terminals originating from the primary, supplementary motor, and dorsal premotor cortical areas in macaque monkeys. J Comp Neurol 396:169-185.

Ruitenberg MJ, Plant G W, Hamers FPT, Wortel J, Blits B, Dijkhuizen PA, Gispen WH, Boer GJ, Verhaagen J. 2003. Ex vivo adenoviral vector-mediated neurotrophin gene transfer to olfactory ensheathing glia: Effects on rubrospinal tract regeneration, lesion size, and functional recovery after implantation in the injured rat spinal cord. J Neurosci 23:7045-7058.

Sasaki S, Isa T, Pettersson LG, Alstermark B, Naito K, Yoshimura K, Seki K, Ohki Y. 2004. Dexterous finger movements in primate without monosynaptic corticomotoneuronal excitation. J Neurophysiol 92:3142-3147.

Schmidlin E, Wannier T, Bloch J, Rouiller EM. 2004. Progressive plastic changes in the hand representation of the primary motor cortex parallel incomplete recovery from a unilateral section of the corticospinal tract at cervical level in monkeys. Brain Research 1017:172-183.

Schmidlin E, Wannier T, Bloch J, Belhaj-Saïf A, Wyss A, Rouiller EM. 2005. Reduction of the hand representation in the ipsilateral primary motor cortex following unilateral section of the corticospinal tract at cervical level in monkeys. BMC Neuroscience 6:56.

Schnell L, Schwab ME. 1990. Axonal regeneration in the rat spinal cord produced by an antibody against myelin-associated neurite growth inhibitors. Nature 343:269-272.

Schucht P, Raineteau O, Schwab ME, Fouad K. 2002. Anatomical correlates of locomotor recovery following dorsal and ventral lesions of the rat spinal cord. Experimental Neurology 176:143-153.

Schwab ME. 2004. Nogo and axon regeneration. Curr Opin Neurobiol 14:118-124.
Thallmair M, Metz GAS, Z'Graggen WJ, Raineteau O, Kartje GL, Schwab ME. 1998. Neurite growth inhibitors restrict plasticity and functional recovery following corticospinal tract lesions. Nature Neurosci 1:124-131.

Tower SS. 1940. Pyramidal lesion in the monkey. Brain 63:36-90.

Von Meyenburg J, Brösamle C, Metz GAS, Schwab ME. 1998. Regeneration and sprouting of chronically injured corticospinal tract fibers in adult rats promoted by NT-3 and the mAb IN-1, which neutralizes myelin-associated neurite growth inhibitors. Exp Neurol 154:583-594.

Wannier T, Schmidlin E, Bloch J, Rouiller EM. 2005. A unilateral section of the corticospinal tract at cervical level in primate does not lead to measurable cell loss in motor cortex. Journal of Neurotrauma 22:703-717.

Weidner N, Ner A, Salimi N, Tuszynski MH. 2001. Spontaneous corticospinal axonal plasticity and functional recovery after adult central nervous system injury. Proceedings of the National Academy of Sciences of the United States of America 98:3513-3518.

Weinmann, O., Schnell, L., Ghosh, A., Montani, L., Wiessner, C., Wannier,T., Rouiller, E., Mir, A. and Schwab, M.E. 2006. Intrathecally infused antibodies against Nogo-A penetrate the CNS and downregulate the endogenous neurite growth inhibitor Nogo-A. Molec. Cell. Neurosci. 32: 161-173

Wohlfarth S. 1932. Die vordere Zentralwindung bei Pyramidenbahnläsionen verschiedener Art. Eine histopathologische Untersuchung. Acta Med Scand Suppl. 46:1-235.

Chapter 5

Fate of rubrospinal neurons after unilateral section of the cervical spinal cord in adult macaque monkeys: effects of an antibody treatment neutralizing Nogo-A

This chapter has been adapted from an article originally published in Journal of Brain Research (P. Wannier-Morino*, E. Schmidlin,*, P. Freund, A. Belhaj-Saif, J. Bloch, A. Mir, M.E. Schwab, E.M. Rouiller and T. Wannier; In Press, 2007)

*** The first two authors contributed equally to the study.**

1.1 Abstract

The present study describes in primates the effects of a spinal cord injury on the number and size of the neurons in the magnocellular part of the red nucleus (RNm), the origin of the rubrospinal tract, and evaluates whether a neutralization of Nogo-A reduces the lesioned-induced degenerative processes observed in RNm. Two groups of monkeys were subjected to unilateral section of the spinal cord affecting the rubrospinal tract; one group was subsequently treated with an antibody neutralizing Nogo-A; the second group received a control antibody. Intact animals were also included in the study. Counting neurons stained with a monoclonal antibody recognizing non-phosphorylated epitopes on neurofilaments (SMI-32) indicated that their number in the contralesional RNm was consistently inferior to that in the ipsilesional RNm, in a proportion amounting up to 35%. The lesion also induced shrinkage of the soma of the neurons detected in the contralesional RNm. Infusing an anti-Nogo-A antibody at the site of the lesion did not increase the proportion of SMI-32 positive rubrospinal neurons in the contralesional RNm nor prevent shrinkage.

Section: Sensory and Motor system

Keywords: Red nucleus, Nogo-A, spinal cord lesion, primate.

Abbreviations

CS: corticospinal
BDNF: brain derived neurotrophic factor
RN: red nucleus
RNm: red nucleus pars magnocellularis
RNp: red nucleus pars parvocellularis
RS: rubrospinal
SCI: spinal cord injury

1.2 Introduction

The effects of spinal cord injury on directly connected supraspinal structures like the magnocellular part of the red nucleus (RNm) are poorly known in primates. In the rat, after a spinal cord lesion at cervical levels, axotomized reticulospinal (RS) neurons shrink and display modification in the expression of various molecules (Egan et al., 1977; Tetzlaff et al., 1991; Novikova et al., 2000; Kwon et al., 2002; Kwon et al., 2004). In this species, the RNm regains a normal aspect if brain derived neurotrophic factor (BDNF) is provided (Liu et al., 1999; Novikova and others, 2000; Kwon and others, 2002). Because neurotrophic substances are uptaken at synapses, the amount of neurotrophic factors accessible to a neuron relates ultimately to the number of synapses that this neuron possesses. Increasing this number may therefore contribute to protect a neuron from the degenerative processes triggered by axotomy.

In the monkey, a unilateral section of the dorsolateral funiculus at cervical levels provoked shrinkage of the axotomized corticospinal (CS) neurons and alteration of their expression of non-phosphorilated neurofilaments, but did not conduct to measurable cell death (Wannier et al., 2005a). For the same lesion, the treatment with an antibody neutralizing the neurite growth inhibitor Nogo-A induced sprouting of CS axons (Freund et al., 2006; Freund et al., 2007). In parallel to these morphological changes, the anti-Nogo-A treatment also enhanced functional recovery (Freund and others, 2006). In monkey, an interruption of the RS tract induced degenerative changes in the RNm (Padel et al., 1981). As the neutralization of Nogo-A in rodents promotes regeneration of CS and sprouting of RS fibers (Raineteau et al., 2002), this treatment could have the same effect in primate. In this case, the improved access to neurotrophic substances may lead to a reduction of the lesion induced degenerative changes in the RNm. The present investigation aims at examining this issue by comparing the number and size of neurons in both RNm in monkeys subjected to a unilateral lesion of the cervical spinal cord and in intact monkeys. Moreover, the effects of a treatment with an antibody neutralizing Nogo-A on RNm neurons will be assessed.

1.3 Results

Location and extent of the cervical lesion

The RS tract is a crossed pathway that runs in the dorsolateral funiculus partially overlapping the lateral corticospinal tract and extending somewhat ventrally. As a consequence of this overlap, the CS and RS tracts cannot easily be segregated on a coronal section of the spinal cord. The extent and the location of the cervical cord hemi-section are shown in Figure 1 for ten of the eleven lesioned monkeys. The total extent of the lesion is given in Table 1 (percentage of hemi-section). To tentatively determine more specifically the extent of the lesion affecting the territory comprising the RS and CS tracts we considered only the lateral funiculus, i.e. the white matter going from the dorsal to the ventral rootlet zone (dashed lines in Fig. 1). A lesion extent was thus recalculated reflecting more accurately the portion of CS and RS tracts affected by the lesion (Table 1: lateral funiculus lesion extent in %). In five of the eleven lesioned monkeys, the section of the lateral funiculus between the dorsal and the ventral rootlets reached 100% of the territory and thus the lesion of the RS tract was considered as complete in these animals (asterisks in Fig. 1). In two animals (Mk-CS and Mk-CB), the lesion covered more than 87% of the lateral funiculus and the territory spared by the lesion was situated most laterally (Fig. 1), a territory normally not occupied by the RS tract. These two monkeys were thus considered as subjected to nearly complete transection of the RS tract (asterisk in parentheses in Fig. 1). In contrast, in three monkeys, the lesion extent in the lateral funiculus was below 75% (open circles in Fig. 1), and therefore the lesion of the RS tract was considered incomplete. Particularly, in Mk-AS the extent of the lesioned lateral funiculus was below 50%.

Figure 1

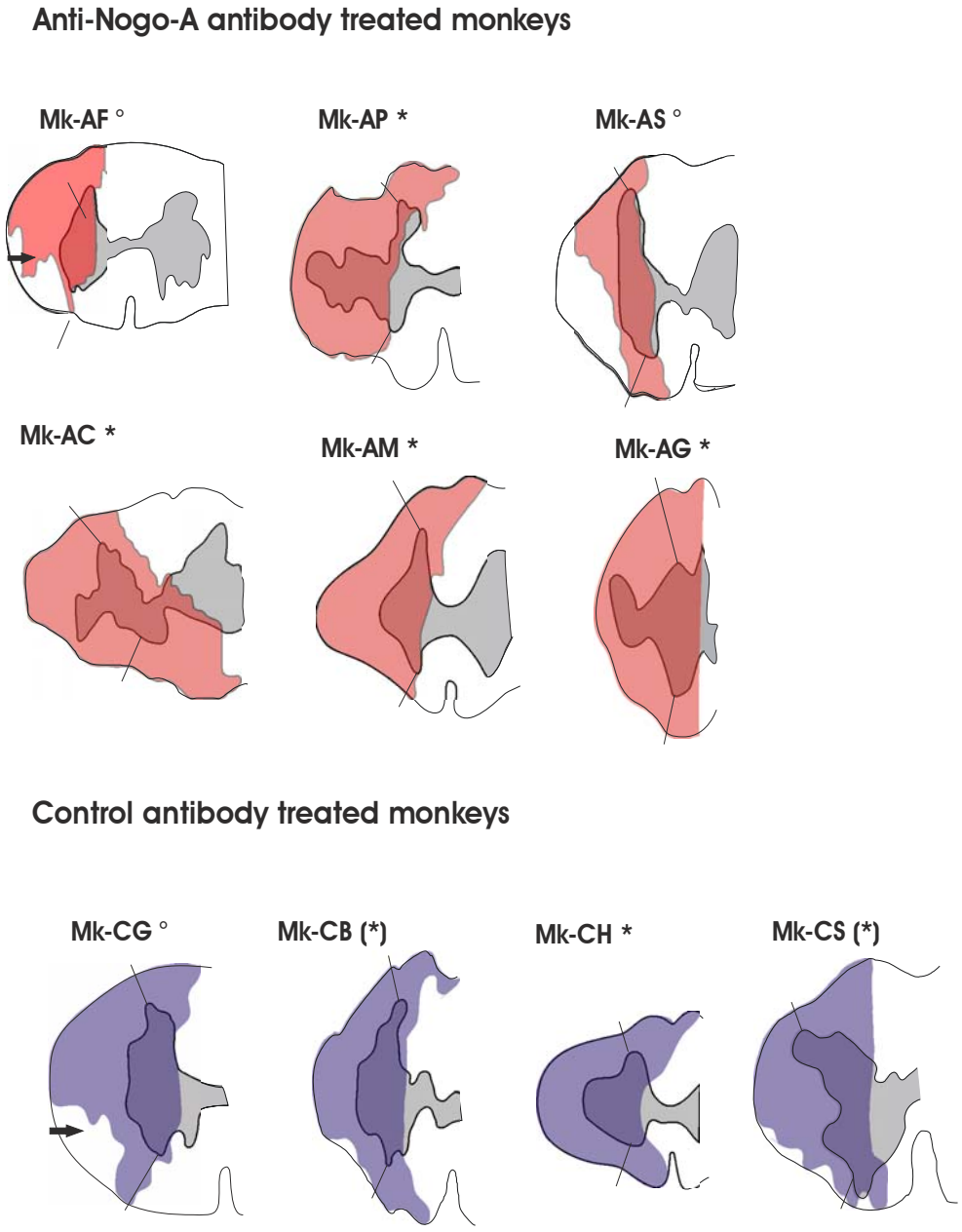

Figure 1

Location and extent of the cervical spinal cord lesions, performed at C7/C8 in the anti-Nogo-A antibody treated animals (six animals, red area) and in the control antibody treated animals (four animals, blue area). In one anti-Nogo-A antibody treated animal (Mk-AT) the lesion extent could not be assessed and thus it is not represented in this figure. Dashed lines indicate the extent of the lateral funiculus, going from the dorsal to the ventral rootlets. Asterisks indicate complete lesion of the zone occupied by CS/RS tracts. Asterisks in parentheses indicate a nearly complete lesion of the CS/RS tracts. Open circles indicate an incomplete lesion of the CS/RS tracts. Arrows in Mk-AF and in

Mk-CG indicate the quadrant of the ventral lateral funiculus where some fibres of the RS tract might have been spared (Mk-CG) or cut (Mk-AF) by the lesion.

The number of SMI-32 positive neurons in the contralesional RNm is reduced in lesioned animals.

The RNm is located in the ventral part of the midbrain. On coronal sections stained for SMI-32, RNm was easily identified by its large and strongly stained neurons, its ovoid shape and its vicinity to the roots of the oculomotor nerve (Fig. 2A). The RNm was clearly distinguished from the parvocellular part of the RN (RNp) which was situated more rostrally, containing smaller, more densely packed and more faintly SMI-32 stained cells (not shown). On Nissl-stained sections adjacent to the SMI-32 labelled ones, large neurons were also visible at low magnification and their number and distribution appeared comparable to the SMI-32 pattern of distribution (Fig. 2 E-F). This observation was confirmed quantitatively in two monkeys (Mk-AF and Mk-CS) by counting the cell nuclei in adjacent sections of the RNm stained respectively for SMI-32 and Nissl (numbers between parentheses in Table 2). For the other animals, as the contour of SMI-32 stained neurons was easier to define than that of Nissl stained cells, we conducted our analysis on SMI-32 stained sections. At first sight, in animals subjected to the cervical lesion, the contralesional RNm exhibited a reduction of the number of SMI-32 positive neurons as compared to the ipsilesional side (Fig. 2 C-D); neurons might have degenerated or shrunken and/or reduced their expression of non-phosphorilated neurofilaments, thus loosing their strong SMI-32 staining (Wannier and others, 2005a). Indeed, faintly stained RNm neurons were visible on the contralesional side at high magnification (400x). RNm neurons were counted on both sides and their somatic cross-sectional area was measured on sections spaced 400 µm apart along the entire rostro-caudal extent of the RNm, only considering SMI-32 labelled cell bodies with a visible nucleus (Fig. 2B).

FIGURE 2

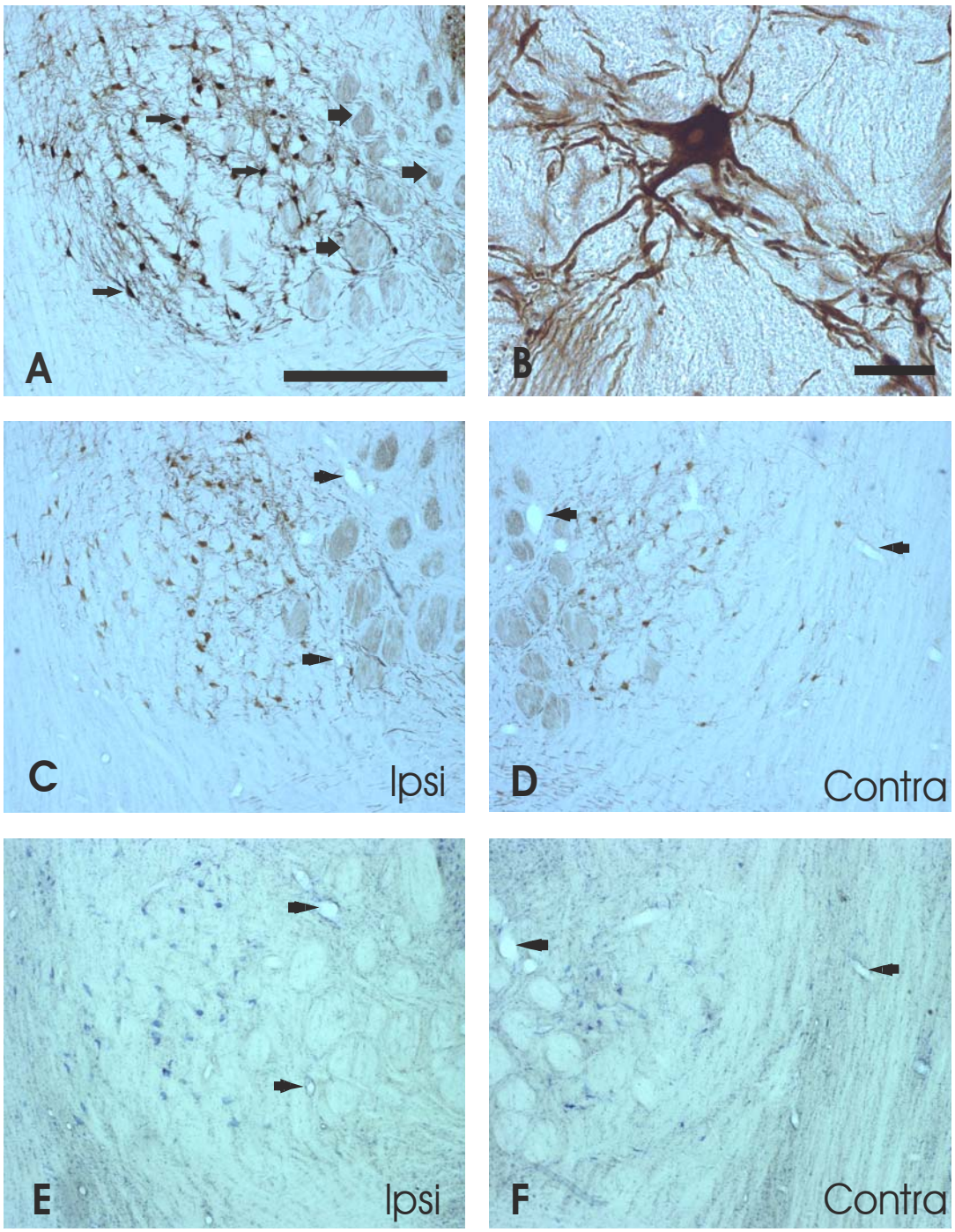

Figure 2

A-D: Photomicrographs of SMI-32 stained frontal sections of the RNm. In panel A the RNm of an intact animal (Mk-IR) is shown. Note the proximity of the RNm with the roots of the oculomotor nerve (large arrows). Large and darkly positive SMI-32 neurons (thin arrows point to a few of them) are loosely packed and are arranged to form a round shaped nucleus. At higher magnification (panel B), neurons show a multipolar shape with several dendritic processes. The neuron in the image has a clearly visible nucleus, which was the

criterion to be included in the morphometric analysis (cell count and somatic size). Panels C and D show the RNm on the ipsi- and contralesional side respectively of a representative animal subjected to a unilateral spinal cord lesion (Mk-CS). Both sides appear less intensively stained if compared to panel A, reflecting individual and methodological variability. In panel D (contralesional RNm) the number of SMI-32 positive cells appears lower than in panel C (ipsilesional RNm). In addition, the intensity of staining appears also reduced in panel D as compared to panel C and A.
E-F: Photomicrographs of Nissl stained sections of the RNm adjacent to sections displayed in C and D, respectively. Arrows in C and E and in D and F respectively indicate the same blood vessels. Similarly to SMI-32 staining, the number of cell bodies appears lower in panel F than in panel E. Scale bar in A (same for C, D, E, F): 1 mm. Scale bar in B: 100 µm.

As the number of sections labelled with SMI-32 antibody and including the RNm was relatively low for each animal (6 to 9), the number of cells counted in each RNm was fairly small (Fig 3A), ranging from 39 neurons (Mk-CB contra) to 174 neurons (Mk-IR right). Indeed, the estimated number of neurons was variable across animals irrespective of the lesion and/or treatment with anti-Nogo-A or control antibodies (Table 2). This variability was best reflected by the RNm cell numbers on each side in the four intact animals (Table 2, rightmost four columns), in which a relative difference in cell number between the two RNm reached up to 25.8 % (Fig. 3A), though not statistically significant. In the eleven monkeys subjected to the cervical lesion, there was a systematic lower number of RNm neurons contralesionally. In three monkeys the difference was statistically significant (Fig. 3A, $p < 0.05$) whereas the difference did not reach significance level in seven monkeys ($0.05 < p \leq 0.1$). The least significant difference was found in the monkey (Mk-CG) subjected to an incomplete transection of the RS tract (Fig. 1, open circle). In Mk-AS the difference could not be statistically evaluated (see methods). To assess further the impact of the lesion, the cell number difference was expressed in percentage between the RNm on both sides for each animal (Fig. 3B and Table 2). For animals with complete or nearly complete lesion of the RS/CS tracts territory (asterisks in Fig. 1), the percentage difference of SMI-32 positive RNm neurons between the two sides ranged from -29.0% to -52.4% (Fig. 3B and C). In contrast, intact monkeys showed a cell number difference between the two RNm, ranging from -3.3% to 25.8%, figures which could be considered as indicative of the inter-individual and intrinsic methodological variability. Interestingly, Mk-AF, which had a relatively restricted lesion extent (73.4 %), exhibited a high cell number difference

between the two RNm (-48.7%). On the other hand Mk-CG, which had also an incomplete lesion comparable to Mk-AF, showed a relatively lower cell number difference (-37.1 %, not significant, see above), although still higher than the values found in intact monkeys. In these two latter monkeys the extent of the lesion in percentage was similar; however when the territory of the lateral funiculus lesioned was considered it appeared that in Mk-AF the part of the lesion going ventro-laterally was coherent with a bigger impact on the RS tract than in Mk-CG (arrows in Fig. 1). Finally in Mk-AS, which had a highly incomplete lesion (below 50%) sparing a large part of the territory occupied by the RS tract (Fig.1), the cell number difference was accordingly comparable to values observed in intact animals.

In the lesioned monkeys, no obvious relationship was found between these values of RNm neurons and the fact that some animals were treated with an anti-Nogo-A whereas other animals received a control antibody (Fig. 3C). To statistically evaluate this observation, we compared the values of cell number difference between the RNm on the two sides expressed in percentage among the three groups of animals (Group 1, red in Fig. 3B: lesioned, anti-Nogo-A antibody treated animals; Group 2, blue: lesioned, control antibody treated animals; Group 3, green: intact animals) using the non parametric Mann and Whitney test. The comparison values between groups 1 and 2 were not statistically significant ($p > 0.05$), confirming thus the observation that the anti-Nogo-A antibody treatment did not prevent a reduction of the number of large SMI-32 positive RNm neurons contralesionally. On the other hand, as compared to intact animals (group 3), the difference in large SMI-32 positive cell number between the two RNm was statistically significant ($p < 0.05$) in the two groups of lesioned monkeys (Fig. 3B).

Figure 3

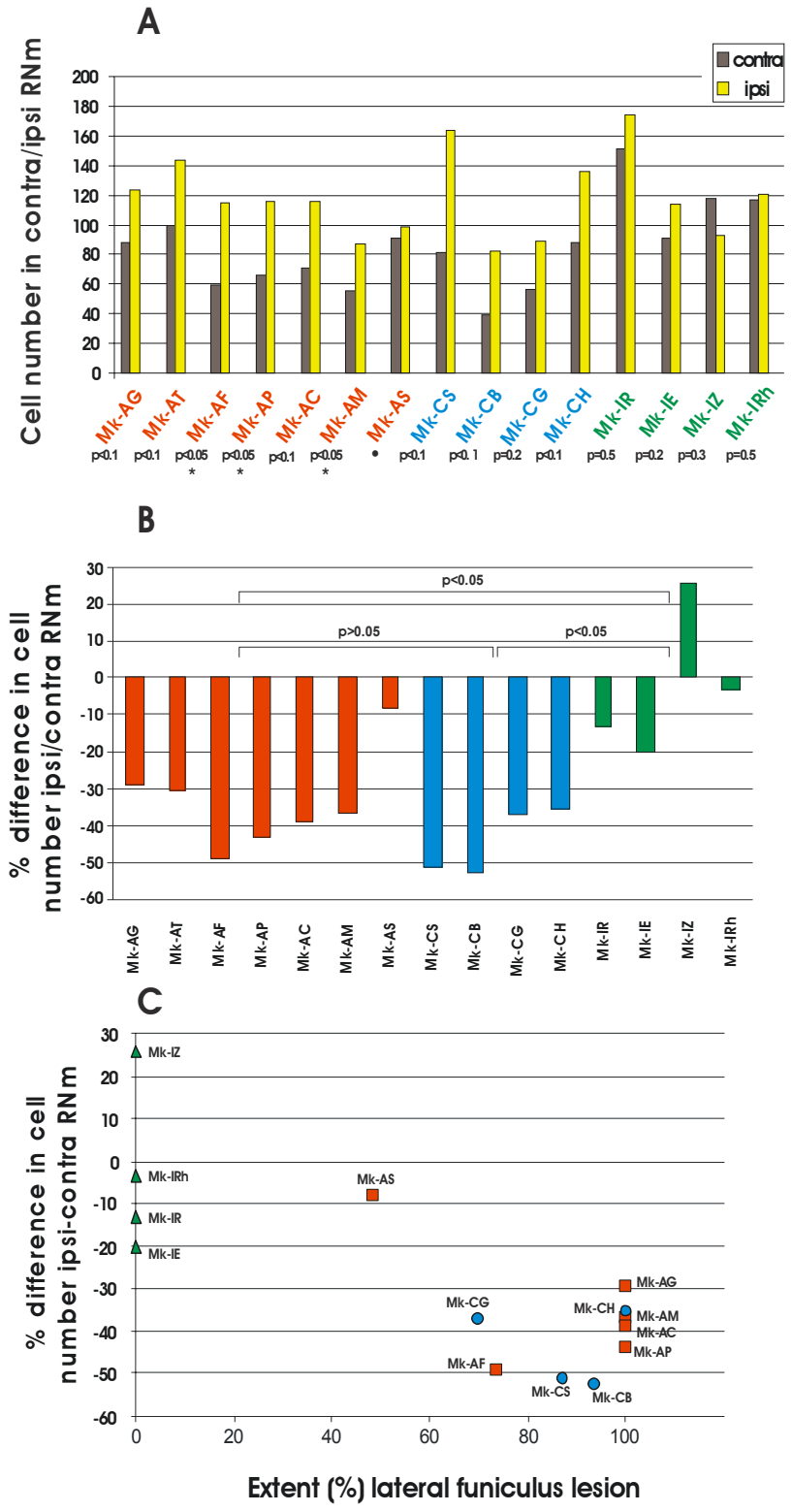

Figure 3

A: Histograms of the number of SMI-32 positive cells (with a visible nucleus) counted in the RNm on the contralesional (brown) and ipsilesional (yellow) sides. The first seven animals (red names)

were subjected to unilateral cervical cord lesion and subsequently treated with the anti-Nogo-A antibody. The next four animals (blue names) were lesioned and treated with a control antibody. The last four animals (green names) were intact. In these latter animals “contra” and “ipsi” corresponded to the left and right RNm, respectively. The statistical significance of the cell number difference between the RNm on the two sides was calculated using the Wilcoxon signed-rank, 1-tailed test. The number of neurons for each histological section of the RNm of both sides throughout the entire extent of the RNm was compared. In three of the lesioned animals this difference was statistically significant ($p < 0.05$, asterisks). In seven lesioned monkeys the difference was not statistically significant ($p< 0.1$ or $p = 0.2$ in Mk-CG). All the intact animals exhibited a cell number difference that was not statistically significant. For Mk-AS the statistical significance could not be calculated (see methods).

B: Difference in the number of SMI-32 positive cells calculated in percentage between the two sides of the RNm in the animals shown in the same order as in panel A. Colour codes indicate the different animal groups as in panel A: in red the lesioned animals, treated with the anti-Nogo-A antibody; in blue the lesioned animals treated with a control antibody; in green the intact animals. In Mk-AS, characterized by an incomplete lesion of the RS tract (less than 50%), the difference appeared comparable to the one of the intact monkeys (“green” animals). Beside this animal, the percentage difference in lesioned animals showed a high variability ranging from 17 to 35%. Note that Mk-CG and Mk-AF have also an incomplete lesion of the RS tract (less than 75%, open circles in figure 1). To statistically evaluate the impact of the anti-Nogo-A or control antibody treatment on the cell number difference between the RNm of the two sides, we compared the values among the three groups of animals. The difference among the two groups of lesioned animals was not statistically significant ($p > 0.05$) whereas the difference between each group of lesioned animals and the group of intact animals was statistically significant ($p < 0.05$).

C: The data shown in panel B were plotted against the extent of the lesion of the lateral funiculus calculated in percentage (see Table 2). Red squares are for lesioned animals treated with the anti-Nogo-A antibody. Blue circles are for lesioned animals treated with a control antibody. Green triangles are for intact animals. For easier comparison with the other animals, the value for Mk-IZ has been set as positive number in this figure. The variability of the values calculated for the lesioned animals appears independent of the fact that the animal was treated with an anti-Nogo-A or a control antibody. Mk-AT is not shown as the lesion extent could not be estimated (see Table 1 and methods).

Do the SMI-32 positive RNm neurons shrink?

As mentioned above, shrinkage of RNm neurons as consequence of the cervical hemisection has also to be considered. To address this issue, we calculated the somatic cross-sectional area of the RNm neurons that were included in the cell counting (Table 2), and these measurements were shown for each monkey as paired box and whisker-plots for the contralesional and ipsilesional sides, respectively (Fig. 4 A-C). Figs. 4A and 4B show the distribution of somatic cross-sectional areas of RNm neurons in the anti-Nogo-A antibody treated and control antibody treated groups for the lesioned monkeys, respectively. In all lesioned monkeys, a systematic and substantial decrease of the cross-sectional somatic area was observed in the contralesional RNm as compared to the ipsilesional RNm. For all lesioned animals, the shrinkage of cross-sectional somatic area of RNm neurons contralesionally was statistically significant (Mann-Whitney *U*-test, $p < 0.05$), irrespective of the treatment with the anti-Nogo-A or with a control antibody. The intact animals, in sharp contrast and as expected, did not show any systematic and significant difference ($p > 0.05$) in neuronal cross-sectional somatic area between left and right RNm (Fig. 4C).

The percentage difference between the median values of the cross-sectional somatic areas on each RNm for each animal was calculated and the values plotted against the extent of the lateral funiculus lesion (Fig. 4D). In intact animals, the difference of the median area between the two RNm ranged from 1.1% to -9.4%. Once more these figures reflect the normal individual and methodological variability. In contrast, all animals subjected to a cervical cord hemisection exhibited a significant shrinkage of the RNm neurons contralesionally, with a difference between the two sides ranging from -13.6% to -36.7 %, not overlapping with the range found for intact monkeys (Fig. 4D).

Figure 4

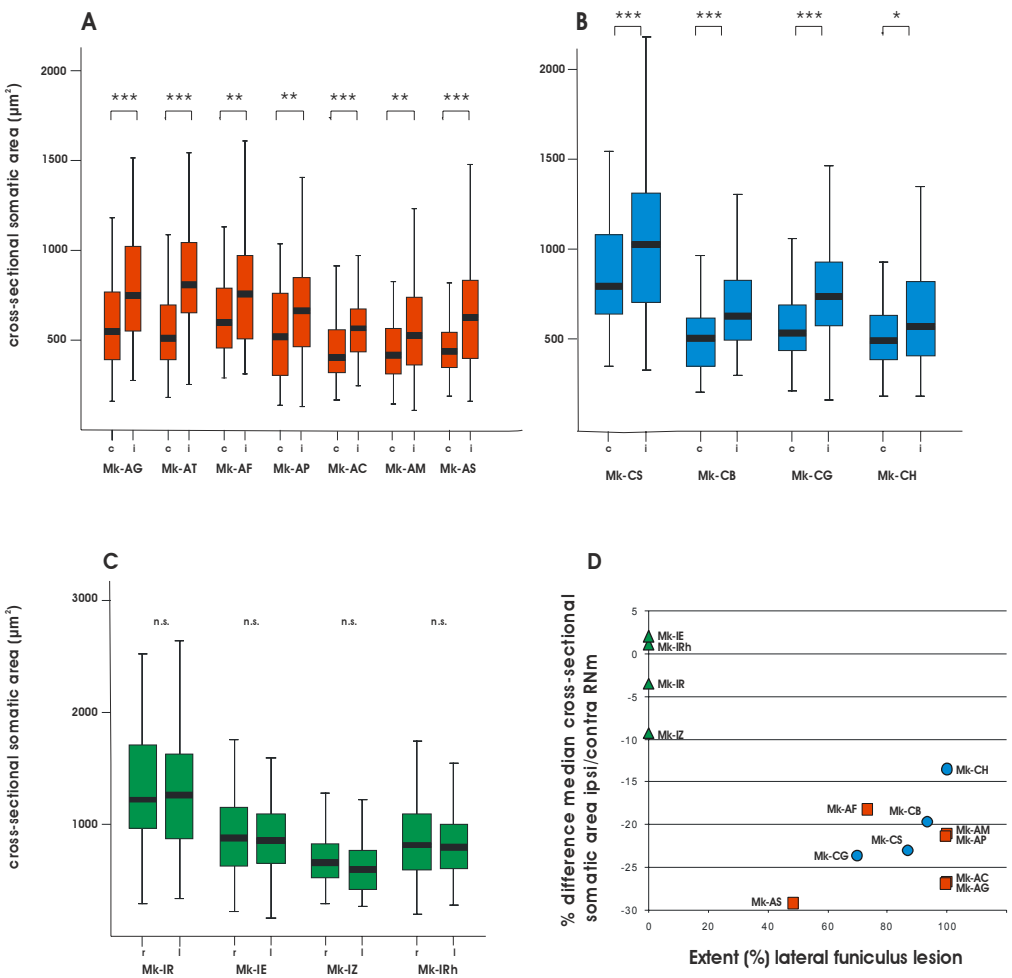

Figure 4

A: Box and whisker plots showing the distribution of somatic cross-sectional areas of SMI-32 positive RNm neurons in lesioned animals treated with an anti-Nogo-A antibody. For each animal the contralesional (c) and the ipsilesional (i) RNm are shown. The soma areas did not follow a normal distribution and therefore were graphically represented in the form of box and whisker plots, emphasizing the median value. Consequently, the statistical analysis was conducted using a non-parametric unpaired test (see below). In the box and whisker plots, the horizontal black line in the box corresponds to the median value, whereas the top and bottom of the box are for the 75 and 25 percentile values respectively. The top and bottom extremities of the vertical lines on each side of the box are for the 90 and 10 percentile values, respectively. A statistical comparison between the two RNm on each side was conducted for each animal using the non-parametric Mann and Whitney test. All animals of this group exhibited a statistically significant difference of soma area across the two RNm of each side (**=p<0.001;***=p<0.0001)

B: Box and whisker plots showing the distribution of somatic cross-sectional areas of SMI-32 positive neurons in lesioned animals treated with a control antibody. For each

animal the contralesional (c) and the ipsilesional (i) RNm are shown. Other conventions are as in panel A. All animals of this group showed a statistically significant difference of soma area across the two RNm on each side (*=p<0.01; ***=p<0.0001).

C: Box and whisker plots showing the distribution of somatic cross-sectional areas of SMI-32 positive neurons in intact animals. The two RNm are indicated here as right (r) and left (l). As expected, the comparisons of cross sectional areas between the RNm on each side did not show any statistically significant difference (n.s. =p>0.05).

D: The difference, expressed in percentage, between the median values of somatic cross-sectional areas of SMI-32 positive neurons in the contralesional and ipsilesional RNm was plotted against the extent of the lateral funiculus lesion expressed in percentage (see Table 2). Red squares are for lesioned animals treated with the anti-Nogo-A antibody. Blue circles are for lesioned animals treated with a control antibody. Green triangles are for intact animals. The variability among values in lesioned animals appears independent of the antibody treatment. Mk-AS which had a rather incomplete lesion (less than 50%) shows a very high (the highest) value of cell surface difference between the two RNm. Mk-CH characterized by a complete lesion has a rather low (but significant, see box plot in B) value of cell surface difference.

1.4 Discussion

In the present investigation we have shown that unilateral cervical cord injury interrupting RS axons also affects the neurons of origin in the contralesional RNm. Although the majority of RS neurons in the contralesional RNm clearly survived to axotomy, there was a significant reduction of the number of SMI-32 positive neurons. In addition, these neurons showed a significant shrinkage of their soma. Finally, our results indicate that treatment with an anti-Nogo-A antibody, applied at the level of the spinal cord lesion, did not reduce the decrease of the number of SMI-32 positive neurons counted in the contralesional RNm or their soma shrinkage.

Lesion extent

In primates both the lateral CS and the RS tracts are found in the lateral funiculus of the spinal cord and influence mostly the distal but also the proximal muscles of the forelimb (Belhaj-Saïf et al., 1998; Belhaj-Saïf and Cheney, 2000). In particular, though in primates the RS tract is reduced in size with respect to other mammals such as cat or rats, it has been shown that after unilateral lesion of the CS tract at the level of the pyramids, the RNm shows a certain degree of functional reorganisation that may contribute to the recovery of motor function for the forelimb (Belhaj-Saïf and Cheney, 2000). However, a lesion of the lateral funiculus at cervical level of the spinal cord will affect both the RS and the CS tracts as in this area the two pathways overlap to some extent, although the RS tract lays slightly more ventrally that the CS tract in the lateral funiculus. Despite the fact that, in the present study, the RS tract was not traced, the analysis of the reconstructed cervical cord hemisections (Fig. 1) allowed assessment of the degree of completeness of RS tract transection, by expressing the lesion extent as the percentage of the quadrant of white matter going from the dorsal to the ventral rootlet zone. Tracing studies in monkeys have shown that the RS tract is included entirely in this quadrant (Holstege et al., 1988; Burman et al., 2000b).

Cell bodies selection and analysis: technical considerations

In the monkey the RNm constitutes the caudal third of the entire RN and it is composed of loosely scattered large cells together with a few smaller cells (Ralston and Milroy, 1989). In individual histological sections large neurons were few and were segregated in small groups among the fibres fascicles of the oculomotor nerve (Fig. 2A). SMI-32 labelled neurons were rather large (Fig. 2B) and showed a radial spread of

relatively large dendrites. This morphology corresponded to the description of monkey RS neurons previously reported (Padel and others, 1981; Burman et al., 2000a).

The number of SMI-32 positive neurons was estimated in one series of sections over the whole extent of the RNm. Thus, we did not count the absolute number of SMI-32 positive neurons in the RNm. Instead, we compared the relative number of RNm cells counted on both sides of the brain of each animal. Because the number of SMI-32 stained neurons in RNm is relatively low (see results), we did not use a stereological probe to estimate their number but we counted all visible nuclei of the labelled cells on the analyzed sections. This approach is considered as adequate as all samples were analyzed using the same procedure and the number of cells is low (Geuna, 2000; Lavenex et al., 2000; Benes and Lange, 2001). In the present case, in addition, the validity of the method is supported *a posteriori* by the absence of overlap between lesioned and intact monkeys in a large group of animals as well as by the absence of difference between the RNm on both sides in intact monkeys.

Cervical cord (C3) hemisection in rat induced, beside other molecular changes, a reduction of neurofilament mRNA in RS neurons (Tetzlaff and others, 1991). This is probably also the case in RS neurons in monkey as the labelling on the contralesional side was fainter than on the ipsilesional side. Thus it might be possible that the SMI-32 antibody would not label some neurons because the expression of the epitope recognised is strongly reduced. However, when we compared Nissl labelled sections of the RNm of lesioned animals to adjacent sections labelled with SMI-32, the numbers of cells found in RNm were comparable (Table 2).

Cell number

Counts of RNm cells on both sides showed inter-individual and methodological variability, as shown for intact monkeys (Fig.3 A, B “green” group) where the percentage difference between the two sides ranged from -3.3 to 25.8% but it was not statistically significant. In lesioned monkeys the difference in the number of SMI-32 positive cells detected in the contralesional and ipsilesional sides was statistically significant in three monkeys (Fig. 3A, $p < 0.05$, asterisk). In the other monkeys the difference was not significant ($p > 0.05$), but as the statistical analysis was done on a relatively small number of data points (cells counted in each section, especially in Mk-CB and Mk-CG), these values indicate a tendency towards a difference in cell number between the two RNm. In these eleven animals, the values of percentage cell difference were rather variable, ranging from -8.1% to -52.4%. Interestingly, the two animals having the highest values (Mk-CS, -51.2% and Mk-CB, -52.4 %) were also the ones having a longer period of

survival after the lesion (around 200 days, Table 1). Otherwise, the high variability could not be systematically correlated to any other parameter.

In the absence of direct evidence of cell death or apoptosis, the question arises as to whether the decrease in the number of SMI-32 positive RNm neurons reported in the present study reflects cell death or rather changes in the phenotype of axotomized RS neurons which then impairs their detection. In the adult rat, some reports have suggested that SCI leads to the death of a sizable proportion of RS neurons (Mori et al., 1997; Houle and Ye, 1999; Novikova and others, 2000), while some other reports have brought evidence that the axotomized RS shrink but survive in an atrophic state (Kwon and others, 2002), (Prendergast and Stelzner, 1976). These discrepancies of interpretation may result from methodological differences; in particular they may reflect the inherent difficulty to detect shrunken neurons. In the case of the monkey, chromatolytic RNm neurons have been observed after SCI, a feature that is consistent with cell death (Bodian, 1946; Padel and others, 1981). Moreover, in investigations of the fate of CS neurons using the same material as in the present report, we observed that CS neurons can be detected on SMI-32 stained material despite their axotomy induced atrophy and phenotype changes (Wannier and others, 2005a; Beaud et al., 2006). These observations suggest that the method was adequate to reveal atrophic neurons and hence that in the primate, some RS neurons die in consequence of an axotomy at the level of the cervical spinal cord. This would in turn indicate that RS neurons in different species react differently to axotomy. In the adult opossum, most RS neurons survive SCI, but a limited proportion of RS neurons consistently disappears, an observation that was interpreted as indicative of limited cell death (Xu and Martin, 1990). Furthermore, this idea is supported by observations on CS neurons. In the adult rat, SCI leads to apoptosis in MI (Hains et al., 2003). However, as mentioned above, in the macaque, the total number of SMI-32 positive cells in layer V of MI remains unchanged (Wannier and others, 2005a), indicating that there occurred no sizeable CS neurons loss. However, there remain space for debate, since after a spinal cord lesion in the macaque, only few apoptotic cells were detected inside the dorsolateral funiculus rostrally to the lesion (Crowe et al., 1997). This data suggests that the lesion induced at most a limited degeneration of the CS and RS axons, and hence that their cells of origin survive. In view of this data, additional evidence is required to establish the exact fate of axotomized RS neurons in the macaque.

Cell size

The measurement of the cross-sectional somatic areas of neurons in the RNm of both sides revealed that in all lesioned animals the contralesional RNm showed a

significant reduction in cell size as compared to the ipsilesional side (Fig. 4). Conversely, in intact animals the cell size difference between the two RNm was not statistically significant. The median values of somatic cross-sectional areas of SMI-32-positive neurons obtained in the four intact monkeys ranged from 601 to 1268 μm, indicating a high inter-individual variability. These values are however in agreement with values previously reported (Padel and others, 1981; Burman and others, 2000a). In lesioned animals the ipsilesional RNm showed median values ranging between 526 and 1023 μm. These values indicated again a considerable individual variability and were comparable, as expected, to the ones observed in intact animals. In contrast, the contralesional RNm showed lower median values ranging from 413 to 787 μm. The box plot distribution and statistical analysis showed that this difference in somatic cross-sectional area between the RNm of the two sides was significant for all lesioned monkeys (Fig. 4 A, B). In contrast, the percentage difference of median values of somatic cross sectional area between the two RNm on each side ranged from 1.1% to -9.4% in intact animals and none was statistically significant. The relationship between the values of cross-sectional area difference and the extent of the lesion was not straightforward. For instance, the lowest percentage difference of somatic cross-sectional area (-13.6%, Mk-CH) was found in an animal with complete transection of the RS/CS tracts, whereas in this animal the cell number difference between the two RNm was relatively high (-35.3%). In general, the poor correlation with parameters such as lesion extent and survival time is due to an individual variability, representing a major aspect of the impact of axotomy at cervical level. This variability is also reflected in the literature by the divergent results reported with respect to cell death and cell body shrinkage.

Anti-Nogo-A antibody treatment

Anti-Nogo-A antibody treatment applied at the level of the spinal cord lesion did influence neither the number nor cross-sectional-somatic area of SMI positive neurons in the contralesional RNm. In other words, the treatment did not have a measurable impact on RS cell body survival or maintenance. Such a protective effect may have been expected as an indirect consequence of the increased number of synaptic boutons which is associated with the sprouting and/or regeneration which is commonly induced by the neutralization of Nogo-A. Indeed, new synapses could provide additional sources of neurotrophic substances and thus help neurons to respond to the damaging effects of axotomy. As no study has yet investigated whether the neutralization of Nogo-A promotes sprouting and/or regeneration of RS neurons in the non-human primate, the question remains as to whether the absence of effects reported here indicates that these neurons

do not generate new synapses in response to the treatment. This view is however rather unlikely, because no effect on the number or volume of SMI-32 neurons was observed for axotomized CS neurons (Beaud and others, 2006). For these neurons, the mechanisms mentioned above should have then entered in action, as the neutralization of Nogo-A has been shown to promote CS axonal sprouting after cervical spinal cord lesion in rats (Bregman et al., 1995; Schwab, 2004; Liebscher et al., 2005), marmoset monkeys (Fouad et al., 2004) and macaque monkeys (Freund and others, 2006; Freund and others, 2007). Nevertheless, the issue of whether anti-Nogo-A antibody treatment enhances sprouting of the RS tract in non-human primates remains an open question that will require future attention.

Experimental procedure

All animals included in the present study belong to a long-term research project on spinal cord lesion from which post-lesion changes in the CS system were described earlier (Schmidlin et al., 2004; Schmidlin et al., 2005; Wannier and others, 2005a; Freund and others, 2006; Freund and others, 2007). To assess the number of RS neurons in this model, midbrain sections including the red nucleus were obtained from 15 adult (3-8 years old) macaque monkeys (*Macaca mulatta* or *Macaca fascicularis*). All experiments were conducted in accordance with the Guide for the care and Use of Laboratory animals (ISBN 0-309-05377-3; 1996) and approved by the local (Swiss) veterinary authority. Following an initial period of 2-3 months during which the animals were trained to perform several manual dexterity tasks until they reached a stable level of performance, 11 of these 15 monkeys were subjected to hemisection of the cervical spinal cord. The lesion consisted of a unilateral transection performed at the C7/C8 border. The manual dexterity performances were assessed for several months post-lesion, until the animals reached a plateau reflecting a stable level of manual dexterity. The behavioural, electrophysiological and neuroanatomical tracing data related to the CS tract derived from these animals were described in previous reports (Schmidlin and others, 2004; Schmidlin and others, 2005; Wannier and others, 2005a; Wannier et al., 2005b; Freund and others, 2006; Freund and others, 2007). The present report is focussed on anatomical aspects dealing specifically with the issue of fate of RS neurons after unilateral cervical section. Therefore, only the methods relevant to this specific issue will be described in detail below. In addition, the anatomical data derived from the 11 lesioned monkeys were compared with data derived from 4 intact monkeys.

Surgical procedures

The surgical procedures for the unilateral spinal cord lesion at C7/C8 level have been described in detail in previous reports; (Schmidlin and others, 2004; Wannier and others, 2005a; Freund and others, 2006; Freund and others, 2007). Briefly, the animal was anesthetized by intramuscular (i.m.) injection of ketamine (Ketalar®; Parke-Davis, 5 mg/kg, i.m.). Before surgery, atropine was injected i.m. (0.05 mg/kg) to reduce bronchial secretions and the animal was treated with the analgesic Carprofen (Rymadil®, 4 mg/kg, s.c.). To assure and monitor deep anesthesia, a catheter was placed in the femoral vein for continuous perfusion with a mixture of propofol 1% (Fresenius ®) and a 4% glucose solution (1 volume of Propofol and 2 volumes of glucose solution). The animal was placed in a ventral decubitus position, with his head kept in a flexed position ventrally to expose the posterior cervical region. Under sterile conditions, a complete C6 laminectomy and an upper C7 hemi-laminectomy were performed to expose the spinal cord. Next, the dura mater was incised longitudinally. To perform the unilateral section of the spinal cord at the C7/C8 border, the dorsal root entry zone, identified under the microscope, was taken as the most medial landmark. From this target, a surgical blade (no 11, Paragon®) was inserted 4 mm in depth perpendicularly to the spinal cord, and the section was prolonged laterally to completely transect the dorsolateral funiculus. The rostro-caudal levels were the dorsal rootlets entering respectively the 7^{th} and the 8^{th} cervical spinal segments. This region corresponds to the rostral zone of the spinal portion covered by the 6^{th} cervical lamina. The muscles and the skin were sutured and the animal recovered from anaesthesia in about half of an hour. After the spinal lesion, the animal was kept alone in a separate cage for a few days, to allow best conditions for recovery. Then, the usual housing in groups with other monkeys was restored. To assess the effect of a regenerative treatment, an osmotic pump (Alzet®, 2ML2, flow: 5 µl/h) delivering either a monoclonal mouse IgG or an antibody neutralizing Nogo-A was inserted subcutaneously between the shoulder blades and changed once after 2 weeks. In order to deliver the antibody in close proximity of the lesion, the free tip of a polyethylene tube attached to the pump was fixed under the dura few mm rostrally to the cervical lesion.

Anti-Nogo-A antibodies

Two monoclonal antibodies (mAbs) against different sites of Nogo-A were employed: the mouse mAb 11C7 was raised against a 18 amino acid sequence of rat Nogo-A (aa623 – 640) close to the most inhibitory region of the Nogo-A protein (Oertle et al., 2003). The second antibody used, mAb hNogo-A recognized the Nogo-A specific region of the human Nogo-A sequence. Both antibodies identify primate Nogo-A monospecifically on Western blots (Oertle and others, 2003; Weinmann et al., 2006; Freund and others, 2006; Freund

and others, 2007). The antibodies were purified as IgGs and concentrated to 3.7-10 mg/ml in PBS (Freund and others, 2007).

Control antibodies

Purified IgG of a mouse mAb directed against wheat auxin (AMS Biotechnology, Oxon/UK) was used as control antibody (concentration: 3.7-10 mg/ml).

Histology

Monkeys were sacrificed at different time points (days) post-lesion (Table 1). For sacrifice, the animal was first sedated with ketamine and subsequently deeply anaesthetized by an intraperitoneal injection of a lethal dose of pentobarbital (90 mg/kg). Monkeys were perfused transcardially with 0.4 litre of 0.9% saline, followed by 4 litres of fixative (4% solution of paraformaldehyde in 0.1 M phosphate buffer, pH=7.6). This fixative was followed by 3 solutions of sucrose of increasing concentration (10% in fixative, 20 and 30 % in phosphate buffer) to prepare the tissue for cryoprotection. For this purpose, after dissection the brain and the spinal cord were additionally stored in a 30% sucrose solution for 1-2 days. Frozen sections of the brain comprising both sides of the midbrain at the level of the RN were cut in the coronal plane at a thickness of 50 µm. The sections were distributed into eight series. The lesion site was reconstructed from camera lucida drawings of individual paralongitudinal consecutive Nissl-stained sections of the cervical spinal cord. The drawings were then aligned to allow reconstruction of the location and extent of the lesion on a transverse view of the spinal cord (Fig. 1), as previously described (Schmidlin and others, 2004; Wannier and others, 2005a). In one monkey (Mk-AT, table 1) the size of the lesion could not be estimated due to poor quality of the spinal cord tissue after histological processing.

A series of brain sections was stained immunocytochemically with a monoclonal SMI-32 antibody (Sternberger Monoclonals, Covance Antibodies, USA). The epitope recognised by the SMI-32 antibody lies on non-phosphorylated regions of the neurofilament protein and is only expressed by particular categories of neurons (Campbell and Morrison, 1989; Tsang et al., 2000). Standard immunohistochemical procedures were used as previously described (Liu et al., 2002). Comparison of adjacent series of sections stained either for Nissl or with the SMI-32 antibody indicated that virtually all neurons in the RNm were labelled by this antibody (see results). As the brain was cut into 8 series (see above), sections stained with the SMI-32 antibody and including entire rostro-caudal extent of the RNm were usually six to nine. For every animal, all sections were included in the analysis.

To evaluate the effect of the lesion on RS neurons, we analysed the series of coronal sections stained for SMI-32 through the midbrain and we identified the position and the extent of the RNm close to the roots of the oculomotor cranial nerve (Fig. 2A) (Paxinos et al., 2000). Well stained SMI-32 positive RNm cells were easily identifiable even using low magnification (x40). In lesioned animals, RNm neurons on the contralesional side were smaller and somewhat more faintly stained than ipsilaterally, and therefore some of them may have escaped detection at low magnification. To circumvent the problem, the quantitative analysis was conducted at higher magnification (x400) for better discrimination. The number of SMI-32 stained RNm cells and the projected surface of their cell body was obtained from digitised photomicrographs using appropriate software (Neurolucida®). The neurons included in this analysis were SMI-32 positive and had a visible nucleus (Fig. 2B). The possibility of sampling the RNm neurons as required by stereological methods appeared not applicable here as the number of neurons responding to the criteria listed above was relatively small. Instead, all RNm neurons filling the above criteria were counted on each individual section. In addition, our aim was not to establish the absolute total number of cells in the RNm but to compare the number and size of neurons in the RNm on each side. This method was shown to be reliable in the motor cortex for the CS neurons (Wannier and others, 2005a). Furthermore, in six animals (data not shown) the cross-sectional area of the nucleus of all neurons included in the counting was calculated. The derived maximal value of the diameter ranged from 8.5 to 20.8 microns. These values were far below the section thickness of 50 µm. Thus, the possibility of introducing significant counting errors by including fractions of the cells is unlikely. Only the soma without the numerous dendritic ramifications was underlined to determine the cell body cross-sectional area. Because of the presence of large dendritic ramifications (Fig. 2B) the cell body contour was in some cases difficult to delineate. Therefore, we considered that, along these large processes, the soma ended at a distance of 20 µm from the nucleus, thus corresponding to the same procedure as used for CS neurons (Wannier and others, 2005a). For comparison, brain sections from four intact animals, which had been included in previous tracing studies (Liu and others, 2002), were used as control material for the SMI-32 analysis of RNm neurons. Counts of SMI-32 positive RNm neurons and measurements of their somatic cross-sectional area were performed for each monkey on both right and left brain side on coronal sections, separated by 400 µm each. The rostro-caudal dimensions of the RNm thus analysed was consistent with the calculated dimensions of the RNm as derived from the atlas of the macaque brain (Paxinos and others, 2000). Each section comprised both the right and left side of the brain (except for

Mk-AS). When cutting the midbrain, care was taken to position the bloc parallel to the coronal plane so that for each section the two RNm were at a similar level. As shown already for the cerebral cortex (Wannier and others, 2005a), althought the sections shrank to some degree, the shrinkage was very similar for the two brain sides on a given section. In other words, cell counts and somatic cross-sectional area measurements were performed on brain halves of comparable thickness for each section analyzed. Consequently, the quantitative comparisons regarding the number of RNm neurons and their somatic cross-sectional area have been conducted on comparable volumes of tissue in RNm. Data were then analysed with the SPSS software for statistical evaluation of the significance of cell number difference and cross-sectional area difference between the RNm neurons on the two sides of midbrain. Statistical analysis on the cell number was conducted by comparing the number of cells in each histological section and on the RNm of each brain side. The data obtained were analysed by means of the Wilcoxon signed-rank, 1-tailed test. In one monkey (Mk-AS) this analysis could not be performed as the two brain sides were processed separately and it was not possible to compare equivalent levels of the RNm for each side. The statistical analysis concerning the cross sectional somatic area was performed by using the non-parametric Mann and Whitney test (see results).

Acknowledgements

The authors wish to thank the technical assistance of Christiane Marti, Georgette Fischer, Monika Bennefeld, Véronique Moret, Françoise Tinguely and Christine Roulin (histology and behavioural evaluations), Josef Corpataux, Bernard Morandi, Bernard Bapst and Laurent Bossy (animal house keeping), André Gaillard (mechanics), Bernard Aebischer (electronics), Laurent Monney (informatics). We thank Prof. Pierre Lavenex for helpful discussion.

Table 1: List of cervical cord lesioned and intact monkeys included in the present study with identification code (same as in Freund et al., 2006 for the lesioned animals).

	Mk-AG	**Mk-AT***	**Mk-AF**	**Mk-AP**	**Mk-AC**	**Mk-AM**	**Mk-AS**	**Mk-CS**	**Mk-CB**	**Mk-CG**	**Mk-CH**	**Mk-IR**	**Mk-IE**	**Mk-IZ**	**MkIRh**
Species	fasc.	fasc.	mul.	fasc.	fasc.	fasc.	asc.	mul.	fasc.	asc.	fasc.	mul.	mul.	fasc.	mul.
Treatment	Anti-Nogo-A (hNogo)	Anti-Nogo-A (hNogo)	Anti-Nogo-A (11C7)	Anti-Nogo-A (11C7)	Anti-Nogo-A (hNogo)	Anti-Nogo-A (hNogo)	Anti-Nogo-A (11C7)	Contr.	Contr.	Contr.	Contr.	Intact	Intact	Intact	Intact
Proportion of hemi-section extent (%)	78	-	56	58	85	80	41	63	75	51	90	0	0	0	0
Lateral funiculus lesion extent (%)	100	-	73.4	100	100	100	48.2	87	93.4	70	100	0	0	0	0
Functional Recovery (%)	100	(100)	57	99	100	96	100	22	78	90	53	-	-	-	-
Completeness of CS/RS section	Yes	-	No	Yes	Yes	Yes	No	Yes	Yes	No	Yes	-	-	-	-
Survival time after lesion (days)	112	97	144	160	135	13	8	282	198	225	140	138	-	-	-	-
Age at sacrifice (years)	3.5	3.75	6.25	6.5	~ 4	~ 4	6.25	4.5	5	~ 4	~ 4	5	~ 5	7.75	6.5

At the time of the experiment, the monkeys had different names, not indicating whether the animal was infused with the control or the anti-Nogo-A antibody or was an intact animal. New names were assigned to the monkeys during the writing of the manuscript to improve its readability, in consistency with Freund *et al*., 2006.

Under species, "mul." is for macaca mulatta while "fasc." is for macaca fascicularis.

The seven anti-Nogo-A antibody treated monkeys are in the seven leftmost columns ("Anti-Nogo-A") with indication of which of the 2 antibodies was used (mAb 11C7 or mAb hNogo-A), whereas the four control antibody treated monkeys ("Contr.") are in the next four columns. The four intact monkeys are in the four rightmost columns.

Proportion of hemi-section extent was calculated as the percentage of corresponding hemicord affected by the lesion on the frontal reconstruction of the cervical cord.

To tentatively determine more precisely the extent of the lesion affecting the RS and CS tracts, the lateral funiculus in the white matter was outlined going from the dorsal to the ventral rootlet zone. This was indicated as lateral funiculus lesion extent.

	Mk-AG	**Mk -AT**	**Mk -AF**	**Mk -AP**	**Mk-AC**	**Mk -AM**	**Mk-AS**	**Mk-CS**	**Mk-CB**	**Mk-CG**	**Mk-CH**	**Mk-IR**	**Mk -IE**	**Mk -IZ**	
Antibody Treatment	Anti-Nogo-A (hNogo)	Anti-Nogo-A (hNogo)	Anti-Nogo-A (11C7)	Anti-Nogo-A (11C7)	Anti-Nogo-A (hNogo)	Anti-Nogo-A (hNogo)	Anti-Nogo-A (11C7)	Contr. C	ontr. C	ontr.	Contr.	Intact	Intact	Intact	I
Lateral funiculus lesion extent (%)	100	*	73.4	100	100	100	48.2	87	93.4	70	100	0	0	0	
Number of SMI cells contralesional	88	10 0	59 (53)	66	71	55	91	81 (82)	39	56	88	51	91	1 17	
Number of SMI cells ipsilesional	124	144	115 (117)	116	116	87	99	166 (158)	82	89	136	174	114	93	
% difference in cell number	-29.0%	-30.6%	-48.7%	-43.1%	-38.8%	-36.8%	-8.1%	-51.2%	-52.4%	-37.1%	-35.3%	-13.2%	-20.2%	25.8%	-
Median cell size contralesional (μm^2)	548.19	510.67	607.3	520.11	413	415.83	441.6	787.53	502.87	556.28	494.03	1223.79	879.19	601	'
Median cell size ipsilesional (μm^2)	750.08	806.18	744.95	661.56	1.1	3.28	526.41	623.6	1023.6	626.31	728.75	571.9	1268.43	862.36	663	'
% difference in median	-26.9%	-36.7%	-18.5%	-	-26.7%	-21.0%	-	-	-	-	-	-3.5%	2%	-	

cell size				21.3%			29.2 %	23.1%	19 .7%	23 .7%	13.6%			9.4%	
Average cell number ipsilesional				114 ± 17					118 ± 21				125 ± 42		

Functional recovery was assessed here for manual dexterity based on the "modified Brinkman board" task (see Freund *et al*., 2006), by giving in percent the ratio of the post-lesion score to the pre-lesion score.

In the row "completeness of RS section", "No" and "Yes" indicate whether the RS transection was considered as partial or as complete, respectively (for further explanation see text).

Survival time: number of days separating the cervical cord hemisection and the sacrifice of the animal.

Age of the animal at sacrifice: for five animals the age was not precisely determined when they were received in our animal facility. Thus, their calculated age at sacrifice is the estimation according to the age attributed at arrival in the animal facility (~).

* In this animal the proportion of hemisection extent and consequently also the RS and CS extent could not be determined for technical reasons (poor quality of histology). In addition, in this same animal the lesion was too caudal and thus the 100% functional recovery cannot be interpreted.

Table 2: Summary of differences in cell number and somatic size in RNm on each side in the monkeys included in the present study.

As in Table 1, the seven anti-Nogo-A antibody treated monkeys are in the seven leftmost columns ("Anti-Nogo-A") with indication of which of the 2 antibodies was used (mAb11C7 or mAb hNogoA), whereas the four control antibody treated monkeys ("Contr.") are in the next four columns. The four intact monkeys are in the four rightmost columns. In lesioned animals the term “contralesional” indicates the RNm opposite to the spinal cord hemisection, whereas “ipsilesional” the RNm situated on the same side of the cervical cord section. In intact animals the contralesional RNm is to be intended as on the right side and the ipsilesional as on the left side.
In Mk-AF and Mk-CS the number of cells in parentheses indicates the number of cells counted in adjacent Nissl stained sections.

* In this animal the total lesion extent and consequently also the RS and CS extent could not be determined for technical reasons (poor histological quality).

1.5 References

Beaud M-L, Wannier T, Schmidlin E, Freund P, Bloch J, Mir A, Schwab ME, Rouiller EM. 2006. Anti-Nogo-A treatment enhanced sprouting of corticospinal axons but did notprevent cell body shrinkage in the motor cortex in adult monkeys subjected to unilateral cervical cord lesion.

Belhaj-Saïf A, Cheney PD. 2000. Plasticity in the distribution of the red nucleus output to forearm muscles after unilateral lesions of the pyramidal tract. In: p 3147-3153.

Belhaj-Saïf A, Hill Karrer J, Cheney PD. 1998. Distribution and characteristics of poststimulus effects in proximal and distal forelimb muscles from red nucleus in the monkey. In: p 1777-1789.

Benes FM, Lange N. 2001. Two-dimensional versus three-dimensional cell counting: a practical perspective. In: p 11-17.

Bodian D. 1946. Spinal projections of brainstem in rhesus monkey, deduced from retrograde chromatolysis. In: p 512-513.

Bregman BS, Kunkel-Bagden E, Schnell L, Dai HN, Gao D, Schwab ME. 1995. Recovery from spinal cord injury mediated by antibodies to neurite growth inhibitors. In: p 439-440.

Burman K, Darian-Smith C, Darian-Smith I. 2000b. Macaque red nucleus: origins of spinal and olivary projections and terminations of cortical inputs. In: p 179-196.

Burman K, Darian-Smith C, Darian-Smith I. 2000a. Geometry of rubro spinal, rubroolivary, and local circuit neurons in the macaque red nucleus. In: p 197-219.

Campbell MJ, Morrison JH. 1989. Monoclonal antibody to neurofilament protein (SMI-32) labels a subpopulation of pyramidal neurons in the human and monkey neocortex. In: p 191-205.

Crowe MJ, Bresnahan JC, Shuman SL, Masters JN, Beattie MS. 1997. Apoptosis and delayed degeneration after spinal cord injury in rats and monkey. In: p 73-76.

Egan DA, Flumerfelt BA, Gwyn DG. 1977. Axon reaction in the red nucleus of the rat. Perikaryal volume changes and the time course of chromatolysis following cervical and thoracic lesions. In: p 13-19.

Fouad K, Klusman I, Schwab ME. 2004. Regenerating corticospinal fibers in the Marmoset (Callitrix jacchus) after spinal cord lesion and treatment with anti-Nogo-A antibody IN-1. In: p 2479-2482.

Freund P, Schmidlin E, Wannier T, Bloch J, Mir A, Schwab ME, Rouiller EM. 2006. Anti-Nogo-A treatment enhances corticospinal tract sprouting and functional recovery after unilateral cervical lesion in adult primates. In: p 790-792.

Freund P, Wannier T, Schmidlin E, Bloch J, Mir A, Schwab ME, Rouiller EM. 2007. Anti-Nogo-A antibody treatment enhances sprouting of corticospinal (CS) axons rostral to an unilateral cervical spinal cord lesion in adult macaque monkey. In: p 644-659.

Geuna S. 2000. Appreciating the difference between design-based and model-based sampling strategies in quantitative morphology of the nervous system. In: p 333-339.

Hains BC, Black JA, Waxman SG. 2003. Primary cortical motor neurons undergo apoptosis after axotomizing spinal cord injury. In: p 328-341.

Holstege G, Blok BF, Ralston DD. 1988. Anatomical evidence for red nucleus projections to motoneuronal cell groups in the spinal cord of the monkey. In: p 97-101.

Houle JD, Ye JH. 1999. Survival of chronically-injured neurons can be prolonged by treatment with neurotrophic factors. In: p 929-936.

Kwon BK, Liu J, Messerer C, Kobayashi NR, McGraw J, Oschipok L, Tetzlaff W. 2002. Survival and regeneration of rubrospinal neurons 1 year after spinal cord injury. In: p 3246-3251.

Kwon BK, Liu J, Oschipok L, Teh J, Liu ZW, Tetzlaff W. 2004. Rubrospinal neurons fail to respond to brain-derived neurotrophic factor applied to the spinal cord injury site 2 months after cervical axotomy. In: p 45-57.

Lavenex P, Steele MA, Jacobs LF. 2000. The seasonal pattern of cell proliferation and neuron number in the dentate gyrus of wild adult eastern grey squirrels. In: p 643-648.

Liebscher T, Schnell L, Schnell D, Scholl J, Schneider R, Gullo M, Fouad K, Mir A, Rausch M, Kindler D, Hamers FP, Schwab ME. 2005. Nogo-A antibody improves regeneration and locomotion of spinal cord-injured rats. In: p 706-719.

Liu J, Morel A, Wannier T, Rouiller EM. 2002. Origins of callosal projections to the supplementary motor area (SMA): a direct comparison between pre-SMA and SMA-proper in Macaque monkeys. In: p 71-85.

Liu Y, Kim D, Himes BT, Chow S, Schallert T, Murray M, Tessler A, Fischer I. 1999. Transplants of fibroblasts genetically modified to express BDNF promote regeneration of adult rat rubrospinal axons and recovery of forelimb function. In: p 4370-4387.

Mori F, Himes BT, Kowada M, Murray M, Tessler A. 1997. fetal spinal cord transplants rescue some axotomized rubrospinal neurons from retrograde cell death in adult rats. In: p 45-60.

Novikova LN, Novikov LN, Kellerth J-O. 2000. Survival effects of BDNF and NT-3 on axotomized rubrospinal neurons depend on the temporal pattern of neurotrophin administration. In: p 776-780.

Oertle T, Van der Haar ME, Bantlow C, Robeva A, Burfeind P, Buss A, Huber AB, Simonen M, Schnell L, Brosamle C, Kaupmann K, Vallon R, Schwab ME. 2003. Nogo-A inhibits neurite outgrowth and cell spreading with three discrete regions. In: p 5393-5406.

Padel Y, Angaut P, Massion J, Sedan R. 1981. Comparative study of the posterior red nucleus in baboons and gibbons. In: p 421-438.

Paxinos G, Huang XF, Toga AW. 2000. The Rhesus monkey brain in stereotaxic coordinates. London: Academic Press.

Prendergast J, Stelzner DJ. 1976. Changes in the magnocellular portion of the red nucleus following thoracic hemisection in the neonatal and adult rat. In: p 163-172.

Raineteau O, Fouad K, Bareyre FM, Schwab ME. 2002. Reorganization of descending motor tracts in the rat spinal cord. In: p 1761-1771.

Ralston DD, Milroy AM. 1989. Red nucleus of *Macaca Fascicularis*: an electron microscopic study of its synaptic organization. In: p 602-620.

Schmidlin E, Wannier T, Bloch J, Belhaj-Saïf A, Wyss A.F., Rouiller EM. 2005. Reduction of the hand representation in the ipsilateral primary motor cortex following unilateral section of the corticospinal tract at cervical level in monkeys. In: p 56.

Schmidlin E, Wannier T, Bloch J, Rouiller EM. 2004. Progressive plastic changes in the hand representation of the primary motor cortex parallel incomplete recovery from unilateral section of the corticospinal tract at cervical level in monkeys. In: p 172-183.

Schwab ME. 2004. Nogo and axon regeneration. In: p 118-124.

Tetzlaff W, Alexander SW, Miller FD, Bisby MA. 1991. Response of facial and rubrospinal neurons to axotomy: changes in mRNA expression for cytoskeletal proteins and GAP43. In: p 2528-2544.

Tsang YM, Chiong F, Kuznetsov D, Kasarskis E, Geula C. 2000. Motor neurons are rich in non-phosphorylated neurofilaments: cross-species comparison and alterations in ALS. In: p 45-58.

Wannier T, Schmidlin E, Bloch J, Rouiller EM. 2005a. A unilateral section of the corticospinal tract at cervical level in primate does not lead to measurable cell loss in motor cortex. In: p 703-717.

Wannier T, Schmidlin E, Bloch J, Rouiller EM. 2005b. A unilateral section of the corticospinal tract at cervical level in primates does not lead to measurable cell loss in motor cortex. In.

Weinmann O, Schnell L, Ghosh A, Montani L, Wiessner C, Wannier T, Rouiller EM, Mir A, Schwab ME. 2006. Intrathecally infused antibodies against Nogo-A penetrate the CNS and downregulate the endogenous neurite growth inhibitor Nogo-A. In: p 161-173.

Xu XM, Martin GF. 1990. The response of rubrospinal neurons to axotomy in the adult opossum, Didelphis virginiana. In: p 46-54.

Chapter 6

Does anti-Nogo-A antibody treatment prevent cell body shrinkage in the motor cortex in adult monkeys subjected to unilateral cervical cord lesion?

This chapter has been adapted from an article originally published in BMC Neurosience (M.-L. Beaud,*, E. Schmidlin,*, T. Wannier*, P. Freund, J. Bloch, A. Mir, M.E. Schwab and E.M. Rouiller; 2008 Jan 14; 9(1):5)

* The first three authors contributed equally to the study.

1.1 Abstract

Background: After unilateral cervical cord lesion at the C7/C8 border interrupting the dorsolateral funiculus in adult monkeys, neutralization of Nogo-A using a specific monoclonal antibody promoted sprouting of corticospinal (CS) axons rostral and caudal to the lesion and, in parallel, improved functional recovery. In monkeys lesioned but not treated with the anti-Nogo-A antibody, the CS neurons in the contralesional primary motor cortex (M1) survived to the axotomy, but their soma shrank. Because the anti-Nogo-A treatment induces regeneration and/or sprouting of CS axons, it may improve access to neurotrophic factors. The question therefore arises as to whether anti-Nogo-A treatment prevents the soma shrinkage observed in the contralesional M1?

Results: Using the marker SMI-32, a quantitative and qualitative anatomical assessment of the pyramidal neurons in the layer V (thus including the CS cells) in M1 was performed and compared across three groups of animals: intact monkeys (n=5); monkeys subjected to the cervical cord lesion and treated with a control antibody (n=4); monkeys with the cervical lesion and treated with anti-Nogo-A antibody (n=5). SMI-32 positive neurons on the side contralateral to the lesion were generally less well stained than those on the ipsilesional hemisphere, suggesting that they expressed less neurofilaments. Nevertheless, in all three groups of monkeys, the amount of SMI-32 positive neurons in both hemispheres was generally comparable, confirming the notion that most axotomized CS neurons survived. However, shrinkage of CS cell body area was observed in the contralesional hemisphere in the two groups of lesioned monkeys. The cell surface shrinkage was found to be of the same magnitude in the monkeys treated with the anti-Nogo-A antibody as in the control antibody treated monkeys.

Conclusion: the anti-Nogo-A antibody treatment did not preserve the axotomized CS cells from soma shrinkage, indicating that the anti-Nogo-A treatment affects morphologically the axotomized CS neurons mainly at distal levels, especially the axon collateralization in the cervical cord, and little or not at all at the level of their soma.

1.2 **Background**

The motor deficits associated with interruption of the CS tract at a segmental level in monkeys were assessed in several studies (Aoki and Mori 1979;Darian-Smith, Cheema, Darian-Smith, Galea, and Ratcliffe 1990;Denny-Brown 1966;Freund et al. 2006;Galea and Darian-Smith 1997a;Galea and Darian-Smith 1997b;Holmes and May 1909;Mettler 1944;Sasaki et al. 2004b;Schmidlin, Wannier, Bloch, and Rouiller 2004)}. More precisely, a surprisingly good and rapid recovery of dexterous finger movements of the ipsilateral hand took place after hemi-section at C3 level in either newborn and juvenile monkeys (Galea and Darian-Smith 1997a,b), or in adult monkeys after hemi-section at C4/C5 (Sasaki et al. 2004) or C7/C8 level (Freund et al. 2006; Schmidlin et al., 2004).

Immediately after the cervical hemi-section and later on during the recovery, there was a dramatic reduction of the CS projection to the hemi-cord caudal to the lesion (Galea and Darian-Smith 1997a),indicating that the spontaneous recovery of manual dexterity was not due to a substantial reconstruction of the lesioned projection but rather to enhancement of the transmission of information from cortex to spinal cord in a reduced number of CS and/or corticobulbospinal projections together with a contribution of a more effective use of spinal circuits.

As far as the fate of the axotomized CS neurons is concerned, some controversy can be found in the literature. Some earlier anatomical studies suggested that pyramidotomy (Pernet and Hepp-Reymond 1975;Wohlfarth 1932) or cervical cord lesion(Holmes and May 1909;Levin and Bradford 1938) induced the death of a substantial part of the large CS neurons in the contralateral primary motor cortex (M1), amounting up to 70% loss (Pernet and Hepp-Reymond 1975;Wohlfarth 1932). In sharp contrast, other authors concluded that there was no retrograde degeneration with breakdown and loss of neurons after section of the CS tract (Davison 1937; Lassek 1942;Tower 1940). In a recent study (Wannier, Schmidlin, Bloch, and Rouiller 2005b) ,the issue of the fate of axotomized CS neurons was re-examined in two monkeys using SMI-32 as a specific marker for pyramidal neurons. We found that, after unilateral lesion of

the dorsolateral funiculus at cervical level (C7-C8), the CS neurons in the contralesional primary motor cortex (M1) survived the axotomy, but their soma shrank (Wannier et al., 2005b).

In a recent report, evidence was provided in monkeys that the functional recovery from unilateral cervical cord lesion and CS axonal sprouting can be enhanced by an antibody treatment neutralizing the neurite growth inhibitor Nogo-A (Freund et al. 2006) extending to the primates previous results obtained in the rat (e.g. Bregman et al., 1995; Liebscher et al. 2005; Schwab 2004). Indeed, several functional readouts of manual dexterity showed a faster and more complete recovery of manual dexterity in a group of six anti-Nogo-A antibody treated monkeys subjected to cervical hemi-section than in a group of six monkeys subjected to a comparable lesion but treated with a control antibody (Freund et al. 2006). Such enhancement of manual dexterity promoted by anti-Nogo-A antibody treatment was associated with an axonal sprouting of CS axons in the cervical cord rostral and caudal to the lesion (Freund et al. 2006). These new fibers could provide the axotomized CS neurons an augmented access to neurotrophic factors compared to that available to the axotomized CS neurons in control antibody treated animals. The goal of the present study was thus to investigate whether the anti-Nogo-A antibody treatment also exert an effect on the CS neurons at the level of their soma in the contralesional motor cortex, for instance by preventing the cell soma shrinkage occurring in the monkeys subjected to cervical lesion and treated with a control antibody (Wannier et al., 2005a). This hypothesis is plausible because, although the anti-Nogo-A antibody was delivered intrathecally in the cervical cord close to the lesion, the antibody was shown to reach the entire brain through the CSF circulation (Weinmann et al. 2006) and, therefore, it may have affected the CS cell bodies in the cerebral cortex as well.

1.3 Results

1. Cervical cord lesion

For the animals subjected to the unilateral spinal cord section, the extent of the lesion was assessed by reconstructing the incision site from histological sections (Fig. 1A). In most monkeys, the lesion completely transected the dorsolateral funiculus, thus corresponding to a complete transection of the CS axons originating from the contralesional hemisphere (as checked with BDA labeling of CS axons in most monkeys; see (Freund et al. 2006). In one monkey (asterisk in Fig. 1A), the dorsolateral funiculus was not completely transected and therefore a few CS axons as well as RS axons were spared by the lesion. The other seven monkeys had a complete transection of the dorsolateral funiculus on the lesioned hemi-cord (Table 1), thus corresponding to a complete interruption of the main CS tract originating from the opposite hemisphere (as discussed in detail earlier in (Freund et al. 2006). The monkeys Mk-AF and Mk-CC clearly had an incomplete lesion of the RS tract, whereas monkeys Mk-CS and Mk-CB possibly had an incomplete lesion of the RS tract (though transected at 95% at least). The RS tract transection was complete in the other four monkeys with complete lesion of the dorsolateral funiculus(Mk-AG, Mk-AC, Mk-AM and Mk-CH).

Figure 1

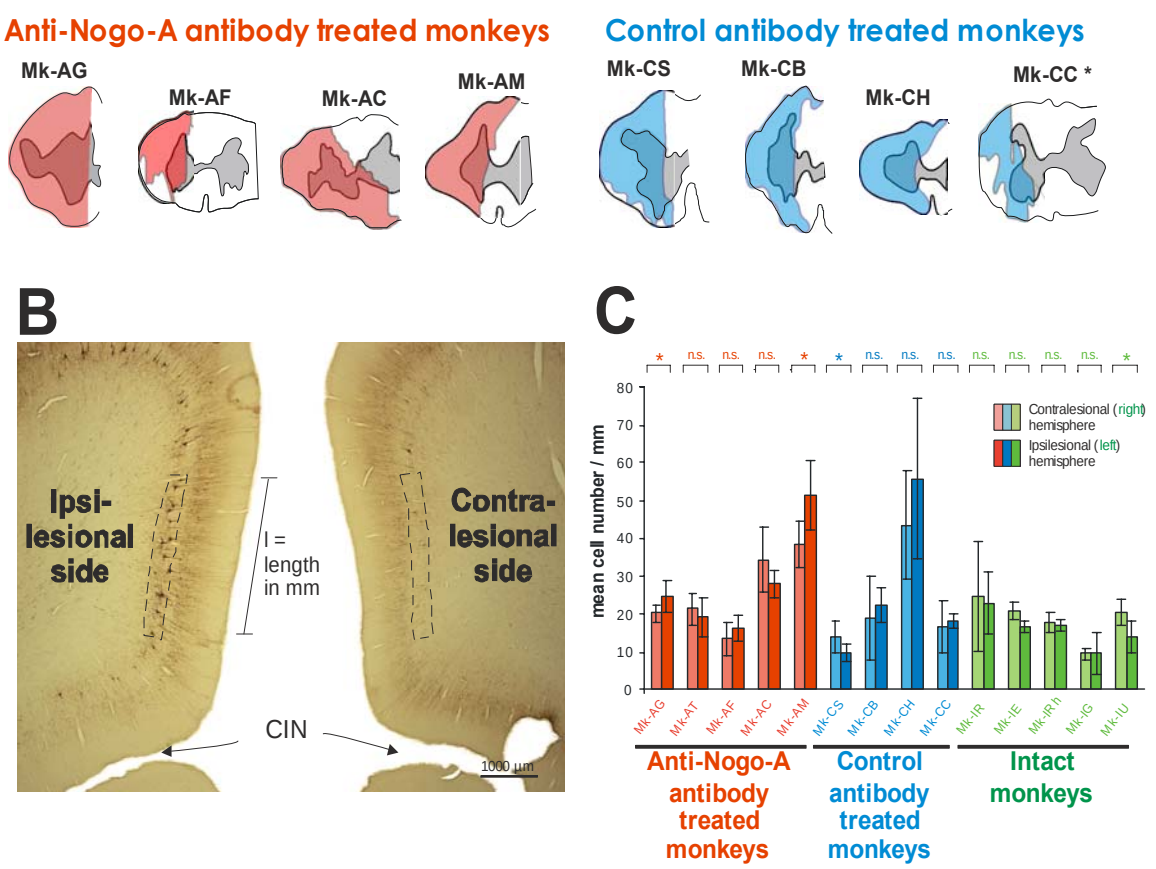

Figure 1: Spinal cord lesion and number of py ramidal neurons in lay er V of the motor cortex

A: Reconstruction from paralongitudinal sections of the lesion performed in eight monkeys at cervical level C7/C8. The lesion area is indicated in red for the anti-Nogo-A antibody treated monkeys and in blue for the control antibody treated monkeys. The gray zone in the center corresponds to the gray matter. In one monkey (Mk-AT), the tissue was damaged in the zone of the cervical cord lesion and it was not possible to precisely assess the position and extent of the lesion. The lesions have already been shown in recent reports (Freund et al., 2006; 2007). Although some lesions (hemi-sections) were on the left side and others on the right side, for simplification they were all represented here as a left side lesion.

B: Photomicrograph showing the part of M1 corresponding to the hindlimb representation on both hemispheres and stained with SMI-32. On both sides, SMI-32 typically labeled the pyramidal cells in the layers III and V. However, typically at such low magnification, the layer V appears more densely stained on the ipsilesional hemisphere than on the contralesional one (see text). The hindlimb area in M1 was thus visible on the same section for the two hemispheres and the observer could thus delineate roughly equally long portions of the layer V in each hemisphere on which the counts were performed (dashed line), as explained in detail earlier (Wannier et al 2005). The length of the portion of layer V in which counts were made (l in mm) was determined for data normalization. CIN = cingulate sulcus.

C: Bar graph indicating the mean number of SMI-32 positive neurons per unit length (and SD) counted in layer V of the hindlimb area in M1 of each hemisphere, on the sample of sections examined in the three groups of monkeys (green is for intact monkeys). * is for $p<=0.05$; n.s. is for $p>0.05$ (t-test for small samples as explained in the methods section).

D: A portion of the hindlimb area in M1, on which morphometric measurements were conducted, is shown at higher magnification, for a typical contralesional hemisphere (left photomicrograph). At low magnification (panel C), due to lighter SMI-32 staining than in the ipsilesional hemisphere, very few SMI-32 positive neurons were visible in layer V. At this magnification (left photomicrograph), some SMI-32 positive neurons appear. The observer then identified at high magnification and at different planes of focus all SMI-32 positive neurons with a visible nucleus in layer V (neurons highlighted on top of a yellow background), as shown on the right photomicrograph. In general, it turned out that, in spite of a lighter SMI-32 staining, the positive neurons with a visible nucleus were on average as numerous as in the ipsilesional hemisphere. In each photomicrograph, the cortical surface is on top and white matter on bottom. The SMI-32 positive neurons are typically found in layer III and layer V.

2. Do some axotomized CS neurons degenerate?

In a recent paper, we reported that the number of SMI-32 positive pyramidal neurons in layer V in M1 was comparable in the contralesional and in the ipsilesional hemispheres in two monkeys subjected to an unilateral cervical lesion (treated with a control antibody), and amounted to a comparable figure as in two intact animals(Wannier, Schmidlin, Bloch, and Rouiller 2005a). In the present study, these data were extended to a total of four monkeys subjected to the cervical lesion (treated with a control antibody) and five intact monkeys (Fig. 1C; blue and green bars, respectively). In the group of intact monkeys, as expected the majority (four out of five) of animals did not show a statistically significant difference of SMI-32 positive neurons between the two hemispheres ($p>0.05$, n.s. in Fig. 1C). However, in one intact monkey (Mk-IU), the number of SMI-32 positive neurons per unit length was significantly higher ($p<0.05$) in the right than in the left hemisphere (Fig. 1C), indicating that even in intact monkeys there may be cases in which the density of SMI-32 positive neurons in layer V of M1 differs between the two hemispheres. Accordingly, there was also one monkey (Mk-CS) in the group of lesioned monkeys treated with the control antibody (blue bars in Fig. 1C) exhibiting an inter-hemispheric difference of the number of SMI-32 positive neurons per unit length ($p<0.05$), whereas in the other three monkeys the difference was not statistically significant. However, still in the group of lesioned monkeys treated with the control antibody (blue bars in Fig. 1C), there was no systematic trend with respect to the side of the lesion. These data thus confirm the notion that axotomy of the crossed CS tract at cervical level in macaque monkeys treated with a control antibody does not lead to significant neuronal loss. As anticipated, the same conclusion applies to the group of five monkeys subjected to cervical cord lesion and treated with anti-Nogo-A antibody (Fig. 1C; red bars): in two monkeys there were slightly more SMI-32 positive neurons in the contralesional hemisphere whereas in the other three monkeys the ipsilesional hemisphere had more SMI-32 positive neurons (in two of them, the difference was statistically significant, but to a similar extent as in the case

observed in each of the other two groups of monkeys). Overall, the unsystematic inter-hemispheric differences in the two groups of lesioned monkeys were generally in the same order of magnitude as those observed in the group of intact monkeys.

3. Does anti-Nogo-A treatment prevent shrinkage of CS neurons after axotomy?

In our recent study (Wannier et al 2005), the two monkeys subjected to the cervical lesion and treated with the control antibody exhibited shrinkage of their soma as a result of the CS axotomy at cervical level. This observation is confirmed here on a larger pool of four control-antibody treated monkeys (Fig. 2A; blue bars): in three of the four monkeys, the SMI-32 positive neurons of layer V were significantly smaller in the contralesional hemisphere than in the ipsilesional one. In the fourth monkey (Mk-CH), no somatic size difference was found, but in this particular animal the quality of the SMI-32 immunostaining was poor, which may in part explain this result. In contrast to the majority of control antibody treated monkeys, the intact monkeys did not show a statistically significant difference in the distribution of somatic area of layer V pyramidal neurons between the two hemispheres (Fig. 2A; green bars). It can be concluded that CS axotomy induced shrinkage of somatic area of the corresponding CS neurons in the lesioned monkeys treated with the control antibody.

Figure 2

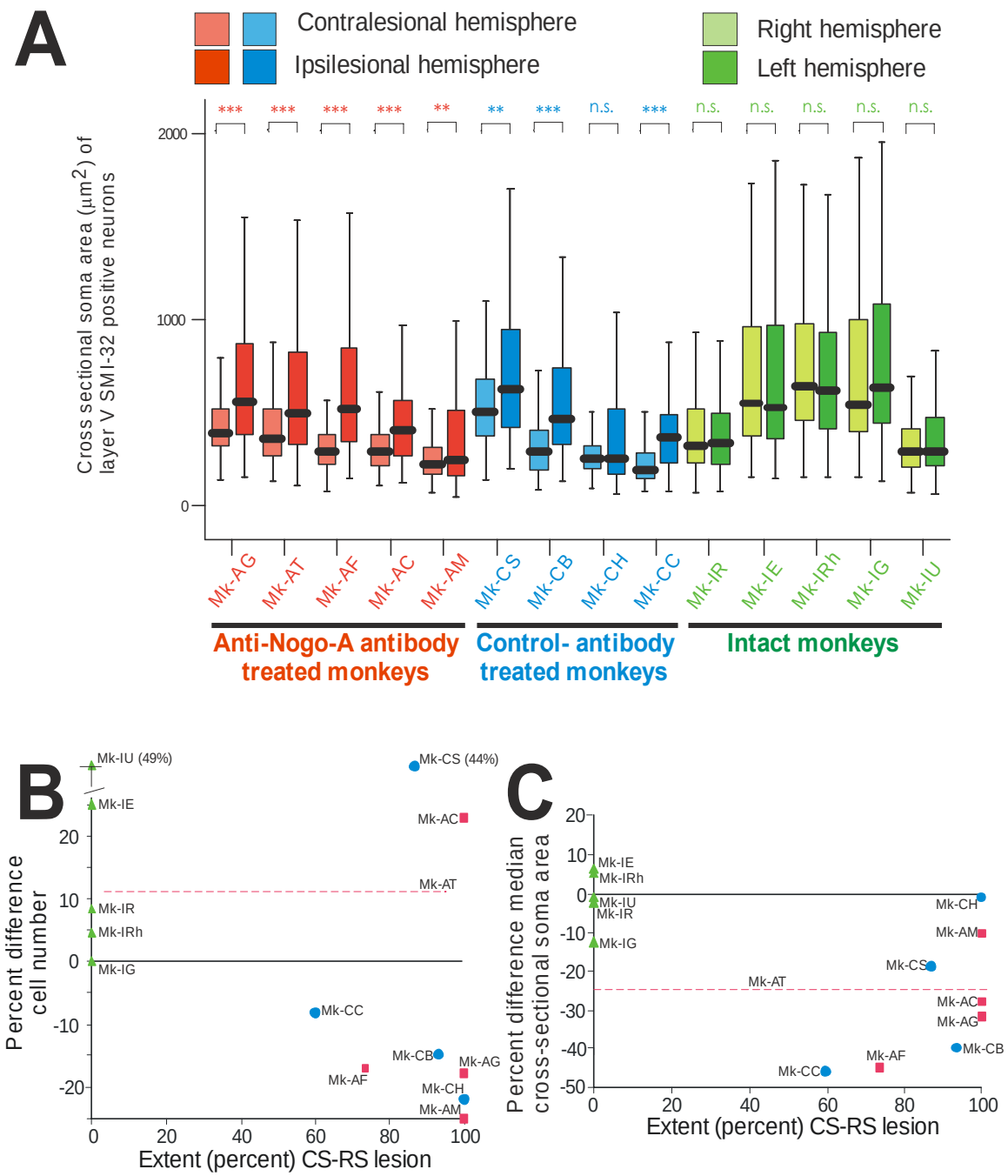

Figure 2: Somatic size of py ramidal neurons in lay er V of the motor cortex and inter-hemispheric differences

A: Box and whisker plots showing the distribution of somatic cross-sectional areas of SMI-32 positive neurons in layer V in M1 for the three groups of

monkeys. In the box and whisker plots, the thick horizontal line in the box corresponds to the median value, whereas the top and bottom of the box are for the 75 and 25 percentile values respectively. The top and bottom extremities of the vertical lines on each side of the box are for the 90 and 10 percentile values, respectively. All but one lesioned monkey (red and blue bars) exhibited a significant inter-hemispheric difference of cross-sectional soma area (*=$p<0.05$; **=$p<0.001$; ***=$p<0.0001$; Mann and Whitney test), whereas in the intact monkeys the difference was not statistically significant (n.s.=$p>0.05$; Mann and Whitney test).

B: Inter-hemispheric percent difference in the number of SMI-32 positive neurons per unit length in layer V in M1 for the same three groups of monkeys as in Figure 1C (same color code), plotted as a function of the lesion extent (percent of the territory corresponding to the CS and RS tracts affected by the lesion). Note that the differences are not systematic with respect to the side of the lesion in the two groups of lesioned animals (red squares and blue circles for the anti-Nogo-A and control antibody treated monkeys, respectively). In the percent comparison, 100% is for the number of SMI-32 positive neurons per unit length on the ipsilesional side (on the left side for the intact monkeys). The green triangles are for the intact monkeys. As the lesion extent could not be determined for Mk-AT (see Table 1), its corresponding percent value was represented by an horizontal dashed line.

C: Inter-hemispheric percent difference of the median value of the cross-sectional soma area of SMI-32 positive neurons in layer V in M1 for the same three groups of monkeys as in panel A, plotted as a function of the lesion extent (percent of the territory corresponding to the CS and RS tracts affected by the lesion). Note that the difference is small for the intact monkeys (green symbols), but it is more prominent and systematic with respect to the side of the lesion for most lesioned monkeys, with considerable overlap between the two groups of lesioned monkeys. Same conventions as in panel B.

To address the issue whether anti-Nogo-A antibody treatment, in addition to enhanced sprouting in the cervical cord near the lesion (Freund et al. 2006; 2007),also prevents shrinkage of the soma of the CS axotomized neurons, the same analysis was conducted here in the group of five anti-Nogo-A antibody treated monkeys. In all five monkeys (Fig. 2A; red bars), the soma cross-sectional areas of SMI-32 positive layer V pyramidal neurons were significantly reduced in the contralesional hemisphere as compared to the ipsilesional one, indicating that the CS axotomized neurons shrank. Moreover, the extent of shrinkage is generally comparable in the anti-Nogo-A antibody treated and control antibody treated monkeys (Fig. 2C). In other words, the anti-Nogo-A antibody treatment did not prevent or reduce shrinkage of the soma of axotomized CS neurons.

The data of the present study are summarized in Figures 2B and 2C, where the inter-hemispheric difference (in percent) of the number of SMI-32 positive neurons per unit length in the layer V of M1 and of the median of their cross-sectional soma area were plotted as a function of the extent of the lesion, estimated in percent of the lateral spinal cord. For the three groups of monkeys, there was no systematic inter-hemispheric difference for the number of SMI-32 positive neurons per unit length in layer V of M1 (Fig. 2B), indicating that the unilateral axotomy of the CS tract did not produce a substantial cell loss in the contralesional hemisphere. Indeed, in the two groups of lesioned monkeys, the inter-hemispheric cell number difference was in the same range as in intact monkeys. On the other hand, as compared to intact monkeys, the cervical hemi-section led to a significant shrinkage of SMI-32 positive cells in layer V of the contralesional M1, irrespective of whether the monkey was treated with a control antibody or an anti-Nogo-A antibody (Fig. 2C).

1.4 Discussio n

Based on a substantially increased number of animals, the present study confirms preliminary data (Wannier, Schmidlin, Bloch, and Rouiller 2005b) indicating that unilateral cervical lesion is not followed by a significant elimination of axotomized CS neurons. This conclusion thus adds a new piece of evidence to the long debated issue of whether CS neurons die after axotomy in monkeys (see introduction). The present data are in line with previous reports claiming that there is no extensive CS cell loss after spinal cord lesion in monkeys (Davison 1937; Lassek 1942; Tower 1940). As compared to the studies which previously addressed this question, the present investigation is based on a specific staining of pyramidal neurons in layer V (SMI-32), allowing better focus on the neurons of interest (CS neurons) than for instance in Nissl staining, as used in most cases previously. Although SMI-32 stains pyramidal cells in layer V in general and not only the CS neurons, the measurements conducted in the present study are thus somewhat more directed towards the subpopulation of CS neurons than measurements conducted for instance in Nissl material, where a much larger population of neurons would be involved. As a consequence, a difference between the two hemispheres affecting the CS neurons after a unilateral cervical lesion is detected with more sensitivity in SMI-32 than in Nissl material. Our measurements thus include the large pyramidal neurons of layer V in the motor cortex, which may possibly be the neurons preferentially expressing Nogo-A, as it was recently reported in the primary somatosensory (barrel) cortex of the rat (Shin, Shim, Hwang, Jung, Park, and Sohn 2006). Whether this is also true in primates and in the motor cortex remains an open question.

To investigate whether cell death occurred in layer V in the contralesional hemisphere, we counted the number of SMI-32 positive neurons in layer V in M1 territories of roughly comparable size delineated on the same section in the two hemispheres. Moreover, the data were normalized with respect to the length of the layer V territory in which the measurements were conducted. Our goal here

was not to establish the absolute number of SMI-32 positive neurons in a given cortical area but rather to compare between the two hemispheres their relative numbers. Furthermore, because the number of SMI-32 stained neurons in the delineated territory of interest was relatively low, we did not use a stereological probe to estimate their number, rather we counted all of them exhibiting their nucleus. This approach is considered as adequate as all samples were analyzed using the same procedure (Lavenex et al 2002; Geuna et al., 2000 ;Benes et al., 2001). More precisely, in a recent morphometrical study in the hippocampus (Lavenex et al 2002) the authors used a true stereological approach to estimate the volume of the structure of interest as well as the total absolute number of neurons. In contrast, to estimate the number of BrdU immunoreactive neurons, the authors did not use a stereological probe because “of the low number of BrdU-labelled cells” (Lavenex et al 2002). In the present case, the number of SMI-32 positive neurons with a visible nucleus in the restricted zone of interest of M1 (layer V) was also very low, thus preventing the use of stereological probe. Furthermore, the data and their reproducibility obtained in the five intact monkeys strongly support the validity of the method used here to establish the number of SMI-32 positive neurons and their cross-sectional somatic area. Indeed, in all five intact monkeys, there was no statistically significant inter-hemispheric difference for their soma area. Furthermore, the number of SMI-32 positive cells did not show substantial inter-hemispheric difference in four out of five intact monkeys. In contrast, the somatic area difference observed in the two groups of lesioned monkeys was considerable and systematic with respect to the side of the lesion (except in one animal, Mk-CH). The morphometrical measurements were conducted in the hindlimb area of M1 and not in the hand area because the latter zone was subjected, in some animals, to extensive intracortical microstimulation (Sasaki et al. 2004a); see also Table 1) and, in all animals, to the injection of an anterograde tracer to label the CS tract (Freund et al. 2006). The hand area in M1 was thus not suitable for an optimal detection of SMI-32 positive neurons as they may be obscured by the presence of the reaction product corresponding to the injection site. The hindlimb area, also affected by the cervical lesion, was

thus more appropriate to conduct the anatomical analysis and we believe that the present data derived from the CS neurons of the hindlimb area is very likely to apply also to the CS neurons of the hand representation.

As shown in Figure 1C, there was no systematic inter-hemispheric difference in the number of SMI-32 positive neurons in the three groups of monkeys, thus supporting the conclusion that the cervical cord hemi-section did not provoque substantial loss of axotomized CS neurons. Considering the results in Figure 1C for the two groups of monkeys subjected to the cervical cord hemi-section (red and blue bar graphs), surprisingly three monkeys (Mk-AT, Mk-AC and Mk-CS) exhibited a higher number of SMI-32 labeled neurons on the contralesional hemisphere. In the first two monkeys, this difference was however not statistically significant, reflecting in part the variability of the method. For the third monkey (Mk-CS), the significant difference may reflect an episodic interhemispheric difference in a minority of monkeys, as actually observed in one intact monkey (Mk-IU in Fig. 1C) out of five intact animals. Nevertheless, the presence of some lesioned monkeys with more SMI-32 positive neurons on the contralesional hemisphere reinforces the conclusion of an absence of elimination of CS axotomized neurons after cervical cord hemi-section. Overall, as shown in Figure 1C, the number of SMI-32 positive neurons varied across animals, most likely reflecting individual variability both in the number of large layer V pyramidal neurons and in the intensity of SMI-32 staining.

The observation that there was no substantial loss of axotomized CS neuron after cervical hemi-section represents a quite favorable outcome for functional recovery. Indeed, the axons that have been severed, although they retract some distance from the lesion (Freund et al., 2007) are still present and potentially in position to regenerate or give rise to collateral sprouting. In other words, the functional recovery does not depend only on CS neurons spared by the lesion or on other preserved descending tracts. In recent reports, we demonstrated that the severed CS axons indeed can give rise to spontaneous axonal sprouting in absence of treatment, but only to a very limited extent

(Freund et al., 2006; 2007). In contrast, an anti-Nogo-A antibody treatment substantially enhanced CS axonal sprouting from the severed axons, as manifested by an increase of axonal arbors rostral to the lesion as well as axonal arbors and swellings caudal to the lesion (Freund et al., 2006; 2007).

As a result of cervical cord hemi-section, the axotomized CS neurons in the contralesional hemisphere exhibit shrinkage of their soma (Fig. 2A, blue bar graphs). Neuron atrophy in response to axotomy is very well known and widely observed, including for cortical neurons. Neuronal metabolism depends on continuous retrograde trophic signals from the targets, which are absent or reduced in case of axotomy. As the normal intact axonal arborization may be much larger than the “spontaneously” newly formed arbor of the few sprouting neurons in the control antibody treated monkeys, the decrease of retrogradely transported trophic signals would thus contribute to the soma shrinkage. In the anti-Nogo-A antibody treated monkeys, although sprouting was enhanced (Freund et al., 2007), the quality and amount of trophic signals may be still insufficient to completely reverse the atrophy. Furthermore, the number of CS axons that successfully sprout and re-establish an axonal arbor with contacts is not precisely known. It is likely that only a relatively limited proportion of axotomized CS neurons managed to re-establish a large axonal arbor and to obtain enough trophic signals to prevent or reverse the atrophy. These few neurons indeed appear in the upper extreme of the soma size distribution (largest cells in Fig. 2A) but, in the anti-Nogo-A antibody treated monkeys, their number is not sufficient to compensate for the large number of shrunk neurons. Finally, the time course has to be taken into consideration. Shortly after the lesion, sprouting neurons are not in an atrophic state and this is true for the initial few weeks after the injury when sprouting takes place. The present morphometric measurements were conducted in our monkeys many months post-lesion at a time point when sprouting was completed. However, as the newly formed axonal arbors may not be as large as intact ones, the total amount of trophic support they receive may still not be enough to maintain their full soma size.

As far as the basic molecular/cellular mechanisms are concerned, it is known that somatic responses to an injury depend upon the intracellular levels of cyclic AMP and activation of transcription factors such as CREB (cAMP responsive element-binding protein; see for reviews(Oertle et al. 2003;Schmidlin et al. 2005). Thus, by increasing the cAMP levels, the neuronal regenerative capacity can be enhanced.

The present study provides evidence that the anti-Nogo-A antibody treatment limits its action on the distal part of the axotomized CS neurons, namely by enhancing axonal sprouting close to the lesion itself, but does not prevent changes taking place at the level of the CS cell body, at least as far as soma size shrinkage is concerned. This conclusion applies to the present experimental conditions and it cannot be excluded that soma shrinkage of axotomized CS neurons could have been better prevented, at least to some extent, if the dose of the anti-Nogo-A antibody would have been higher or if it would have been delivered not only near the cervical lesion but also at cortical level. Indeed, although the anti-Nogo-A antibody delivered intrathecally near the lesion site penetrates into the CNS, the penetration was less complete in the brain than in the spinal cord (Weinmann et al. 2006; Liu et al., 2002).

To our knowledge, the issue of CS neurons elimination after spinal cord lesion and treatment with anti-Nogo-A antibody has not been investigated before, even in rodents and therefore the present observation of an absence of anti-Nogo-A antibody treatment effect on the shrinkage of axotomized CS neurons is original. The issue of whether the anti-Nogo-A antibody treatment can contribute to rescue cells from elimination after axotomy could not be addressed here as there was no CS neuron loss, even in the control antibody treated monkeys. The absence of CS cell loss after cervical lesion contrasts with the number of RS neurons detected in the contralesional magnocellular red nucleus (RNm), which was up to 30% lower than in the ipsilesional RNm (Liu et al., 2002). However, in the latter study conducted on the same groups of lesioned monkeys, it was observed that the anti-Nogo-A treatment did not impact on the RS neurons, as

the number of detected RS neurons was comparable in the anti-Nogo-A antibody and in the control antibody treated monkeys.

1.5 Methods

The present data have been derived from a long-term protocol, described earlier in detail(Freund et al. 2006;Schmidlin, Wannier, Bloch, Belhaj-Saïf, Wyss, and Rouiller 2005;Schmidlin, Wannier, Bloch, and Rouiller 2004;Wannier, Schmidlin, Bloch, and Rouiller 2005a) ,conducted on monkeys subjected to unilateral cervical cord lesion at the C7/C8 border, in accordance with the Guide for the Care and Use of Laboratory Animals (ISBN 0-309-05377-3; 1996) and approved by local (Swiss) veterinary authorities. The present study aimed at comparing three groups of monkeys (Table 1): (i) Intact monkeys (n=5); (ii) Monkeys subjected to the cervical hemi-section and treated with anti-Nogo-A antibody (n=5); (iii) Monkeys subjected to the cervical hemi-section and treated with a control antibody (n=4).

Two monoclonal antibodies (mAbs) against different sites of the neurite inhibitor protein Nogo-A were employed (Table 1; see also (Freund et al. 2007) for more detail on the antibodies) in the group of anti-Nogo-A antibody treated monkeys: the mouse mAB 11C7 was raised against a 18 amino acid sequence of rat Nogo-A (aa623 – 640) close to the most inhibitory region of the Nogo-A protein (Oertle et al. 2003). The second antibody used, mAb hNogo-A recognized the Nogo-A specific region of the human Nogo-A sequence. Both antibodies identify primate Nogo-A monospecifically on Western blots (Campbell and Morrison 1989;Weinmann et al. 2006). The antibodies were purified as IgGs and concentrated to 3.7-10 mg/ml in PBS. In the control antibody treated monkeys, purified IgG of a mouse mAb directed against wheat auxin (AMS Biotechnology, Oxon/UK) was used as control antibody (concentration: 3.7-10 mg/ml).

Briefly, the main steps of the protocol conducted on the lesioned monkeys were the following. First, an intensive pre-lesion training was initially performed in order to establish a stable behavioral score in manual dexterity tasks involving both hands (Freund et al. 2006). A unilateral lesion was performed at the C7/C8 border (see Wannier et al. 2005; Freund et al. 2006) and the antibody (either control or anti-Nogo-A) was administered intrathecally a couple of mm rostral to the lesion. The manual dexterity tests were conducted at regular intervals for several months post-lesion, until the animals reached a plateau reflecting a stable level of functional recovery. Anterograde tracers were injected mainly in the hand representation of the primary motor cortex (M1) bilaterally to label the CS tract (Freund et al. 2006; 2007). The monkeys were sacrificed under deep anesthesia and perfused transcardially with fixatives (Wannier et al. 2005).Frozen sections comprising each of the two hemispheres were cut in the coronal plane at a thickness of 50 m. The spinal cord was cut in the paralongitudinal plane at the site of the lesion and transversally at the level of the first cervical segments as well as of thoracic segments caudal to the lesion. The lesion was reconstructed using SMI-32 stained material in all monkeys as previously reported (Wannier et al. 2005; Freund et al. 2006) and its extent was expressed quantitatively by the percent of the territory delimited by two lines starting from the central channel and extending to the dorsal and ventral rootlets, thus covering completely the lateral funiculus and hence the zone occupied by the main CS and rubrospinal (RS) tracts. A series of brain and spinal cord sections was treated immunocytochemically with SMI-32 antibody in order to visualize in the cerebral cortex the layers III and V pyramidal neurons (Fig. 1B), as recently described in detail(Tsang, Chiong, Kuznetsov, Kasarskis, and Geula 2006). The epitope recognised by the SMI-32 antibody lies on non-phosphorylated regions of neurofilament protein and is only expressed by specific categories of neurons (Campbell & Morrison, 1989; Tsang et al., 2006).

SMI-32 positive neurons (only those exhibiting the nucleus) in the primary motor cortex (M1) on both hemispheres were counted under the microscope at high magnification (400x), in a territory including layer V at the same dorso-

ventral location and defined of roughly equal length on both hemispheres (zone delineated with a dashed line in Fig. 1B). The typical appearance of SMI-32 positive neurons in layer V of M1 was illustrated in a recent report (see Figure 3 in Wannier et al., 2005). At low magnification, as staining was stronger on the ipsilesional hemisphere, the number of SMI-32 positive neurons seems to be lower on the contralesional side (Fig. 1B). This is however a wrong impression as, at higher magnification (Fig. 1D), several SMI-32 positive neurons appear on the contralesional hemisphere (Fig. 1D): at high magnification, even lightly stained SMI-32 positive neurons can reliably be detected. On each section and separately for each hemisphere, the total number of SMI-32 positive neurons was divided by the length (in mm) of the territory in which the analysis was conducted (l in mm in Fig. 1B). Moreover, the somatic cross-sectional silhouette area of these SMI-32 positive neurons in layer V was determined, as described in detail earlier [17]. In each monkey, four to six coronal histological sections were taken along the rostrocaudal extent of M1 (separated by 800 m each) in which the analysis of SMI-32 positive neurons in layer V was conducted.

The number of SMI-32 positive neurons per unit length (mm) obtained in a given section was averaged across the sections analyzed in each monkey, separately for the two hemispheres, and a standard deviation was obtained reflecting the variability from one section to the next (Fig. 1C). The statistical comparison of the number of SMI-32 positive neurons per unit length between the two hemispheres was based on a paired t-test for small samples applied on the four to six sections analyzed in each monkey. A statistically significant difference of the number of SMI-32 positive neurons in layer V between the two hemispheres was obtained for a t value corresponding to $p<=0.05$ (df=3 to 5 for 4 to 6 sections analyzed, respectively). The soma areas did not follow a normal distribution (wider dispersion for large somatic areas than small ones) and therefore they were graphically represented in the form of box and whisker plots (putting emphasis on the median value rather than the mean value; Fig. 2A). Accordingly, the statistical comparison of soma areas of SMI-32 positive neurons between the two hemispheres was conducted for each animal using the non-

parametric unpaired Mann and Whitney test (Fig. 2A), with a significance level of $p<=0.05$.

1.6 List of abbreviations

CS = corticospinal
M1 = primary motor cortex
Mk = monkey
RNm = magnocellular red nucleus
RS = rubrospinal
SCI = spinal cord injury

1.7 Authors' contributions

EMR designed the study, contributed to the experiments and analysis of the data, and drafted the manuscript. MLB conducted the morphological measurements in most monkeys, contributed to the analysis and wrote a preliminary version of the manuscript in the context of her Master thesis. ES and TW designed the study, carried out the experiments, the morphological measurements on some monkeys and analyzed the corresponding data. PF contributed to the experiments and the analysis of the data. JB designed the study and performed the cervical lesions. AM contributed to the study design and antibody protocol. MES contributed to the study design and general concept, antibody protocol and data analysis. All authors read, commented and approved the final manuscript.

1.8 Acknow ledgements

The authors wish to thank the technical assistance of Véronique Moret, Françoise Tinguely Christiane Marti, Monika Bennefeld, Georgette Fischer and Christine Roulin (histology and behavioral evaluations), Josef Corpataux, Bernard Morandi, Bernard Bapst and Laurent Bossy (animal house keeping), André Gaillard (mechanics), Bernard Aebischer (electronics), Laurent Monney (informatics).

Grant Sponsors: Swiss National Science Foundation, grants No 31-43422.95, 31-61857.00, 310000-110005 (EMR), 31-63633 (MS) and 4038043918/2 (PNR-38); Novartis Foundation; The National Centre of Competence in Research (NCCR) on "Neural plasticity and repair"; The *Christopher Reeves* Foundation (Spinal Cord Consortium, Springfield, N.J.).

1.9 Referneces

Aoki M, Mori S: Recovery of hindlimb movement elicited by motor cortical stimulation after spinal hemisection in monkeys. In *Integrative control functions of the brain*. Edited by Ito M. Amsterdam: Elsevier; 1979:152-154.

Benes FM, Lange N: Two-dimensional versus three-dimensional cell counting: a practical perspective. *TINS* 2001, 24: 11-17.

Bernhard CG, Bohm E, Petersen J: Investigations on the organization of the cortico-spinal system in monkeys (Macaca mulatta). *Acta physiol scand* 1953, 29, Suppl. 106: 79-103.

Bregman BS, Kunkel-Bagden E, Schnell L, Dai HN, Gao D, Schwab ME: Recovery from spinal cord injury mediated by antibodies to neurite growth inhibitors. *Nature* 1995, 378,:498-501.

Campbell MJ, Morrison JH: Monoclonal antibody to neurofilament protein (SMI-32) labels a subpopulation of pyramidal neurons in the human and monkey neocortex. *J Comp Neurol* 1989, 282: 191-205.

Davison C: Syndrome of the anterior spinal artery of the medulla. *Arch Neurol* 1937, 37: 91-107.

Denny-Brown D: *The Cerebral Control of Movements.* Liverpool: Liverpool University Press; 1966.

Freund P*, Schmidlin E*, Wannier T*, Bloch J, Mir A, Schwab ME *et al.*: Nogo-A-specific antibody treatment enhances sprouting and functional recovery after cervical lesion in adult primates. *Nature Med* 2006, 12: 790-792.

Freund P, Wannier T, Schmidlin E, Bloch J, Mir A, Schwab ME, Rouiller EM: Anti-Nogo-A antibody treatment enhances sprouting of corticospinal axons rostral to a unilateral cervical spinal cord lesion in adult macaque monkey. *J Comp Neurol* 2007, 502, 644-659.

Galea MP, Darian-Smith I: Corticospinal projection patterns following unilateral section of the cervical spinal cord in the newborn and juvenile macaque monkey. *J Comp Neurol* 1997a, 381: 282-306.

Galea MP, Darian-Smith I: Manual dexterity and corticospinal connectivity following unilateral section of the cervical spinal cord in the macaque monkey. *J Comp Neurol* 1997b, 381: 307-319.

Geuna S: Appreciating the difference between design-based and model-based sampling strategies in quantitative morphology of the nervous system. *J Comp Neurol* 2000, 427: 333-339.

Harel NY, Strittmatter SM: Can regenerating axons recapitulate developmental guidance during recovery from spinal cord injury? *Nat Rev Neurosci* 2006, 7:603-616.

Holmes G, May WP: On the exact origin of the pyramidal tracts in man and other mammals. *Brain* 1909, 32: 1-43.

Lassek AM: The pyramidal tract. A study of retrograde degeneration in the monkey. *Arch Neurol* 1942, 48: 561-567.

Lavenex P, Steele MA, Jacobs LF: The seasonal pattern of cell proliferation and neuron number in the dentate gyrus of wild adult eastern grey squirrels. *Eur J Neurosci* 2000, 12: 643-648.

Levin PM, Bradford FK: The exact origin of the cortico-spinal tract in the monkey. *J Comp Neurol* 1938, 68: 411-422.

Liebscher T, Schnell L, Schnell D, Scholl J, Schneider R, Gullo M, Fouad K, Mir A, Rausch M, Kindler D, Hamers FPT, Schwab ME: Nogo-A antibody improves regeneration and locomotion of spinal cord-injured rats. *Ann Neurol* 2005, 58:706-719.

Liu J, Morel A, Wannier T, Rouiller EM: Origins of callosal projections to the supplementary motor area (SMA): A direct comparison between pre-SMA and SMA-proper in macaque monkeys. *J Comp Neurol* 2002, 443: 71-85.

Mettler FA: Observations on the consequences of large subtotal lesions of the simian spinal cord. *J Comp Neurol* 1944, 81: 339-360.

Oertle T, Van der Haar ME, Bandtlow CE, Robeva A, Burfeind P, Buss A, Huber AB, Simonen M, Schnell L, Brösamle C, Kaupmann K, Vallon R, Schwab ME: Nogo-A inhibits neurite outgrowth and cell spreading with three discrete regions. *J Neurosci* 2003, 23: 5393-5406.

Pernet U, Hepp-Reymond M-C: Retrograde Degeneration der Pyramidenbahnzellen im motorischen Kortex beim Affen (Macaca fascicularis). *Acta Anat (Basel)* 1975, 552-561.

Sasaki S, Isa T, Pettersson LG, Alstermark B, Naito K, Yoshimura K *et al.*: Dexterous finger movements in primate without monosynaptic corticomotoneuronal excitation. *J Neurophysiol* 2004, 92: 3142-3147.

Schmidlin E, Wannier T, Bloch J, Belhaj-Saïf A, Wyss A, Rouiller EM: Reduction of the hand representation in the ipsilateral primary motor cortex following unilateral section of the corticospinal tract at cervical level in monkeys. *BMC Neuroscience* 2005, 6:56.

Schmidlin E, Wannier T, Bloch J, Rouiller EM: Progressive plastic changes in the hand representation of the primary motor cortex parallel incomplete recovery from a unilateral section of the corticospinal tract at cervical level in monkeys. *Brain Research* 2004, 1017: 172-183.

Schwab ME: Nogo and axon regeneration. *Curr Opin Neurobiol* 2004, 14:118-124.

Shin JW, Shim ES, Hwang GH, Jung HS, Park JH, Sohn NW: Cell size-dependent Nogo-A expression in layer V pyramidal neurons of the rat primary somatosensory cortex. *Neurosci Lett* 2006, 394: 117-120.

Thallmair M, Metz GAS, Z'Graggen W J, Raineteau O, Kartje GL, Schwab ME: Neurite growth inhibitors restrict plasticity and functional recovery following corticospinal tract lesions. *Nature Neurosci* 1998, 1:124-131.

Tower SS: Pyramidal lesion in the monkey. *Brain* 1940, 63: 36-90.

Tsang YM, Chiong F, Kuznetsov D, Kasarskis E, Geula C: Motor neurons are rich in non-phosphorilated neurofilaments: cross-species comparison and alteration in ALS. *Brain Res* 2006, 861: 45-58.

Walmsley AR, Mir AK: Targeting the Nogo-A signalling pathway to promote recovery following acute CNS injury. *Curr Pharm Des* 2007, 13:2470-2484.

Wannier T, Schmidlin E, Bloch J, Rouiller EM: A unilateral section of the corticospinal tract at cervical level in primate does not lead to measurable cell loss in motor cortex. *Journal of Neurotrauma* 2005, 22: 703-717.

Wannier-Morino P*, Schmidlin E*, Freund P, Belhaj-Saif A, Bloch J, Mir A, Schwab ME, Rouiller EM, Wannier T: Fate of rubrospinal neurons after unilateral section of the cervical cord in adult macaque monkeys: effects of an antibody treatment neutralizing Nogo-A. Brain Res. (in revision) 2007.

Weinmann O, Schnell L, Ghosh A, Montani L, Wiessner C, Wannier T, Rouiller E, Mir A, Schwab ME: Intrathecally infused antibodies against Nogo-A penetrate the CNS and downregulate the endogenous neurite growth inhibitor Nogo-A. *Molec Cell Neurosci* 2006, 32: 161-173.

Wohlfarth S: Die vordere Zentralwindung bei Pyramidenbahnläsionen verschiedener Art. Eine histopathologische Untersuchung. *Acta Med Scand* 1932, Suppl. 46: 1-235.

Table 1: List of cervical cord lesioned and intact monkeys included in the present study with identification code (same as in [10]).

	Mk-AG	Mk-AT	Mk-AF	Mk-AC	Mk-AM	Mk-CS	Mk-CB	Mk-CC	Mk-CH	Mk-IR	Mk-IE	Mk-IZ	Mk-IRh	Mk-IG
species	fasc.	fasc.	mul.	fasc.	fasc.	mul.	fasc.	fasc.	fasc.	mul.	mul.	fasc.	mul.	mul
Antibody Treatment	Anti-Nogo-A (hNogo)	Anti-Nogo-A (hNogo)	Anti-Nogo-A (11C7)	Anti-Nogo-A (hNogo)	Anti-Nogo-A (hNogo)	Contr.	Contr.	Contr.	Contr.	-	-	-	-	-
Hemi-section total extent (%)	78	*	56	85	80	63	75	38	90	-	-	-	-	-
Completeness of dorsolateral funiculus section	Yes	*	Yes	Yes	Yes	Yes	Yes	No	Yes	-	-	-	-	-
RS and CS lesion extent (%)	100	*	73	100	100	87	93	61	100	-	-	-	-	-
Functional Recovery (%)	100	(100)*	57	100	96	22	78	83	53	-	-	-	-	-
Completeness of CS/RS section	Yes	*	No	Yes	Yes	Yes	Yes	No	Yes	-	-	-	-	-
Survival time after lesion (in days)	112	97	144	135	138	198	225	105	138	-	-	-	-	-
ICMS	no	no	yes	no	no	yes	no	yes	no	no	no	no	no	no

At the time of the experiment, the lesioned monkeys had different names, not indicating whether the animal was infused with the control or the anti-Nogo-A antibody, corresponding to a double blind procedure (except Mk-AF, Mk-CS and Mk-CC). New names were assigned to the monkeys during the writing of the manuscript to improve its readability, in consistency with (Freund et al. 2006).

Under species, "mul." is for macaca mulatta while "fasc." is for macaca fascicularis.

The five anti-Nogo-A antibody treated monkeys are in the five leftmost columns ("Anti-Nogo-A") with indication of which of the two antibodies was used (mAB11C7 or mAB hNogo-A), whereas the four control antibody treated monkeys ("Contr.") are in the next four columns. The five intact monkeys are in the five rightmost columns.

Total hemi-section extent was calculated as the percentage of corresponding hemi-cord affected by the lesion on the frontal reconstruction of the cervical cord.

To tentatively determine more precisely the extent of the RS and CS lesions a quadrant of the lateral funiculus in the white matter was outlined going from the dorsal to the ventral rootlet zone. This was indicated as RS and CS lesion extent.

Functional recovery was assessed here for manual dexterity based on the "modified Brinkman board" task (see Freund et al. 2006) by giving in percent the ratio of the post-lesion score to the pre-lesion score.

In the row “completeness of RS section”, “No” and “Yes” indicates whether the RS transection was considered as partial or as complete, respectively (for further explanation see text).

Survival time: number of days separating the cord hemi-section from the sacrifice of the animal.

* In this animal the total hemi-section extent and consequently also the RS and CS extent could not be calculated for technical reasons (poor quality of histology). In addition in this same animal the lesion was too caudal and thus the 100% functional recovery cannot be interpreted.

ICMS is for intracortical microstimulation. “Yes” means that the corresponding monkeys were subjected to extensive ICMS both pre- and post-lesion in order to study the change of motor maps (somatotopy) in relation to the lesion (see Schmidlin et al. 2004; 2005).

CHAPTER 7

Discussion

1.1 Neutralizing Nogo-A in SCI macaque monkeys: Summary

The present investigation aimed at assessing the effects on nerve fiber plasticity and the amount and time course of spontaneous recovery when neutralizing antibodies against Nogo-A were infused intrathecally after a unilateral cervical spinal cord lesion in adult primates. The understanding of such mechanisms in the non-human primate is of strategic significance in the context of ongoing research leading to translational attempts to treat SCI patients. In particular, such knowledge derived from the non-human primate model is crucial, because of the potential difficulties in translating work in the rat model of spinal cord injury to the human condition (Courtine et al., 2007). In macaque monkeys, we used skilled tasks, such as the prehension of objects with the precision grip, the ballistic arm movement test and food grasping to test functional recovery of manual dexterity in control and anti- Nogo-A antibody treated monkeys.

We found that neutralization of Nogo-A promoted regenerative sprouting of CS (and possibly other) axons around the lesion and into the denervated spinal cord in macaque monkeys (Freund et al., 2006; Freund et al., 2007), in line with previous observation in marmoset (Fouad et al., 2004).

In particular, anti-Nogo-A antibody treatment decreased the normally occurring retrograde degeneration of the axotomized CS axons: the number of terminal retraction bulbs formed by the axotomized CS axons was smaller in the group of anti-Nogo-A antibody treated monkeys than in the group of control antibody treated monkeys and the terminal retraction bulbs were closer to the lesion (**Chapter 4** : Fig. 2). Thus, anti-Nogo-A antibody treatment reduced axonal dieback. More CS axons grew into the lesion scar, but their regeneration through the scar tissue remained unsuccessful. Scar associated growth inhibition factors mainly account for this blockade of regeneration (Rhodes and Fawcett, 2004).

The anti-Nogo-A antibody treatment enhanced the presence of CS axon arbors in the grey matter rostral to the lesion, the number of CS axon arbors (possibly corresponding to CS axon collaterals) passing from the white to the grey matter and, finally, the number of CS fibers crossing the segmental midline at C5 level

(Freund et al. 2007). These measurements show that axonal sprouting was induced by neutralizing the neurite outgrowth inhibitor Nogo-A after a cervical lesion, and that some CS collaterals were in a position to grow around the lesion in order to re-innervate the spinal cord territory caudal to the lesion deprived of CS input.

We believe that these axons sprouting around the lesion make an important contribution to the incomplete but significantly enhanced reconstruction of the CS fiber plexus caudal to the lesion in the anti-Nogo-A antibody treated monkeys (Freund et al., 2006), more so than the fibers attempting to regenerate and to re-enter the lesion itself.

For the first time we report that nearly full recovery in a specific behavioural task measuring manual dexterity (Freund et al 2006, 2007b) parallels the reorganization of the CS tract in anti-Nogo-A antibody treated monkeys. Thus the enhanced growth of the CST may be part of a neural substrate for promoting better and faster recovery of manual dexterity as compared to control antibody treated monkeys.

However, axotomized CS and RN neurons exhibited in control and anti-Nogo-A antibody treated monkeys a similar shrinkage of their cell soma (Beaud et al. 2007). In contrast to CS neurons where the number of SMI-32 positive neurons remains similar in both hemispheres, a reduced number of positive stained RN neurons were found in the contralesional RNm (Wannier-Morino et al. 2007). In conclusion, the anti-Nogo-A antibody treatment did not preserve the axotomized CS and RN cells from soma shrinkage, indicating that in our experimental conditions the anti-Nogo-A antibody treatment affects morphologically the axotomized CS neurons mainly at distal levels, especially the axon collateralization in the cervical cord, and little or not at all at the level of their soma.

1.2 Lesion variability

Spinal cord injuries are well-known to trigger a cascade of secondary tissue reactions due to bleeding, ischemia and inflammation, which lead to substantial variability within groups of animals and remain a crucial concern in the context studies investigating behavioral recovery.

In the present investigation thirteen monkeys were subjected to a unilateral partial section of the spinal cord aiming at completely interrupting the decussated component of the CST which runs in the dorsolateral funiculus (Rouiller et al., 1996; Lacroix et al., 2004). Histological reconstructions demonstrated a considerable variability in the extent of the lesion. In some animals the lesion covered an area of 45% of the total surface of the hemicord, whereas in others it affected up to 90%.

However, in an experimental injury situation, the key prerequisite for studying regeneration is the completeness of the transection of the studied fiber tract. In our investigation, the crucial criterion for a complete lesion was not only the extent of the lesion as it appears in reconstructed cross sections for each monkey, but the full interruption of the corticospinal (CS) tract as assessed by anterograde transport of the tracer BDA from the hand area of motor cortex. Based on our criteria, 9 out of 13 monkeys had a complete lesion of the CS tract in the dorsolateral funiculus. Furthermore, among the animals considered for the tracing analysis of axonal arbors caudal to the lesion, only a single animal, Mk-CP, had an incomplete CS lesion, as shown by the presence of a few BDA-labeled CS axons not transected at the level of the lesion.

The extensive functional recovery of manual dexterity which depends on lesion size may be due to pathways others then the CST. However, to what extent the variability of the lesions affected the degree of recovery, by involving other descending tracts such as the rubrospinal, reticulospinal, tectospinal and vestibulospinal tracts was not addressed in the present investigation at least at

the anatomical level (Hashimoto and Fukuda, 1991; Schucht et al., 2002; Fouad et al., 2005). Without doubt, the functional roles of these different descending tracts are not independent and, to address the impact of a lesion to one of them would require the comparison of several monkeys with the same lesion of the RS and CS tracts and assess the effects of lesions of graded extent aimed at the ventral column for instance. Due to restrictions in the use of non-human primates, the contribution to manual deficits of damage to separate territories of the cervical cord could not be addressed in the present study.

However, the mean of the extent of the ventral column lesions in the control antibody treated monkeys (28.5%) was almost identical to that of the anti-Nogo-A antibody treated monkeys (28%; Table 2 of **Chapter 2**). This remains true if one considers separately the subgroup of monkeys retained for the statistics of functional recovery (treated: 33.6 %; control: 30.5%). Note also that the only animal, Mk-AC, which had a full section of both the dorsolateral and ventral funiculi was treated and recovered better than anyone of the control antibody treated animals, which all had some portion of their ventral funiculus remaining intact (Fig. 1 in **Chapter 2**).

An additional important aspect of inter-animal variability is due to processes of scar formation and inflammation. CNS scars are well-known to contain a variety of neurite inhibitory factors other than the CNS myelin and neuron associated Nogo-A (Moon and Fawcett, 2001; Rhodes et al., 2003; Rhodes and Fawcett, 2004). Inflammatory cells, on the other hand, are known to secrete cytokines and growth factors in CNS injury situations; some of these factors are effective neurite growth promoters (Schnell et al., 1994). Because complete serial sections series were prepared for the reconstruction of BDA-labeled CS fibers in our study, we had no control over the detailed anatomy of scar formation and inflammation. The variability in the extent of regenerative sprouting, growth of fibers around the injury site and elongation into the caudal spinal cord may well be influenced by these very complex tissue reactions.

1.3 Time course of manual dexterity recovery

After injury at spinal level, ascending as well as descending pathways are affected. In a complete lesion situation a transmission of information below the lesion is completely abolished whereas, in an incomplete SCI, information can bypass the lesion using intact or partially intact pathways. In any case sensory as well as motor deficits are the consequence. The motor deficits associated to interruption of the CS tract at a segmental level in monkeys were assessed in several studies (Aoki and Mori 1979; Cheema, 1990; Denny-Brown 1966; Freund et al. 2006; Galea and Darian-Smith 1997a; Galea and Darian-Smith 1997b; Holmes and May 1909; Mettler 1944; Sasaki et al. 2004; Schmidlin, et al., 2004). A surprisingly good and rapid recovery of dexterous finger movements of the ipsilateral hand took place after hemi-section at C3 level in either newborn and juvenile monkeys (Galea and Darian-Smith 1997a,b), or in adult monkeys after hemi-section at C4/C5 (Sasaki et al. 2004) or C7/C8 level (Freund et al. 2006; Schmidlin et al., 2004).

The above mentioned authors report persisting deficits of manual dexterity, in line with our data demonstrating that the recovery of manual dexterity is incomplete in a control situation (Fig. 1). In contrast, neutralization of Nogo-A by specific antibodies infused intrathecally leads to impressive functional manual dexterity recovery and enhanced regenerative CS sprouting and elongation in adult primates. The absence of detectable malfunctions such as allodynia supports the present view that the newly formed connections of sprouting axons reached meaningful targets. The extent of sprouting was not sufficient to reach the lumbar segment and may explain partially the absence of functional recovery of grasping with the hindlimb in anti-Nogo-A antibody treated monkeys.

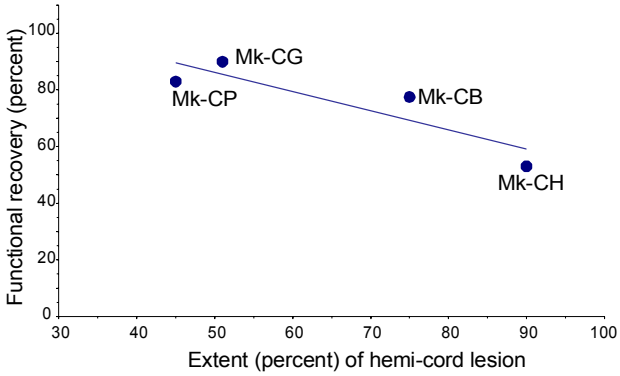

Figure 1: Behavioural data derived from the assessment of manual dexterity. In control-antibody treated monkeys the data indicates that the recovery of manual dexterity is inversely correlated to lesion extent. All monkeys show a persisting deficit in manual dexterity.

In the context of spontaneous vs. anti-Nogo-A antibody enhanced recovery a critical issue remains the lesion level at C7/C8. In the macaque monkey a lesion introduced at this level reflects an incomplete lesion for fine finger controlled hand manipulation. CS neurons from the hand area terminate mainly in spinal segments from C5 down to Th2 and the main afferent input to the hand from the opposing fingers (thumb and index) enter the spinal cord at C5-C7. Whereas the anti-Nogo-A antibody treated monkeys show an enhanced recovery, the variability of the lesion level which can amount up to some mm, has to be taken into consideration as a contributing factor to functional recovery.

1.4 Scar formation, regeneration and regenerative sprouting

In the context of the fiber tract lesions, the term regeneration is clearly defined as re-growth of injured axons. The initial outgrowth over short distances has been called “regenerative sprouting” by Ramon y Cajal; elongation of these fibers over longer distances is often simply referred to as “regeneration”. Following anti-Nogo-A antibody treatment in the rodent model of SCI true regeneration across and around the glia scar was observed (Schnell and Schwab, 1990; Schnell and Schwab, 1993; Liebscher et al., 2005). When Nogo-A was neutralized in monkeys the phenomena of regeneration in the sense of elongation from the axon stump was observed, but remained very limited and the elongating axons never crossed successfully the scar tissue. Rather regenerative sprouting of the

injured CST occurred. Most important, histological reconstructions showed that caudal to the lesion, the anti-Nogo-A antibody treated monkeys had longer cumulated axonal arbor lengths than the control antibody treated monkeys (Figure 3 in **Chapter 2**). These fibers were analyzed many months after the injury following antibody treatment; they had a healthy appearance and had characteristic typical varicosities and terminal buttons. Due to the long standing injury, there is no reason to assume that these fibers would be degenerating rather they represent newly grown fibers.

It appears that in the context of fiber elongation the enhanced reconstruction of the CST tract in anti-Nogo-A antibody treated monkeys was successful because spared tissue served as a bridge to circumvent the lesion, thus limiting the approach at least in the context of SCI to incomplete SCI patients. However, incomplete SCI patients represent up to 70% of the whole injury population and therefore will, if successful in the clinical trial, address the majority of SCI patients.

The BDA injections were targeted mainly to the hand area of M1 and therefore most labeled fibers are mainly directed to spinal levels C7-Th2, in other words one to three spinal segments below the lesion.

In the first two monkeys (Mk-CC, Mk-CS), the survival time after BDA injection was set to three weeks, as used before in intact monkeys. However the tracer did not reach the cervical segments suggesting that the cervical lesion substantially slowed down the anterograde axonal transport of BDA. These animals were not considered further for the anatomical analysis (see Table 1 of **Chapter 2**). In contrast, a much longer survival time (60 days) allowed transport of BDA up to thoracic level in the other ten monkeys (see Table 1 of **Chapter 2**).

The number of CS labeled axons observed at C5 level on transverse sections (up to 2282; see Table 1 of **Chapter 2**) appears low considering that the total number of CS axons was estimated to be 400'000 and that the number of CS neurons retrogradely labeled after tracer injection in the upper spinal cord amounted up to 72'000 in the entire frontal lobe (Dum and Strick, 1991). A few

explanations may account for this. First of all, only 50% of the precentral CS axons originate from M1 (Dum and Strick, 1991; He et al., 1993; He et al., 1995). Secondly, the BDA injections formed patchy territories leaving in between zones where there was no or less uptake. Thirdly, the BDA injections did not cover the entire M1; instead they were focused to the hand (forelimb) representation. Fourthly, a contingent of CS axons terminates above C5. In addition, BDA infusion was limited to the rostral bank of the central sulcus and therefore the whole rostral part of M1 was not injected. Furthermore, as compared to other anterograde tracers such as WGA-HRP for instance, the uptake of BDA appears less prominent. However, to explain the surprisingly low number of CS axons labeled with BDA in the present study, one may consider the likely possibility that the very fine axons making the majority of the CS tract are not labeled or escaped detection at light microscopy level, as suggested by our observation that most BDA labeled CS axons visible in our material at C5 level are relatively large in diameter. In this context, for the same reason, one cannot exclude that some fine CS axons unlabeled with BDA or undetected at light microscopic level were spared by the lesion.

The quantitative analysis of the presence of BDA-labeled CS axon arbors below the lesion was limited to a distance of 3 mm, because it is the area where one expects most of the arborisation and where the motoneurons involved in the control of manual dexterity tested in our behavioral assessment are located.
A systematic quantitative evaluation of the maximal distance at which BDA-labeled CS axons are present caudal to the lesion would make sense only if the tracer BDA would have been injected not mainly in the hand area but also massively in cortical areas projecting to the hindlimb, which was not the case in the present study. In other words, as our data are focused on the hand representation, the true potential of the anti-Nogo-A antibody treatment in term of maximal distance of regeneration remains unknown in macaque monkeys, and would require further experiments.

In the present study, young adult monkeys (3.5 – 6.9 years old at time of sacrifice) were subjected to the spinal cord lesion (Table 1). It cannot be excluded that some of the axonal sprouting (although limited) observed in the control antibody treated monkeys occurred due to the relatively juvenile state of some of the animals and would not have taken place in older animals. Similarly, it is not established whether the enhancement of sprouting due to the anti-Nogo-A treatment would have reached the same extent in older animals. Nevertheless, our animals had an age at the time of the lesion of 3.5 years or more, at which the myelination of the CS tract reached the adult stage, as full myelination was reported to last as long as 36 months (Olivier et al., 1997). As far as the CS tract is concerned, the animals included in the present study can thus be considered as adult monkeys.

1.5 Problem of statistics with a small population

The statistical analysis for the validation of our data remains an important point.
An intrinsic difficulty of lesion studies on humans and monkeys is the inevitable variability in lesion location and extent between individuals. The impact being even more substantial on our nonhuman primate model of SCI for which ethical considerations drastically limit the number of animals. Moreover, the monkeys motivational and attentional states vary from day to day thus influencing strongly the readout of the behavioural test.
In rodents, the inter-individual variability is dealt with in part by increasing the number of animals included in the treated and control groups. In the present investigation, in order to reduce the inter-animal variability, we paired monkeys for behavioural evaluation that were conducted by one experimenter in the same conditions. However, statistical analysis was performed by treatment group and not by pairs. Six control antibody treated monkeys and seven anti-Nogo-A antibodies treated were assessed for functional recovery whereas only eight

monkeys fulfilled the inclusion criteria for the anatomical tracing data (see paragraph 1.4).

The statistical test indicating a significant functional recovery as reported in **Chapter 2** was based on a single parameter: the percentage of manual dexterity recovery between the individual groups. Yet, Figure 1 indicates an inverse relationship of functional recovery to lesion size and thus needs to be taken into consideration for statistical examination. Therefore, in a second report extending the behavioural data, the variability related to the lesion extent was taken into account statistically, by introducing a non-parametric statistical test comparing the anti-Nogo-A antibody treated and control antibody treated monkeys with assessment of both the percent of recovery and lesion extent. More importantly, a new parameter was introduced for the same task, namely the “contact time”, defined as the time required grasping the first food pellet aimed by the monkey. This new parameter demonstrates more accurately the manual dexterity as it focuses on the precision grip between thumb and index finger, a prerogative of primates including humans (Lemon and Griffiths, 2005). The difference of functional recovery were statistically significant ($P<0.05$; two dimensional Mann- and Whitney test) for parameters, the contact time and the score.

1.6 Fate of CS and RS neurons after spinal cord injury

The debate whether axotomized CS neurons die after axotomy remains controversial. On the one side a substantial loss of CS neurons was detected after pyramidotomy (Pernet and Hepp-Reymond, 1975) or cervical lesion (Holmes and May, 1909) but others did not observe any retrograde degeneration with breakdown and loss of neurons after section of the CS tract (Tower, 1940). Moreover, in primates the effect of axotomy on RS neurons is not known in contrast to the rat where cell shrinkage is observed (Novikova et al., 2000). In the present investigation we used a specific staining of a subpopulation of neurons in layer V, the pyramidal neurons and RS neurons of the RNm allowing a better

focus on the neurons of interest than for instance in Nissl staining that stains a much larger population of neurons. As a consequence, a difference between the two hemispheres and red nuclei affecting the CS and RS neurons after a unilateral cervical lesion is detected with more sensitivity in SMI-32 than in Nissl material.

Our findings show that CS and RNm neurons shrink and that anti-Nogo-A antibody treatment does not prevent cell shrinkage. Despite the wide diffusion of the antibody reaching also the brain through the CSF circulation (Weinmann et al., 2006) this may seem surprising.

However, normal neuronal functioning depends on the neurotrophic substances acquired via the numerous synapses. Hence after injury enhanced sprouting, as observed in the anti-Nogo-A antibody treated monkeys (Freund and others, 2006; Freund and others, 2007) should lead to enhanced synapse formation and thus could provide the neuron with more neurotrophic support as not sprouting neurons after injury. However, if one considers that the number of sprouting CS and RNm neurons after injury may be limited to a small population and that the newly formed axonal arbors may not be as large as intact axons the amount of neurotrophic support would not be sufficient to maintain their full soma size. Moreover, such minor difference between the cell sizes may not be detectable by the methods used in this investigations.

Because the number of SMI-32 stained neurons is relatively low in both cortical layer and red nucleus, we did not use a stereological probe to estimate their number but we counted all visible nuclei of the labelled cells on the analyzed sections. This approach is considered as adequate as all samples were analyzed using the same procedure and the number of cells is low (Geuna, 2000; Lavenex et al., 2000; Benes and Lange, 2001). In the present case, in addition, the validity of the method is supported *a posteriori* by the absence of overlap between lesioned and intact monkeys in a large group of animals.

1.7 Reconstruction of the injured CST, a mechanism of recovery?

During recovery after CNS lesion, extensive plastic re-organization of neuronal networks at cortical level as well as spinal level have been observed in rodents (Bareyre et al., 2004), non-human primates (Schmidlin et al., 2004) and humans (Dietz, 1992; Ward et al., 2003). In the case of incomplete SCI spared tissue functions as a bridge for regenerating fibers. In addition the spared tissue conserves pathways that can takeover function after injury and thus may represent the substrate for compensatory mechanism.

In the present study, reflecting an incomplete SCI situation, a substantial reorganization of the injured CST tract was observed in anti-Nogo-A antibody and limited in control antibody treated monkeys. As compared to control antibody treated monkeys, the anti-Nogo-A antibody treated monkeys exhibited an increased cumulated axon arbor length and a higher number of axon arbors going in the medial direction from the white to the grey matter. Higher in the cervical cord (at C5 level), the anti-Nogo-A treatment enhanced the number of corticospinal fibers crossing the midline, suggesting axonal sprouting. In conclusion, the anti-Nogo-A antibody treatment enhanced axonal sprouting rostral to the cervical lesion (Freund et al 2007); some of these fibers grew around the lesion and into the caudal spinal segments (Freund et al. 2006). Among the possible mechanisms leading to the partial reconstruction of the CS tract caudal to the lesion, sprouting from the CS tract that originates from the ipsilesional hemisphere can be ruled out, at least in control antibody treated monkeys. After reversible inactivation using the GABA antagonist muscimol (brown syringes in Fig 2) of the ipsilesional motor cortex the recovered manual dexterity score was not affected (Schmidlin and others, 2004; Schmidlin et al., 2005). On the other hand, reversible inactivation of the contralesional motor cortex reduced the ability of the ipsilesional hand to obtain the recovered manual dexterity score (Schmidlin et al., 2005), indicating that the spontaneous reconstruction of the CS tract caudal to the lesion occurs from axons originating from the contralesional hemisphere in the form of sprouting of the transected CS

axons (green solid lines in Fig. 2) and/or sprouting of the undecussated CS projection not affected by the lesion, crossing the midline below the lesion (yellow solid lines in Fig. 2).

After injection of an anterograde tracers into the hand area of M1 90 % of the CS projection run in the contralateral dorsolateral funiculus (90%) whereas the other 10 % do not decussate and thus remain unaffected by the cervical lesion (Rouiller et al. 1996; Lacroix et al. 2004). However, the present study did not address the possibility that some CS axon arbors observed caudal to the lesion (**Chapter 2**) could result from sprouting arising from these undecussated CS axons (Fig. 2). In rats subjected to a spinal cord lesion interrupting the main CS tract, axon sprouting from the intact ventral CS tract was indeed found to play an important role in the spontaneous post-lesion recovery (Weidner et al., 2001). CS fibers from the intact side have been seen to cross the spinal cord midline in rats after unilateral pyramidotomy and anti-Nogo-A antibody application (Thallmair et al., 1998).

Descending tracts other than the CS projection were not labeled in the present investigation and therefore it remains uncertain how much they were affected by the lesion, as well as to what extent the anti-Nogo-A antibody treatment enhanced sprouting of the rubrospinal, reticulospinal, tectospinal and vestibulospinal tracts for instance as observed in the rat (Thallmair et al., 1998; Raineteau et al., 2001).

1.8 Takeover of indirect pathways

To recover from an injury to the CNS injured fiber tracts can respond in terms of regeneration and/or regenerative sprouting (Schwab, 2002). The latter mechanism can also be observed from fiber tracts not directly affected by the lesion (Thallmair and others, 1998; Raineteau et al., 2002; Cafferty and Strittmatter, 2006).

In non-human primates subjected to a unilateral section of the CST the ipsilateral descending portion of the CST responded to injury by compensatory sprouting. However, as these animals were mature, the effect of CST sprouting remained very limited and may not play a significant role for the recovery of manual dexterity (Galea and Darian-Smith, 1997a; Galea and Darian-Smith, 1997b). It was observed that both CS as well as RN atrophy and therefore cannot solely contribute to functional recovery to the extent as observed in the hemisected primates (Galea and Darian-Smith, 1997a; Galea and Darian-Smith, 1997b). At least in the cat, reticulospinal tract neurons do not atrophy after cervical hemisection. This may offer a neural substrate for descending inputs onto ipsilateral motoneurons in form of commissural axons sprouting rostral and caudal to lesion to reconnect to pre-existing spinal circuits. In the recovery weeks these connections could be reinforced by increasing crosstalk through corticocortical connections between the different corticospinal populations. In the latter study on primate hemisection of the cervical cord, Galea and Darian-Smith attributed a substantial part of the functional recovery of the precision grip in the lesioned monkeys to the remaining fibres of the reticulospinal tract spared by their model of lesion (Galea and Darian-Smith, 1997a; Galea and Darian-Smith, 1997b), though no direct evidence supports this hypothesis in macaque monkeys.

Another possible neural adaptation mechanism promoting functional recovery is the use and exploitation of intrinsic circuits of the spinal cord. It was shown that spontaneous sprouting of lesioned axons can contribute to recovery in absence

of long distance regeneration via collaterals that connect to long distance propriospinal fibers themselves forming a new circuit caudal to lesion (Bareyre et al. 2004). These networks are called ‘detour circuit’ that allow spinal interneural circuits to take over new functions in order to compensate for the deprived input (Galea and Darian Smith 1997; Bareyre et al. 2004).

In addition, further intraspinal reorganization has been observed following mid-thoracic hemisection in rodents: After a recovery time of eight weeks the number of direct contacts between long propriospinal axon terminals and lumbar motoneurons is doubled. This two fold increase demonstrates that neural population not directly affected by the lesion respond to injury and create novel axonal circuits (Bareyre and others, 2004).

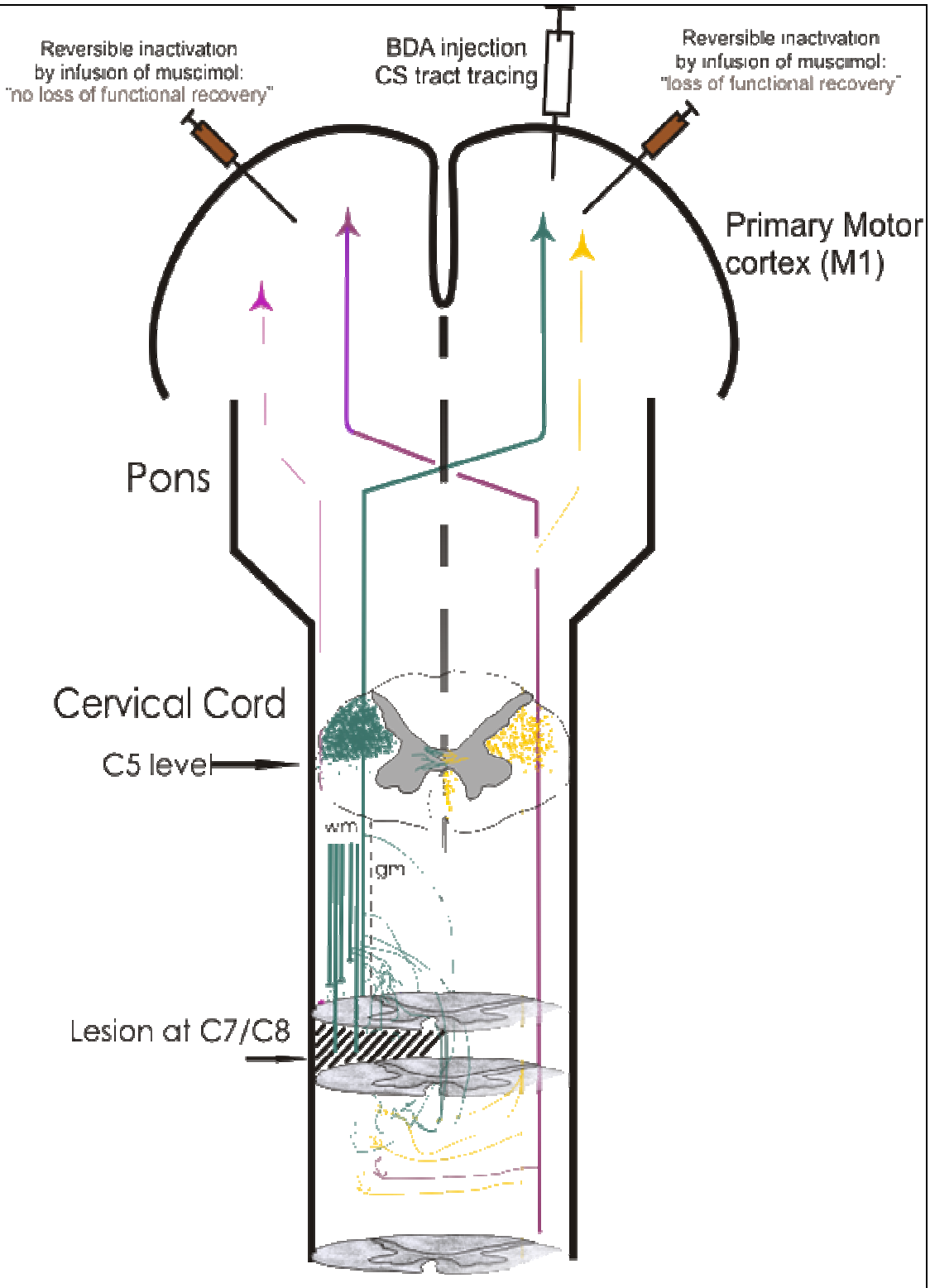

Figure 2 : Schematic representation of the macaque monkey corticospinal (CS) projection originating from the right primary motor cortex (M1) as seen at cervical cord level, as a result of BDA injection (empty syringe) in the right motor cortex. At C5 level,

on a frontal section of the cervical cord, green dots indicate the location and distribution of the CS axons, forming the dorsolateral funiculus (dlf) contralateral to the injection site and the uncrossed CS axons, present in the dorsolateral and ventral funiculi ipsilateral to the injection site. At C7/C8 level, the ensemble of black oblique lines represents the cervical lesion performed in the present study. Rostral to the lesion, parallel green thick lines represent CS axons in the dorsolateral funiculus, interrupted by the lesion. Axonal sprouting is represented by thinner lines arising from the thick green lines above, into and around the lesion.

The brown syringe is for pharmacological reversible inactivation experiments of the contralesional primary motor cortex (M1), (Schmidlin and others, 2004). The thick vertical dashed line represents midline, whereas the thin vertical dashed line represents the boundary between the white (wm) and the grey (gm) matter.

1.9 Adaptive strategies to compensate for loss of function

In an incomplete SCI condition, the large information normally projected to the spinal cord via the CST for reach and grasp movements is greatly reduced and remains a “bottleneck” situation. The decreased transmission rates from the cortex to the cervical cord may influence the animal to adopt new strategies to achieve its intention with simpler and slower actions which nevertheless are still effective. It is known that in SCI patients as well as in experimentally induced SCI animals the use of adaptive strategies for the recovery of limb function is important. In cats this has been observed for grasping after high cervical lesions (Alstermark et al., 1987) and in rats for walking by involving axial movements (Giszter et al., 1998). Such change in strategy has also been observed in monkeys for a precision grip task after cervical dorsal rhizotomy (Darian-Smith and Ciferri, 2005) and locomotion in thoracical hemisected monkeys (Courtine et al., 2005).

In the present investigation it was observed that especially control antibody treated monkeys made use of new adaptive strategies. In particular, during the

modified “Brinkman Board task” the monkeys tucked their thumb into the palm of the hand. As a consequence the opposed thumb served as an opposing platform for the index finger in order to achieve a successful retrieve.

In anti-Nogo-A antibody treated monkeys adaptive strategies at least during the dexterity test were rarely observed. A question then arises to what extent the limited sprouting of the CST tract in control antibody treated monkeys implies the need for such adaptation mechanism? Due to the limited number of control monkeys the question is difficult to answer. However the comparison of the sprouting occurring rostral to the lesion with the numbers of axonal swellings caudal to lesion indicates a correlation between the rostral and caudal occurring anatomical reorganization (Fig 4 E, **Chapter 4**); supporting the notion that the contingent of CS axons growing around the lesion in the grey matter is an anatomical correlate of the functional recovery observed in the anti-Nogo-A antibody treated animals.

1.10 Perspectives:

Combined anti-Nogo-A / BDNF treatment: Neutrophic support?

In the present investigation we revealed that axotomized CS and RN neurons exhibited significant shrinkage of their cell soma size after a unilateral cervical lesion (Beaud et al. 2007; Wannier-Morino et al. 2007). In addition, positive SMI-32 stained RS neurons were less numerous on the contralateral side of injury, possibly indicating cell loss. Infusion of anti-Nogo-A antibodies did not prevent atrophy of the axotomized CS and RS neurons. Rather its effect was at the distal end of the axotomized axons leading to regenerative CS sprouting (Freund and others, 2006; Freund and others, 2007).

Neuronal metabolism depends on continuous retrograde trophic signals from the targets, which are absent or reduced in case of axotomy. As the normal intact axonal arborization may be much larger than the “spontaneously” newly formed

arbors of the few sprouting neurons the decrease of retrogradely transported trophic signals may in part explain soma shrinkage. Although in the anti-Nogo-A antibody treated monkeys sprouting was enhanced (Freund and others, 2006; Freund and others, 2007), the quality and amount of neurotrophic signals may still not be sufficient to reverse atrophy completely.

In line with our data, adult rats subjected to cervical axotomy undergo a marked atrophy of rubrospinal neurons (RSNs) within the first month together with a decline in expression of regeneration-associated genes such as GAP-43 and Tα1-tubulin (Bregman et al., 1998; Broude et al., 1999). Can this be attributed in part to the lack of neutrophic factors?

The neutrophin factor family comprises the nerve growth factor (NGF), the brain derived brain growth factor (BDNF) (Leibrock et al. 1998), neutrophin-3 (NT-3) and neutrophin-4/5 (NT-4/5). All known members bind to two different types of receptors, the *trk* tyrosine kinases and the neurotrophin receptor p75. Neutrophins mediate via these receptors neuronal survival, neural differentiation during development, maintenance of neural phenotype and modulation of synaptic efficacy in the adult CNS (Bonhoeffer, 1996).

In consequent studies using a battery of administration techniques to supply neutrophic factors such as BDNF, NT-3 and NT-4/5 showed that axotomized RSNs and other supraspinal neurons in adult rats after cervical lesion did not atrophy, in contrast to untreated (Bregman and others, 1998; Liu et al., 2002). Following BDNF and NT-4/5 administration in the vicinity of RSNs neurons GAP-43 and Tα1-tubulin gene expression was increased. In addition, infusion of BDNF enhanced the numbers of RSNs axons regenerating into a sciatic nerve implanted into the cervical cord at the level of injury (Kobayashi et al., 1997) Moreover, following BDNF administration at CS cell bodies after SCI in adult rats, CS neurons established new connections onto spared descending interneurons (Vavrek et al., 2006) and collateral sprouting (Coumans et al., 2001; Hiebert et al., 2002). The restoration of anatomical connections was associated with recovery of locomotor function (Coumans and others, 2001).

In conclusion, the aforementioned studies add up evidence that indeed lack of neutrophic factors leads to cell soma atrophy; itself a detrimental process to functional recovery. In contrast, exogenous administration of neutrophins, such as BDNF, can prevent neural atrophy, stimulate axonal sprouting and promotes functional recovery.

As the anti-Nogo-A antibody treatment did not prevent cell body shrinkage of CS and RS neurons (Beaud et al., 2007; Morino-Wannier et al. 2007), we hypothesized that a combination of anti-Nogo-A antibodies and BDNF infusion could prevent cell atrophy of these neurons. In addition, BDNF infusion could contribute to the restoration of anatomical connections, making the reconstruction of the CST as observed when neutralizing Nogo-A (Freund and others, 2006; Freund and others, 2007) more beneficial in supporting functional recovery.

In ongoing investigations three monkeys received a combination of anti-Nogo-A and BDNF being intrathecally infused. Despite a complete hemisection, these animals recovered manual dexterity to a greater extend then control antibody treated animals, in line with the anti-Nogo-A antibody treatment. In the ongoing anatomical investigation we have found that at least in two of the three treated animals cell soma atrophy of RN neurons was more limited then in control and anti-Nogo-A antibody treated animals.

Measuring grip and load force to monitor forelimb recovery?

Tasks that have been commonly used to gain insights into control and recovery of manual dexterity usually involve a monkey removing food pellets from wells in a “Klüver” or “Brinkman board” task using the precision grip, the opposition of thumb and index finger (Nudo and Milliken, 1996; Friel and Nudo, 1998; Liu and Rouiller, 1999; Freund and others, 2006). The success and temporal measures are the most commonly recorded parameters. However, dexterous manipulation of objects requires also a precise control of the forces applied to objects held between two or more digits.

This precise control over the digit forces is important for successful completion of complex daily tasks, such as writing and food preparation. Measuring forces applied by the hand and digits during a task should provide a sensitive measure to monitor recovery reflecting the level of coordination of several joints and muscles. In order to measure these deficits and to monitor its recovery in the nonhuman primate we developed a so-called “Drawer Pulling task”: This device allows analyzing the recovery of the grip force exerted by the fingers on the drawer knob, the load force exerted to pull the drawer, the time to pull the drawer open and the time required to pick a food reward out of the drawer. A torque motor allows generating a force of chosen constant amplitude to oppose the pulling force.

So far, we have investigated the recovery of four adult macaque monkeys performing the task. The macaques were either treated with a control antibody (N=2) or with a combination of BDNF and of an antibody neutralizing Nogo-A (N=2). During the pre-lesion period the strength of the grip force and load force covaried. However, immediately after the lesion the hand homolateral to the lesion was impaired and, during the first trials depending on the resistance amplitude tested, pulling time increased. A control antibody treated monkey with an incomplete lesion of the corticospinal tract (CST) exhibited a persistent significant loss of grip and load forces at the highest resistance amplitude (6.5 N) and an increase in pulling time for the lowest resistance amplitude (0.5 N). In contrast an anti-Nogo-A / BDNF treated monkey with a complete CST lesion recovered fully its grip force, load force and pulling time under the same conditions for this specific task. Picking time returned for both monkeys to pre-lesion level. The recovery profile of one of the two remaining animals corresponds to that of the control antibody treated animal, whereas that of the second animal corresponds to that of the combined anti-Nogo-A / BDNF treated animal. However, the experimenter is presently blind to the treatment of the two other monkeys, and to the size of their lesion. These data suggests that the unimanual drawer-pulling task is a useful tool to detect a motor deficit after a

unilateral spinal cord lesion and to monitor the time course and extent of recovery.

Repair of neural pathways by olfactory ensheathing cells

After injury to the spinal cord, axons first attempt to regenerate but fail because of the myelin inhibitory environment and the lack of proper glia pathways that nerve fibres require for their elongation. Transplantation of olfactory ensheathing cells into the lesion site is being investigated as a procedure to re-establish glia pathways.

The failure of injured axons to regenerate within the adult CNS does not apply to the olfactory bulb containing the olfactore ensheathing glia cells. During development the olfactory ensheathing cells develop from a placode on the surface of the body (Raisman, 1985; Raisman and Li, 2007) and therefore need to tunnel their way through intervening mesenchym to reach the olfactory bulb. Electron microscopy studies show that these cells consist of a thin cytoplasmic sheet that is curved over to enclose a tunnel-like space. Through this tunnel approximately 1000 olfactory fibres make their way to the olfactory bulb (Field et al., 2003). It was shown that by transplanting such cells into the lesion site, analogous to the reasoning of the experiments conducted by David and Aaguyo (David and Aguayo, 1981), the property of axons to re-enter the astrocytic environment could be translated. The transplanted cells appear to migrate with regenerating axons through the nonpermissive astrocytic environment towards specific denervated spinal cord laminae (Li and Raisman, 1993; Ramon-Cueto and Nieto-Sampedro, 1994). Most important, the enhanced long distance regeneration was shown to lead to impressive functional recovery of rats with injured CST(Li et al., 1997; Ramon-Cueto et al., 2000).

Clinical demonstration of the effectiveness of transplanting the olfactory ensheating cells would open a door to treating a wide variety of currently incurable injuries of the brain and the spinal cord. At present two neurosurgical groups (Dobkin et al., 2006; Lima et al., 2006a) have adopted transplantation of

olfactory tissue as a clinical approach to treat spinal cord injuries and one reports preliminary data of enhanced functional recovery(Lima et al., 2006b).

1.11 Conclusion

The present thesis demonstrates a remarkable functional recovery of manual dexterity when Nogo-A is neutralized in adult non-human monkeys subjected to a cervical spinal cord lesion. CS sprouting into and around the lesion paralleled the observed functional recovery of manual dexterity. We believe that this enhanced anatomical reorganization may in part contribute to the observed enhanced functional recovery of manual dexterity. This result is a further promising step towards clinical application.

The demonstration of nerve fiber plasticity within the mature spinal cord, a process being paralleled by significant functional recovery opens exiting perspectives for therapeutic approaches after SCI in humans. However, for an optimal future treatment aiming at restoring function after SCI, a combination of different approaches to overcome the barrier and inhibitory constitutes will be required (Thuret and Moon, 2006). In this line one could imagine to combine the anti-Nogo-A antibody treatment with the auto transplantation of olfactory ensheathing cells. This double treatment would allow neutralizing the inhibitory myelin and in addition provide the regenerating axons a proper glia pathways.

1.12 Reference List

Alstermark B, Lundberg A, Pettersson LG, Tantisira B, Walkowska M. 1987. Motor recovery after serial spinal cord lesions of defined descending pathways in cats. Neurosci Res 5:68-73.

Bareyre FM, Kerschensteiner M, Raineteau O, Mettenleiter TC, Weinmann O, Schwab ME. 2004. The injured spinal cord spontaneously forms a new intraspinal circuit in adult rats. Nat Neurosci 7:269-277.

Benes FM, Lange N. 2001. Two-dimensional versus three-dimensional cell counting: a practical perspective. In: p 11-17.

Bonhoeffer T. 1996. Neurotrophins and activity-dependent development of the neocortex. Curr Opin Neurobiol 6:119-126.

Bregman BS, Broude E, McAtee M, Kelley MS. 1998. Transplants and neurotrophic factors prevent atrophy of mature CNS neurons after spinal cord injury. Exp Neurol 149:13-27.

Broude E, McAtee M, Kelley MS, Bregman BS. 1999. Fetal spinal cord transplants and exogenous neurotrophic support enhance c-Jun expression in mature axotomized neurons after spinal cord injury. Exp Neurol 155:65-78.

Cafferty WB, Strittmatter SM. 2006. The Nogo-Nogo receptor pathway limits a spectrum of adult CNS axonal growth. J Neurosci 26:12242-12250.

Coumans JV, Lin TTS, Dai HN, MacArthur L, McAtee M, Nash C, Bregman BS. 2001. Axonal regeneration and functional recovery after complete spinal cord transection in rats by delayed treatment with transplants and neurotrophins. J Neurosci 21:9334-9344.

Courtine G, Bunge MB, Fawcett JW, Grossman RG, Kaas JH, Lemon R, Maier I, Martin J, Nudo RJ, Ramon-Cueto A, Rouiller EM, Schnell L, Wannier T, Schwab ME, Edgerton VR. 2007. Can experiments in nonhuman primates expedite the translation of treatments for spinal cord injury in humans? Nat Med 13:561-566.

Courtine G, Roy RR, Raven J, Hodgson J, McKay H, Yang H, Zhong H, Tuszynski MH, Edgerton VR. 2005. Performance of locomotion and foot grasping following a unilateral thoracic corticospinal tract lesion in monkeys (*Macaca mulatta*). Brain 128:2338-2358.

Darian-Smith C, Ciferri MM. 2005. Loss and recovery of voluntary hand movements in the macaque following a cervical dorsal rhizotomy. J Comp Neurol 491:27-45.

David S, Aguayo AJ. 1981. Axonal elongation into peripheral nervous system "bridges" after central nervous system injury in adult rats. Science 214:931-933.

Dietz V. 1992. Human neuronal control of automatic functional movements: Interaction between central programs and afferent input. Physiol Rev 72:33-69.

Dobkin BH, Curt A, Guest J. 2006. Cellular transplants in China: observational study from the largest human experiment in chronic spinal cord injury. Neurorehabil Neural Repair 20:5-13.

Dum RP, Strick PL. 1991. The origin of corticospinal projections from the premotor areas in the frontal lobe. J Neurosci 11:667-689.

Field P, Li Y, Raisman G. 2003. Ensheathment of the olfactory nerves in the adult rat. J Neurocytol 32:317-324.

Fouad K, Klusman I, Schwab ME. 2004. Regenerating corticospinal fibers in the Marmoset (*Callitrix jacchus*) after spinal cord lesion and treatment with the anti-Nogo-A antibody IN-1. Eur J Neurosci 20:2479-2482.

Fouad K, Schnell L, Bunge MB, Schwab ME, Liebscher T, Pearse DD. 2005. Combining Schwann cell bridges and olfactory-ensheathing glia grafts with chondroitinase promotes locomotor recovery after complete transection of the spinal cord. J Neurosci 25:1169-1178.

Freund P, Schmidlin E, Wannier T, Bloch J, Mir A, Schwab ME, Rouiller EM. 2006. Nogo-A-specific antibody treatment enhances sprouting and functional recovery after cervical lesion in adult primates. Nature Med 12:790-792.

Freund P, Wannier T, Schmidlin E, Bloch J, Mir A, Schwab ME, Rouiller EM. 2007. Anti-Nogo-A antibody treatment enhances sprouting of corticospinal axons rostral to a unilateral cervical spinal cord lesion in adult macaque monkey. J Comp Neurol 502:644-659.

Friel KM, Nudo RJ. 1998. Recovery of motor function after focal cortical injury in primates: compensatory movement patterns used during rehabilitative training. Somatosens Mot Res 15:173-189.

Galea MP, Darian-Smith I. 1997a. Manual dexterity and corticospinal connectivity following unilateral section of the cervical spinal cord in the macaque monkey. J Comp Neurol 381:307-319.

Galea MP, Darian-Smith I. 1997b. Corticospinal projection patterns following unilateral section of the cervical spinal cord in the newborn and juvenile macaque monkey. J Comp Neurol 381:282-306.

Geuna S. 2000. Appreciating the difference between design-based and model-based sampling strategies in quantitative morphology of the nervous system. In: p 333-339.

Giszter SF, Kargo WJ, Davies M, Shibayama M. 1998. Fetal transplants rescue axial muscle representations in M1 cortex of neonatally transected rats that develop weight support. J Neurophysiol 80:3021-3030.

Hashimoto T, Fukuda N. 1991. Contribution of serotonin neurons to the functional recovery after spinal cord injury in rats. Brain Res 539:263-270.

He S-Q, Dum RP, Strick PL. 1995. Topographic organization of corticospinal projections from the frontal lobe: Motor areas on the medial surface of the hemisphere. J Neurosci 15:3284-3306.

He S-Q, Dum RP, Strick PL. 1993. Topographic organization of corticospinal projections from the frontal lobe: Motor areas on the lateral surface of the hemisphere. J Neurosci 13:952-980.

Hiebert GW, Khodarahmi K, McGraw J, Steeves JD, Tetzlaff W. 2002. Brain-derived neurotrophic factor applied to the motor cortex promotes sprouting of corticospinal fibers but not regeneration into a peripheral nerve transplant. Journal of Neuroscience Research 69:160-168.

Holmes GL, May WP. 1909. On the exact origin of the pyramidal tracts in man and other mammals. Brain 32:1-42.

Kobayashi NR, Fan DP, Giehl KM, Bedard AM, Wiegand SJ, Tetzlaff W. 1997. BDNF and NT-4/5 prevent atrophy of rat rubrospinal neurons after cervical axotomy, stimulate GAP-43 and Talpha1-tubulin mRNA expression, and promote axonal regeneration. J Neurosci 17:9583-9595.

Lacroix S, Havton LA, McKay H, Yang H, Brant A, Roberts J, Tuszynski MH. 2004. Bilateral corticospinal projections arise from each motor cortex in the macaque monkey: A quantitative study. J Comp Neurol 473:147-161.

Lavenex P, Steele MA, Jacobs LF. 2000. The seasonal pattern of cell proliferation and neuron number in the dentate gyrus of wild adult eastern grey squirrels. In: p 643-648.

Lemon RN, Griffiths J. 2005. Comparing the function of the corticospinal system in different species: Organizational differences for motor specialization? Muscle Nerve 32:261-279.

Li Y, Field PM, Raisman G. 1997. Repair of adult rat corticospinal tract by transplants of olfactory ensheathing cells. Science 277:2000-2002.

Li Y, Raisman G. 1993. Long axon growth from embryonic neurons transplanted into myelinated tracts of the adult rat spinal cord. Brain Res 629:115-127.

Liebscher T, Schnell L, Schnell D, Scholl J, Schneider R, Gullo M, Fouad K, Mir A, Rausch M, Kindler D, Hamers FPT, Schwab ME. 2005. Nogo-A antibody improves regeneration and locomotion of spinal cord-injured rats. Ann Neurol 58:706-719.

Lima C, Pratas-Vital J, Escada P, Hasse-Ferreira A, Capucho C, Peduzzi JD. 2006a. Olfactory mucosa autografts in human spinal cord injury: a pilot clinical study. J Spinal Cord Med 29:191-203.

Lima C, Pratas-Vital J, Escada P, Hasse-Ferreira A, Capucho C, Peduzzi JD. 2006b. Olfactory mucosa autografts in human spinal cord injury: a pilot clinical study. J Spinal Cord Med 29:191-203.

Liu Y, Himes BT, Murray M, Tessler A, Fischer I. 2002. Grafts of BDNF-producing fibroblasts rescue axotomized rubrospinal neurons and prevent their atrophy. Experimental Neurology 178:150-164.

Liu Y, Rouiller EM. 1999. Mechanisms of recovery of dexterity following unilateral lesion of the sensorimotor cortex in adult monkeys. Exp Brain Res 128:149-159.

Moon LDF, Fawcett JW. 2001. Reduction in CNS scar formation without concomitant increase in axon regeneration following treatment of adult rat brain with a combination of antibodies to TGFβ_1 and β_2. Eur J Neurosci 14:1667-1677.

Novikova LN, Novikov LN, Kellerth JO. 2000. Survival effects of BDNF and NT-3 on axotomized rubrospinal neurons depend on the temporal pattern of neurotrophin administration. Eur J Neurosci 12:776-780.

Nudo RJ, Milliken GW. 1996. Reorganization of movement representations in primary motor cortex following focal ischemic infarcts in adult squirrel monkeys. J Neurophysiol 75:2144-2149.

Olivier E, Edgley SA, Armand J, Lemon RN. 1997. An electrophysiological study of the postnatal development of the corticospinal system in the macaque monkey. J Neurosci 17:267-276.

Pernet U, Hepp-Reymond M-C. 1975. Retrograde Degeneration der Pyramidenbahnzellen im motorischen Kortex beim Affen (Macaca fascicularis). Acta Anat (Basel)552-561.

Raineteau O, Fouad K, Bareyre FM, Schwab ME. 2002. Reorganization of descending motor tracts in the rat spinal cord. Eur J Neurosci 16:1761-1771.

Raisman G. 1985. Specialized neuroglial arrangement may explain the capacity of vomeronasal axons to reinnervate central neurons. Neuroscience 14:237-254.

Raisman G, Li Y. 2007. Repair of neural pathways by olfactory ensheathing cells. Nat Rev Neurosci 8:312-319.

Ramon-Cueto A, Cordero MI, Santos-Benito FF, Avila J. 2000. Functional recovery of paraplegic rats and motor axon regeneration in their spinal cords by olfactory ensheathing glia. Neuron 25:425-435.

Ramon-Cueto A, Nieto-Sampedro M. 1994. Regeneration into the spinal cord of transected dorsal root axons is promoted by ensheathing glia transplants. Exp Neurol 127:232-244.

Rhodes KE, Fawcett JW. 2004. Chondroitin sulphate proteoglycans:preventing plasticity or protecting the CNS? J Anat 204:33-48.

Rhodes KE, Moon LDF, Fawcett JW. 2003. Inhibiting cell proliferation during formation of the glial scar: Effects on axon regeneration in the CNS. Neuroscience 120:41-56.

Rouiller EM, Moret V, Tanné J, Boussaoud D. 1996. Evidence for direct connections between the hand region of the supplementary motor area and cervical motoneurons in the macaque monkey. Eur J Neurosci 8:1055-1059.

Schmidlin E, Wannier T, Bloch J, Belhaj-Saïf A, Wyss A, Rouiller EM. 2005. Reduction of the hand representation in the ipsilateral primary motor cortex following unilateral section of the corticospinal tract at cervical level in monkeys. BMC Neuroscience 6:56.

Schmidlin E, Wannier T, Bloch J, Rouiller EM. 2004. Progressive plastic changes in the hand representation of the primary motor cortex parallel incomplete recovery from a unilateral section of the corticospinal tract at cervical level in monkeys. Brain Research 1017:172-183.

Schnell L, Schneider R, Kolbeck R, Barde Y-A, Schwab ME. 1994. Neurotrophin-3 enhances sprouting of corticospinal tract during development and after adult spinal cord lesion. Nature 367:170-173.

Schnell L, Schwab ME. 1993. Sprouting and regeneration of lesioned corticospinal tract fibres in the adult rat spinal cord. Eur J Neurosci 5:1156-1171.

Schnell L, Schwab ME. 1990. Axonal regeneration in the rat spinal cord produced by an antibody against myelin-associated neurite growth inhibitors. Nature 343 no 6255:269-272.

Schucht P, Raineteau O, Schwab ME, Fouad K. 2002. Anatomical correlates of locomotor recovery following dorsal and ventral lesions of the rat spinal cord. Experimental Neurology 176:143-153.

Schwab ME. 2002. Differing views on spinal cord repair - Response. Science 296:1400.

Thallmair M, Metz GAS, Z'Graggen WJ, Raineteau O, Kartje GL, Schwab ME. 1998. Neurite growth inhibitors restrict plasticity and functional recovery following corticospinal tract lesions. Nature Neurosci 1:124-131.

Thuret S, Moon LDF. 2006. Therapeutic interventions after spinal cord injury. Nat Rev Neurosci 7:628-643.

Tower SS. 1940. Pyramidal lesion in the monkey. Brain 63:36-90.

Vavrek R, Girgis J, Tetzlaff W, Hiebert GW, Fouad K. 2006. BDNF promotes connections of corticospinal neurons onto spared descending interneurons in spinal cord injured rats. Brain 129:1534-1545.

Ward NS, Brown MM, Thompson AJ, Frackowiak RSJ. 2003. Neural correlates of motor recovery after stroke: a longitudinal fMRI study. Brain 126:2476-2496.

Weidner N, Ner A, Salimi N, Tuszynski MH. 2001. Spontaneous corticospinal axonal plasticity and functional recovery after adult central nervous system injury. Proceedings of the National Academy of Sciences of the United States of America 98:3513-3518.

Weinmann O, Schnell L, Ghosh A, Montani L, Wiessner C, Wannier T, Rouiller E, Mir A, Schwab ME. 2006. Intrathecally infused antibodies against Nogo-A penetrate the CNS and downregulate the endogenous neurite growth inhibitor Nogo-A. Mol Cell Neurosci 32:161-173.

Ward,N.S., Frackowiak,R.S. (2003a). Age-related changes in the neural correlates of motor performance. *Brain* 126(4), 873-888. ISSN: 0006-8950

Ward NS, Brown MM, Thompson AJ, Frackowiak RSJ. (2003c). Neural correlates of motor recovery after stroke: a longitudinal fMRI study. *Brain* 2003; 126:2476-2496

Ward NS, Newton JM, Swayne OBC, Lee L, Frackowiak RSJ, Thompson AJ, Greenwood RJ, Rothwell JC. The relationship between brain activity and peak grip force is modulated by corticospinal system integrity after subcortical stroke. *Eur J Neurosci* 2007;25(6):1865-73.

Beaud M-L, Wannier T, Schmidlin E, Freund P, Bloch J, Mir A, Schwab ME, and Rouiller EM. 2006. Anti-Nogo-A treatment enhanced sprouting of corticospinal axons but did not prevent cell body shrinkage in the motor cortex in adult monkeys subjected to unilateral cervical cord lesion [abstract]

Leibrock J, Lottspeich F, Hohn A, Hofer M, Hengerer B, Masiakowski P, *et al.* (1989). Molecular cloning and expression of brain-derived neurotrophic factor. *Nature* 341:149–152.

Curriculum Vitae Patrick Freund

W: Department of Physiology
University of Fribourg
Pérolles
Rue du Musée 5
CH-1700 Fribourg
Switzerland
Phone: 004126 300 86 88
Fax: 004126 300 96 75
Email: Patrick.Freund@unifr.ch

H: Grande Rue 69
CH-1700 Fribourg
Switzerland
Phone : 0041788852868

Education/School	1986-1990	German School Beijing (China)
	1991-2000	Goerdeler Gymnasium Paderborn (Germany)
	10.06.2000	Abitur (A-Levels)
Civilian Service	01.07.2000 – 30.08.2001	Assistant Teacher in a School for Children with special needs in Hermanus (Western Province, South Africa)
Education/ University	15.03.2002 – 07.02.2005	Biology at the Bilingual University of Fribourg (Switzerland)
	15.10.2003	Bilingual (French/German) Bachelor of Science degree in Biology
	07.02.2005	Bilingual (French/German) Master of Science degree in Biology (Neurophysiology)
	01.04.2005 – 30.01.2008	PhD degree in Neurophysiology at the University of Fribourg
	15.10.2005 – present	Medical student: Physikum (Semester: 5)

Internships	15.07.1999 – 08.08.1999	Internship on a farm (Le Mans, France)
	01.09.2001 – 29.02.2001	Internship as a nurse in the 'Brüder Krankenhaus Paderborn' (Germany)
	01.06.2003 – 31.10.2003	Field Assistant in an Ecological Experiment (Fribourg, Switzerland)
Proficiencies	Knowledge of languages: German, English, French (fluent)	
	PC: Office, Frontpage, Adobe Photoshop, Microsoft Photoshop, Corel 13, MatLab, Spike2, SPSS, NeuroLucida	
Interests	Reading, Sports, Stamps, Farming, Hiking, Fishing, Climbing	

BIBLIOGRAPHY – Patrick Freund – 2007

FULL-LENGTH ARTICLES:

1. **P. Freund**[*], E. Schmidlin[*], T. Wannier[*], J. Bloch, A. Mir, M. E. Schwab and E. M. Rouiller: *Anti-Nogo-A enhances sprouting and functional recovery after cervical lesion in adult primates.* Nat Med. 2006 Jul; 12(7):790-2. Epub 2006 Jul 2; [*] = equal contribution

2. **P. Freund,** Eric Schmidlin, Thierry Wannier, J. Bloch, A. Mir, M.E. Schwab and E. M. Rouiller: *Challenges to the report of Nogo antibody effects in primates.* **Nat Med**. 2006 Nov;12(11):1231-2; author reply 1232-3

3. **P. Freund**[*], T. Wannier[*], E. Schmidlin[*], J. Bloch, A.Mir, M.E. Schwab and E.M. Rouiller: *Anti-Nogo-A antibody treatment enhances sprouting of corticospinal (CS) axons rostral to an unilateral cervical spinal cord lesion in adult macaque monkey* **J Comp Neurol**. 2007 Jun 1;502(4):644-59*; [*] = equal contribution*

4. P. Wannier-Morino[*], E. Schmidlin[*], **P. Freund**, A. Belhaj-Saif, J. Bloch, A. Mir, M.E. Schwab, E.M. Rouiller and T. Wannier : *Fate of rubrospinal neurons after unilateral section of the cervical spinal cord in adult macaque monkeys. In Press in* ***Journal of Brain Research*** *;[*] = equal contribution*

5. M.-L. Beaud[*], T. Wannier[*], E. Schmidlin[*], **P. Freund**, J. Bloch, A. Mir, M.E. Schwab and E.M. Rouiller: Anti-Nogo-A antibody treatment enhanced sprouting of corticospinal axons but did not prevent cell body shrinkage in the motor cortex in adult monkeys subjected to cervical hemi-cord lesion **BMC Neurosci**. 2008 Jan 14;9(1):5; [*] = equal contribution

6. **P. Freund** *, E. Schmidlin*, J. Bloch, A. Mir, M.E. Schwab, E.M. Rouiller and Thierry Wannier: *Anti-Nogo-A antibody treatment promotes manual dexterity after unilateral cervical lesion in adult primates: behavioural data. Submitted to* ***Journal of Neurosience****;* * *= equal contribution*

7. CJ. Spicher, F. Mathis, B. Degrange, **P. Freund,** EM. Rouiller, *Static mechanical allodynia is a paradoxical painful hypoesthesia. In Press in* ***Somatosens. Mot. Res****.*

8. E. Schmidlin*, **P. Freund***, C. Jouffrais*, P. Wannier, M. Beaud, E. Rouiller and T. Wannier: *Structural characterization including Corticospinal Tract tracing of Polymicrogyria in an adult macaque monkey: case report*
   In preparation for **Brain**; * *= equal contribution*

Abstracts:

1. **P. Freund**, T. Wannier, E. Schmidlin, J. Bloch, A. Mir, M.E. Schwab and E.M. Rouiller : *Density of corticospinal (CS) fibers caudal to a cervical hemisection in monkeys correlates w ith behavioral r ecovery and both are enhanced by anti-Nogo-A treatment* ; Society for Neuroscience Meeting, Washington DC (2005)

2. T. Wannier, E. Schmidlin, **P. Freund**, J. Bloch, A. Mir, M.E. Schwab and E.M. Rouiller : *Behavioral recovery from cer vical hemis ection in monkeys is enhanced by anti-Nogo-A treatment* ; Society for Neuroscien ce Meeting, Washington DC (2005)

3. **P. Freund**, T. Wannier, E. Schmidlin, J. Bloch, A. Mir, M.E. Schwab and E.M. Rouiller : *Regenerative sprouting of co rticospinal (CS) fiber s following c ervical he misection in monkeys correlates with behavioral recovery and both are enhanced by anti-Nogo-A treatment* ; 5th Forum of European Neuroscience, Vienna (2006)

4. **P. Freund**, T. Wannier, E. Schmidlin, M-L. Beaud, J. Bloch, A. Mir, M.E. Schwab and E.M. Rouiller: *Anti-Nogo-A-specific antibody treatment fosters recovery of m anual dexterity from unila teral spinal cord injury in adult monkeys*; 7th Göttingen Meeting to the German Neuroscience Society (2007)

5. S. Bashir, M.-L. Beaud, **P. Freund**, M. Kaeser, A. Wyss, A. Belhaj-Saif, J. Bloch, D. Debatisse, A. Mir, E. Pralong, E.M. Rouiller, M.E. Schwab and T. Wannier: *Characterization of early soma tosensory evoked potentials (SEPs) to electrical s timulation of the m edian nerve in adult macaqu e monkeys: intact and spinal les ioned animals*. Joint meeting SNN- NCCR-Neuro-SSMS (2007), Berne (Switzerland)

6. **P. Freund**, B. Wilm, C. Baltes, M. Rudin, E.M. Rouiller, M.E. Schwab, S. Kollias and T. Wannier: *Characterizing the extent of spinal cord lesion in monkeys: com parison of m agnetic resonance imaging (MRI) data with histological reconstructions* . Joint meeting SNN-NCCR-Neuro-SSMS (2007), Berne (Switzerland)

7. **P. Freund**, M-L. Beaud, J. Bloch, A. Mir, M.E. Schwab , E.M. Rouiller and T. Wannier: *Effects of a unilateral cervical lesion on the perform ance of a drawer-pulling task in control anti body and c ombined anti-Nogo-A / BDNF treated adult m acaque m onkeys;* Society for Neuroscience Meeting, San Diego (2007)

8. S. Bashir, M. Kaeser, ML Beaud, **P.Freund**, A. Belhaj-Saif, J.Bloch, D.Debatisse, E. Pralong, EM Rouiller, ME Schwab, T Wannier: *Effects of a combination of ketam ine and medetomidine hy drochloride (KM) anaesthesia on somatosensory evoked potentials (SSEPs) obtained by electrical s timulation of the m edian nerve in macaques* ; Society for Neuroscience Meeting, San Diego (2007)

9. **P. Freund,** E. Schmidlin, J. Bloch, A. Mir, M.E. Schwab, E.M. Rouiller and T. Wannier**:** *In adult macaque monkeys a unila teral section of the dorsal funiculus induces a reducti on of the num ber of SMI-32 positive neurons in the ipsilesional External Cuneat us Nu cleus (ECU) that is prevented by anti-Nogo-A antibody treatm ent;* 6th Forum of European Neuroscience, Geneva (2008)

10. M.-L. Beaud, E. Schmidlin, **P. Freund** , J. Bloch, A. Mir, M.E. Schwab, E.M. Rouiller and T. Wannier*: In adult m acaque monkeys subje cted to an incomplete spina l cord injury, numer ous large SMI-32 positive fibers wer e observed into the lesion site.* 6th Forum of European Neuroscience, Geneva (2008)

Book Review:

Handbook for Somatosensory Rehabilitation

Spicher CJ, Montepellier, Paris, Saurmaps Medical (2006)

Invitations as speaker:

Breaking News in Neuroscience at 5th Forum of European Neuroscience, Vienna *(***2006)**